

**DESIGN AND IMPLEMENTATION OF EMBEDDED
ARCHITECTURE USING SOFT-COMPUTING
TECHNIQUES FOR PARAMETRIC OPTIMIZATION
OF MIMO WIRELESS SYSTEM**

**A thesis submitted for the award of the
Degree of
DOCTOR OF PHILOSOPHY**

**in
Electrical Engineering**

**By
Pooja S. Suratia**



**ELECTRICAL ENGINEERING DEPARTMENT,
FACULTY OF TECHNOLOGY AND ENGINEERING,
THE MAHARAJA SAYAJIRAO UNIVERSITY OF BARODA,
VADODARA – 390 001
GUJARAT, INDIA.
MARCH-2014**

**Design and Implementation of Embedded Architecture
Using Soft-Computing Techniques for Parametric Optimization
of MIMO Wireless System**



By
Pooja S. Suratia



**ELECTRICAL ENGINEERING DEPARTMENT,
FACULTY OF TECHNOLOGY AND ENGINEERING,
THE MAHARAJA SAYAJIRAO UNIVERSITY OF BARODA,
VADODARA – 390 001
GUJARAT, INDIA.
MARCH-2014**

**Dedicated
to
My Family and Teachers**

Certificate

This is to certify that the thesis entitled, “**Design and Implementation of Embedded Architecture Using Soft-Computing Techniques for Parametric Optimization of MIMO Wireless System**” submitted by **Pooja S. Suratia** in fulfillment of the degree of **DOCTOR OF PHILOSOPHY** in Electrical Engineering Department, Faculty of Technology and Engineering, The Maharaja Sayajirao University of Baroda, Vadodara is a bonafide record of investigations carried out by her under my guidance and supervision. In my opinion the standards fulfilling the requirements of the Ph.D. Degree as prescribed in the regulations of the University has been attained.

Prof. Satish K. Shah

Guide,

Electrical Engineering Department,
Faculty of Technology and Engineering,
The Maharaja Sayajirao University of Baroda,
Vadodara.

Dr. Satish K. Joshi

Head,

Electrical Engineering Department,
Faculty of Technology and Engineering,
The Maharaja Sayajirao University of Baroda,
Vadodara.

Dean,

Faculty of Technology and Engineering,
The Maharaja Sayajirao University of Baroda,
Vadodara.

Declaration

I, Pooja S. Suratia hereby declare that the work reported in this thesis entitled, “**Design and Implementation of Embedded Architecture Using Soft-Computing Techniques for Parametric Optimization of MIMO Wireless System**” submitted for the degree of **DOCTOR OF PHILOSOPHY** in Electrical Engineering Department, Faculty of Technology and Engineering, The Maharaja Sayajirao University of Baroda, Vadodara, is original and has been carried out in the Electrical Engineering Department, Faculty of Technology and Engineering, The Maharaja Sayajirao University of Baroda, Vadodara. I further declare that this thesis is not substantially the same as one, which has already been submitted in part or in full for the award of any degree or academic qualification of this University or any other Institution or examining body in India or abroad.

March 2014

Pooja S. Suratia

Acknowledgment

I express my thanks to Almighty for providing me inspiration, strength and patience to accomplish my work with support of all concerned, a few of them I am trying to acknowledge.

I would like to express my deepest appreciation to my research guide, Prof. Satish K. Shah, for his admirable way of supervising the work, invaluable guidance, assistance and support throughout this research. His positive efforts in pointing the need of the research, suggestions and encouragement has resulted in research work. My sincere thanks to, Dr. Satish K. Joshi, Head, Electrical Engineering Department, for providing valuable guidance.

An extended acknowledgment to Mr.Jagdish Sanghani for his support and technical guidance to develop Wireless Control of Robot. My sincere thanks to the entire team of Edutech Systems, Vadodara for providing their effective guidance and assistance during my experimental work. My sincere thanks to E-corner Consultants Pvt. Ltd, Vadodara for providing laboratory facilities for the research work. I also thank Mr. Nirmalkumar Reshamwala, student of Master of Engineering, Electrical Engineering Department for his kind support and technical help.

The project is sponsored by the Department of Science and Technology (DST), Government of India under Women Scientists Scheme (A) (SR/WOS-A/ET-05/2011).

I also thank all those people who have helped me directly or indirectly but have gone unnoticed. My special thanks to my family for their endless encouragement and inspiration throughout the educational years of my life. Last but not least, thanks to all my fellow friends and colleagues for their continuous encouragement.

Pooja S. Suratia

Abstract

Wireless communication has emerged as one of the largest and fastest growing sectors of the telecommunication industry. One of the major advances in this field has been the shift from Single-Input Single-Output (SISO) paradigm to Multi-Input Multi-Output (MIMO) scheme. LTE-Advanced acquired the official designation of International Mobile Telecommunications-Advanced (IMT-Advanced), to achieve the requirements for 4G standards.

Research work concentrates on the capacity analysis of MIMO systems and Throughput optimization techniques for LTE-A Downlink Physical Layer. To demonstrate the theoretical advances in MIMO Communication, Rapid Prototyping and field trials are essential. Basic Hardware Architecture for MIMO Communication system and System Design methodology for development of MIMO Wireless Platform is presented in this work.

The MIMO Channel Estimation in LTE-A Downlink Physical Layer is carried out using Artificial Neural Network (ANN) architectures as they consist of learning ability to solve real-world problems. ANN architectures designed for MIMO Channel Estimation are analyzed by means of simulation using MATLAB based Vienna LTE-A Link Level Simulator. To further enhance the LTE-A Link Level Throughput the ANN weights are optimized using Genetic Algorithm(GA).

Fuzzy Logic (FL) Decision model is developed for switching between MIMO modes to maximize the throughput of LTE-A Downlink Physical Layer. Based on the Channel Condition Number and Receive SNR at the receiver, decision can be made to select the appropriate MIMO mode to enhance the throughput of the system. The FL decision model is capable of selecting the MIMO mode based on the channel conditions to maximize the throughput of the system. Simulations are carried out for performance analysis of proposed FL Decision model using LTE-A Link Level Simulator.

Proposed techniques are implemented on Xilinx Atlys Spartan 6 Development kit and TMS320C6713 DSK in close-loop simulation with LTE-A Link Level Simulator in order to perform the real time implementation. Comparative analysis between MATLAB Simulation, FPGA and DSP implementation results is carried out based on the throughput for LTE-A Downlink Physical Layer.

Contents

Certificate	iv
Declaration	v
Acknowledgments	vi
Abstract	vii
List of Tables	ix
List of Figures	x
List of Acronyms	x
1 Introduction	1
1.1 Evolution of Wireless Access Technologies	3
1.2 Significance of research	3
1.3 Thesis Organization	5
2 Background and Related work: MIMO Wireless Communication	7
2.1 Introduction	7
2.1.1 MIMO Wireless System model	7
2.2 MIMO Channel Capacity Analysis	8
2.2.1 Shannon capacity of wireless channels	9
2.2.2 Ergodic Capacity	13
2.2.3 Outage Capacity	16
2.3 MIMO Performance Gains	18
2.3.1 Spatial Multiplexing Gain	18
2.3.2 Spatial Diversity Gain	18
2.3.3 Array Gain	19
2.3.4 Interference Canceling Gain	20
2.4 Tradeoffs in MIMO Wireless System	20
2.4.1 Diversity-Multiplexing Tradeoff	21
2.5 MIMO Transmission Techniques	23
2.6 GUI for Capacity and Performance Analysis	24
2.7 Concluding Remarks	26
3 Conceptual Design of MIMO Wireless Systems	27
3.1 Introduction	27
3.2 System Design Methodology	27
3.2.1 Hardware Concept of MIMO Wireless System	28
3.2.2 MIMO Wireless Testbeds and Prototypes	31
3.3 Model-Based Design for Rapid Prototyping	31
3.3.1 Mathworks Model-based Design	32
3.3.2 MATLAB Design Tools for FPGA	33
3.3.3 MATLAB Design Tools for DSP	35

3.4	Case Study: Wireless control of FTE Robot	36
3.4.1	Overview of FTE Robot	37
3.4.2	Wireless Module	39
3.4.3	Implementation	40
3.5	Concluding Remarks	42
4	Long Term Evolution-Advanced: Downlink Physical Layer	43
4.1	Introduction	43
4.2	E-UTRAN Architecture and Protocol Stack	45
4.3	LTE Downlink Physical Layer	48
4.3.1	LTE Frame and Subframe Structure	48
4.3.2	Downlink Slot Structure	49
4.3.3	Downlink Physical Channel Processing	51
4.4	MIMO Downlink Transmission modes	53
4.4.1	Transmit Diversity	53
4.4.2	Spatial Multiplexing	53
4.5	LTE-A Downlink Link Level Simulator	55
4.5.1	LTE Transmitter	56
4.5.2	Channel Model	57
4.5.3	LTE Receiver	57
4.5.4	Simulation Results	58
4.6	Results Summary	63
4.7	Concluding Remarks	66
5	Soft-Computing Techniques and Development Tools	67
5.1	Overview of Soft-Computing Techniques	67
5.2	Fuzzy Logic System	69
5.2.1	MATLAB Simulation-Fuzzy Logic Toolbox	71
5.3	Artificial Neural Networks	73
5.3.1	McCulloch and Pitts Model of Neuron	73
5.3.2	ANN Network Architectures	75
5.3.3	Designing Neural Network	76
5.3.4	MATLAB Simulation: Neural Network Toolbox	77
5.4	Genetic Algorithms	80
5.4.1	Introduction	80
5.4.2	MATLAB Simulation: Global Optimization Toolbox	81
5.5	Applications of Soft Computing Techniques in Wireless Communication	83
5.6	Concluding Remarks	84
6	Artificial Neural Network Based MIMO Channel Estimation	85
6.1	Introduction	85
6.2	LTE-A MIMO channel estimation	85
6.3	ANN based MIMO Channel Estimation	87
6.3.1	ANN Simulation Parameters and results	90
6.4	ANN trained by Genetic Algorithm for MIMO Channel Estimation	93
6.4.1	ANN-GA Simulation Parameters and Result	95
6.5	Concluding Remarks	96

7	Fuzzy Logic Decision model for MIMO mode switching	97
7.1	Introduction	97
7.2	MIMO Channel Condition Number	97
7.2.1	Statistics of Demmel Condition Number	98
7.3	Investigation of Switching Point between TxD and OLSM for 2x2 MIMO	104
7.4	FL Decision model for MIMO mode switching	105
7.4.1	Fuzzification	106
7.4.2	Fuzzy Rule Base	107
7.4.3	Defuzzification	108
7.4.4	FL Decision Algorithm	108
7.5	Simulation Parameters and Results	109
7.6	Conclusion	115
8	Hardware Implementation of Throughput Optimization Algorithms	116
8.1	Embedded Architecture Implementation	116
8.1.1	XUP Atlys Spartan-6 Development Kit	117
8.1.2	TMS320C6713 DSP Starter Kit	118
8.1.3	Implementation of FL Decision model for MIMO mode switching	119
8.1.3.1	Implementation on Atlys Spartan 6 Development kit	120
8.1.3.2	Implementation on TMS320C6713 DSP Starter Kit	121
8.1.3.3	Implementation Results	123
8.1.4	Implementation of ANN based MIMO Channel Estimation	127
8.1.4.1	Implementation on TMS320C6713 DSP Starter Kit	128
8.1.4.2	Implementation Results	128
8.2	Concluding Remarks	132
9	Conclusion and Further developments	133
9.1	Research Contributions	133
9.1.1	Channel Capacity Analysis and Conceptual Design of MIMO Wireless System	133
9.1.2	Performance Analysis of LTE-A Downlink Physical Layer	134
9.1.3	Throughput Optimization of LTE-A Downlink Physical Layer	135
9.1.3.1	ANN based Channel Estimation Technique	135
9.1.3.2	FL Decision model for MIMO mode switching	135
9.1.3.3	GUI developed for performance analysis of MIMO Wireless System	136
9.2	Further Developments	137
10	Bibliography	138
	Appendix A: User manual for GUI of Embedded Architecture Using Soft-Computing Techniques for Parametric Optimization of MIMO Wireless System	162
	Appendix B: Development Tools and Software programs	168
	Appendix C: Photo Gallery	171
	Appendix D: Research Publications	174
	Appendix E: Training Programs attended based on Research Work	176

List of Tables

1.1	Generations of Wireless Technology	3
2.1	MIMO Performance Gains and its effects	18
3.1	MATHWORKS Products for Rapid Prototyping on DSP and FPGA	32
3.2	FTE Robot Specifications	38
3.3	Technical Specifications of wireless module	39
3.4	List of Commands to control FTE Robot	42
4.1	3GPP release of radio access technologies	44
4.2	3GPP LTE Physical Layer Specifications and Reports	48
4.3	LTE Downlink Resource Grid Parameters	49
4.4	LTE Transmission Modes	53
4.5	LTE-A Downlink Link Level Simulator General Files	55
4.6	LTE Transmitter Steps and related MATLAB Function Files	56
4.7	Channel Models	57
4.8	LTE Channel Model Generation MATLAB Function Files	57
4.9	LTE Receiver Steps and related Matlab Function Files	58
4.10	Simulation Parameters	63
4.11	Comparison of TxD and OLSM for SNR=5dB	63
5.1	List of FIS Editor Blocks and description	71
5.2	List of MATLAB Functions for Designing FIS	72
5.3	List of MATLAB Functions for Genetic Algorithm	83
6.1	MATLAB Function to design ANN Networks	91
6.2	Simulation parameters for ANN	91
6.3	Simulation Parameters for ANN-BPA and ANN-GA for MIMO Channel Estimation	95
7.1	Channel Condition Number and its indications	98
7.2	Switching point between TxD and OLSM for 2x2 MIMO	104
7.3	Characteristics of FL Decision model	106
7.4	Variables for FL Decision model	106
7.5	FL Decision model Rule base	108
7.6	Initial Selection of Simulation Parameters	109
8.1	Summary of throughput results for various case scenarios for FL Decision model	127
8.2	Summary of throughput results for case scenarios for ANN Channel estimation	132
B. 1	Software Development Tools with Description	168
B. 2	Hardware Development Tools with Description	168
B. 3	FIS Files	169
B. 4	MATLAB files with Description	169
B. 5	MATLAB Simulink model files	169
B. 6	GUI Figure files	170

List of Figures

2.1	MIMO wireless communication model	8
2.2	SIMO System-Channel Capacity	11
2.3	MISO System-Channel Capacity	11
2.4	MIMO System-Channel Capacity	12
2.5	Capacity vs Number of receive antenna for SIMO system	14
2.6	Capacity vs Number of transmit antenna for MISO system	14
2.7	Capacity vs Number of receive antenna for MIMO system	15
2.8	10 percent Outage capacity of MIMO System	17
2.9	90 percent Outage capacity of MIMO System	17
2.10	BER for different diversity order	19
2.11	Diversity Multiplexing trade-off of MIMO System	22
2.12	Diversity Multiplexing tradeoff of MISO and MIMO system	22
2.13	MIMO Transmission techniques and their performance gains	23
2.14	GUI for MIMO Wireless Simulator	25
2.15	Comparison of ZF, ML and MMSE reciver for V-BLAST Technique	25
2.16	Comparison of BER for Diversity Techniques: Alamouti, STBC and STTC	26
3.1	System Design Methodology	29
3.2	Basic Hardware Architecture of MIMO	30
3.3	Model Based Design Methodology	33
3.4	Programming and Verification steps for FPGA	34
3.5	Programming and Verification steps for DSP	36
3.6	Front View of FTE Wireless Robot	37
3.7	Back View of FTE Wireless Robot	37
3.8	Snapshot of SiLabs IDE	38
3.9	FTE Robot with Wireless module connection	40
3.10	Connections between FTE Robot and Wireless Module	40
3.11	Snapshot of Pololu Wixel Configuration Utility	41
3.12	Implementation of Wireless Control of FTE Embedded Robot	41
4.1	Performance of LTE MIMO with different antenna schemes	44
4.2	E-UTRAN Architecture	45
4.3	E-UTRA radio interface protocol architecture	46
4.4	Frame Structure Type 1 (FDD)	49
4.5	LTE Resource Grid	50
4.6	LTE Physical Channel Processing with Uplink Feedback	51
4.7	Downlink Physical Layer Processing	52
4.8	2x2 Transmit Diversity Transmission Mode	54
4.9	Open Loop Spatial Multiplexing	54
4.10	Close Loop Spatial Multiplexing	54
4.11	Structure of Link Level Simulator	55
4.12	Throughput v/s SNR for MIMO antenna configuration in LTE-A	59
4.13	Throughput and BLER for Transmit Diversity	60
4.14	Throughput and BLER for Spatial Multiplexing	61

4.15	Throughput and BLER for Transmit Diversity and Spatial Multiplexing	62
4.16	Comparison of MIMO Transmission modes in LTE-A	64
4.17	Throughput for Transmission modes with Flat rayleigh	65
4.18	Comparison of Throughput for SNR=30dB	65
5.1	Various Problem Solving Techniques	68
5.2	Fuzzy Logic System	69
5.3	Fuzzy Inference System Editors and Viewers	71
5.4	FLC in Simulink	72
5.5	McCulloch-Pitts model neuron	73
5.6	Artificial Neuron	74
5.7	(a) Feed-forward (FNN) and (b) Recurrent Neural Network (RNN) Architectures	75
5.8	Neural Network Toolbox	77
5.9	Neural Network Simulink model	78
5.10	Neural Network Toolbox Simulink Blocks	79
5.11	Genetic Algorithm Basic Structure	81
5.12	Optimization App in Global Optimization Toolbox	82
6.1	Reference Signals for LTE-A antenna ports	86
6.2	ANN based Channel estimation	88
6.3	Feedforward Neural Network	89
6.4	Radial Basis Network	89
6.5	Layer Recurrent Neural Network	90
6.6	Generalized Regression Neural Network	90
6.7	Throughput v/s SNR for TxD 2x2 for various ANN Channel estimation	92
6.8	Throughput v/s SNR for CLSM 2x2 for various ANN Channel estimation	92
6.9	Comparison of Elapsed Time for different MIMO Channel Estimation Techniques	93
6.10	ANN-GA based Channel Estimation	94
6.11	Throughput v/s SNR for ANN-BPA and ANN-GA MIMO Channel Estimation	96
7.1	Channel capacity with varying SNR	100
7.2	Channel capacity with varying Condition Number	100
7.3	CDF of SCN for Uncorrelated Rayleigh Channel	101
7.4	PDF of SCN for Uncorrelated Rayleigh Channel	101
7.5	CDF of SCN for semicorrelated Rayleigh Channel	102
7.6	PDF of SCN for semicorrelated Rayleigh Channel	102
7.7	Switching point between 2x2 TxD and OLSM for different transmit correlation	104
7.8	Block Diagram for FL Decision based MIMO mode Switching	105
7.9	Membership function for Channel Condition Number	107
7.10	Membership function for Receive-SNR	107
7.11	User Interface for FL Decision model for MIMO mode switching	110
7.12	Comparative Analysis of FL Decision Model for Initial mode of TxD 4x2	111
7.13	Comparative Analysis of FL Decision Model for Initial mode of OLSM 2x2	112
7.14	Comparative Analysis of FL Decision Model for Initial mode of OLSM 4x2	113
7.15	Comparative Analysis of FL Decision Model for Initial mode of TxD 4x2.	114
8.1	Design Flow for Real-time Implementation on Target Hardware	116
8.2	XUP Atlys Spartan-6 Development Kit	117
8.3	Functional Block Diagram of Atlys board	118

8.4	TMS320C6713 DSP Starter Kit	119
8.5	Functional Block Diagram of DSK 6713	119
8.6	Simulink Models for FL Decision model for HDL Co-simulation and FIL Simulation	120
8.7	ModelSim Simulator Results	121
8.8	Simulink Model for FL Decision model for SIL and PIL Simulation	122
8.9	Code Composer Studio IDE Window	123
8.10	Throughput Analysis of Case 1 Scenario	124
8.11	Throughput Analysis of Case 2 Scenario	124
8.12	Throughput Analysis of Case 3 Scenario	125
8.13	Throughput Analysis of Case 4 Scenario	125
8.14	Throughput Analysis of Case 5 Scenario	126
8.15	Throughput Analysis of Case 6 Scenario	126
8.16	ANN based MIMO Channel Estimation Simulink Model	127
8.17	Throughput Analysis of GRNN Case 1	129
8.18	Throughput Analysis of GRNN Case 2	129
8.19	Throughput Analysis of GRNN Case 3	130
8.20	Throughput Analysis of GRNN Case 4	130
8.21	Throughput Analysis of GRNN Case 5	131
8.22	Throughput Analysis of GRNN Case 6	131
9.1	Throughput for different antenna configuration in LTE-A Downlink Physical Layer	134
9.2	Comparison of Throughput for GRNN channel estimation and implementation . . .	135
9.3	Comparison of throughput for FL Decision model and hardware implemntation . .	136
9.4	GUI for analysis of MIMO Communication System	137
A. 1	GUI for Design and Implementation of Embedded Architecture Using Soft-Computing Techniques for Parametric Optimization of MIMO Wireless System	162
A. 2	GUI for MIMO Wireless Simulator	163
A. 3	Features of MIMO Wireless Simulator	164
A. 4	MIMO WS GUIs for performance analysis	164
A. 5	STTC performance analysis GUI	165
A. 6	GUI for FL decision model for MIMO mode switching	165
A. 7	Programming XUP Atlys board through MATLAB FIL model	166
A. 8	Programming C6713DSP through MATLAB PIL model	166
A. 9	GUI for Throughput Analysis for ANN based MIMO channel estimation	167
B. 1	FTE Robot with Wireless module: 1)FTE Robot, 2)Connecting wires between Robot and Wireless Module and 3)Wireless Module.	171
B. 2	Wireless Control of FTE Robot setup: 1)Remote Computer, 2) FTE Robot with wireless module, 3) Transmitter Wireless Module, 4) JTAG Adapter Connector . .	171
B. 3	DSP Starter Kit: 1)TMS320C6713 DSP, 2)JTAG Emulation, 3)Power Jack, 4)USB Port, 5)Memory Expansion and 6)AIC23 Codec with peripherals	172
B. 4	DSP Setup: 1)CPU Core2Duo with Software tools installed, 2)TMS320C6713 DSK, 3)Power Cable and 4)USB Cable	172
B. 5	XUP Atlys Board: 1)Spartan-6 LX 45, 2)Adept USB Port, 3)Power Jack, 4)Ethernet connector, 5)VHDC connector and 6)LEDs, Slide Switches and Push buttons . . .	173
B. 6	FPGA Setup: 1)CPU Core2Duo with Software tools installed, 2)USB cable, 3)Power cable, 4)Atlys board, 5)Gigabit Ethernet crossover cable	173

List of Acronyms

- 1G** First Generation
- 2G** Second Generation
- 3G** Third Generation
- 3GPP** 3rd Generation Partnership Project
- 4G** Fourth Generation
- ADC** Analog-to-Digital Converter
- AM** Acknowledged Mode
- AMC** Adaptive Modulation and Coding
- ANN** Artificial Neural Network
- ARQ** Automatic Repeat Request
- ART** Adaptive Resonance Theory
- ASIC** Application Specific Integrated Circuits
- AWGN** Additive White Gaussian Noise
- BB** Baseband Processing Unit
- BER** Bit Error Rate
- BLER** Block Error Rate
- BPA** Back-Propagation Algorithm
- CAE** Computer Aided Engineering
- CCS** Code Composer Studio
- CDF** Cumulative Distribution Function
- CDMA** Code Division Multiple Access
- CLSM** Close-Loop Spatial Multiplexing
- CP** Cyclic Prefix
- CPLD** Complex Programmable Logic Device
- CQI** Channel Quality Indicator
- CRS** Cell-specific Reference Signal
- CSI** Channel State Information
- DAC** Digital-to-Analog Converter

DCI Downlink Control Information

DDR Double Data Rate

DMA Diversity, Multiplexing and Array gain

DM-RS Demodulation Reference Signals

DMT Diversity and Multiplexing tradeoff

DSK DSP Starter kit

DSP Digital Signal Processor

EC Evolutionary Computation

EDA Electronic Design Automation

EDGE Enhanced Data for Global Evolution

EE Energy Efficiency

EMIF External Memory Interface

eNB Evolved Base Stations-eNodeB

EPC Evolved Packet Core

E-UTRA Evolved- Universal Terrestrial Radio Access

E-UTRAN Evolved-UMTS Terrestrial Radio Access Network

FDD Frequency Division Duplexing

FIS Fuzzy Inference System

FIL FPGA-in-the-loop

FL Fuzzy Logic

FLC Fuzzy Logic Controller

FNN Feed-forward Neural Network

FPGA Field Programmable Gate Arrays

FTE Faculty of Technology and Engineering

GA Genetic Algorithms

GPP General Purpose Processors

GPRS General Packet Radio Service

GRNN General Regression Neural Network

GSM Global System for Mobile Communications

GUI Graphical User Interface

HARQ Hybrid Automatic Repeat Request

HDL Hardware Description Language

HDMI High-Definition Multimedia Interface

HSDPA High Speed Downlink Packet Access

HSPA High Speed Packet Access

HSUPA High Speed Uplink Packet Access

i.i.d Independent Identically Distributed

I2C Inter-Integrated Circuit

IDE Integrated Development Environment

IMT- Advanced International Mobile Telecommunications-Advanced

IMT-2000 International Mobile Telecommunications-2000

IR Infrared

ISE Integrated Software Environment

ITU International Telecommunications Union

JTAG Joint Test Action Group

LCD Liquid Crystal Display

LED Light Emitting Diode

LOS Line-Of-Sight

LRN Layered Recurrent Network

LS Least Square

LTE Long Term Evolution

LTE-A Long Term Evolution-Advanced

MAC Medium Access Control

MATLAB Matrix Laboratory

MBMS Multimedia Broadcast Multicast Services

MCS Modulation and Coding Scheme

MF Membership Function

MIMO Multiple-Input Multiple-Output

MISO Multi-Input Single-Output

MIMO-WS Multi-Input Multi-Output Wireless Simulator

ML Maximum Likelihood

MME Mobility Management Entity

MMS Multimedia Messaging Service

MMSE Minimum Mean Square Error

NAS Non-Access Stratum

OFDMA Orthogonal Frequency Division Multiplexing Access

OLSM Open-Loop Spatial Multiplexing

OSTBC Orthogonal Space-Time Block Code

PAR Place-and-route

PDP Power Delay Profile

PDSCH Physical Downlink Shared Channel

PIL Processor-in-the-Loop

PMI Precoder Matrix Indicator

PDCCP Packet Data Convergence Protocol

PDF Probability Density Function

PDN Packet Data Network

P-GW Packet Data Network Gateway

PHY Physical Layer

PR Probabilistic Reasoning

PSTN Public Switched Telephone Network

QAM Quadrature Amplitude Modulation

QPSK Quadrature Phase Shift Keying

QoS Quality of Service

RACH Random Access Channel

RAM Random-Access Memory

RB Resource Blocks

RI Rank Indicator

RBF Radial Basis Function
RBNN Radial Basis Neural Network
RF Radio frequency
RLC Radio Link Control
RNN Recurrent Neural Network
ROHC Robust Header Compression
RP Rapid Prototyping
RRC Radio Resource Control
RS Reference Signal
RTW Real-Time Workshop
SC-FDMA Single-Carrier Frequency Division Multiple Access
SDRAM Synchronous Dynamic Random-Access Memory
SE Spectral Efficiency
S-GW Serving Gateway
SM Spatial Multiplexing
SOM Self-organizing Map
STC Space Time Coding
STTC Space-Time Trellis Code
SDU Service Data Unit
SIL Software-in-the-Loop
SIMO Single-Input Multi-Output
SISO Single-Input Single-Output
SMS Short Message Service
SNR Signal-to-Noise Ratio
TDD Time Division Duplexing
TI Texas Instruments
TM Transparent Mode
UE User Equipment
TRT Throughput-Reliability Tradeoff

UART Universal Asynchronous Receiver/Transmitter

UCI Uplink Control Information

UM Unacknowledged Mode

UMTS Universal Mobile Telecommunications System

UP User Plane

USB Universal Serial Bus

USRP Universal Software Radio Peripheral

UE User Equipment

V-BLAST Vertical Bell-Labs Layered Space-Time Architecture

VHDC Very-High-Density Cable

W-CDMA Wideband Code Division Multiple Access

WiFi Wireless Fidelity

WiMax Worldwide Interoperability for Microwave Access

Wimax2 Wireless MAN-advanced

WLAN Wireless Local Area Network

XUP Xilinx University Program

ZF Zero-Forcing

Introduction

Wireless communication has emerged as one of the largest sectors of the telecommunication industry, evolving from a niche business in the last decade to one of the most promising areas for growth in the 21st century [1]. To appreciate the growth of the wireless sector, it is worth noting that in 1990 there were only 10 million mobile subscribers worldwide. Today there are approximately 6 billion mobile subscribers worldwide [2]. Emerging demands for ubiquitous networks, high data rate multimedia based services and high spectral efficiency are the key drives for the continued technology evolution in wireless communications. Wireless communication is inherently limited by the available spectrum and impaired by signal fading, increasing interference and multi-path propagation. Hence, to achieve capacity needs for future wireless systems without increasing the required spectrum, accomplishment of implementation of advanced communication techniques is necessary. To satisfy the demand for next generation wireless communication networks, MIMO technology is mandatory.

MIMO wireless communication system constitutes a key technology for next generation wireless communication. It employs multiple antennas at both transmitter and receiver end of communication link. MIMO has emerged as one of the most promising approaches for high bit rates, small error rates and increased channel capacity without consuming extra bandwidth or transmit power [3]. MIMO concepts have been under development for many years for both wireless and wire-line systems. One of the earliest MIMO-to-wireless communication application came in 1984 with groundbreaking developments by Jack Winters of Bell Laboratories [4]. MIMO is now being integrated into many wireless standards like 3G and 4G wireless communication systems [5], IEEE 802.11n Wireless Local Area Network (WLAN) standard [6], IEEE 802.20 mobile broadband wireless access system [7] and the 3rd Generation Partnership Project(3GPP) LTE (Long Term Evolution) of Wide-band Code Division Multiple Access (W-CDMA) [8].

The 3GPP's LTE represents a major advance in cellular technology. LTE also called as Evolved-Universal Terrestrial Radio Access (E-UTRA) represents a radical new step towards 4G mobile to cope up with the increasing throughput requirements of the future wireless cellular systems [9]. MIMO schemes are now moving into mainstream communication systems. This has led to MIMO being standardized in 3GPP Rel-6 and Rel-7 of the UTRAN specifications [10]. Support for multi-antenna transmission was an integral part of LTE from the first release. MIMO technologies have been widely used to improve downlink peak rate, cell coverage, as well as average cell throughput. To achieve this diverse set of objectives, LTE adopted various MIMO transmission schemes such as

Transmit Diversity, Spatial Multiplexing (including Open-Loop Spatial multiplexing (OLSM) and Close-loop spatial multiplexing (CLSM)) and Beamforming [11].

LTE-A physical layer is highly efficient for conveying both data and control information between an Enhanced Base Station (eNB) and Mobile User Equipment (UE). The LTE Physical layer employs advanced technologies of wireless cellular systems. These includes multiplexing schemes: Orthogonal Frequency Division Multiplexing Access (OFDMA) and Single-Carrier Frequency Division Multiple Access (SC-FDMA), MIMO antenna schemes: 2x2, 4x4 upto 8x8, Adaptive modulation and coding (AMC) schemes, duplexing schemes: Time Division Duplexing (TDD) and Frequency Division Duplexing (FDD), and bandwidth flexibility [12]. Research and development of signal processing algorithms for Long Term Evolution (LTE) requires a realistic, flexible, and standard-compliant simulation environment [13]. In the development and standardization of LTE, as well as in the implementation process of equipment manufacturers, simulations are necessary to test and optimize algorithms and procedures [14]. MATLAB based Vienna LTE-A Link Level Simulator [15], has been used in the research work for investigation and analysis of channel estimation, MIMO Gains, MIMO Transmission Techniques and feedback for LTE-A Downlink Physical Link Layer.

Recently, various MIMO wireless testbed based on DSP and FPGA have been developed to verify the theoretical performance gains and to investigate practical issues in MIMO implementation [16, 17]. These systems are realized by computationally complex algorithms, requiring new digital hardware architectures to be developed. Embedded Processors are suitable for computation of extensive applications. Software simulations provide more flexibility, but the true performance of the system can only be known by developing a hardware wireless platform and performing measurements and tests in the target environment [18, 19].

Soft Computing with its roots in Fuzzy Logic (FL), Artificial Neural Network (ANN), and Evolutionary Computation has become one of the most important research and application fields for wireless communication in the last decade. Wireless communication systems are associated with much uncertainty and imprecision due to a number of stochastic processes such as time-varying characteristics of the wireless channel caused by the mobility of transmitters, receivers, objects in the environment and mobility of users. This reality has fueled numerous applications of Soft-Computing techniques in mobile and wireless communications [20].

1.1 Evolution of Wireless Access Technologies

Evolution of wireless access technologies is about to reach its Fourth Generation (4G). Looking at past, wireless access technologies have followed different evolutionary paths aimed at unified target: performance and efficiency in high mobile environment. The First Generation (1G) has fulfilled the basic mobile voice, while the Second Generation (2G) has introduced capacity and coverage. This is followed by the Third Generation (3G), which had quest for data at higher speeds, which is further realized by the 4G [21].

Over the years mobile technology have made breakthrough in the world of telecommunication and has become an indispensable equipment for everyone. On examining the revolutionary transformations from 1G to 4G, the technology has evolved with advanced features and usage patterns. The brief history of Generation of Wireless Technology from First Generation to Fourth Generation, with their respective Data Bandwidths, Services and Features are listed in Table 1.1.

Generation	1G	2G	2.5G	3G	3.5G	4G
Start	1970-1980	1991-2000	2001-2004	2004-2005	2006-2010	2011-Now
Data Bandwidth	2 Kbps	64 Kbps	144 Kbps	2 Mbps	> 2Mbps	1 Gbps
Technology	Analog Cellular	Digital Cellular CDMA	GPRS, EDGE,	CDMA 2000, UMTS, Wi-Fi	WiMax-LTE	Wi-Fi LTE
Service	Voice	Digital Voice, SMS, Packet Size Data	SMS, MMS	Integrated High Quality Audio, Video & Data	High speed Internet application	Dynamic, Information access, Wearable Devices
Switching	Circuit	Circuit, Packet	Packet	Packet	All Packet	All Packet
Core Network	PSTN	PSTN	PSTN	Packet N/W	Internet	Internet

Table 1.1: Generations of Wireless Technology

1.2 Significance of research

Emerging trends for high data rate and high spectral efficiency are key drivers for the evolving technology in wireless communication. The major technical challenges to achieve high data rate and system performance, can be overcome by incorporating the advanced technical techniques in physical layer to enable truly ubiquitous network capabilities. The research work focuses on maximizing the Throughput of LTE-A Downlink Physical Layer.

The receiver in MIMO system, requires the knowledge of Channel State Information (CSI) in order to recover the transmitted signal properly. Channel estimation in MIMO systems is an active

research area and challenging task. Several channel estimation methods have already been studied by different researchers for MIMO systems [22,23]. In wireless communications, the channel variability due to multi-path fading hardens the problem of channel estimation and optimization. Channel estimation by ANN has been deployed in MIMO-OFDM system, with different Neural Network architectures [24,25]. The research work proposes ANN based MIMO Channel Estimation Technique for LTE-A Downlink Physical Layer. Comparative analysis with traditional method, Least Square (LS) has been carried out as a part of research work. ANN based MIMO Channel Estimator is further tuned using Genetic Algorithm for optimization of Neural Network Weights to give better performance.

There exist trade-off between Spatial Multiplexing and Diversity Techniques [26]. Both the gains are not possible to achieve simultaneously. Hence switching algorithms are applied to MIMO system to get advantage of both the systems [27]. The condition number is a well known indicator of the spatial selectivity of a MIMO wireless channel [28]. In MIMO context, the condition number indicates the multipath richness of the channel. Many adaptive MIMO systems [29] that have been proposed employ the condition number as a criterion for choosing appropriate MIMO Scheme. This has motivated the author to design Fuzzy Logic Decision model for MIMO mode switching based on Channel Condition Number and Receive Signal-to-noise-ratio (SNR) for Throughput optimization of LTE-A Downlink Physical Layer.

During the last years, MIMO technology has attained great attractions in the area of wireless communications. The hardware implementation of MIMO algorithms becomes a challenging task as the complexity of the MIMO system increases. The developed Throughput Optimization algorithms for LTE-A Downlink Physical Layer are implemented and real-time close-loop verification has been carried out for performance analysis. The ANN based Channel Estimation Algorithm and the FL Decision model is implemented on FPGA using FPGA-in-the-Loop (FIL) Simulation and with DSP using Processor-in-the-Loop (PIL) Mode in close loop with LTE-A Link Level Simulator.

The features and discussions of research carried out in the thesis includes:

- Performance Analysis of MIMO Techniques and MIMO Channel capacity Analysis.
- Development of Conceptual Design and basic hardware architecture for MIMO Wireless System
- Design of GUI based MIMO-WS (Multi-Input Multi-Output Wireless Simulator) for Capacity and Performance Analysis of various MIMO Techniques.
- Comparative Performance Analysis of various MIMO Transmission modes in LTE-A Down-

link Physical Layer

- Design and simulation of ANN Based MIMO Channel Estimation for LTE-Advanced Downlink Physical Layer .
- Design and development of GA algorithm for Tuning ANN Network Parameters used in MIMO Channel estimation .
- Design and development of FL Decision model for MIMO mode switching for Throughput Optimization of LTE-A Downlink Physical Layer.
- Implementation of proposed algorithms on FPGA and DSP. Comparative performance analysis of software simulation and hardware implementation results.

1.3 Thesis Organization

The thesis is organized as follows:

Chapter: 1 This chapter provides an overview and the context for the remainder of the thesis. It also introduces the Evolution of Wireless Access Technologies. It presents the significance of research work to be carried out in the thesis.

Chapter: 2 Chapter gives theoretical background of MIMO wireless communication systems. It describes various MIMO performance gains and trade offs. MIMO capacity analysis for various antenna configuration is discussed. Various MIMO transmission schemes is discussed. MIMO Wireless Simulator (MIMO-WS) GUI developed for MIMO Capacity and transmission techniques analysis is briefly described.

Chapter: 3 This chapter discusses the conceptual design of MIMO wireless system. It describes the Design methodology for MIMO system and relevant decisions. It gives an overview of software development tools for analysis of DSP and FPGA implementation. Mathworks model based design for DSP and FPGA verification is discussed. A case study for wireless communication has been developed to study the wireless control of Mobile Robots. The Wireless module and the procedural steps has been briefly described.

Chapter: 4 The chapter discusses the Downlink Physical Layer of LTE-A systems in detail. It gives an overview of MIMO Transmission modes in LTE-A. Performance evaluation of MIMO Transmission modes is evaluated using MATLAB based Vienna LTE-A Link Level Simulator. Throughput and Block Error Rate (BLER) analysis for MIMO modes is carried out and discussed.

Chapter: 5 Chapter gives an concise overview and theoretical background of soft-computing techniques such as Fuzzy Inference System (FIS), ANN and GA. Applications of soft-computing techniques in various fields of wireless communication has been reviewed. Toolboxes available for deploying soft computing techniques in MATLAB and used in research work for the design and testing of proposed techniques are described in detail.

Chapter: 6

Channel estimation technique for LTE-A Downlink Physical Layer based on ANN and ANN trained by GA has been discussed in chapter. Comparative performance analysis of the proposed techniques with traditional Least Square (LS) method has been carried out. Also, channel estimators were designed using various Neural network Architecture: Back-propagation Neural Network (BPN), Layered Recurrent Neural Network (LRN), General Regression Neural Network (GRNN) and Radial Basis Function Neural Network (RBFN). Simulation parameters and result analysis for various ANN based MIMO channel estimators are discussed.

Chapter: 7

In this chapter, a Fuzzy Logic Decision model for MIMO mode switching that maximizes the throughput of LTE-A Downlink Physical Layer is briefly described. In particular two MIMO modes are considered: Transmit Diversity and Open Loop Spatial Multiplexing in LTE-A context. The decision for selection of MIMO mode is based on the Channel Condition Number and Receive SNR. The designed FL Decision model is verified using Vienna LTE-A Link Level Simulator. The simulation parameters and results are presented in the chapter. Analysis of Channel condition number has been studied and its effect on throughput and switching point for MIMO has been investigated in detail.

Chapter: 8 The chapter describes the implementation of the proposed algorithms described in Chapter 6 and 7, on embedded platforms using Software tools like Code Composer Studio (CCS) and Xilinx Development Suite. Real time Implementation of developed algorithms on FPGA using FIL Simulation and on DSP using PIL Mode is discussed in detail. Comparative performance analysis of MATLAB simulations, FPGA and DSP results is presented.

Chapter: 9 Conclusion and further developments has been elaborated in this chapter.

Chapter: 10 Thesis ends with Bibliography which includes the list of references used in each chapter.

Background and Related work: MIMO Wireless Communication

2.1 Introduction

Wireless communication is one of the great success stories of recent years, offering users levels of mobility and services never available before. The success of future wireless communication systems depends on meeting, or exceeding, the needs, requirements and interests of users and society as a whole. This will require an increase in spectral efficiency to allow high data rates and high user capacities far beyond those of 2G or 3G systems [1]. This goal is particularly challenging for systems that are power, bandwidth, and complexity limited. However, the domain which can be exploited to increase the channel capacity is the use of multiple transmit and receive antennas. Pioneering work by Foschini [2] and Telatar [3] ignited much interest in this area by predicting significant higher bit rates compared to single-antenna systems. The use of multiple antennas for wireless communication systems has gained overwhelming interest during the last decade [4]. MIMO is now being integrated into many wireless standards like 3G and 4G wireless communication systems [5].

Throughout this introductory chapter, an attempt has been made to present MIMO channel capacity analysis, performance gains offered by MIMO architecture and trade-offs in MIMO wireless communication system.

2.1.1 MIMO Wireless System model

The MIMO wireless communication system investigated in this work consists of n_T transmitting and n_R receiving antennas, the descriptor used is (n_T, n_R) . The input and output relation of MIMO communication system model is commonly represented by the vector notation as:

$$y = Hx + n \quad (2.1)$$

where \mathbf{x} is $(n_T \times 1)$ transmit symbol vector, \mathbf{y} is the $(n_R \times 1)$ receive vector, \mathbf{H} is $(n_R \times n_T)$ channel matrix, and \mathbf{n} is $(n_R \times 1)$ Additive White Gaussian Noise (AWGN) vector at a given instant of time as shown in Figure 2.1 .

In channel matrix \mathbf{H} , h_{ij} represents the complex gain of the channel between the j^{th} transmitter and i^{th} receiver. For a MIMO system represented by Equation 2.1, with n_T transmit antennas and n_R receive antennas, the channel matrix \mathbf{H} is given by Equation 2.2.

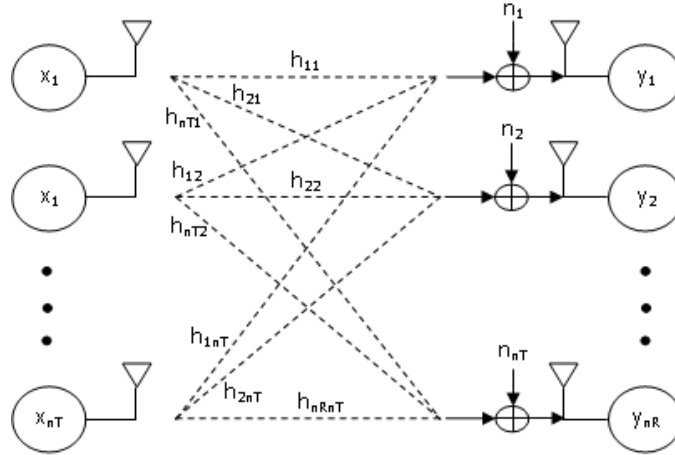


Figure 2.1: MIMO wireless communication model

$$H = \begin{bmatrix} h_{11} & h_{12} & \cdots & h_{1n_T} \\ h_{21} & h_{22} & \cdots & h_{2n_T} \\ \vdots & \vdots & \ddots & \vdots \\ h_{n_R1} & h_{n_R2} & \cdots & h_{n_Rn_T} \end{bmatrix} \quad (2.2)$$

In rich scattering environment with no specular component of the signal i.e Line-Of-Sight (LOS), the channel gains $|h^{ij}|$ are usually Rayleigh distributed [6]. It is assumed that the entries of channel \mathbf{H} are Independent Identically Distributed (i.i.d) Gaussian, complex and each entry is of zero mean with independent real and imaginary parts. Each entry of \mathbf{H} has uniformly distributed phase and Rayleigh distributed magnitude with expected magnitude square equal to unity. This is intended to model a Rayleigh fading channel with enough physical separation within the transmitting and the receiving antennas to achieve independence in the entries of \mathbf{H} as in Equation 2.3.

$$H_{ij} = \text{Normal}(0, 1/\sqrt{2}) + i.\text{Normal}(0, 1/\sqrt{2}) \quad (2.3)$$

The Rayleigh channel model considered here is similar to that in Foschini's work [2]. Considering the described MIMO wireless channel model, the capacity analysis for SISO, SIMO, MISO and MIMO system is carried out in following section. The capacity analysis are plotted using Matrix Laboratory (MATLAB).

2.2 MIMO Channel Capacity Analysis

The MIMO systems can be studied from two different perspectives: one concerns performance evaluation in terms of error probability of practical systems, the other concerns the evaluation of

the information-theoretic (Shannon) capacity [7]. For the latter, the Shannon capacity of MIMO communication systems in terms of Ergodic capacity and Outage capacity is briefly discussed. The capacity analysis for different types of MIMO channels are discussed in [8–10]. All these analyses showed that MIMO systems in Rayleigh-fading environments can potentially provide enormous channel capacity.

The inspiration for research and applications of wireless MIMO systems was mostly triggered by the initial Shannon capacity results obtained independently by Bell Labs researchers E. Telatar and J. Foschini. In this section we examine the capacity aspects of MIMO wireless communication systems.

2.2.1 Shannon capacity of wireless channels

Information theory is very broad mathematical framework, which has its roots in communication theory, as founded by Shannon in his well known paper [11]. Information theory deals with measurement and transmission of information through a channel. Shannon's law defines the theoretical maximum rate at which error free digits can be transmitted over a bandwidth limited channel in the presence of noise as given in Equation 2.4.

$$C \leq B \log_2 \left(1 + \frac{S}{N} \right) \quad (2.4)$$

where C is the effective channel capacity in bits per second; B is the channel bandwidth in hertz and S/N is the SNR of the communication signal to the Gaussian noise interference expressed as a straight power ratio.

Single-Input Single-Output

Given a Single-Input Single-Output (SISO) channel corrupted by an AWGN noise, at a level of SNR denoted by ρ , the capacity (rate that can be achieved with no constraint on code or signaling complexity) can be written as in Equation 2.5 [12]:

$$C = \log_2(1 + \rho|h|^2) \quad b/s/Hz \quad (2.5)$$

where $|h|^2$ is the normalized complex gain of a fixed wireless channel.

Single-Input Multiple-Output

Single-Input Multi-Output (SIMO) system consists of single transmit antenna and multiple receive antenna. This system is also known as Receive Diversity. It is mainly used to enable receiver

to receive signal from number of independent sources to combat the effect of fading. As we deploy more receiver antennas the statistics of capacity improve with n_R receive antennas. The capacity of SIMO system is given by [13]:

$$C = \log_2\left(1 + \rho \sum_{i=1}^{n_R} |h_i|^2\right) \quad \text{b/s/Hz} \quad (2.6)$$

where h_i is the gain of i^{th} receive antenna. As shown in Figure 2.2, by increasing the value of n_R there is logarithmic increase in capacity. This is due to the spatial diversity which reduces fading and due to high SNR of the combined antennas.

The increase in capacity due to SNR improvement is limited because the SNR is increasing inside the log function in Equation 2.6. In summary, SIMO systems are good at improving the channel capacity performance due to the spatial diversity effect, but this effect saturates with increase in the number of antennas. SIMO system is not acceptable in systems where the receiver is located in mobile device such as mobile equipment, as the receiver processing will be limited by size and battery drain.

Multiple-Input Single-Output

Multi-Input Single-Output (MISO) system consists of multiple transmit antennas and single receive antenna, termed as Transmit Diversity. In such systems, the redundant data is transmitted from transmitter and receiver receives the optimum signal to extract the required data. For MISO system, it is assumed that the transmitter does not have the channel knowledge. MISO system with n_T transmit antennas and one receive antenna, the channel capacity is given as in Equation 2.7, where the normalization by n_T ensures a fixed total transmit power.

$$C = \log_2\left(1 + \frac{\rho}{n_T} \sum_{i=1}^{n_T} |h_i|^2\right) \quad \text{b/s/Hz} \quad (2.7)$$

As shown in Figure 2.3, as the number of transmit antenna increases the channel capacity increases and has a logarithmic relationship with n_T . The advantage of using MISO compared to SIMO, is that the number of antennas are on the transmitter side. In systems like Base station as transmitter it is acceptable to have number of transmit antennas due to space for antennas, size and battery life.

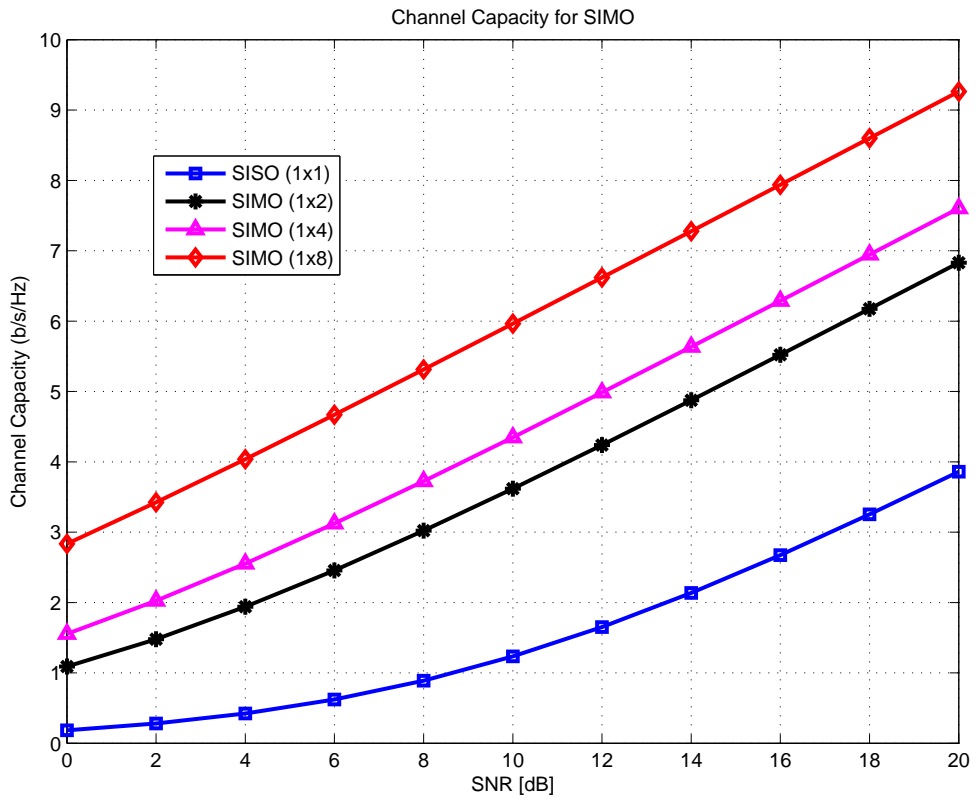


Figure 2.2: SIMO System-Channel Capacity

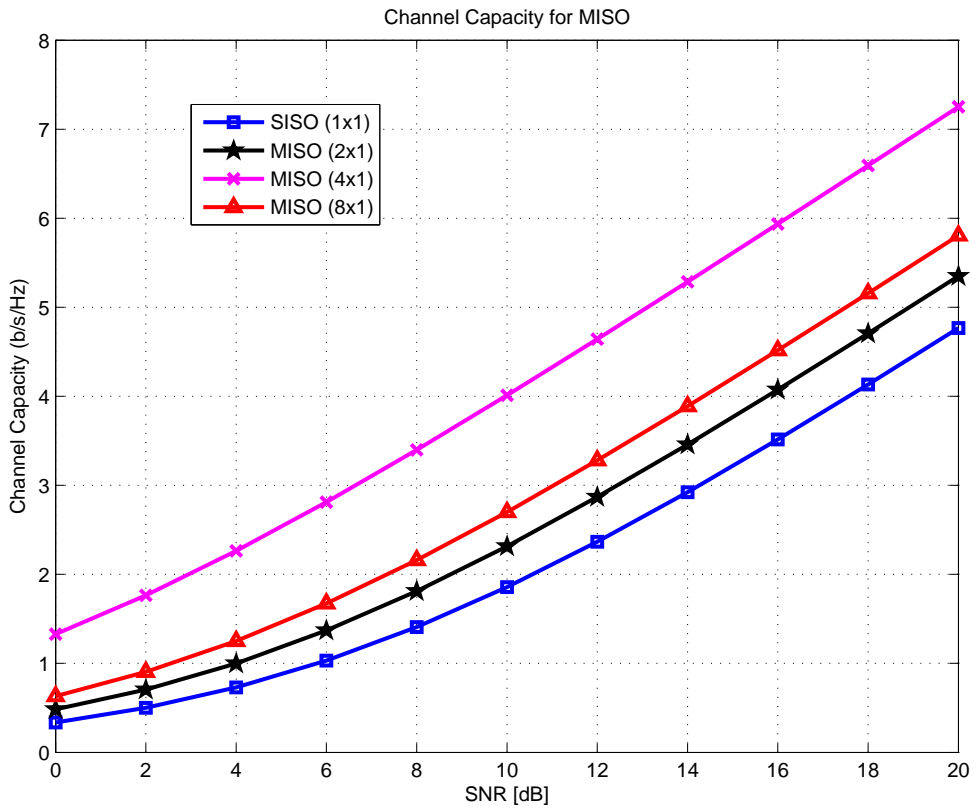


Figure 2.3: MISO System-Channel Capacity

Multiple-Input Multiple-Output

Now, we consider the use of diversity at both transmitter and receiver giving rise to a MIMO system. For n_T transmit antennas and n_R receive antennas, the capacity equation is given by Equation 2.8

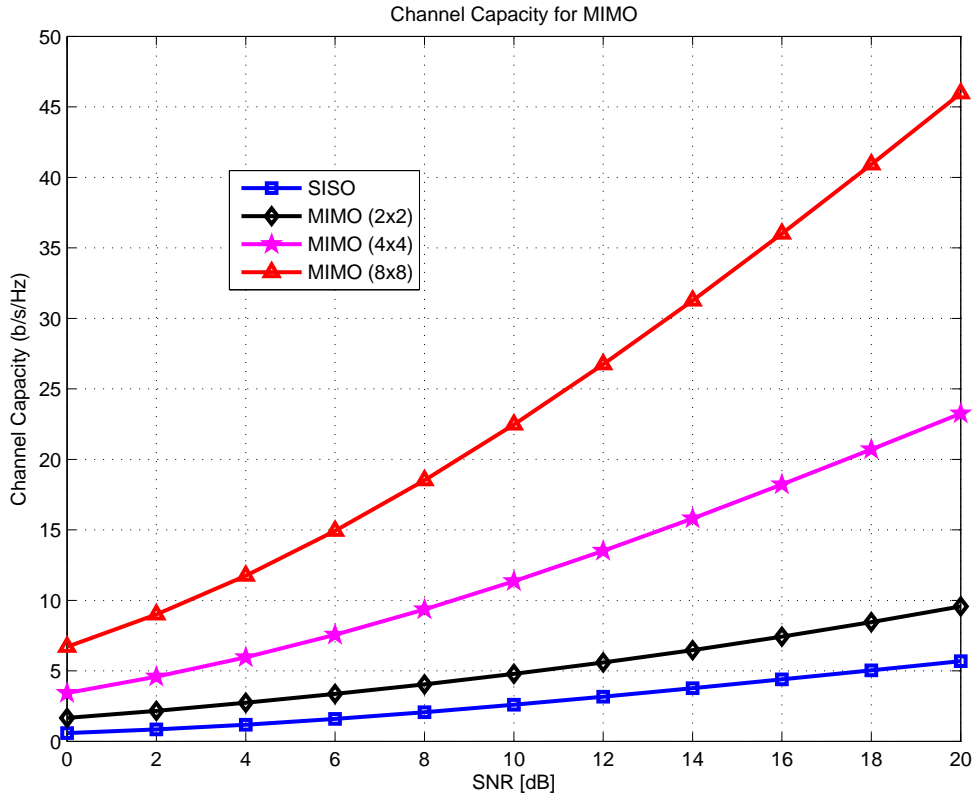


Figure 2.4: MIMO System-Channel Capacity

$$C = \log_2 \left[\det \left(I_{n_R} + \frac{\rho}{n_T} H H^* \right) \right] \quad \text{b/s/Hz} \quad (2.8)$$

where (*) means transpose-conjugate. As shown in Figure 2.4, as the number of transmit and receive antenna increases, the channel capacity linearly increases with the term $\min(n_T, n_R)$.

To further consider the random variations of the wireless channel, there are two notions of capacity for fading channel [14]. They are as follows:

- 1) Ergodic Capacity: It is the capacity achieved by encoding each message across multiple channel realizations and
- 2) Outage Capacity: It is the rate achieved under a constraint on the outage probability. Outage analysis quantifies the level of channel capacity performance that is guaranteed with a certain level of reliability. These capacities for MIMO communication systems are briefly examined.

2.2.2 Ergodic Capacity

For finite number of transmit and receive antennas, E. Telatar [3] derived the analytical expression for the ergodic (or mean) capacity of i.i.d Rayleigh flat-fading MIMO channels by using the eigenvalue distribution of the Wishart matrix \mathbf{W} in integral form involving the Laguerre polynomials. The calculation of the mean capacity involves the channel \mathbf{H} , in terms of the eigenvalues $\lambda_1 \dots \lambda_m$ of \mathbf{W} where

$$W = \begin{cases} HH^*, & n_R < n_T \\ H^*H, & n_R \geq n_T \end{cases} \quad (2.9)$$

An exact calculation of the ergodic capacity with $n_T = t$ transmitters and $n_R = r$ receivers under power constraint P yields [[3],Equation 8]:

$$C = \int_0^\infty \log\left(1 + \frac{P\lambda}{t}\right) \sum_{k=0}^{m-1} \frac{k!}{(k+n-m)!} [L_k^{n-m}(\lambda)]^2 \lambda^{n-m} e^{-\lambda} d\lambda \quad (2.10)$$

where $m = \min(n_R, n_T)$ and $n = \max(n_R, n_T)$, and L_k^{n-m} is the associated Laguerre polynomial of order k given as:

$$L_k^{n-m}(x) = \frac{1}{k!} e^x x^{m-n} \frac{d^k}{dx^k} (e^{-x} x^{n-m+k}) \quad (2.11)$$

SIMO-Ergodic Capacity

For SIMO system, $n_T = 1$ and $n_R = r$, hence $m = 1$ and $n = r$ in Equation 2.10. The capacity is given as [[3],Equation 9]:

$$C_{SIMO} = \frac{1}{\Gamma(r)} \int_0^\infty \log(1 + P\lambda) \lambda^{r-1} e^{-\lambda} du \quad (2.12)$$

Simulation results of the ergodic capacity v/s number of receive antenna is as shown in Figure 2.5. From the graph we can say that as number of receive antenna increases the ergodic capacity increases. For system with large number of receive antennas, the capacity is asymptotic to $\log(1+Pr)$.

MISO-Ergodic Capacity

For MISO System the value of r in Equation 2.10 equals to one. The ergodic capacity is given by [[3],Equation 10]:

$$C_{MISO} = \frac{1}{\Gamma(t)} \int_0^\infty \log\left(1 + \frac{P\lambda}{t}\right) \lambda^{t-1} e^{-\lambda} du \quad (2.13)$$

The MISO Ergodic capacity of given by integral in Equation 2.13 is plotted in Figure 2.6. The

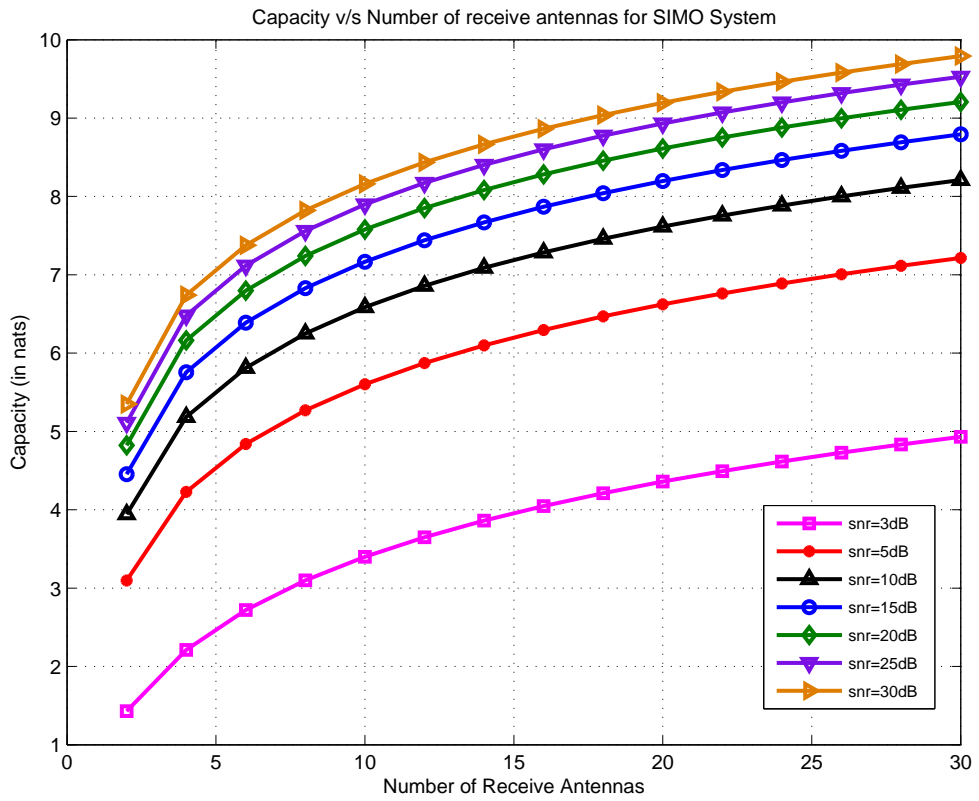


Figure 2.5: Capacity vs Number of receive antenna for SIMO system

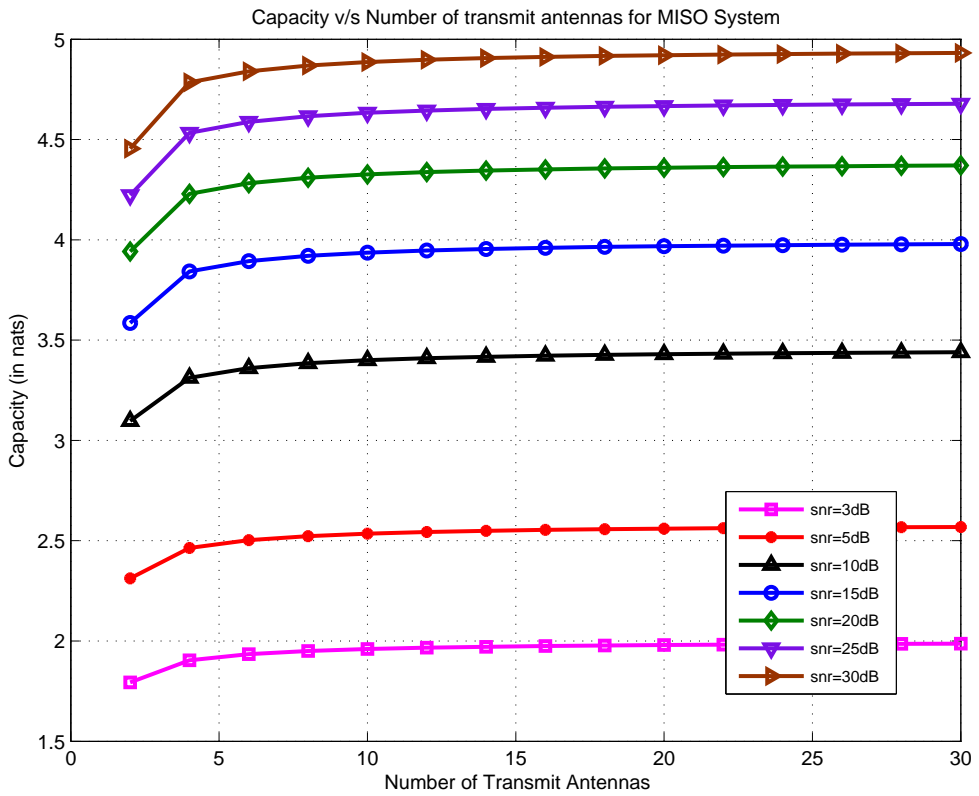


Figure 2.6: Capacity vs Number of transmit antenna for MISO system

plot is for number of transmit antennas v/s Capacity. From the plot we can observe that as the number of transmit antennas increases the capacity approaches to $\log(I+P)$.

MIMO-Ergodic Capacity

For MIMO system, with $r = t, n = m = r$, the capacity is given by [[3],Equation 11]:

$$C_{MIMO} = \int_0^{\infty} \log\left(1 + \frac{P\lambda}{r}\right) \sum_{k=0}^{r-1} L_k(\lambda)^2 e^{-\lambda} d\lambda \quad (2.14)$$

where $L_k = L_k^0$ is the Laguerre polynomial of order k .

Figure 2.7 shows this capacity for number of antenna configurations and SNR. It can be shown that the channel capacity grows proportional with the minimum number of antennas $\min(n_R, n_T)$ outside and no longer inside the log function. Hence from theoretical analysis, for idealized random channels, limitless capacities can be obtained if we can afford the cost and space of many antennas and RF chains. In practical applications the capacity is dictated by the transmission algorithms selected and by the physical channel characteristics.

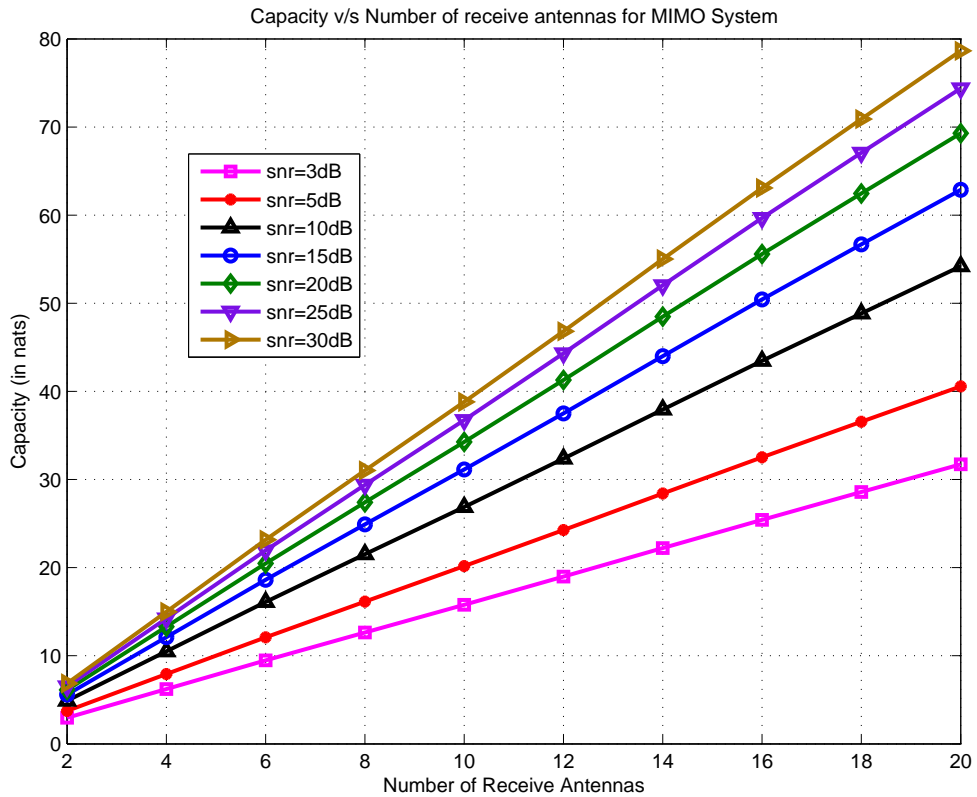


Figure 2.7: Capacity vs Number of receive antenna for MIMO system

2.2.3 Outage Capacity

Since the MIMO channel capacity is a random variable, it is meaningful to consider its statistical distribution. A particularly useful measure of its statistical behavior is the so-called Outage Capacity. With Outage Capacity, the channel capacity is associated to an Outage probability. If the channel capacity falls below the outage capacity, there is no possibility that the transmitted block of information can be decoded with no errors, whichever coding scheme is employed. The probability that the capacity is less than the outage capacity denoted by C_{out} is q . It is represented as:

$$Pr(C \leq C_{out}) = q \quad (2.15)$$

Outage Capacity is the information rate that is guaranteed for $(100 - q) \%$ of the channel realizations, given by [15]:

$$Pr(C(H) \geq C_{out}(q)) = q\% \quad (2.16)$$

The outage capacity is more relevant measure than the ergodic channel capacity, because it describes in some way the quality of the channel [16]. For a targeted outage probability p_o , the capacity with outage is the maximal rate for which the outage probability is smaller than p_o [17]. The outage capacity describes the rate at which reliable transmission can be guaranteed with a certain probability.

Denoting ρ is the probability of an outage event, the outage capacity is given as the rate R that satisfies the below equation:

$$\rho = Pr[C(t) < R] = Pr[\log_2 \det(I_{n_R} + \frac{\rho}{n_T} HH^*) < R] \quad (2.17)$$

The capacity for a fixed outage probability of 10% is as shown in Figure 2.8. And for a fixed outage probability of 90% is shown in Figure 2.9.

Summarizing the results of Ergodic and Outage Capacity for MIMO wireless communication systems, it can be concluded that large channel capacity is obtained using multiple antennas at transmitter and receiver. But the results are based on the assumptions that rich scattering environment provides independent transmission paths from each transmit antenna to each receive antenna i.e. Rayleigh channel is considered and perfect channel knowledge is known at the receiver. Hence, for a single-user system with MIMO architecture can achieve channel capacity which grows linearly with $\min(n_T, n_R)$ as compare to SISO system. The channel capacity is highly dependent on the nature of CSI at the transmitter and receiver, the channel SNR and antenna correlations. Channel ca-

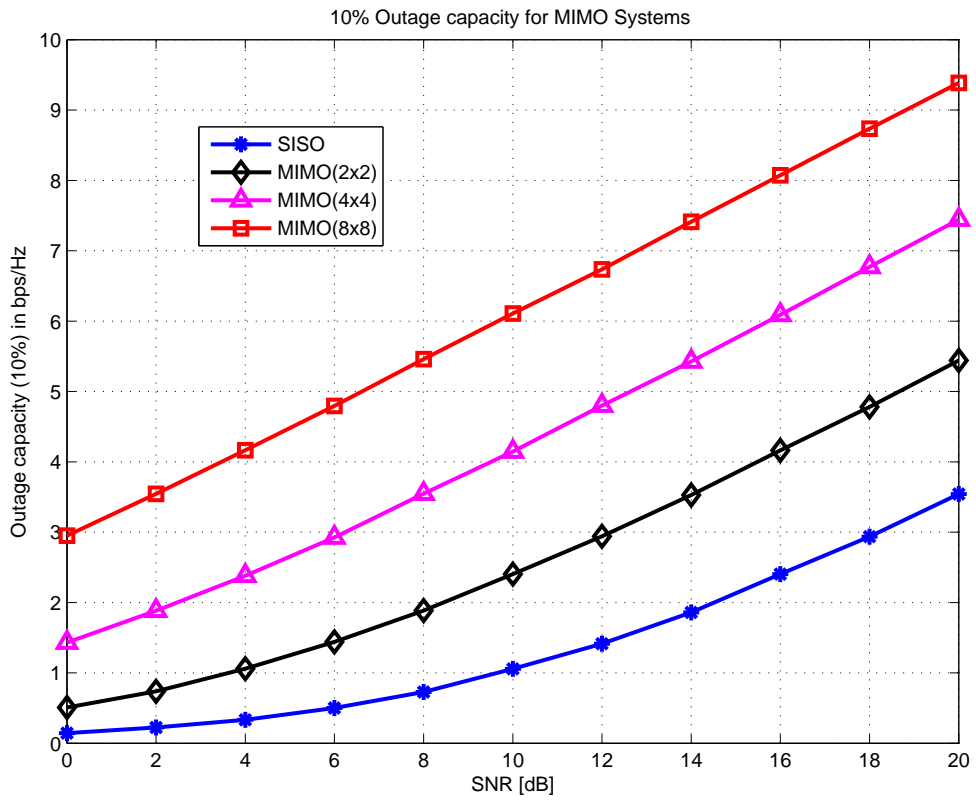


Figure 2.8: 10 percent Outage capacity of MIMO System

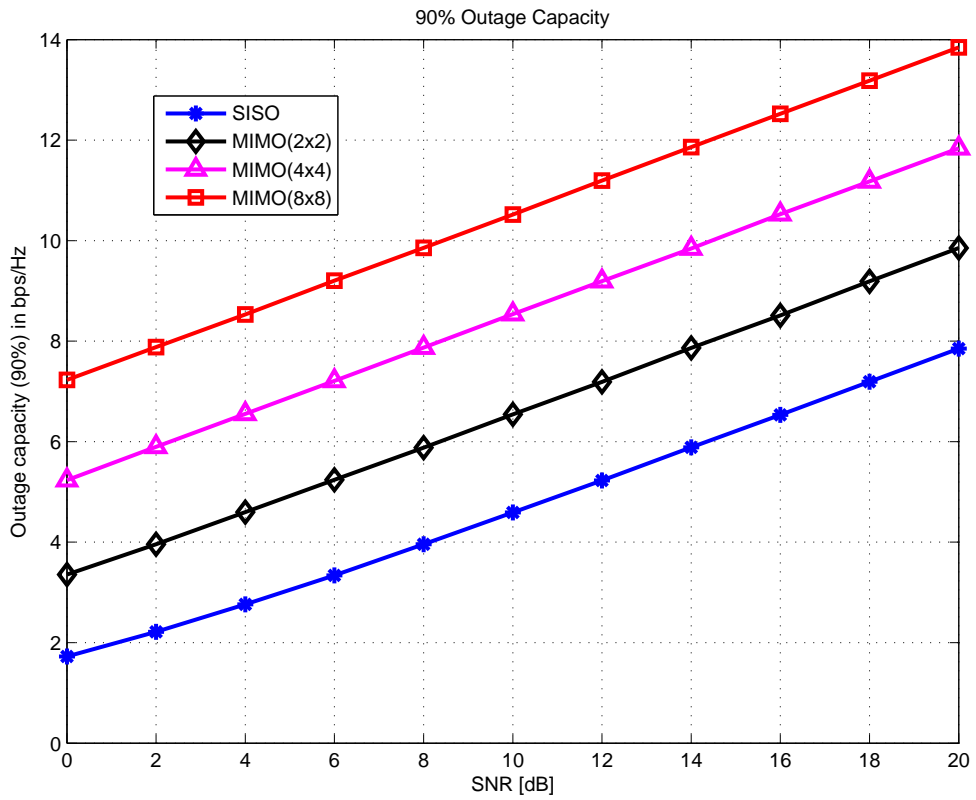


Figure 2.9: 90 percent Outage capacity of MIMO System

capacity limits based on realistic assumptions regarding CSI and time-varying channels are discussed briefly in [18].

2.3 MIMO Performance Gains

In wireless communication, spectral efficiency is of paramount importance due to high data rate demands of multimedia services. Usage of MIMO is considered as a promising way to achieve the necessary demands of spectral efficiency. MIMO system offers new degrees of freedom, which have to be used carefully to get the benefit of a MIMO system [19]. For a system where the channel is unknown at the transmitter and perfectly known at the receiver the MIMO performance gains and their respective effects on system performance are summarized in Table 2.1 [20].

MIMO Performance Gains	Effects
Spatial Multiplexing Gain	Increase Spectral Efficiency and capacity
Spatial Diversity Gain	Increase Link Reliability
Array Gain	Increase Coverage and QoS
Interference Cancellation gain	Reduce co-channel Interference and Increase cellular capacity

Table 2.1: MIMO Performance Gains and its effects

The performance improvements resulting from the use of MIMO systems are due to Spatial Multiplexing gain, Spatial Diversity gain, Array gain and Interference Cancellation gain. In this section each of these leverages gains are briefly reviewed. Various MIMO gain trade-offs are also discussed and analyzed.

2.3.1 Spatial Multiplexing Gain

Spatial Multiplexing gain is achieved in MIMO systems by transmitting independent data signals from individual antennas. Under the assumption of channel with rich scattering and independently faded channel paths, the receiver can separate different streams, resulting in increase in channel capacity. This increase in channel capacity is obtained for no additional power or bandwidth expenditure. The spatial multiplexing gain is given by [21]:

$$\lim_{SNR \rightarrow \infty} \frac{R(SNR)}{\log(SNR)} = r \quad (2.18)$$

where $R(SNR)$ is the data rate at SNR and r is the spatial multiplexing gain.

2.3.2 Spatial Diversity Gain

Diversity in the context of MIMO systems is the ability of system to improve link reliability by providing multiple independent fading parallel signal paths between transmitter and receiver. If multiple antennas are placed sufficiently far apart, the channel path gains between different antenna

pairs fade independently, and, thus, independent signal paths are created. Diversity proves to be a powerful technique to mitigate the effects of fading in wireless systems [22].

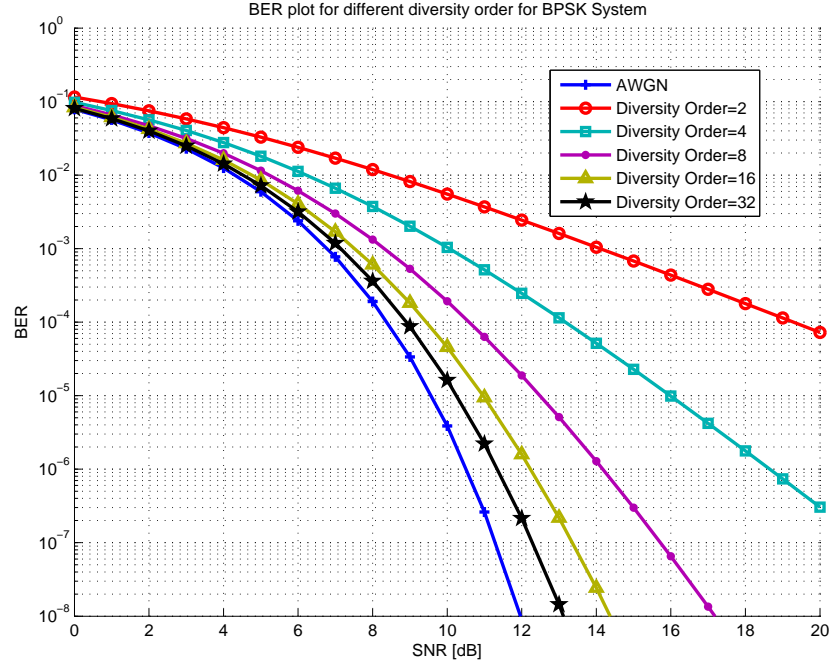


Figure 2.10: BER for different diversity order

Diversity Order: It is the number of independently fading signal paths between transmitter and receiver. Full diversity order for flat-fading spatially white MIMO channel of $n_T \times n_R$ is achieved in case of MIMO system with n_T transmit antenna and n_R receive antennas. Capacity of fading channel approaches to an AWGN channel when the diversity order goes to infinity [23]. Figure 2.10 shows the effect of diversity order on the BER for Rayleigh Fading channel for BPSK system. It is seen that as the diversity order increases, the BER decreases and approaches nearer to AWGN channel BER. This plot was plotted using MATLAB based BERTool [24].

Diversity Gain: It is a measure of the decay of the probability of error with respect to the SNR. This quantity is given by [21]:

$$\lim_{SNR \rightarrow \infty} \frac{\log P_e(SNR)}{\log(SNR)} = -d \quad (2.19)$$

where $P_e(SNR)$ is the average probability of error at SNR and d is the diversity gain.

2.3.3 Array Gain

Array gain can be made available through processing at the transmitter and the receiver and results in an increase in average receive SNR due to coherent combining effect. This increase in

average receive SNR relative to single-antenna average SNR is termed as Array Gain [25]. Array gain improves coverage by improving the received SNR through coherent combining of the signals arriving at the receive antenna array.

2.3.4 Interference Canceling Gain

Interference canceling gain reduces co-channel interference, thus increases cellular system capacity by nulling out undesired interfering signals. Co-channel interference arises due to frequency reuse in wireless channels. Interference reduction requires knowledge of the desired signal channel. Interference reduction can be achieved by combining the signals in order to suppress the interference signal by using proper multiantenna spatial weighting scheme at the receiver to improve the average SNR at the receiving end [26,27].

In general it is not possible to exploit all the leverages of MIMO technology simultaneously due to conflicting demands on the spatial degrees of freedom. The degree to which these conflicts are resolved depends upon the transmission techniques and transceiver design.

2.4 Tradeoffs in MIMO Wireless System

In recent developments in wireless communication systems, MIMO has been extensively applied in various wireless standards to increase the system performance dramatically. To date MIMO have been utilized for both spatial multiplexing approaches to increase spectral efficiency [28,29] or for spatial diversity to improve error performance [30]. The pioneering work by Zheng and Tse in the excellent groundbreaking paper [31] showed that both diversity and multiplexing gains can be simultaneously obtained, but there is a tradeoff between how much of each type of gain any MIMO scheme can extract: higher spatial multiplexing comes at the price of sacrificing diversity. The optimal Diversity and Multiplexing tradeoff (DMT) in Rayleigh i.i.d channels was studied. Further in [32], the DMT framework was completed by including array gain to cope with limitations of DMT. The derived Diversity, Multiplexing and Array gain (DMA) analysis gave more insight into the relation between reliability and transmission rate in MIMO Systems.

Based on elegant formulation of DMT, Azarian and El Gamal [33] introduced a new notion called the Throughput-Reliability Tradeoff (TRT), between the throughput, as quantified by the transmission rate, and reliability, as quantified by the so-called outage probability in Block Fading channel for high SNR-regime. Similarly, the Power-Bandwidth tradeoff [34,35] and Spectral Efficiency (SE) and Energy Efficiency (EE) Tradeoff [36] is also studied for MIMO Systems.

2.4.1 Diversity-Multiplexing Tradeoff

As discussed in previous sections, for i.i.d. Rayleigh fading MIMO channel with n_T transmit and n_R receive antennas has a maximum diversity gain of $n_T X n_R$. On the other hand, the channel capacity scales with $\min(n_T, n_R)$, which is the number of spatial degrees of freedom in the channel. This section analyses the DMT between the error probability and the data rate of a system [31].

As in [31, 32], for family of codes $C(snr)$ of block length n_S , employs a different code $C(snr)$ with rate $R(snr)$ at each SNR level. A MIMO coding scheme $C(snr)$ is said to achieve a spatial multiplexing gain r , a diversity gain $d(r)$, and an array gain $a(r)$ if the data rate satisfies following equations:

$$\lim_{snr \rightarrow \infty} \frac{R(snr)}{\log(snr)} = r \quad (2.20)$$

with $0 \leq r \leq \min(n_T, n_R)$

and the outage probability satisfies

$$\lim_{snr \rightarrow \infty} \frac{\log P_{out}(r, snr)}{\log(snr)} = -d(r) \quad (2.21)$$

$$\lim_{snr \rightarrow \infty} \frac{P_{out}(r, snr)}{snr^{-d(r)}} = a(r)^{-d(r)} \quad (2.22)$$

Observe that definitions in 2.21 and 2.22 induce the following approximation of the high-SNR behavior of the outage probability when R satisfies 2.20

$$P_{out}(r, snr) \sim (a(r) \cdot snr)^{-d(r)} \quad (2.23)$$

where \sim denotes asymptotic equivalence as $snr \rightarrow \infty$.

The optimal tradeoff curve $d^*(r)$ between the diversity gain and the spatial multiplexing gain that can be achieved by any scheme in the Rayleigh-fading multiple-antenna channel for the case where block length $l \geq m + n - 1$ is given by piecewise-linear function connecting the points $(k, d^*(k))$, $k = 0, 1, \dots, \min(m, n)$, where

$$d^*(r) = (m - k)(n - k) \quad (2.24)$$

where, $d_{max}^* = mn$ and $r_{max}^* = \min(m, n)$.

The optimal tradeoff curve for various MIMO antenna configurations is plotted in Figure 2.11. As seen the maximum achievable spatial multiplexing gain is the total number of degrees of freedom

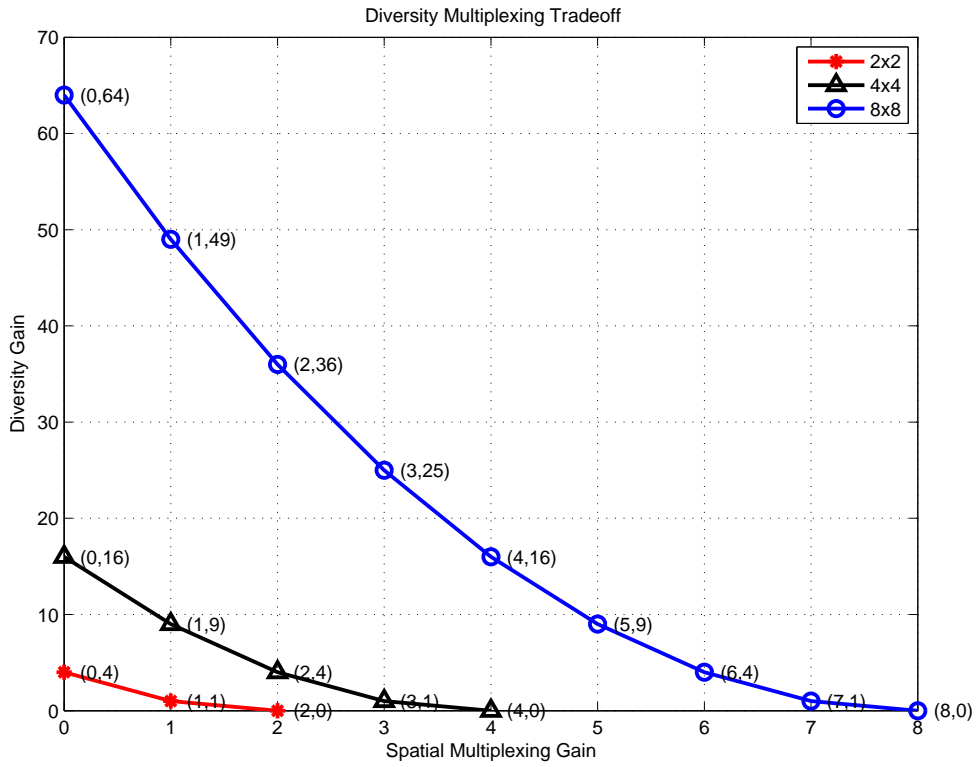


Figure 2.11: Diversity Multiplexing trade-off of MIMO System

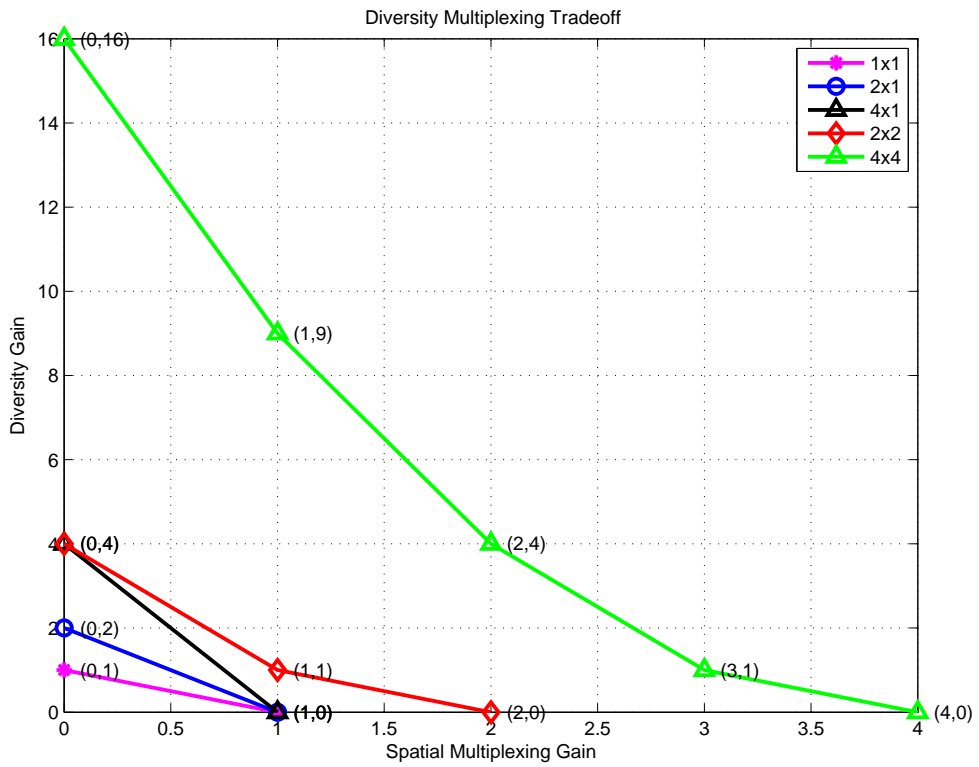


Figure 2.12: Diversity Multiplexing tradeoff of MISO and MIMO system

provided by the channel given by $\min(m, n)$. The curve intersects the y axis at the maximal diversity gain given by mn , corresponding to the total number of random fading coefficients that a scheme can average over. It can be concluded that as we increase the diversity gain by increasing the $\min(m, n)$ from 2 to 4, the supported spatial multiplexing gain also increases by 2 to 4 i.e. the entire tradeoff curve shifts by a factor of $\min(m, n) = 2$.

Similarly comparing the optimal tradeoff for various MISO and MIMO techniques as shown in Figure 2.12. It can be shown that as we increase the diversity gain by increasing the number of transmit antennas from 2 to 4, the spatial multiplexing gain remains same. But when we compare the results for 4x1 and 2x2 the maximal diversity gain remains similar equal to 4, but the spatial multiplexing gain increase from 1 to 2. Hence there clearly exist tradeoff between spatial multiplexing and diversity gain achieved by MIMO Wireless Communication Systems.

2.5 MIMO Transmission Techniques

MIMO wireless systems have gained overwhelming interest during the last decade which has evolved rapidly. The last ten years of research efforts are recapitulated, with focus on spatial multiplexing and spatial diversity techniques [37]. MIMO techniques can be mainly categorized as: Spatial Multiplexing (SM) MIMO, Spatial Diversity MIMO and Beamforming Techniques. Various MIMO techniques, their respective performance gains and their categorization is as shown in Figure 2.13.

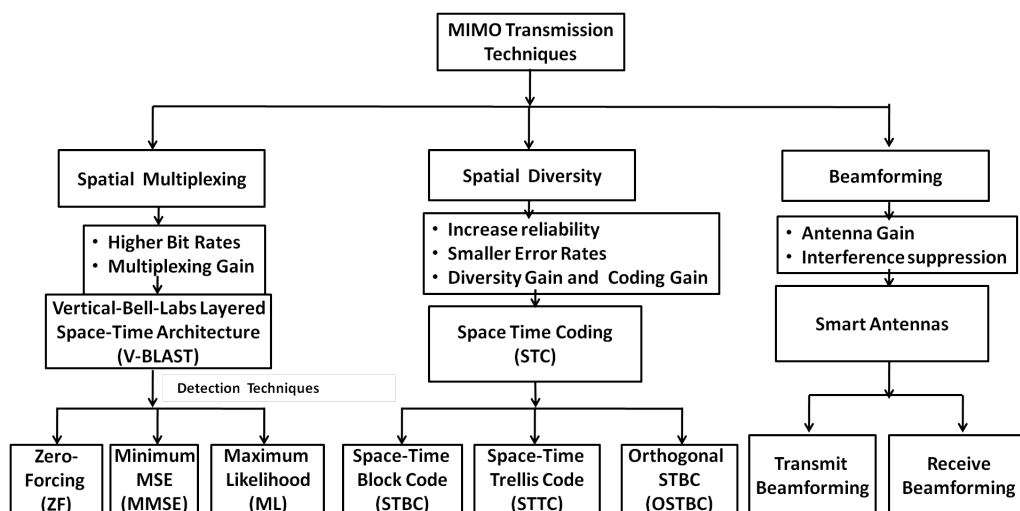


Figure 2.13: MIMO Transmission techniques and their performance gains

A well-known spatial multiplexing scheme is the Vertical Bell-Labs Layered Space-Time Architecture (V-BLAST) [38]. The high spectral efficiency achievement in MIMO SM system is

due to the fact that, in rich scattering environment the transmitted signals received at the receiver are highly uncorrelated at each receiving antennas. The receiver exploits this property to separate signals enabling simultaneous reception of multiple spatial streams.

In contrast to SM, Spatial diversity techniques aim at providing higher bit rates [39]. Diversity Techniques exploits the received copies of transmitted data to minimize fading effects. If no channel information is available, the signals can be transmitted from different antenna through Space-Time Coding (STC). It provides both Space and Time diversity. Space-time coding schemes [40,41] that achieve Spatial Diversity are Space-Time Trellis Code (STTC) [42], Alamouti's transmit diversity scheme [30], and Orthogonal Space-Time Block Code (OSTBC) [43, 44].

Beamforming is an advanced technology that offers a significantly improved solution to reduce the interference levels and improve the system capacity. They are used to create a certain required antenna directive pattern to give the required performance. Beamforming can be achieved by either transmit beamforming to receive beamforming. Joint transmit and receive beamforming can be implemented to get the advantage of both.

2.6 GUI for Capacity and Performance Analysis

MIMO systems have gain interest due to its performance gains and various transmission techniques. Researchers have studied MIMO Channel capacity and analysis of MIMO transmission techniques. Motivated by various studies based on MIMO Wireless Systems, MATLAB based Multiple-Input Multiple-Output Wireless Simulator (MIMO-WS) is developed to ease the comparative and performance analysis of MIMO Systems. MIMO-WS is able to carry out the Capacity Analysis for various antenna configurations and performance analysis in terms of BER for various MIMO Transmission Techniques. V-BLAST Spatial multiplexing can be analyzed for different receiver techniques: ZF, ML and MMSE. Spatial diversity techniques: Alamouti and STTC is also compared in terms of BER. The snapshot of the developed GUI is as shown in Figure 2.14. The description and operating procedure is explained in detail in Appendix A.

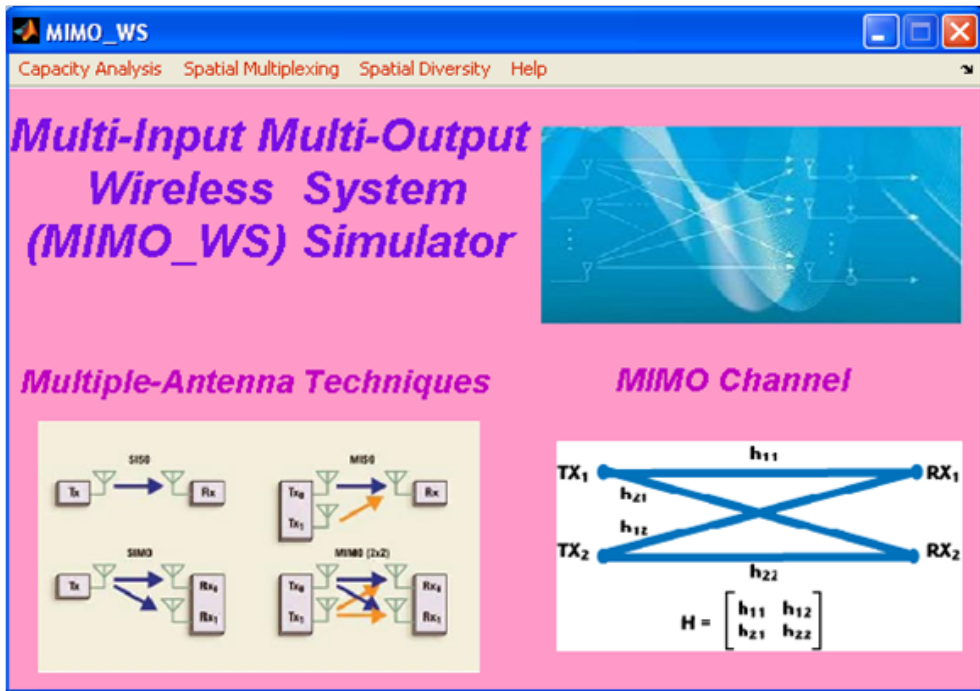


Figure 2.14: GUI for MIMO Wireless Simulator

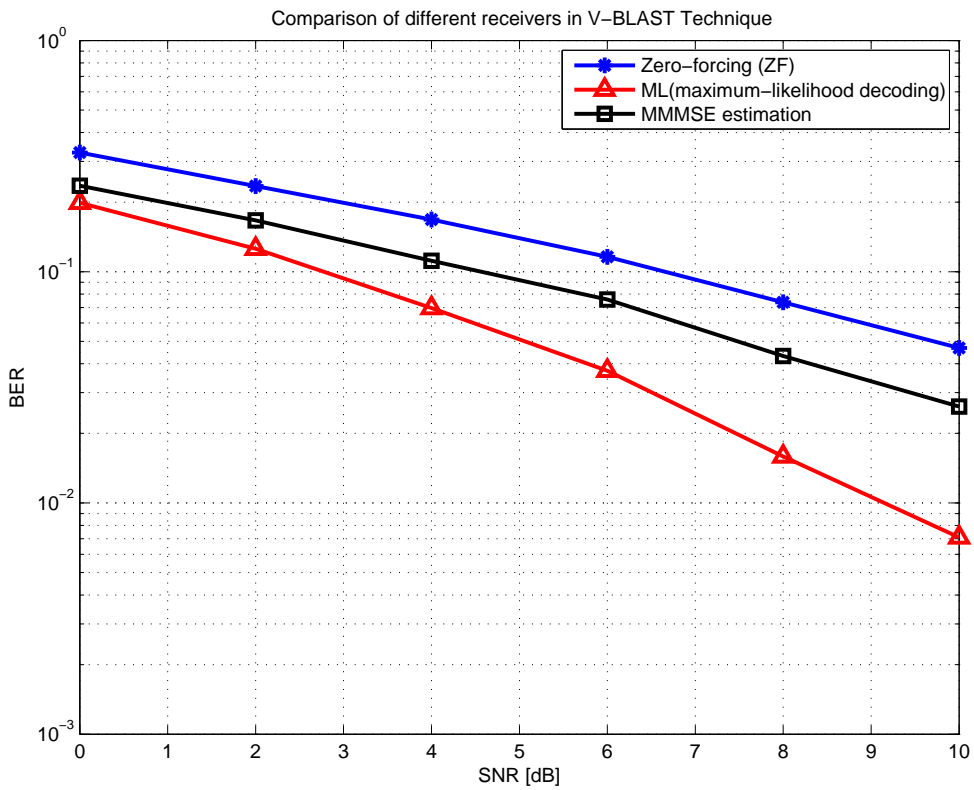


Figure 2.15: Comparison of ZF, ML and MMSE receiver for V-BLAST Technique

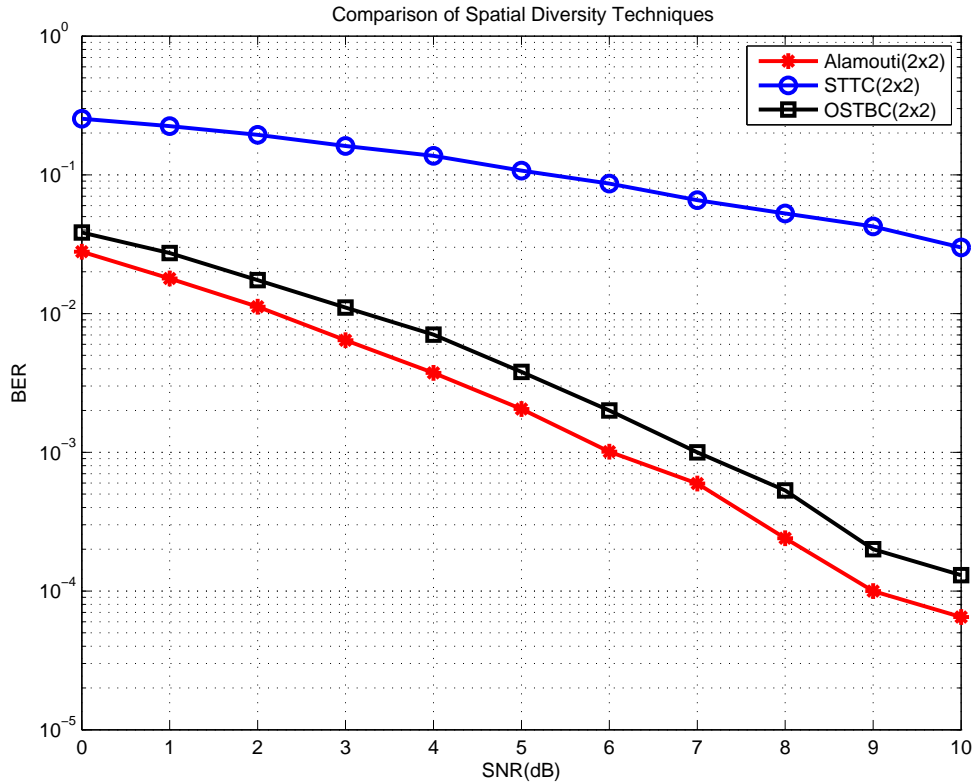


Figure 2.16: Comparison of BER for Diversity Techniques: Alamouti, STBC and STTC

Figure 2.15 shows the comparative performance analysis of 2x2 V-BLAST technique for different receivers. ML detection technique outperforms ZF and MMSE receivers as SNR increases. To achieve target BER of 0.01dB, we need SNR=3dB in V-BLAST system with the ML detector, and SNR=4.5dB in the MMSE and SNR = 7dB with ZF receiver. Figure 2.16 shows comparison of different spatial diversity techniques BER v/s SNR plot. Alamouti code gives minimum BER when compared to OSTBC and STTC. At SNR = 5dB, Alamouti Scheme gives BER of 2.05×10^{-3} , OSTBC gives 3.8×10^{-3} and STTC results in BER of 0.107.

2.7 Concluding Remarks

MIMO technology is an advanced technique which promises high capacity as compared to traditional systems. Capacity analysis of MIMO system is carried out in comparison with SISO systems. Performance gains achieved from MIMO Technology is discussed in detail. Tradeoff between MIMO Transmission Techniques i.e Spatial Multiplexing and Transmit Diversity is analyzed and discussed in brief. MIMO Wireless Simulator GUI is developed to ease the channel capacity and performance analysis of MIMO Wireless System.

Conceptual Design of MIMO Wireless Systems

3.1 Introduction

The ever-growing demands for high-speed data and multimedia services are the driving forces behind the requirements for future wireless communication systems. Next-generation communication evolution towards 4G promises to meet the demands for ubiquitous communication. Hence, the complexity of communication systems has grown dramatically in search for higher system capacity, higher data rates, and bandwidth efficiency. To meet the demand for ubiquitous communication and the ability to access and share information, wireless appliances and the supporting networking infrastructure must be able to integrate complex algorithms with adequate computing and signal processing capabilities. In order to meet the capacity needs for future wireless systems without increasing the required spectrum, accomplishment of implementation of advanced communication techniques is necessary. MIMO promises high bit rates, small error rates, reliability, increased channel capacity over rich scattering wireless channels without consuming extra bandwidth or transmit power when compared to conventional single antenna technologies [1].

Software simulations provide flexibility, but the true performance of the system can only be known by developing a hardware wireless platform and performing measurements and tests in the target environment. Recently, various MIMO wireless testbeds based on DSP and FPGA have been developed to verify the theoretical performance gains and to investigate practical issues in MIMO implementation. Overview of various MIMO Testbed for physical layer of MIMO communications is given in [2]. MIMO Communication systems are realized by computationally complex algorithms, requiring new digital hardware architectures to be developed. This chapter describes the System Design Methodology and Basic Hardware Concept for designing MIMO Wireless platform development. Mathworks model based design and MATLAB based programming and verification tools for FPGAs and DSPs are also discussed briefly in this chapter.

3.2 System Design Methodology

Next-generation communication systems promise to deliver a wide variety of new features, such as improved battery life, smaller size, high-definition video and high-bandwidth Internet connections. In designing of such systems, the development and integration of several computationally-intensive algorithms which enable these new features are to be incorporated. In spite of their performance enhancing capabilities, most of the research on MIMO technology up to the moment is based on theoretical studies. To verify the laid concepts of any newly developed system or standards,

Rapid Prototyping (RP) implementations is the most popular methodology [3, 4].

Rapid Prototype implementations and field trials are an essential part of the verification of new system concepts and standards. Consequently, extensive prototyping efforts have been carried out for current technologies such as WLAN [5] and 3GPP/LTE [6]. A prototype is the initial realization of a research concepts, either as a reference, or as a vehicle for future developments and improvements. The software simulations of the developed system based on research requirements often make numerous assumptions and depend on mathematical models. Examples are the assumption of perfect channel knowledge at the receiver or mathematical model of wireless channel. From an implementation point of view, prototyping efforts have the advantage of pointing out complexity issues early in the design cycle of a newly developed systems. In RP approach, to develop real-time algorithms on testbed, first the simulation implementation is done, then the simulation is migrated to the testbed and, finally real-time implementation is obtained. The speed and complexity of MIMO-based system requires comprehensive design and verification process including both hardware and software. Experiments in real-world scenarios by means of hardware implementations are necessary to measure the actual performance of system. Figure 3.1 describes the System Design Methodology for MIMO Wireless Platform. The scope of this design methodology extends from specification to implementation on Wireless Platform. According to Functional Description or Specifications various system modeling tools, software tools are chosen and based on hardware specifications, hardware simulation tools and verification is carried out and finally the Wireless platform is developed for implementation of Wireless Communication System.

For RP, design time of a new system is more critical than other factors like cost and power consumption. A major focus is therefore on the efficiency of the tools that are being used in the development process. Based on the system specifications, system modeling and simulation tools like MATLAB Simulink is used for system simulation analysis. Once the system is analyzed in Simulink, the hardware simulation and verification is carried out and finally the integration, measurement and testing is done.

3.2.1 Hardware Concept of MIMO Wireless System

The past decade has shown distinct advances in the theory of MIMO techniques for wireless communication systems. Now, the time has come to demonstrate this progress in terms of applications, where the intermediate step towards a customized product consists of more or less rapid prototyping. Due to the multitude of different MIMO schemes and different applications and standards, an ideal prototyping platform requires a high degree of flexibility and modularity in order

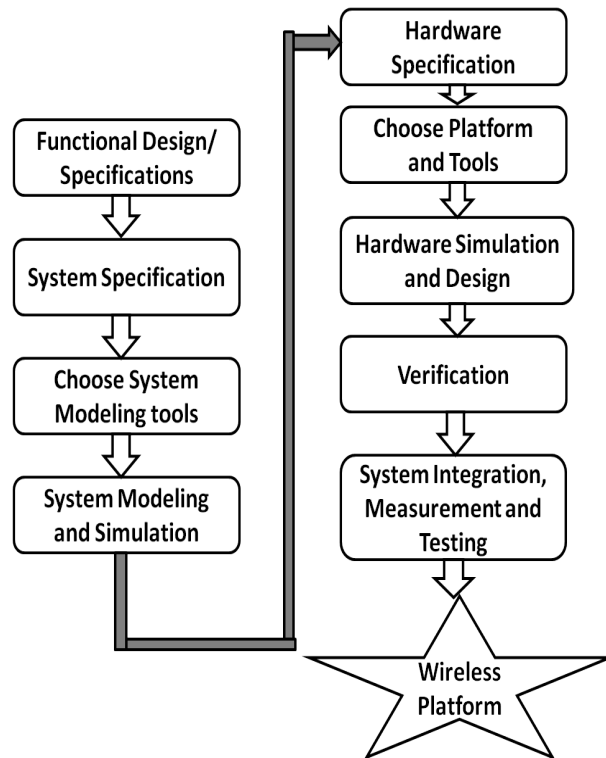


Figure 3.1: System Design Methodology

to be qualified for a wide range of potential applications. MIMO implementation is still facing a lot of challenges. There are different hardware processing platforms available for implementing high performance algorithms for MIMO Wireless system. Following are the processing platform options [7]:

- General purpose processors (GPP),
- Digital signal processors (DSPs),
- Field programmable gate arrays (FPGAs) and
- Application specific integrated circuits (ASICs),

Hardware implementation of the wireless system can be achieved using GPPs, but it faces difficulties when dealing with high processing systems. FPGAs are suitable for fast implementation, quick hardware verification and is re-programmable, whereas ASIC is designed for a particular application. DSP are suitable for complex computation of digital signal processing algorithms. The integration of powerful FPGAs and DSPs is feasible for testing MIMO algorithms for real-time systems as we can get advantage of both processing units. DSP provides a specialized core with multiple-functional units, which are optimized for digital signal processing operations like filtering

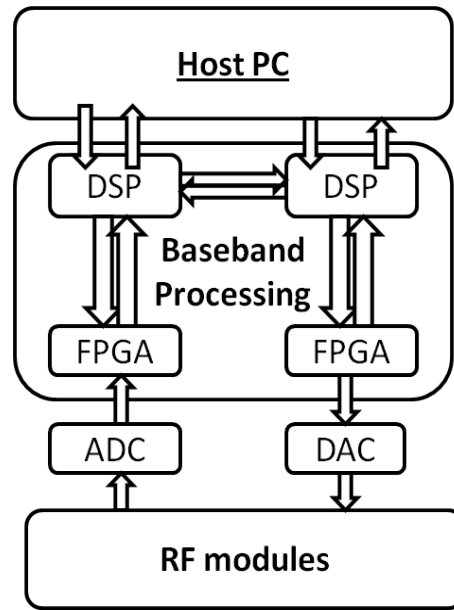


Figure 3.2: Basic Hardware Architecture of MIMO

and transformations. FPGA has the ability to provide special hardware structures in parallel, and to handle high data rates without affecting the other algorithms. It is also convenient to split the real-time implementation into several steps: firstly, a fixed-point code is implemented on DSP and, afterwards, the software modules that do not meet time requirements are migrated to FPGA [8, 9].

Figure 3.2 shows the Basic Hardware Architecture of MIMO Communication System. It consists of two units: Analog RF Unit (RF) and Baseband Processing Unit (BB). The first stage consists of the RF modules mixing the signals of each antenna from RF to BB following the receiver path, the next stage consists of the Analog-to-digital converter (ADC) and Digital-to-analog converter (DAC).

The succeeding FPGA stage allows high-speed parallel data processing for various processing tasks. Therefore, the FPGA stage covers the complete MIMO front end, i.e. antenna filtering operations, the synchronization of time and frequency, the signal modulation and demodulation, and all other regular processing operations. The FPGA operates on the incoming high-data-rate digital signal and reduces the data-rate step wise, so that the subsequent DSP stage is not over strained.

In the DSP stage, all less regular MIMO processing takes place, i.e. algorithms which are under study. Among the hardware platform and its components, a rich set of software tools is required to develop DSP- and/or FPGA-based applications in an efficient and fast way.

3.2.2 MIMO Wireless Testbeds and Prototypes

Since the foundation of MIMO Wireless Communication Systems, considerable effort is dedicated to the demonstration of the capabilities of the technology to investigate the performance of MIMO in real-world scenarios. Hence, various demonstrators and testbeds for MIMO communication have been developed [10]. Testbeds involve real-time transmission in a wireless environment and thus allow experiments with physical channels and RF Frontends. Whereas RP involves designing transmitter and receiver hardware architectures for future products [11]. In 1998, Foschini and a team from AT&T Research Labs developed the first prototype using VBLAST Technique [12], to verify the predicted gains of Spatial Multiplexing MIMO Technique.

The testbeds mainly consist of DSPs, FPGAs combined with ASICs for performance-critical system components, RF frontends equipped with a number of antennas and interfacing to the digital baseband transceiver. The MIMO Wireless channel is either a physical channel or is implemented using a hardware radio frequency emulator. The signal is processed either in real-time mode or offline-mode. Various demonstrators and testbeds developed have been proven to be initial research tools for the development of new technologies [13].

Various MIMO Communication Testbeds that provide physical layer functionality are based on the Universal Software Radio Peripheral (USRP) from Ettus Research [14] together with the GNU software radio [15], the wireless open-access research platform (WARP) from Rice University [16] or OpenAirInterface systems developed by EURECOM [17]. Since then a number of universities have developed their own testbeds and experimental platforms to perform MIMO measurements and real-time experiments. Many of these systems are based on offline processing of sampled data and use commercially available prototyping platforms. These again are often intended to perform channel measurements and to verify the performance of algorithms considering implementation issues. However, some implementations are also capable and specifically designed for real-time operation to consider implementation complexity.

3.3 Model-Based Design for Rapid Prototyping

The development of embedded systems consists of a prototyping phase for feasibility studies, testing and verification of final product. Prototyping of embedded software/hardware systems is essential as it shortens the path from specifications to the implementation on target hardware [18].

Embedded Systems development organizations are seeking to adopt Model-Based Design to take advantage of enhanced ability to deal with complexity, reduce time-to-market, reduced cost, and improved quality [19]. MATLAB, Simulink and various signal processing tools provide an

integrated workflow for verifying, prototyping and implementing wireless communication systems. Algorithm development for hardware targets involves converting the high-level concept codes into a version that uses low-level arithmetic or logical operations. Many rapid prototyping platforms are available such as DSP, FPGA, or mixtures of DSP and FPGA [20–22]. Various software simulation tools are provided by the manufacturer to ease the development of communication system. These tools can be integrated with MATLAB Simulink to provide a path from block diagram to system integration such as Xilinx System Generator and Link to CCS/Real-time workshop.

The ability to efficiently construct models combined with associated tools and systematic methodologies primes Model-Based Design for success by providing a complete solution that enables concurrent engineering, performance analysis, automatic test generation, building efficient specifications and execution models, code generation and optimization, and automatic refinement through different abstraction levels [23]. Following sections discuss the Mathworks model based design methodology, software simulation tools and design workflow for DSP and FPGA.

3.3.1 Mathworks Model-based Design

Model-Based Design is a systematic method to generate test cases from models of system requirements. It allows evaluation of requirements independent of algorithm design and developments. For embedded deployment automatic codes can be generated and test benches can be created for system verification using available processing tools. Model-Based Design [24] offers an efficient and cost-effective way to develop complex embedded systems for a variety of applications. Model-Based design involves using Computer Aided Engineering (CAE) Tools to simulate system behavior, verifying research requirements, designing system models, generating software for prototyping and continuous testing on hardware target throughout the development process.

Embedded C Code Generation and Verification (DSP)	HDL Code Generation and Verification (FPGA)
Embedded Target for TI C6000 DSP, Link for Code Composer Studio, Real-Time Workshop, Real-Time Workshop Embedded Coder, Stateflow Coder	Link for ModelSim, Filter Design HDL Coder Synplify DSP (Synplicity) Xilinx System Generator for DSP DSP Builder (Altera)

Table 3.1: MATHWORKS Products for Rapid Prototyping on DSP and FPGA

MATLAB provides various tools for Model-Based Design of FPGA and DSP. Table 3.1 lists MATHWORKS products for Embedded C-Code generation for DSP and HDL Code generation and verification for FPGA. Figure 3.3 shows the design methodology for Mathworks Model based

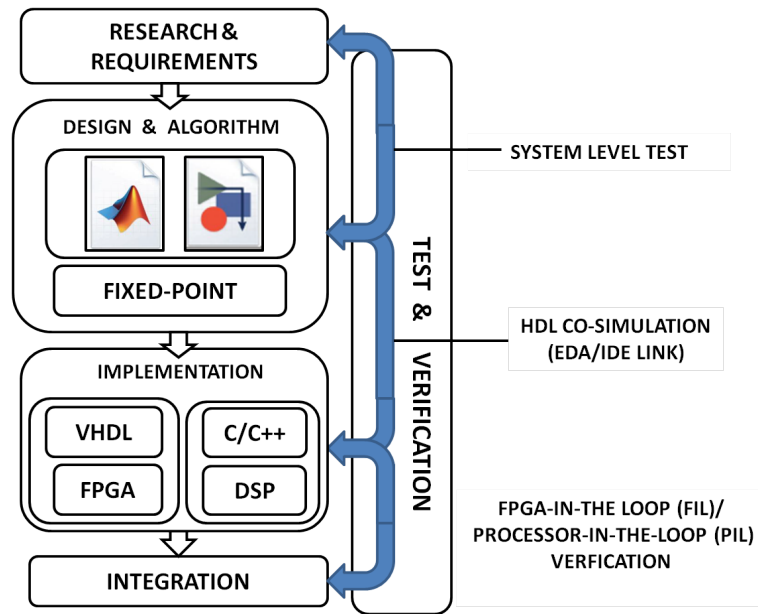


Figure 3.3: Model Based Design Methodology

design, the test and verification of algorithms developed for DSP and FPGA including the Hardware Co-simulation, test and verification on the target hardware.

3.3.2 MATLAB Design Tools for FPGA

Using FPGA for complex systems enables engineers to rapidly evaluate algorithm and architecture tradeoffs quickly. They can also test designs under real world scenarios without incurring the heavy time penalty associated with HDL simulators [25]. FPGA are used for prototyping ASIC workflows for hardware verification and early software development. To improve the performance running high-throughput, high-performance applications, algorithm designers are increasingly using FPGAs to prototype and validate innovations instead of using traditional processors [26]. However, many algorithms are implemented in MATLAB due to the simple-to-use programming model and rich analysis and visualization capabilities. For FPGA development, several design suites are available. Targeting at Xilinx FPGAs, three major players are well-known: Xilinx Corporation with its Integrated Software Environment (ISE) [27], Mentor Graphics Corporation with its FPGA advantage suite [28], and Synplicity Inc. with its synthesis and verification solutions [29]. Model-Based Design using HDL code generation enables engineers to efficiently produce FPGA prototypes.

The process for translating MATLAB designs to FPGA target hardware consists of following steps:

- 1) Model the algorithm in MATLAB Simulink
- 2) Convert the model to Fixed point using Fixed point Toolbox

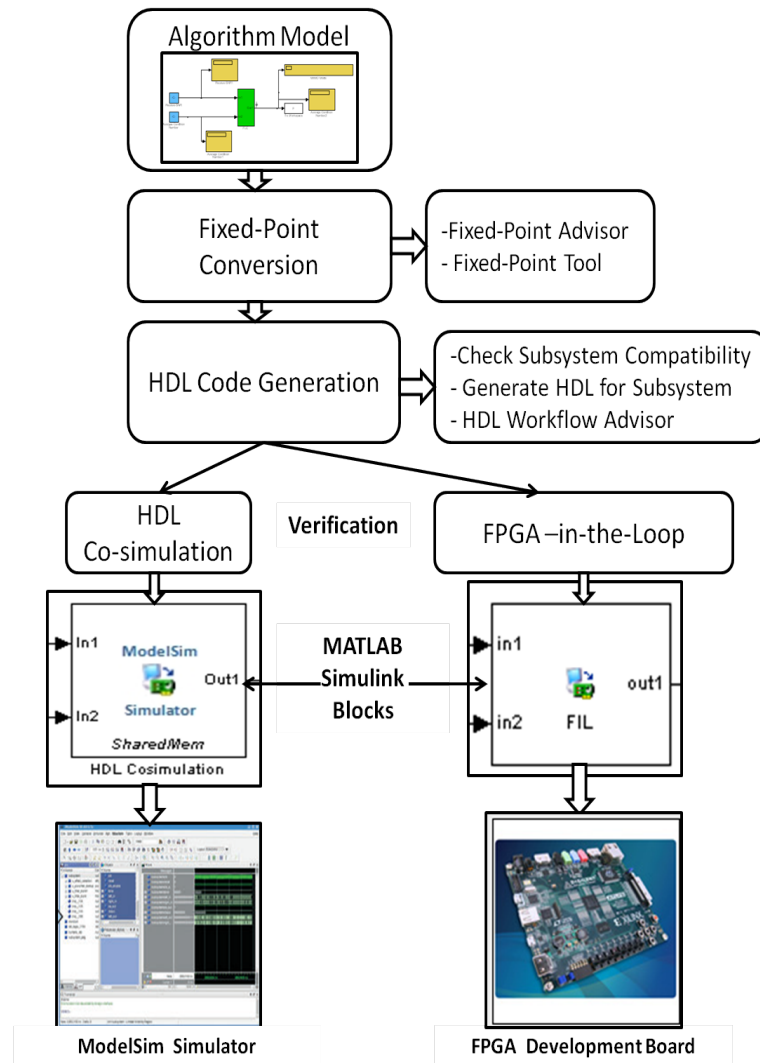


Figure 3.4: Programming and Verification steps for FPGA

- 3) Use HDL Workflow Advisor to generate the HDL code of the algorithm
- 4) Use HDL Co-simulation Wizard with Modelsim for HDL Verification
- 5) Use FPGA-in-the-Loop to download the code to target, for testing and verification in loop.

Figure 3.4 shows the steps for Programming FPGA using HDL coder Workflow Advisor. Electronic Design Automation (EDA) Simulator Link [30] Toolbox provides a co-simulation interface between MATLAB Simulink and HDL simulator Mentor Graphics ModelSim. Using EDA Simulator Link we can verify a VHDL implementation against Simulink model or MATLAB algorithm. HDL co-simulation enables engineers to reuse Simulink models to drive stimuli into the HDL simulator and perform system-level analysis of the simulation output interactively. While HDL simulation provides only digital waveform output, HDL co-simulation provides complete visibility into

the HDL code, as well as access to the full suite of system-level analysis tools of Simulink. When engineers observe a difference between expected results and HDL simulation results, co-simulation helps them to better understand the system-level effect of the mismatch.

FPGA based verification (also referred to as FPGA-in-the-loop (FIL) simulation) of the algorithm increases confidence that the algorithm will work in the real world. Implementation of HDL code on FPGA boards to enable FIL verification for running test scenarios faster. This approach ensures that the algorithm will behave as expected in the real world. This enables engineers to run test scenarios faster than with host-based HDL simulation.

3.3.3 MATLAB Design Tools for DSP

For DSP-based development [31], Mathworks offers with Simulink and the Real-Time Workshop (RTW) [32] a seamless tool for fast prototyping in DSP based systems. This approach also offers the possibility of hardware-in-the-loop simulation, where parts of the application may run on the target DSP and others run on the host computer. Other methodologies, such as The Mathworks Real-Time Workshop in combination with the Embedded Target for the TI TMS320C6000 DSP Platform [33] allow mapping a Simulink block diagram composed of pre-existing algorithm blocks to a single DSP. Texas Instruments (TI) Code Composer Studio (CCS) is an Integrated Development Environment (IDE) for TI embedded processors . It comprises of compilers for each TI's device families and suite of tools like source code editor, project build environment, debugger, real-time operating system for development and debugging the developed embedded applications.

As shown in Figure 3.5, the DSP Design flow for programming and verification of developed algorithm on DSP. For the algorithm developed in MATLAB Simulink, the C/C++ code is generated using Code Generation Tools and Embedded Coder Toolbox. Target Preference is set to the Texas Instruments Code Composer Studio and the DSP Target Board used for verification.

Once the C code is generated and the subsystem for the algorithm is created, Software-in-the-Loop (SIL) or Processor-in-the-Loop (PIL) is performed for verification. With SIL simulation, we can verify the behavior of source code of the developed algorithm on the host computer. In SIL mode, the simulink executes the referenced model by generating the production code using the model reference target preference set in the model. The code is compiled in the C Compiler and verification is carried out. SIL mode is a convenient option to verify the code when the target hardware is not available. With PIL simulation, we can verify the compiled object code that we want to deploy, the object code runs on the real target hardware or on instruction set simulator. In PIL mode, the C code generated for the algorithm model is cross-compiled and executed on the

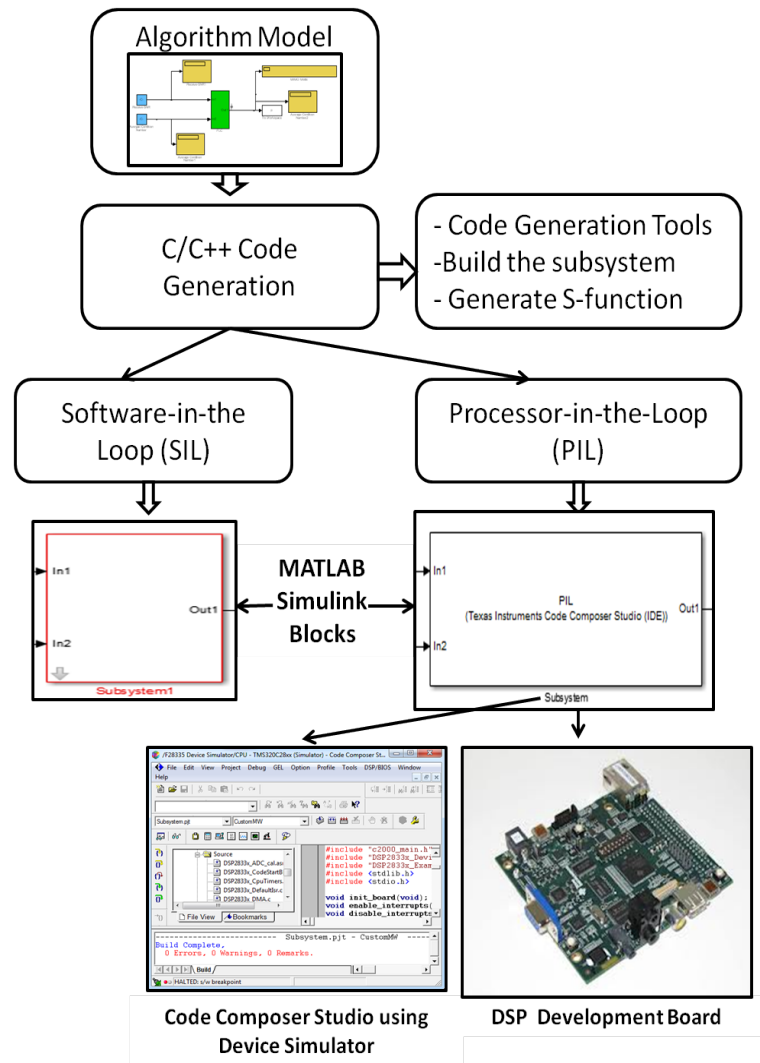


Figure 3.5: Programming and Verification steps for DSP

target processor or an equivalent instruction set simulator.

3.4 Case Study: Wireless control of FTE Robot

Wireless communication systems have range of applications for mobile robots. It includes industrial applications, agricultural robotics applications, underwater applications, and numerous military applications [34]. Wireless Sensor Networks are developed for search and rescue applications, with the use of mobile robot integrated with wireless camera [35]. Wireless control of mobile robot is done by Radio frequency (RF) Communication. Numerous wireless technologies like Zigbee and Bluetooth can be used to control the robot through remote computer, joystick etc. Here an attempt has been made to control Mobile Robot using wireless modules, to gain in-depth knowledge about wireless concepts and implementation challenges of working with practical wireless applications.

The Faculty of Technology and Engineering (FTE) Robot is a mobile device which has features like Line Follower and Maze Follower. The Robot is featured around C8051F340 microcontroller, which is reprogrammed to establish a wireless communication link between Robot and remote computer. Specific commands are generated to control the movements of Robot. It is possible to control two robots simultaneously by control commands from remote computer. This section discusses the design and implementation of Wireless control of FTE robot through remote computer. It gives overview of the FTE Robot and Wireless module specifications.

3.4.1 Overview of FTE Robot

FTE robot, as shown in Figure 3.6, is developed by Mr. Jagdish Sanghani for educational purpose for Department of Electrical Engineering, Faculty of Technology and Engineering, The Maharaja Sayajirao University of Baroda, India. The robot can be used for research in Embedded systems and Robotics. It focuses on the microcontroller C8051F340A [36] from SILABS. Figure 3.7 shows the back view of the FTE Robot with all the hardware connections.



Figure 3.6: Front View of FTE Wireless Robot



Figure 3.7: Back View of FTE Wireless Robot

The specifications of various components in FTE Robot is listed in Table 3.2. The robot con-

Components	Specifications
C8051F340A	8051-compatible microcontroller core, 64 kB Flash, ADC,SMBus, 6x PWM 2x UARTs, I2C, SPI, Four general purpose 16-bit counter/timers,
I2C based LCD	16x2
Micro metal Geared DC motors	Gear ratio-30:1, Free-run speed at 6V: 440 rpm
IR Sensor	Tolerance of + -0.15mm.
LEDs	Green, Red and Blue.
Full-Bridge Motor Driver	peak output currents up to + -2.8 A and operating voltages up to 36 V
PIZO Sounder	Sound Output 90(dB Min Typ)
On-board battery	3AAA batteries (1.5V each)

Table 3.2: FTE Robot Specifications

sists of various components like IR sensors, micro metal geared motors, I2C based Liquid Crystal Display (LCD), Pizo sounder, user pushbuttons, Light Emitting Diode (LED) and various other components. It consists of on-board Joint Test Action Group (JTAG) debugger for testing the robot operation using HyperTerminal. It also consists of LEDs to show the ON/OFF status of the power supply.

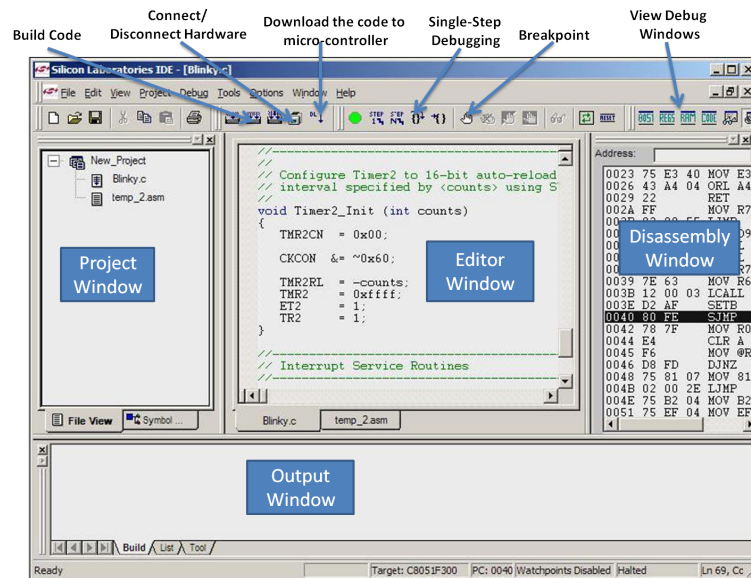


Figure 3.8: Snapshot of SiLabs IDE

The FTE robot is programmed using Silabs IDE, which has Keil C compiler [37, 38]. The snapshot of the Silabs IDE is as shown in Figure 3.8. Using the IDE the programs can be debugged, and downloaded to the micro-controller using USB Debug Adapter. All the programs to control the

Robot movements, motors speed and the direction of motors are written in C language [39]. The testing of the programs is done using the Hyperterminal [40] connected to the Robot for debugging purpose. Functions are written for each command and they are executed using the main file. The program is initially tested on C8051F34X Development Kit [41].

3.4.2 Wireless Module

The wireless module is a general-purpose programmable module, which features 2.4 GHz radio and Universal Serial Bus (USB) from Pololu Robotics and Electronics [42]. The wireless module is based around the CC2511F32 microcontroller from Texas Instruments [43], which has an integrated radio transceiver, 32 KB of flash memory, 4 KB of RAM and USB interface. Table 3.3 lists the Technical Specifications of wireless module. The Wireless module can be connected using USB connection to configure the module and to transmit and receive data. USB connection also provides power to the module.

CC2511F32	2.4 GHz system-on-chip (SoC), 32 kB of Flash, 4 kB of RAM 8051 MCU, 7 12 bit ADC, Two USARTs.
Radio	Frequency: 2400 2483.5 MHz, with 256 channels Range: approximately 50 feet (under typical conditions indoors) Bit rate: programmable, up to 350 kbps Effective data rate: up to 10 KB/s
Operating current	up to approximately 30 mA
Operating voltage	2.76.5 V

Table 3.3: Technical Specifications of wireless module

Wireless module is connected to the micro-controller using UART for serial communication. Figure 3.9 shows the FTE Robot with the Wireless module connection. The Wireless Module is connected to the Robot with UART and power supply connections. To connect micro-controller to wireless module, GND, TX and RX connections are made to establish a connection link between FTE Robot and wireless module for communication as shown in Figure 3.10. The wireless module is configured using Wixel Configuration Utility. We can read, write or configure wixel module using this utility. Using Application Configuration the specifications like baud rate, serial mode and radio channel is configured. For this particular application, Wireless Serial Application is used to control robot using remote computer.

Wireless Serial application connects two wireless modules together to make a wireless bidirectional link. It uses RF bit rate of 350 kbps and can reach a range of approximately 50 feet under

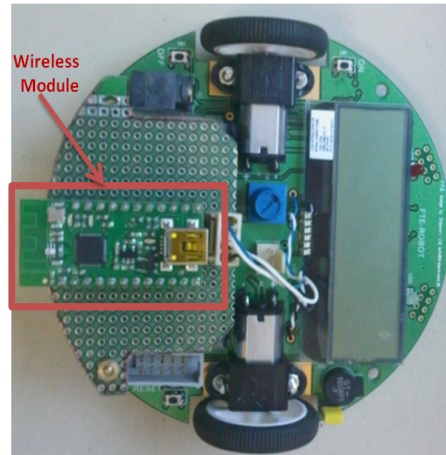


Figure 3.9: FTE Robot with Wireless module connection

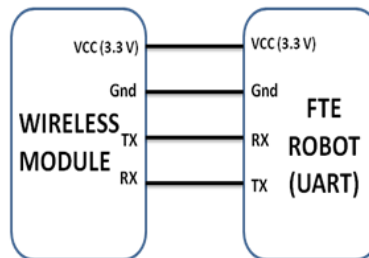


Figure 3.10: Connections between FTE Robot and Wireless Module

typical indoor. conditions. Applications for wireless module can be developed using Eclipse IDE for C/C++ Developers.

The programming of Wireless Module was done in Eclipse IDE [44]. The Wireless Serial Application was used to control robot movements. Pololu Wixel Configuration Utility as shown in Figure 3.11 shows the snapshot of Wixel Configuration Utility, with the App configuration for the Wireless Serial Application. Baud rate is set to 9600 and the radio channel is set to 128. Serial mode 0 is selected which is the Auto-Detect Serial mode and it automatically choose the serial mode based on how the module is being powered. Various parameter like baudrate and radio-channel parameter are adjusted. For this particular case study the baud rate of the transmitter, receiver wireless modules and that of robot's UART is set to 9600 bps.

3.4.3 Implementation

Once the FTE Robot and the wireless modules are programmed, the entire system is implemented as shown in Figure 3.12. The FTE Robot movements in desired direction is controlled by the commands from the wireless module. The transmitter wireless module which gives direction to robot is connected to the USB port of remote computer. The movement of robot is controlled by

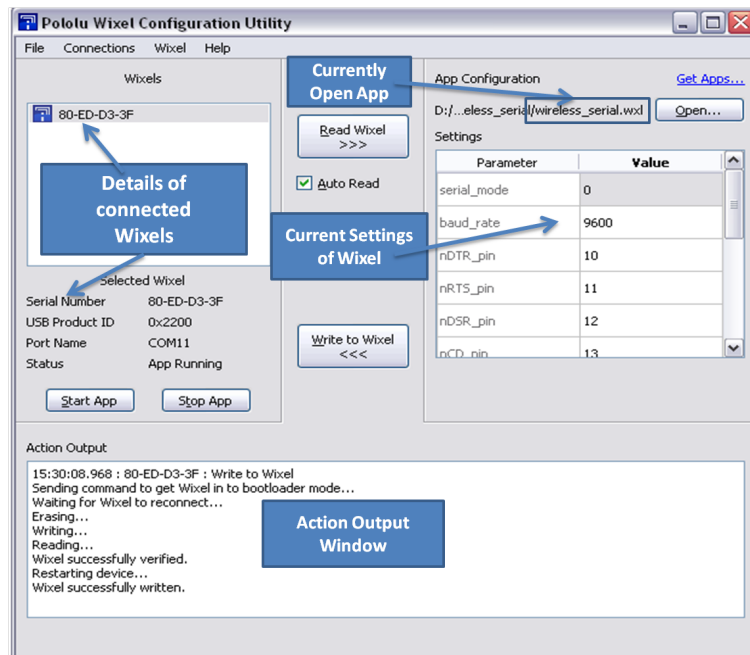


Figure 3.11: Snapshot of Pololu Wixel Configuration Utility

controlling the direction and speed of motors which control the wheel motion. The commands are given with the help of numeric keypad and the list of commands is listed in Table 3.4. The receiver wireless module is connected to the FTE robot through UART as discussed in Section 3.4.2.

To remotely control robot from remote computer, Wireless Serial application is used [45]. It turns pair of wireless modules into wireless USB/TTL serial link for communication between a remote computer and a micro-controller (in our case c8051F340 on FTE Robot).

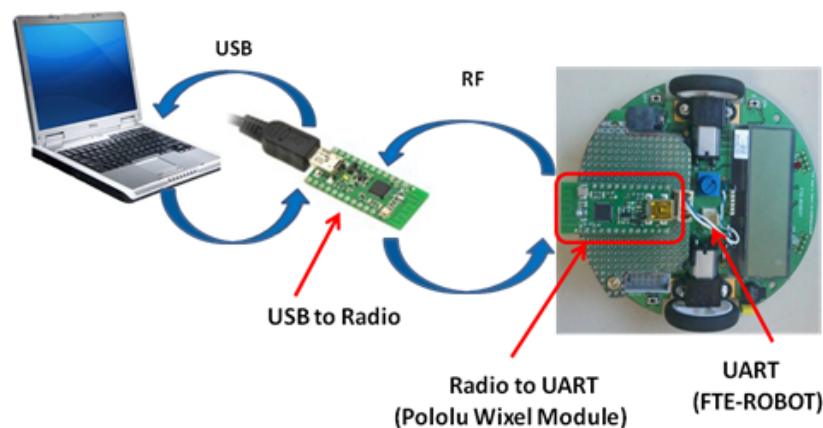


Figure 3.12: Implementation of Wireless Control of FTE Embedded Robot

Using the wireless module the remote computer is successfully able to control the FTE Robot movements. The commands for the Direction, Start and Stop for robot are successfully working.

Commands From PC	Operation By Robot
0	Robot-Reverse
1	Robot-45-degree-Left
2	Robot-180-turn
3	Robot-45-degree-Right
4	Robot-left-turn
5	Robot-stop
6	Robot-right-turn
7	Robot-90-Degree-left-turn
8	Robot-Forward
9	Robot-90-Degree-right-turn

Table 3.4: List of Commands to control FTE Robot

When two FTE Robots are connected with wireless modules, both robots are simultaneously controlled by only single remote computer commands. Wireless Networks with more than two FTE robots can be remotely controlled by remote computer. Also two robots can communicate with each other and transfer of data can be achieved. As further development, for search and rescue operation application camera and voice recorder can be embedded on the robot.

3.5 Concluding Remarks

This chapter discusses the system design methodology flow for designing Wireless Platform for experimental evaluation of developed algorithms. Rapid prototyping of MATLAB based model based design for algorithm implementation on DSP and FPGA is briefly described. MATLAB based PIL Simulation for DSP and FIL Simulation for FPDA design and development is described. PIL and FIL modes are used in this research work for verification of optimization algorithms developed for MIMO Wireless Communication System. Wireless Control of FTE Robot was carried out, and their design flow and steps are discussed in the chapter. The practical implementation of Wireless System gave technical experience and knowledge to author to work with Wireless Communication Systems.

Long Term Evolution-Advanced: Downlink Physical Layer

4.1 Introduction

The International Telecommunications Union (ITU), the organization that sets the international standards for next-generation mobile technology, introduced family of standards for 3G termed as International Mobile Telecommunications-2000 (IMT-2000). It included systems like Universal Mobile Telecommunication System (UMTS), CDMA 2000, GSM Evolution-EDGE [1]. International Telecommunications Union-Radio communications sector (ITU-R) specified a set of requirements for 4G standards, termed as International Mobile Telecommunications-Advanced (IMT-Advanced). IMT-Advanced mobile systems provide access to wide range of telecommunication services including advanced mobile services, supported by mobile and fixed networks, which are increasingly packet-based [2]. In 2012, ITU approved the specifications for IMT-Advanced, and determined that LTE-Advanced and Wireless MAN-advanced (WiMAX2) should be accorded the official designation of IMT-Advanced [3].

The 3rd Generation Partnership Project (3GPP) unites telecommunications standard development organizations, known as Organizational Partners. The scope of 3GPP is to prepare, approve and maintain globally applicable Technical Specifications and Reports for a 3rd Generation Mobile System based on the evolved GSM core networks, and the radio access technologies (i.e UTRA for Frequency Division Duplex (FDD) and Time Division Duplex(TDD) modes). The success of 3GPP subsequently lead organizations to the development of GSM, GPRS and EDGE technical specifications and reports. Recently it has completed the development of the 3GPP LTE and LTE-Advanced technical specifications and reports [4].

The 3GPP has developed specifications for mobile technologies from GSM to LTE-Advanced, differentiated by releases [5]. The first 3GPP release of the UMTS standard took place in 1999. Since then number of 3GPP radio access technologies and systems were released, each adding further functionality. 3GPP releases, their respective freeze year and Specifications are summarized in Table 4.1.

Each progressive 3GPP radio access technologies provides a high degree of continuity in the evolving systems by delivering higher data rates, quality of service and cost efficient. 3GPP introduced evolution of 3G System in 2008, Release-8 termed as Long Term Evolution (LTE) towards the need of IMT-2000. The advanced version of LTE termed as Long Term Evolution-Advanced (LTE-A) was introduced in Release 10 which satisfies the requirement for IMT-Advanced.

3GPP Release	Technology	Freeze Year
Release 99	Specified first UMTS 3G networks: W-CDMA	March 2000
Release 4	TDD	March 2001
Release 5	Introduced HSDPA	March - June 2002
Release 6	HSUPA, MBMS	December 2004 - March 2005
Release 7	HSPA+ Improvements to QoS and EDGE Evolution	December 2007
Release 8	LTE OFDMA, MIMO based radio interfaces	December 2008
Release 9	LTE Enhancements	December 2009
Release 10	LTE-A fulfills IMT-Advanced 4G requirements	March 2011
Release 11+	Further LTE Enhancements	September 2012

Table 4.1: 3GPP release of radio access technologies

To achieve the target data rate of LTE and eventually 4G, many new techniques are necessary. Multiple-Input Multiple-Output (MIMO) is one key technique among them because of its ability to enhance the radio channel capacity of cellular systems at no extra cost of spectrum.

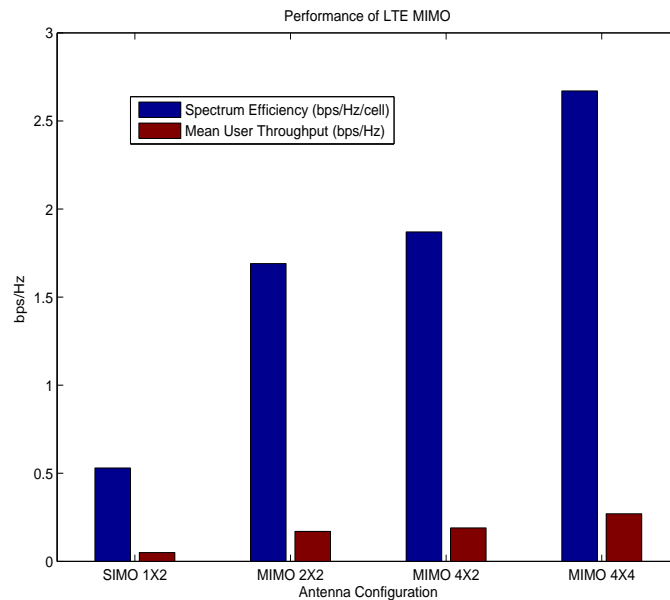


Figure 4.1: Performance of LTE MIMO with different antenna schemes

LTE-A downlink performance evaluation for MIMO configurations (2x2 and 4x4) are compared based on LTE Requirements [6]. As shown in Figure 4.1, Spectrum efficiency and Mean User throughput, increases as the number of antennas at transmitter and receiver increases in MIMO

configuration. The Spectrum efficiency of SIMO with 1x2 configurations is 0.53 bps/Hz/cell and that of 2x2 is 1.69 bps/Hz/cell and 2.67bps/Hz/cell for 4x4. The Mean User throughput (bps/Hz) analysis is also shown. The results are for 20 MHz bandwidth, 64 QAM modulations and FDD mode.

4.2 E-UTRAN Architecture and Protocol Stack

The network architecture of LTE is as shown in Figure 4.2 comprises of following components [7](Chapter 2):

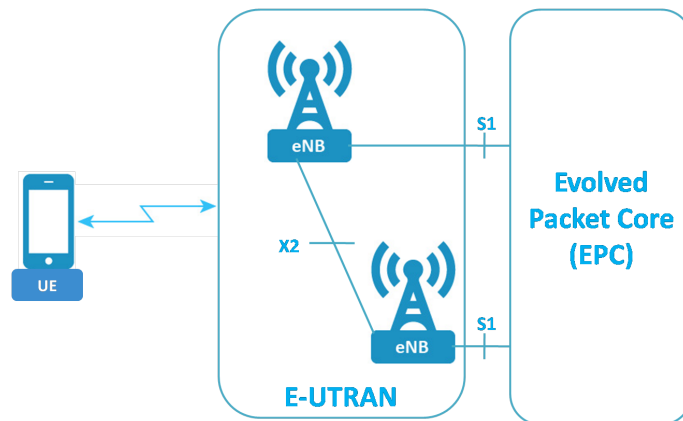


Figure 4.2: E-UTRAN Architecture

- User Equipment (UE): The internal architecture of the user equipment for LTE is identical to that in UMTS and GSM, which is basically a Mobile Equipment.
- Evolved-UMTS Terrestrial Radio Access Network (E-UTRAN): The E-UTRAN handles the radio communications between the mobile and EPC and consists of evolved base stations, called eNodeB. Each eNB connects with EPC by means of S1 interface and connected to nearby eNB by the X2 interface, which is mainly used for signaling and packet forwarding during handover.
- Evolved Packet Core (EPC): The EPC consists of components like Mobility Management Entity (MME), Serving Gateway (S-GW) and Packet Data Network (PDN) Gateway(P-GW).

The E-UTRA radio interface protocol architecture is as shown in Figure 4.3 consists of three layers [8]:

Layer 1: Physical Layer (PHY)

Layer 2: Medium Access Control (MAC)

Layer 3: Radio Resource Control (RRC)

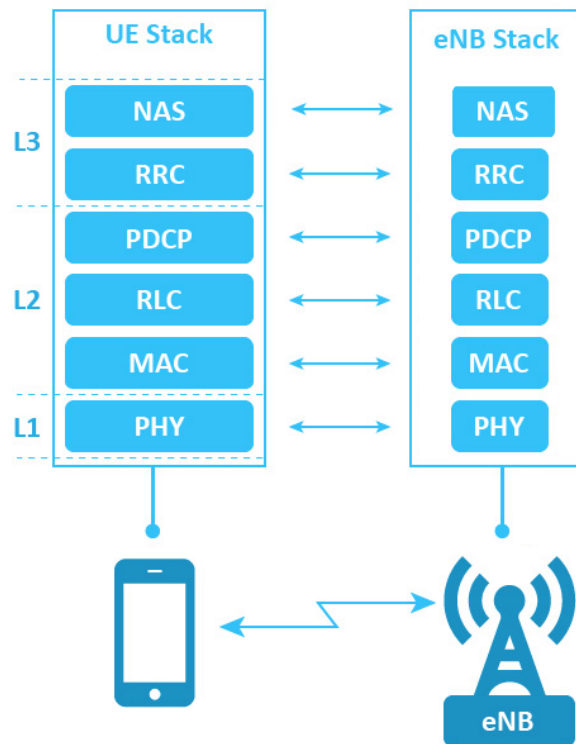


Figure 4.3: E-UTRA radio interface protocol architecture

The physical layer interfaces the MAC, sub-layer of Layer 2 and the RRC, Layer of Layer 3. The Physical (PHY) layer is the basis of base station-to-mobile device connectivity. The PHY interfaces with Layer 2 and Layer 3 and offers data transport services to higher layers. The multiple access scheme for the LTE physical layer is based on Orthogonal Frequency Division Multiplexing (OFDM) with cyclic prefix (CP) in the downlink, and on Single-Carrier Frequency Division Multiple Access (SC-FDMA) with cyclic prefix in the uplink.

The 3GPP TS 36.200 series describes the PHY Layer specifications. Layers 2 and 3 are described in the 3GPP TS 36.300 series. The services provided by each protocol stack and their features are listed below:

Non-Access Stratum (NAS) [9]

- Session management
- Mobility management
- Security procedures

Radio Resource Control (RRC) [10]

- System information handling
- Idle mode procedures handling
- Security management on radio interface
- NAS messages encapsulation and de-encapsulation and delivery to NAS protocols

Packet Data Convergence Protocol (PDCP) [11]

- User Plane (UP) path features: ciphering, robust header compression (ROHC)
- Control Plane (CP) path features: ciphering, integrity
- In-sequence delivery to higher layers
- Re-transmissions handling at handover

Radio Link Control (RLC) [12]

- Transparent Mode (TM) features: buffering
- Unacknowledged Mode (UM) features: segmentation / concatenation of SDUs, buffering
- Acknowledged Mode (AM) features: error correction handling through ARQ, segmentation / concatenation and re-segmentation of SDUs, buffering
- In-sequence delivery to PDCP, duplicate detection and discarding

Medium Access Control (MAC) [13]

- Mapping between logical channels and transport channels
- Interface towards PHY and RLC
- Logical channels multiplexing and priority handling
- Resource allocation and link adaptation
- HARQ and RACH processing
- Feedback creation and processing

PHY abstraction (MAC-PHY interface)

- Data transfer
- HARQ / DCI / UCI information exchange and feedback

- Sending of scheduling request
- Transport to Physical channels mapping

LTE downlink PHY processing accepts data and control streams from MAC Layer in the form of transport blocks. Transmission with MIMO is supported with configurations in the downlink with two or four transmit antennas in Release 8 and upto eight transmit antennas in Release 10 and two or four receive antennas in Release 8 and upto eight receive antennas in Release 10, which allow multi-layer transmissions with up to four streams or eight streams respectively [8, 14]. The 3GPP Physical Layer specification for the LTE and LTE-A radio technology is given in specification 36 series. The list of various Technical Specifications and Reports are given in Table 4.2.

Specification Number	Contents
TS 36.201	E-UTRA; LTE physical layer; General description
TS 36.211	E-UTRA; Physical channels and modulation
TS 36.212	E-UTRA; Multiplexing and channel coding
TS 36.213	E-UTRA; Physical layer procedures
TS 36.214	E-UTRA; Physical layer; Measurements
TR 36.912	Feasibility study for Further Advancements for E-UTRA (LTE-A)
TR 36.913	Requirements for further advancements for E-UTRA (LTE-A)

Table 4.2: 3GPP LTE Physical Layer Specifications and Reports

4.3 LTE Downlink Physical Layer

4.3.1 LTE Frame and Subframe Structure

In LTE, the uplink and downlink transmissions are organised into radio frames of 10ms, consisting of 10 subframes, each consisting of OFDM symbols. Two radio frame structures are supported:

- Type 1, applicable to FDD,
- Type 2, applicable to TDD.

In Frame Structure Type 1 (FDD), radio frame contains downlink or uplink subframes depending on link directions. The uplink and downlink transmissions have different bandwidths, i.e they are separated in frequency domain. Each radio frame is 10ms long and consists of 20 slots of length 0.5ms each, numbered from 0 to 19. Each slot of radio frame consists of 7 OFDM Symbols. OFDM Symbols consists of Cyclic prefix for timing and synchronization of signals. Detailed timing and samples of CP and OFDM Symbols are as shown in Figure 4.4.

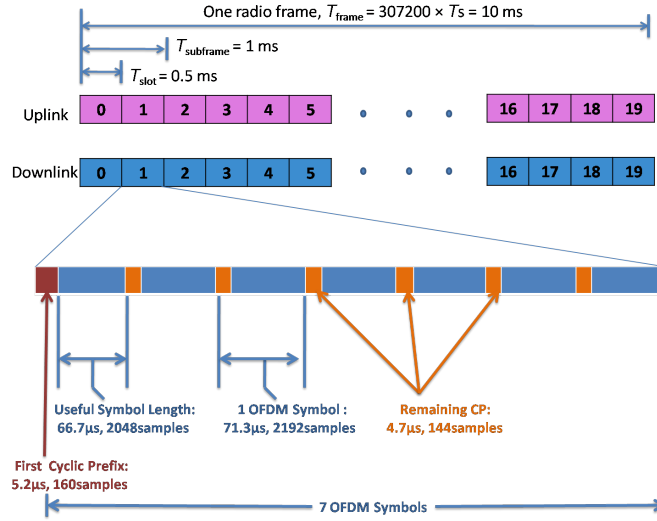


Figure 4.4: Frame Structure Type 1 (FDD)

4.3.2 Downlink Slot Structure

In Downlink, the transmitted signal in each slot of 0.5ms is described by a resource grid of $N_{RB}^{DL} N_{SC}^{RB}$ subcarriers and N_{symp}^{DL} OFDM symbols [14]. The parameters for Downlink resource grid for transmission bandwidth of 1.4MHz are listed in Table 4.3. For multi-antenna transmission, there is one resource grid defined per antenna port. Each element in resource grid is defined by the index pair (k, l) in a slot where k and l are the indices in the frequency and time domain respectively.

Symbols	Definitions	Value
BW	Transmission Bandwidth	1.4MHz
T_s	Basic time unit	$\frac{1}{15000 \times 2048}$ seconds
T_{frame}	Radio Frame Duration	$307200 \times T_s = 10\text{ms}$
$T_{subframe}$	Subframe Duration	1ms
T_{slot}	Slot Duration	0.5ms
N_{Sym}^{DL}	Number of OFDM symbols in a downlink slot	7
N_{RB}^{DL}	Downlink bandwidth configuration	6
N_{SC}^{RB}	Resource block size in the frequency domain	12 subcarriers
(k, l)	Resource block size in the frequency domain	$k = 0$ to $k = N_{RB}^{DL} \times N_{SC}^{RB} - 1$ $l = 0$ to $l = N_{symp}^{DL} - 1$
Δf	Sub carrier spacing	15kHz

Table 4.3: LTE Downlink Resource Grid Parameters

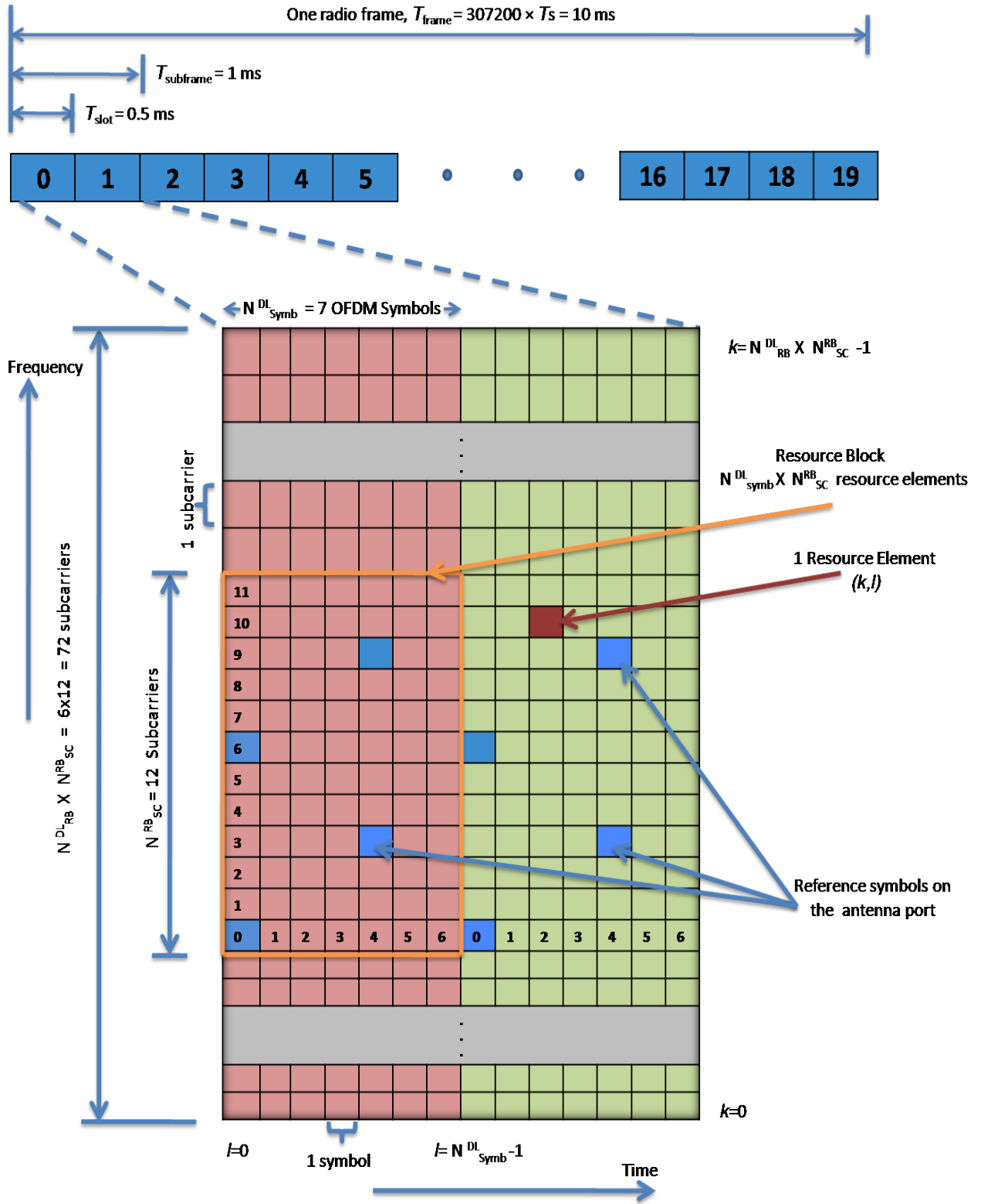


Figure 4.5: LTE Resource Grid

A physical resource block is made up of $N_{Sym}^{DL} \times N_{SC}^{RB}$ resource elements, corresponding to one slot in time domain and 180kHz in frequency domain. For 1.4 MHz bandwidth with Normal Cyclic Prefix. As shown in Figure 4.5, one slot consists of 7 OFDM symbols in time domain and 12 consecutive subcarriers in frequency domain.

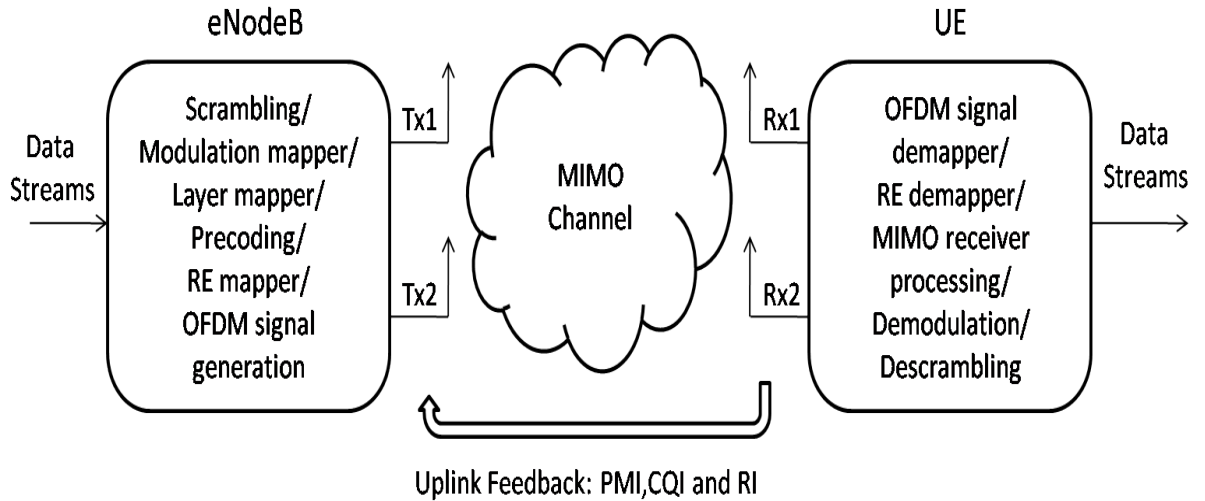


Figure 4.6: LTE Physical Channel Processing with Uplink Feedback

4.3.3 Downlink Physical Channel Processing

LTE physical layer is highly efficient for conveying both data and control information between an eNB and UE. Novel technologies such as multiplexing techniques, MIMO antenna schemes, duplexing schemes, flexible bandwidth, AMC schemes are employed to improve performance [14]. The uplink feedback values Channel Quality Indicator (CQI), Rank Indicator (RI) and Precoding Matrix Indicator (PMI) are calculated at the receiver, and is feedback to the eNodeB. The CQI performs selection of modulation scheme (QPSK, 16-QAM or 64 QAM). The RI gives information about the useful number of layers for layer mapping and PMI gives information regarding precoding matrix for the precoder [15–17].

Figure 4.6 shows LTE Downlink Physical channel processing for system with two antennas at eNodeB and UE each. The Physical channel processing consists of Scrambling, Modulation, Layer Mapping, Precoding, Resource Element Mapper and OFDM signal generation. The Layer Mapping and Precoding are for Multi-Antenna Processing. The MIMO Processing in Physical Downlink Shared Channel (PDSCH) Channel is briefly described in Figure 4.7.

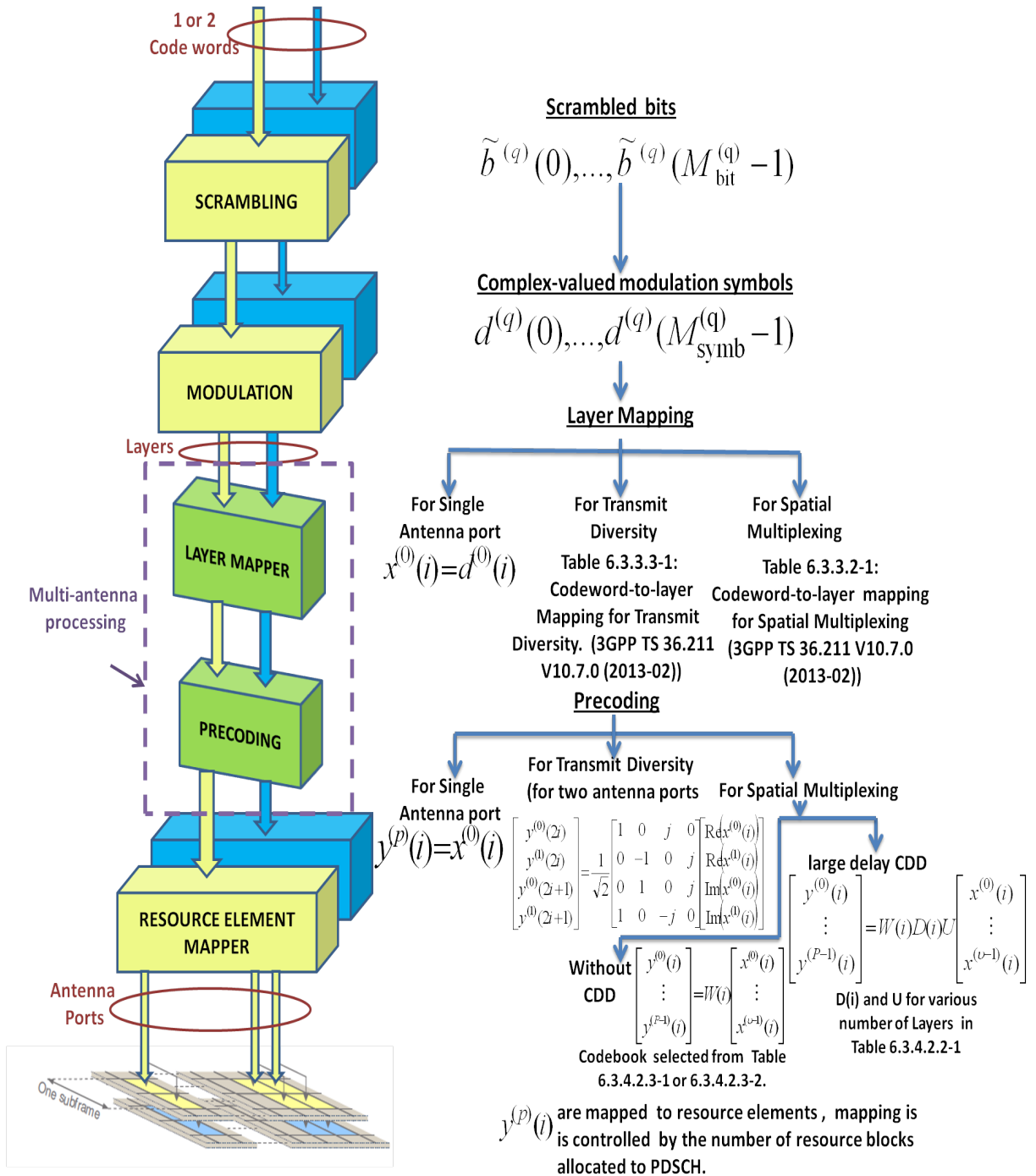


Figure 4.7: Downlink Physical Layer Processing

4.4 MIMO Downlink Transmission modes

MIMO technology is based on transmitting and receiving data streams with multiple antennas, utilizing uncorrelated communication channels. MIMO performance depends on number of parameters like number of transmit and receive antennas, reference signals, channel estimation techniques and feedback parameters from UE to eNB. LTE R8 and R9 support MIMO technology with upto 4 transmit and receive antennas in downlink. Release 10 extends MIMO support with upto 8 transmit and receive antennas. 3GPP LTE/LTE-A defines nine multi-antenna transmission modes (TMs) [18–21], listed in Table 4.4.

Mode	Release	Description
1	R8	Single Antenna Transmission
2	R8	Transmit Diversity
3	R8	Open Loop Spatial Multiplexing
4	R8	Close Loop Spatial Multiplexing
5	R8	Multi-User MIMO
6	R8	CLSM-Single Transmission Layer
7	R8	Beamforming
8	R9	Dual Layer beamforming
9	R10	Eight Layer Spatial Multiplexing

Table 4.4: LTE Transmission Modes

LTE/LTE-A supports various MIMO Transmission modes. The two main multi-antenna techniques, which have different performance gains and which are implemented in different ways are discussed below.

4.4.1 Transmit Diversity

Transmit Diversity mode achieves Spatial Diversity by transmitting redundant information sequences from multiple antenna ports. It uses only one codeword and the number of layers are equal to the number of antenna ports. Transmit Diversity uses Alamouti like coding for transmission of codewords. This mode is suitable for cell edge where the channel condition is complex and interference is large, or high-mobility or for low SNR situations [22]. Figure 4.8 shows 2x2 Transmit Diversity Transmission mode.

4.4.2 Spatial Multiplexing

Spatial Multiplexing mode achieves higher bit rates by transmitting multiple parallel data streams. It uses one or two codewords and the number of layers is less than or equal to number of antenna ports. The number of layers in Spatial multiplexing depends on the MIMO channel Rank. It is suitable for high UE mobility, for good channel conditions and provides high data transmission rate.

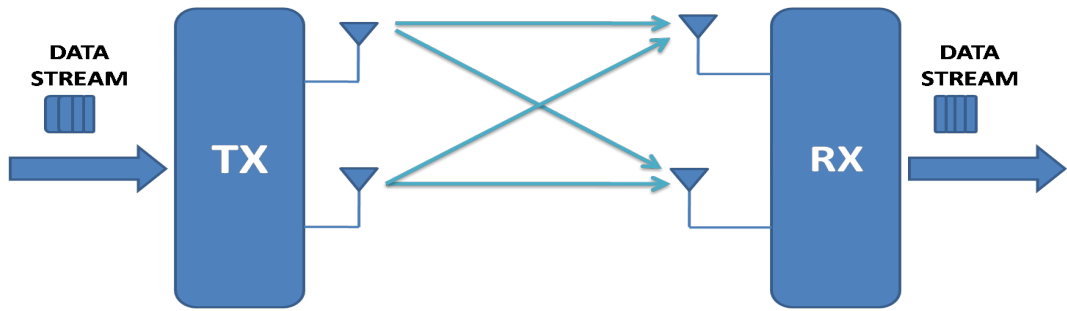


Figure 4.8: 2x2 Transmit Diversity Transmission Mode

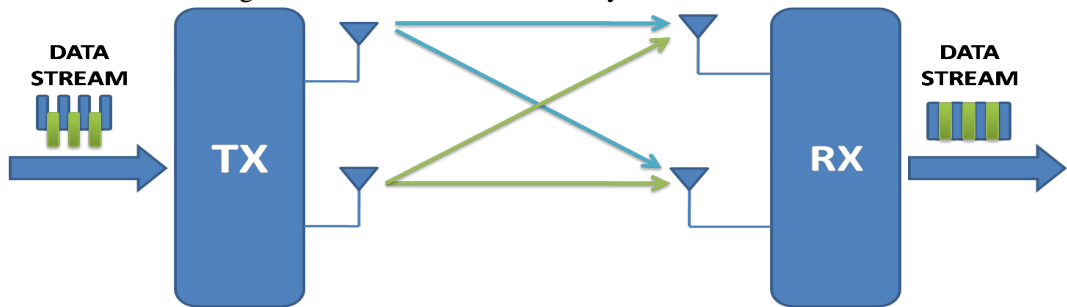


Figure 4.9: Open Loop Spatial Multiplexing

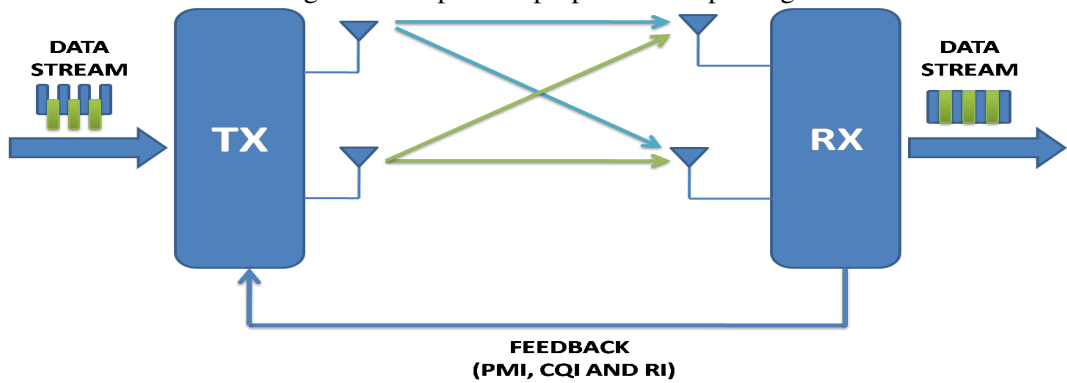


Figure 4.10: Close Loop Spatial Multiplexing

Figure 4.9 and 4.10 shows the concept of Open-Loop Spatial Multiplexing (OLSM) and Close-Loop Spatial Multiplexing (CLSM) Transmission modes respectively. The term closed loop in CLSM refers specifically to the loop that is created by feeding back the CQI, PMI and RI to eNB.

4.5 LTE-A Downlink Link Level Simulator

Vienna LTE-A Downlink Link Level simulator is a MATLAB-based link level simulation environment for 3GPP-LTE-A. The open source code of the simulator is available under an academic non-commercial use license [23, 24]. The LTE-A link level simulator consists of transmitting eNodeB, receiver User Equipments (UEs), a downlink channel model over which only the Physical Downlink Shared Channel (PDSCH) is transmitted, signaling information and an error-free uplink feedback channel with adjustable delay as shown in Figure 4.11. The eNodeB and UE are linked by the channel model, which is used to transmit the downlink data. The performance of Link Level Simulation can be analyzed using Bit Error Rate (BER), Block Error Rate (BLER) and Throughput (Mbps). The MATLAB-based Downlink Physical Layer (Link Level) simulator v1.1 [25, 26], consists of main files for performing simulation, saving and plotting the results, as listed in Table 4.5. The LTE-A simulator are implemented in MATLAB and require Communication Toolbox and Signal Processing Toolbox.

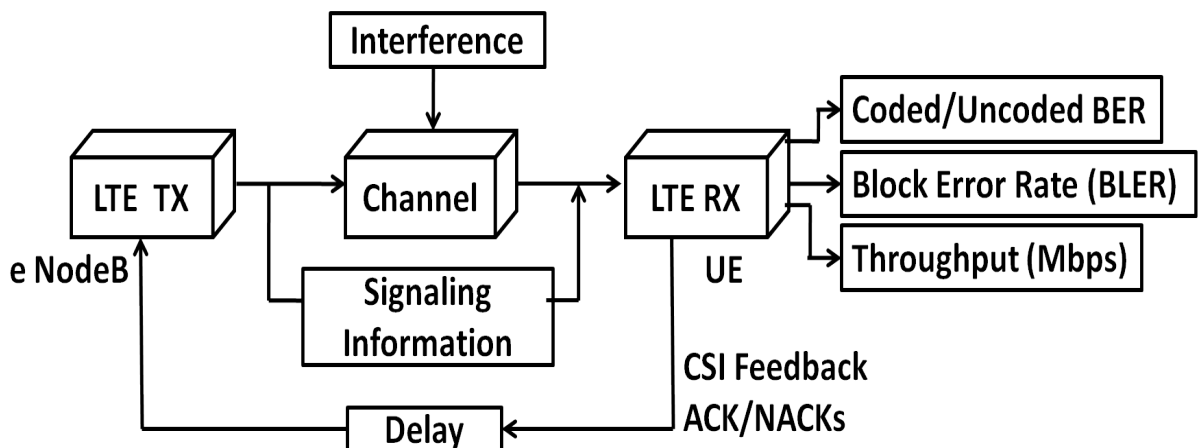


Figure 4.11: Structure of Link Level Simulator

Simulation Procedure	MATLAB Files
Run LTE Simulation	LTE_sim_main
Parallel Simulation	LTE_sim_main_par
Normal Simulation	LTE_sim_main_single
Plot Results	LTE_sim_result_plots
Load Parameters	LTE_load_parameters
Load dependent Parameters	LTE_load_parameters_dependent
Generate dependent Parameters	LTE_load_parameters_generate_elements

Table 4.5: LTE-A Downlink Link Level Simulator General Files

4.5.1 LTE Transmitter

LTE downlink transmission is based on Orthogonal Frequency Division Multiplex Access (OFDMA). The LTE downlink physical resources are represented by a time-frequency resource grid in which each resource element corresponds to one OFDM subcarrier during one OFDM symbol interval. These resource elements are grouped into Resource Blocks (RBs) as shown in Figure 4.5. Physical Downlink channel processing for LTE-A is briefly discussed in Section 4.3.3. The LTE Downlink Transmission steps and their related MATLAB function files of LTE-A Downlink Link Level Simulator are listed in Table 4.6.

Steps for LTE Transmitter	Matlab Files, functions and parameters
Generation of the transmit signal	LTE_TX
Read pregenerated reference signals	LTE_common_gen_Reference_Signal
Generation of other channels	LTE_common_gen_PBCH, LTE_common_gen_PDCCH
Generation of synchronization signals and Initialization of signals	LTE_common_gen_Synchronization_Signal
Scheduler	UE_MCS_and_scheduling_info
Add the scheduler information to the downlink channel	UE_MCS_and_scheduling_info(uu)
Get what HARQ process was assigned to this TX	UE_output(ue_num).HARQ_process
Get the number of data and coded bits from the scheduler	UE_MCS_and_scheduling_info(uu). N_coded_bits(cw)
Generate data bits	tx_data_bits
Coding of the bits	LTE_tx_turbo_encode, LTE_tx_turbo_rate_matcher, LTE_tx_DLSCH_encode
Scrambling of the bits	LTE_common_scrambling
Symbol mapping	LTE_params.SymbolAlphabet
Layer mapping	LTE_common_layer_mapping
Determination of Codebook index	LTE_common_gen_8TX_codebook
Pre-Coding	LTE_precoding, LTE_tx_precoding, LTE_common_get_precoding_matrix
OFDM symbol assembly	CHmapping, PrimMapping and SecMapping
Zero padding, IFFT, add CP	LTE_params.Index_TxCyclicPrefix
Mapping of antenna port to antenna	LTE_map2antenna

Table 4.6: LTE Transmitter Steps and related MATLAB Function Files

4.5.2 Channel Model

The LTE-A Downlink Link Level Simulator supports block and fast-fading channel filtering. In the block-fading case, the channel is constant during the duration of one subframe (1 ms). In the fast-fading case, time-correlated channel impulse responses are generated for each sample of the transmit signal. The frequency-selective channels are modeled by the ITU and 3GPP Power Delay Profiles (PDPs). The LTE-A Link Level Simulator supports various channel models as listed in Table 4.7: The channel models are as defined for the ITU-R evaluation of IMT-2000 [27].

Channel Models	Abbreviations
VehA	Vehicular A
VehB	Vehicular B
PedA	Pedestrian A
PedB	Pedestrian B
PedBcorr	Pedestrian Correlated B
AWGN	Additive White Gaussian Noise
flat Rayleigh	Rayleigh Flat Fading
flatraycorr	Rayleigh Flat Fading Correlated
TU	Typical Urban
RA	Rural Area
HT	Hilly Terrain
Winner-II	Winner Channel Model

Table 4.7: Channel Models

The MATLAB files which generate the channel matrix and channel noise are listed in Table 4.8

Channel Model	MATLAB Files
Generate channel matrix	LTE_channel_matrix
Filter the output of transmitter and add noise	LTE_channel_model

Table 4.8: LTE Channel Model Generation MATLAB Function Files

4.5.3 LTE Receiver

Each UE receives the signal transmitted by the eNodeB and performs the reverse physical-layer processing of the transmitter. The Receiver processing consists of steps as shown in Table 4.9. LTE-A requires UE feedback to adapt the transmission to the current channel conditions. The LTE-A standard received signal specifies three feedback indicators for that purpose: CQI, RI, and PMI. The CQI is employed to choose the appropriate Modulation and Coding Scheme (MCS), such as to achieve a predefined target BLER, whereas the RI and the PMI are utilized for MIMO pre-processing.

Steps for Receiver	Matlab Files and Parameters
Receive signal, demodulate and decoding	LTE_RX
Introduce carrier frequency offset	LTE_params.introduce_frequency_offset
Read pregenerated reference signals	LTE_params.Reference_Signal
Generation of synchronization signals and Initialization of signals	LTE_params.usePBCH, LTE_params.usePDCCH, LTE_params.Sync_Signal
Carrier Frequency Offset Compensation	LTE_rx_freq_sync
Remove CP, FFT, remove zeros	LTE_params.Index_RxCyclicPrefix LTE_params.NfftCP, fft
Disassemble reference symbols	RefMapping
extract the signal on pilots positons	
Channel and noise estimation	LTE_channel_estimator
Disassemble symbols	CHmapping, PrimMapping and SecMapping
Perform detection	LTE_detecting
Undo layer mapping	LTE_get_user_layers
Demapper	LTE_demapper
Descrambling of the bits	LTE_common_scrambling
Decoding of the bits	LTE_rx_DLSCCH_decode LTE_rx_turbo_decode, LTE_rx_turbo_rate_matcher
Precoding feedback calculation	LTE_feedback

Table 4.9: LTE Receiver Steps and related Matlab Function Files

The MATLAB based Vienna LTE-A Link Level Simulator is briefly discussed in this section. The Simulator is used in this research work to carry out the performance analysis in terms of BLER and Throughput for various MIMO Transmission Modes. The Simulation results and concluding remarks are presented in following section.

4.5.4 Simulation Results

Throughput Analysis of various MIMO Antenna configuration for LTE-A Downlink Physical Link Layer is as shown in Figure 4.12. Throughput of LTE-A Link layer increases as the number of antenna increases from 2x2 to 4x4 and to 8x8. Comparative Performance analysis for various MIMO Transmission modes were performed using MATLAB based LTE-A Link Level Simulator. Table 4.10 shows the Simulation Parameters used for the simulation.

As shown in Figure 4.13 (a) the SISO is compared with Transmit Diversity Scheme for 2x1 and 4x2 antenna scheme. At 30dB, throughput of SISO is 5.043 Mbps which is higher than that of 2x1 (4.869Mbps) and 4x2 (4.616 Mbps).

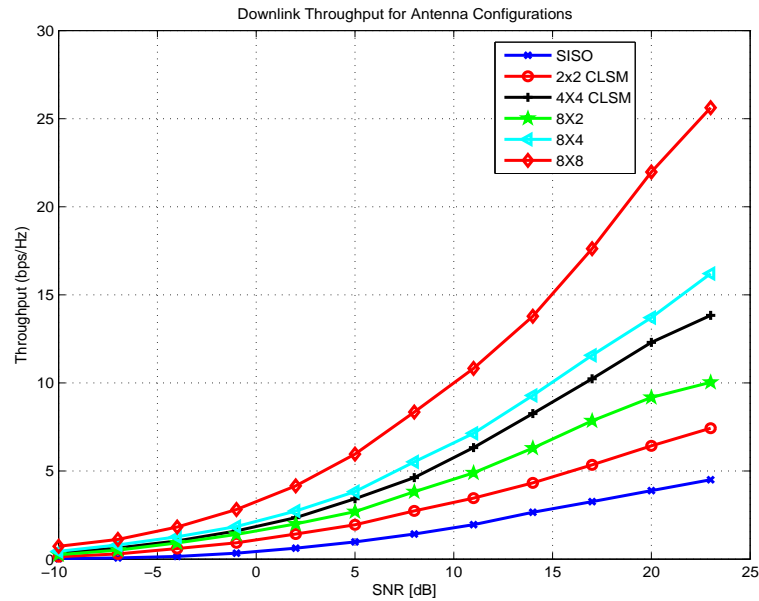


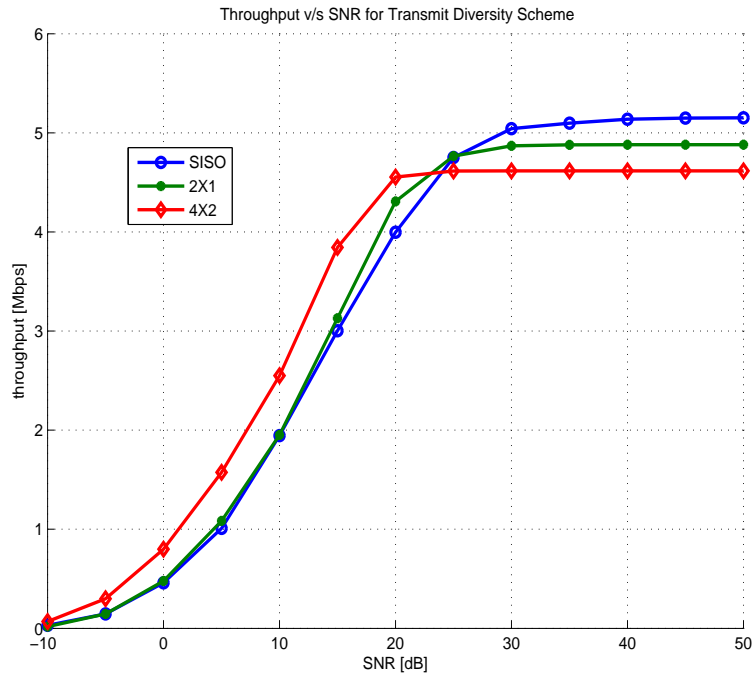
Figure 4.12: Throughput v/s SNR for MIMO antenna configuration in LTE-A

But when we compare Block Error Rate as shown in Figure 4.13 (b), 4x2 Transmit diversity has lowest BLER of $8X10^{-3}$ as compare to 2x1 ($66X10^{-3}$) and SISO ($194X10^{-3}$), at 0dB. Hence, as we increase the number of antennas at transmitter side the throughput decreases, but BLER increases as compare to SISO case.

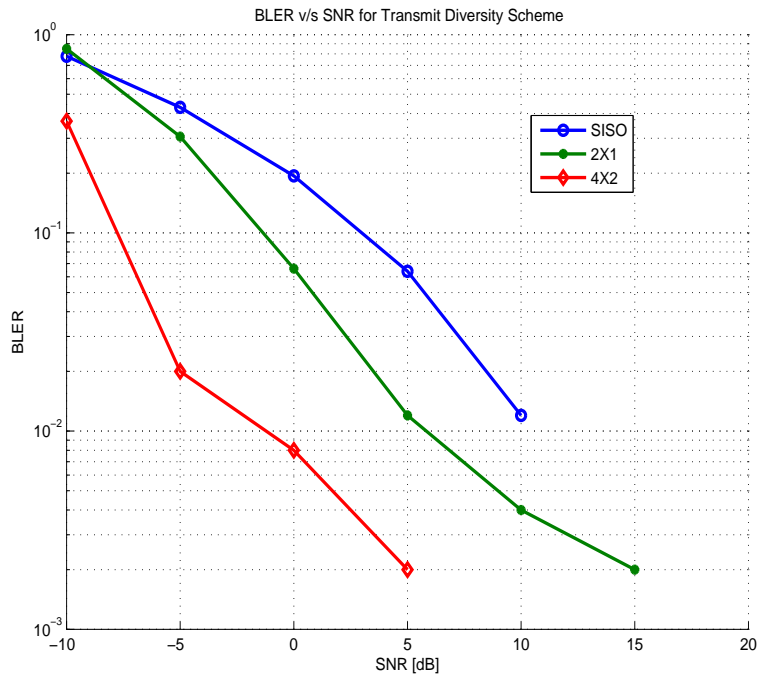
As shown in Figure 4.14 (a) the SISO is compared with OLSM and CLSM Scheme for 2x2 antenna scheme. Throughput of SISO System is lower when compared to OLSM and CLSM due to the effect of Spatial Multiplexing Gain. At 30 dB, throughput of SISO is 5.043 Mbps whereas that of OLSM is 9.257 Mbps and CLSM is 9.396 Mbps. The CLSM scheme has higher throughput due to the feedback indicators which gives information regarding channel conditions, rank and precoding indicators to the eNB. But when we compare the BLER as shown in Figure 4.14 (b), CLSM has lowest BLER as compare to SISO and OLSM. At 0 dB, BLER of CLSM is $3.745X10^{-3}$, for OLSM $12.92X10^{-3}$ and of SISO is $194X10^{-3}$.

Hence, Throughput of OLSM Scheme is higher as compare to SISO, but at high SNR the TxD has lower throughput compare to SISO. Spatial Multiplexing and TxD have lower BLER when compared to SISO.

As shown in Figure 4.15 (a), the SISO is compared with both Transmit Diversity and OLSM for 2x2 antenna scheme. At 30 dB, throughput of OLSM (9.257 Mbps) is highest when compared to TxD (4.88 Mbps) and SISO (5.043 Mbps). But when we compare BLER as shown in Figure 4.15 (b), 2x2 TxD has lowest BLER of $4X10^{-3}$ as compare to OLSM which has $12.929X10^{-3}$.

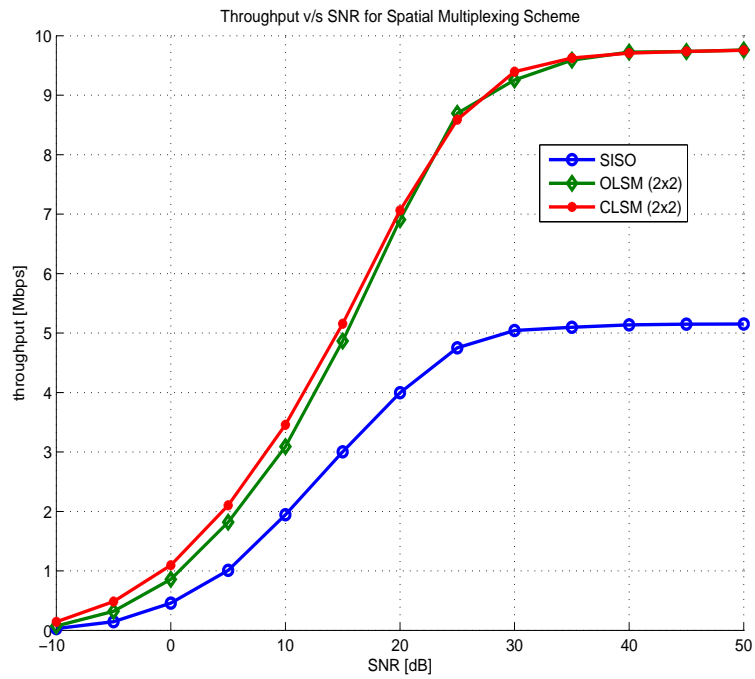


(a) Throughput for Transmit Diversity

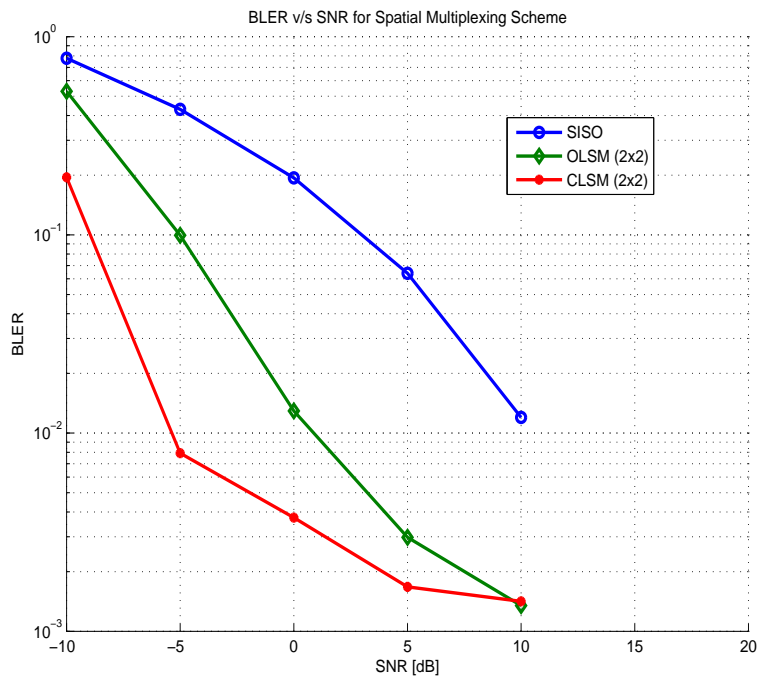


(b) BLER for transmit diversity

Figure 4.13: Throughput and BLER for Transmit Diversity

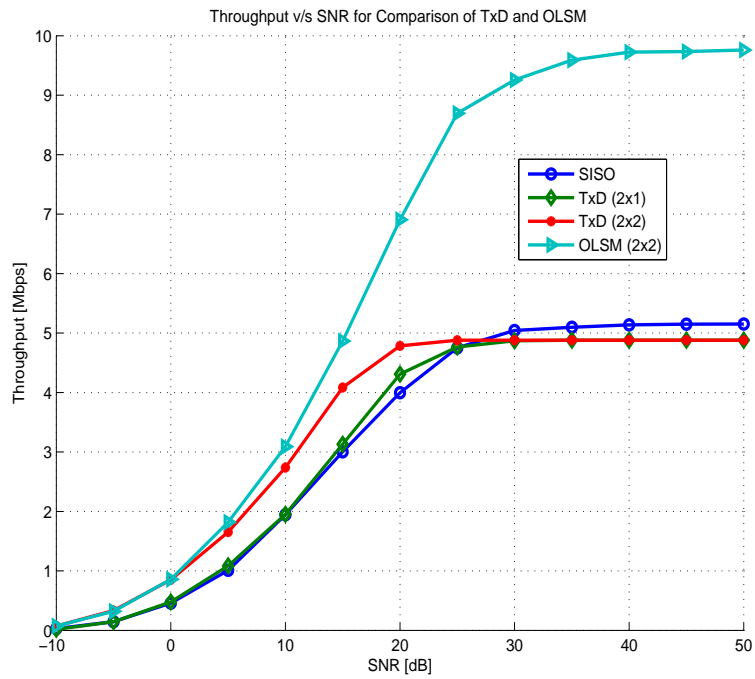


(a) Throughput for OLSM

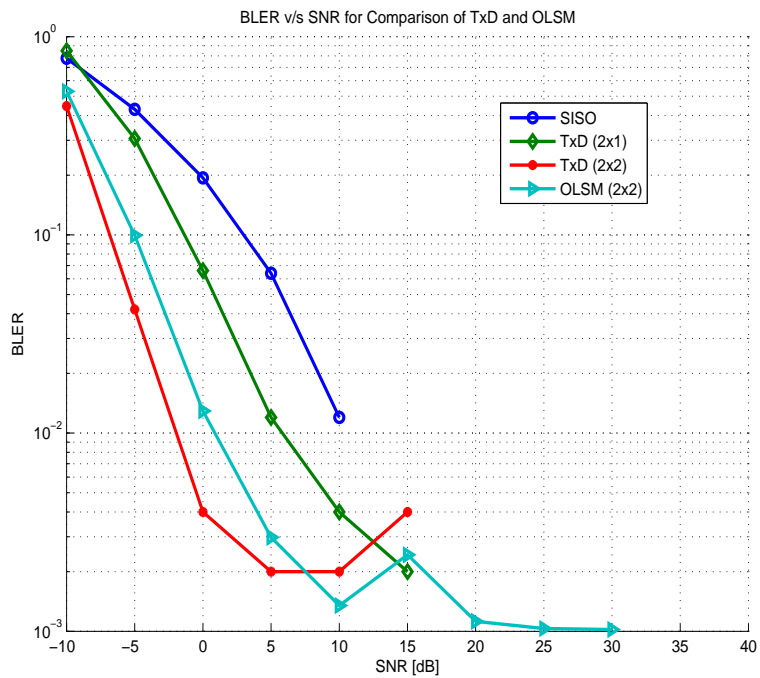


(b) BLER for OLSM

Figure 4.14: Throughput and BLER for Spatial Multiplexing



(a) Throughput for TxD and OLSM



(b) BLER for TxD and OLSM

Figure 4.15: Throughput and BLER for Transmit Diversity and Spatial Multiplexing

Parameters	Value
Number of Sub frames	500
Transmission Bandwidth	1.4 MHz
Number of UE	1
Number of eNodeB	1
Sub-frame duration	1ms
Sub-carrier spacing	15 kHz
Channel Estimation	Perfect
TTI length	1 ms
OFDM Cyclic Prefix	Normal
Simulation Configuration	SU-MIMO
Antenna schemes	SISO, TxD, OLSM and CLSM
MIMO receiver	ZF (Zero Forcing)
Channel Model Filtering	Block Fading
Channel type	Flat Rayleigh
Scheduler Type	Best CQI

Table 4.10: Simulation Parameters

Hence Spatial Multiplexing gives highest throughput, but the BLER is higher than that of TxD. The results discussed conclude the Diversity-Multiplexing Tradeoff for MIMO communication systems as discussed in previous chapter.

4.6 Results Summary

This section presents the summary of the results of Throughput and BLER for MIMO Techniques in LTE-A Physical Downlink Layer. Figure 4.16 shows the comparative analysis of TxD and OLSM MIMO Transmission modes for Rayleigh flat-fading channel and at SNR equal to 5dB. The tabular results are given in Table 4.11. It can be observed from the results that OLSM 2x2 has highest throughput of 1.81 Mbps as compared to SISO and TxD, but TxD 2x2 has lowest BLER of 2×10^{-3} when compared to other techniques.

Transmission Mode	Throughput	BLER
SISO	1.085	0.064
TxD (2x1)	1.009	0.012
TxD (2x2)	1.654	0.002
OLSM (2x2)	1.818	0.003

Table 4.11: Comparison of TxD and OLSM for SNR=5dB

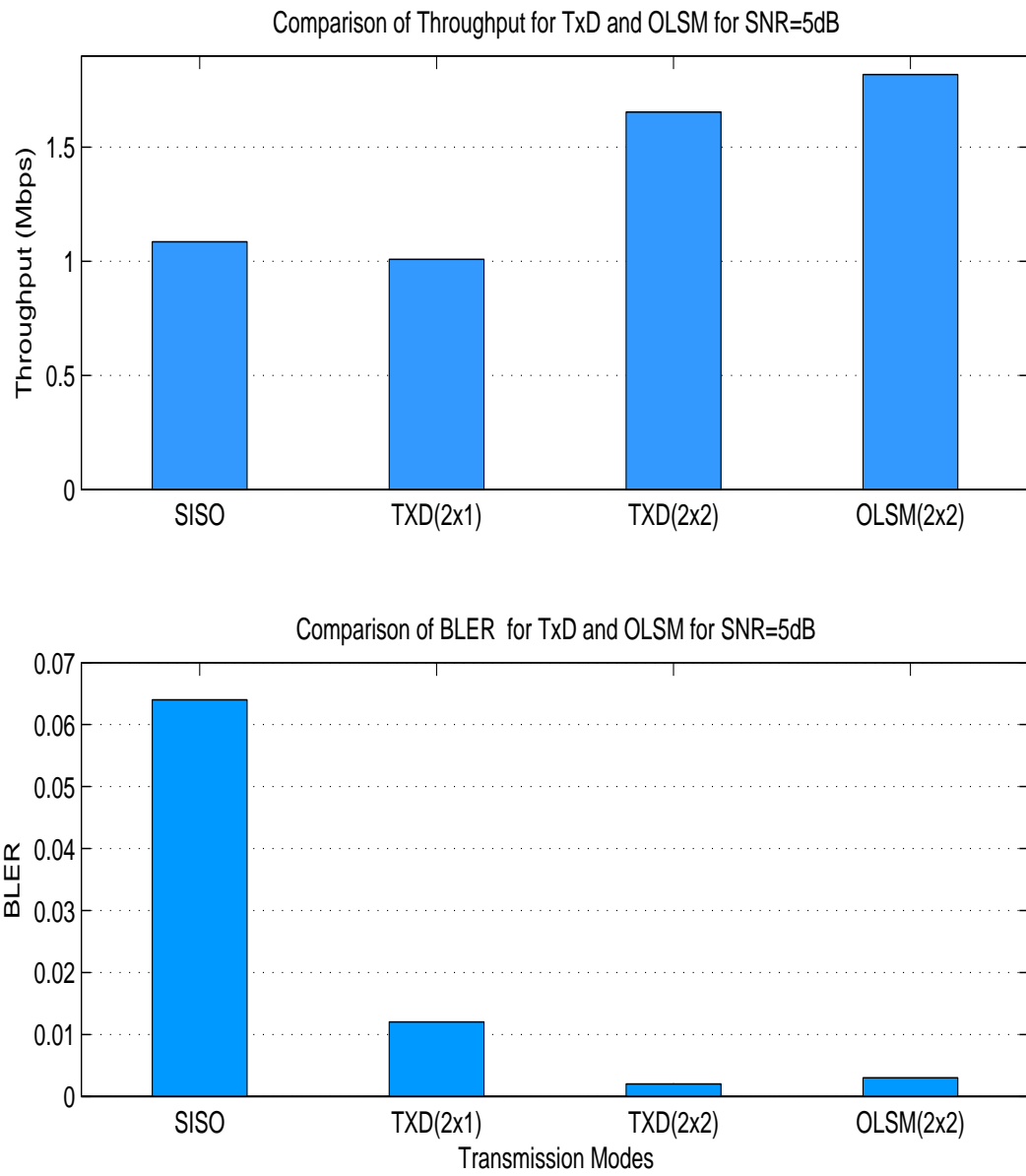


Figure 4.16: Comparison of MIMO Transmission modes in LTE-A

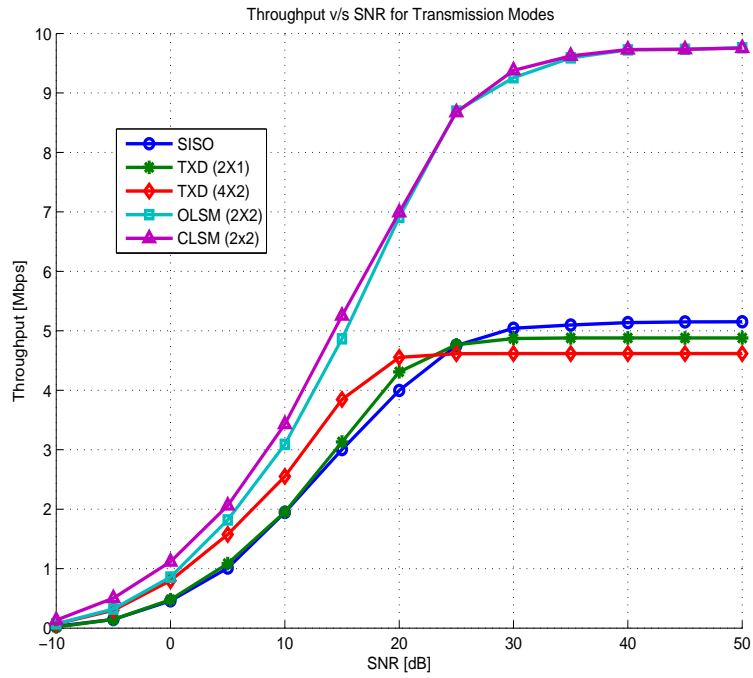


Figure 4.17: Throughput for Transmission modes with Flat rayleigh

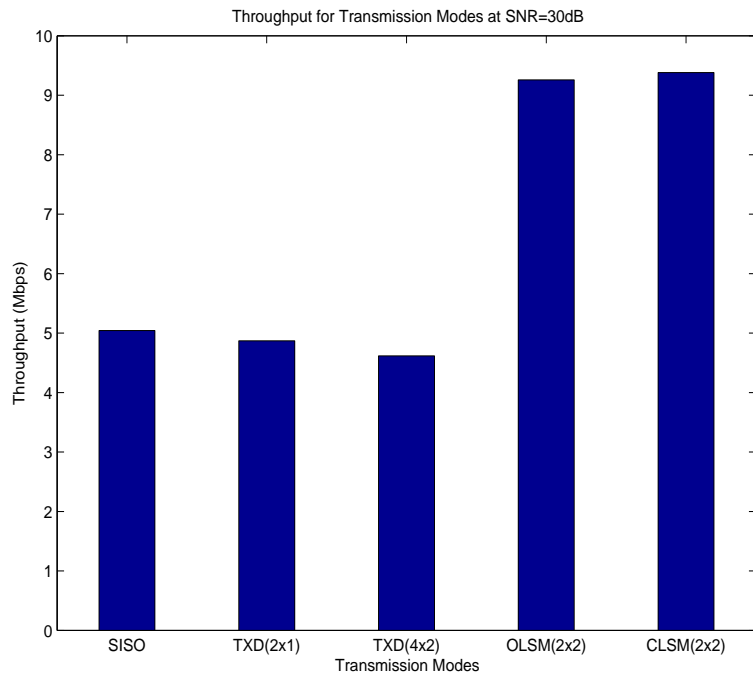


Figure 4.18: Comparison of Throughput for SNR=30dB

Hence we can conclude that OLSM offers high bit rates by transmitting independent information sequences over multiple antennas simultaneously. Whereas, low error rates is achieved with TxD by transmitting and/or receiving redundant signals representing the same information sequence. Comparative analysis of throughput v/s SNR for all MIMO Transmission schemes are as shown in Figure 4.17 and the throughput at SNR=30dB is as shown in Figure 4.18. It can be seen the CLSM scheme has highest throughput as compare to SISO ,TxD and OLSM.

4.7 Concluding Remarks

This chapter describes the LTE-A Downlink Physical Layer in detail. The MIMO transmission modes are explained in detail. Vienna LTE-A Link Level Simulator is briefly described. Simulation results for various MIMO Transmission modes is carried out. Spatial Multiplexing offers highest throughput, whereas Transmit diversity results into lowest BLER. Hence the tradeoff between transmit Diversity and Spatial multiplexing is verified for LTE-A Downlink Physical Layer with simulation results presented.

Soft-Computing Techniques and Development Tools

5.1 Overview of Soft-Computing Techniques

Real world problems have to deal with systems which are non-linear, time-varying in nature with uncertainty and high complexity. The computing of such systems is study of algorithmic processes which describe and transform information: their theory, analysis, design, efficiency, implementation, and application. Conventional computing/Hard computing requires exact mathematical model and lot of computation time [1]. For such problems, methods which are computationally intelligent, possess human like expertise and can adapt to the changing environment, can be used effectively and efficiently. Soft Computing is an evolving collection of artificial intelligence methodologies aiming to exploit the tolerance for imprecision and uncertainty that is inherent in human thinking and in real life problems, to deliver robust, efficient and optimal solutions and to further explore and capture the available design knowledge [2]. Soft computing utilizes computation, reasoning and inference to reduce computational cost by exploiting tolerance for imprecision, uncertainty, partial truth and approximation. Numerous Soft Computing-based methods and applications have been reported in the literature in a variety of scientific domains. The advances in application of Soft Computing Techniques in various demanding domains has promoted its use in industrial applications [3,4].

Soft Computing with its roots in fuzzy logic, artificial neural network, and evolutionary computation has become one of the most important research field applied to numerous engineering areas such as Aircraft, Communication networks, computer science, power systems and control applications. Soft Computing Techniques comprises of core methodologies: Fuzzy Systems (FS), including Fuzzy Logic (FL); Evolutionary Computation (EC), including Genetic Algorithms (GAs); Artificial Neural Networks (ANN), including Neural Computing (NC); Machine Learning (ML); and Probabilistic Reasoning (PR) [5]. Where PR and FL systems are based on knowledge-driven reasoning, whereas, ANN and EC, are data-driven search and optimization approaches. List of various problem Solving Techniques are as shown in Figure 5.1.

Soft Computing Techniques consists of rich knowledge representation, knowledge acquisition and knowledge processing for solving various applications. These techniques can be deployed as individual tools or be integrated in unified and hybrid architectures. The fusion of Soft Computing techniques causes a paradigm shift in engineering and science fields, which could not be solved with the conventional computational tools. Soft Computing has gain importance in the application fields for wireless communication in the last decade. Wireless communication systems are associated with

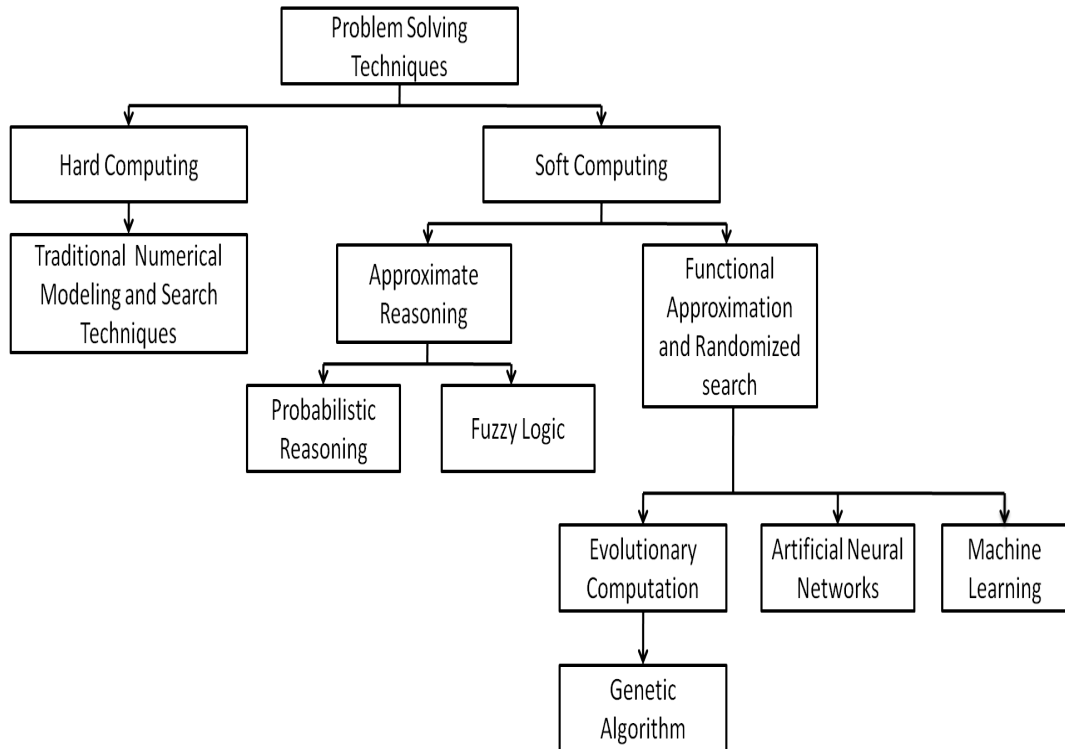


Figure 5.1: Various Problem Solving Techniques

much uncertainty and imprecision due to a number of stochastic processes such as time-varying characteristics of the wireless channel caused by the mobility of transmitters, receivers, objects in the environment and mobility of users. This reality has fueled numerous applications of soft computing techniques in mobile and wireless communications [6]. The role of soft computing in the domain of wireless systems can be classified into three broad categories, namely, optimization, prediction and uncertainty management [7]. Evolutionary algorithms are mostly used for optimization. Neural networks and other learning systems are used for different types of prediction tasks. Uncertainties arising due to incomplete modeling and measurements are handled using fuzzy logic, either in stand-alone manner or in conjunction with the optimization and prediction algorithms.

This chapter discusses the theoretical understanding of core Soft Computing Techniques i.e FL, ANN and GA in detail. Also the simulation of these systems with MATLAB based Toolboxes is presented. Various methods of using the tools for application oriented programming techniques is briefly discussed. The advances of application of Soft Computing Techniques in the vast field wireless communication is reviewed and presented in the chapter.

5.2 Fuzzy Logic System

Fuzzy systems are based on fuzzy logic, a generalization of traditional Boolean logic which is extended to handle the concept of partial truth i.e values between “complete true” and “complete False”. Fuzzy Logic provides a set of mathematical methods for representing information in a way that resembles natural human reasoning and deals with system uncertainty and vagueness [9]. Concepts of fuzzy sets, fuzzy logic and fuzzy control have been introduced and developed by L.Zadeh in a series of articles spanning several years [10–13]. Fuzziness is imprecision or vagueness, a fuzzy proposition may be true to some degree. For example we use a linguistic variable like short, tall, very tall for HEIGHT or maybe young, old for AGE. Fuzzy logic is viewed as a formal mathematical theory for the representation of uncertainty [14, 15].

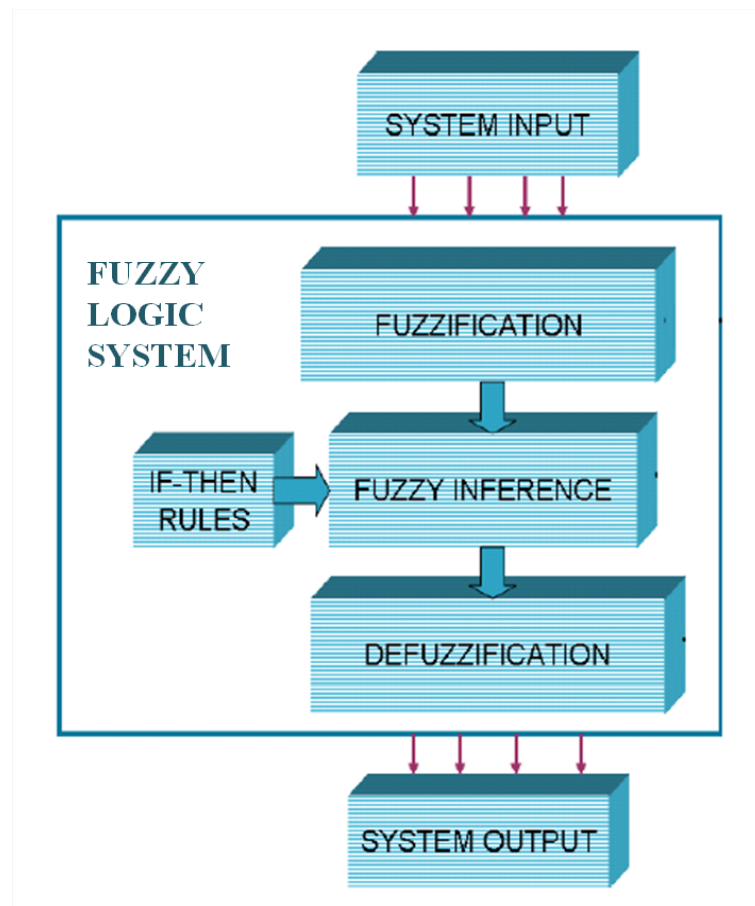


Figure 5.2: Fuzzy Logic System

A Fuzzy Logic System is an expert system that uses a collection of fuzzy membership functions and fuzzy IF-THEN rule base, instead of Boolean logic, to reason about data. The rules in a Fuzzy Logic System are of a form as following:

IF (x is LOW) AND (y is HIGH) THEN (z is MEDIUM),

IF (premise) THEN (Conclusion)

where x and y are input variables for known data values, z is an output variable for an output data to be computed, LOW is a membership function (fuzzy subset) defined on the set of x , HIGH is a membership function defined on the set of y , and MEDIUM is a membership function defined on the set of z . The antecedent (the rules premise, between IF and THEN) describes to what degree the rule applies, while the consequent (the rules conclusion, following THEN) assigns a membership function to each of one or more output variables. The set of rules in a Fuzzy Logic System is known as the rule base or knowledge base. Figure 5.2 shows the Fuzzy Logic System Block Diagram.

Algorithm 5.1 Fuzzy Logic Algorithm

- Initialization:

- Define Linguistic variables and terms
- Construct Membership Functions
- Construct Rule Base

- Fuzzification: Convert crisp input data to fuzzy values using the membership functions

- Inference: Evaluate the rules in the rule base and combine the results in rule base

- Defuzzification: Convert output data to non-fuzzy values

The Fuzzy Inference Process consists of following steps [16]:

- Fuzzification: The membership functions defined on the input variables are applied to their actual values, to determine the degree of truth for each rule premise.
- Fuzzy Inference Engine: The truth value for the premise of each rule is computed, and applied to the conclusion part of each rule. This results in one fuzzy subset to be assigned to each output variable for each rule. The aggregation method min or product is used as inference rules. After Inference, the composition of all fuzzy sets is carried out. Under composition, all of the fuzzy subsets assigned to each output variable are combined together to form a single fuzzy subset for each output variable. Usually max or sum is used.
- Defuzzification: It convert the fuzzy output set to a crisp number. There are many defuzzification methods [17, 18]. The Fuzzy Logic Algorithm steps is as given in Algorithm 5.1.

For modeling, simulation and design of Fuzzy Logic Systems usage of simulation software packages has become apart of engineering practice. MATLAB consists of Fuzzy Logic Toolbox

that allows designers to create fuzzy systems, the description of the features of the Fuzzy Logic Toolbox is described in next Section.

5.2.1 MATLAB Simulation-Fuzzy Logic Toolbox

The Fuzzy Logic Systems can be designed and simulated using MATLAB Fuzzy Logic Toolbox [19]. The Fuzzy Logic Toolbox, provides functions and GUI based editors for building Fuzzy Inference System (FIS).

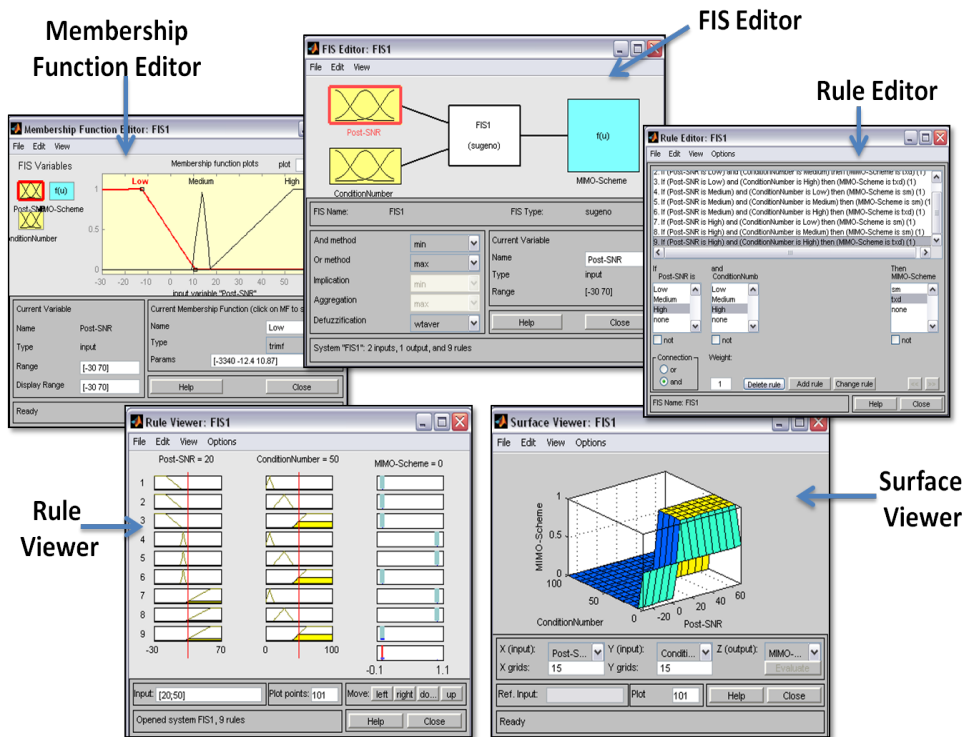


Figure 5.3: Fuzzy Inference System Editors and Viewers

FIS Editor Blocks	Description
FIS Editor	Display general Information about FIS
Membership Function Editor	Display and edit the MFs associated with the input and output variables of FIS
Rule Base Editor	View and edit fuzzy rules
Rule Viewer	View detailed behavior of a FIS to help es diagnose the behavior of specific rul
Surface Viewer	Generates a 3-D surface from two input variables and the output of FIS

Table 5.1: List of FIS Editor Blocks and description

FIS editor is a GUI which contains editors and viewers for building rule sets, defining membership functions and for analyzing the behavior of FIS. The toolbox also has ability to embed FIS

in Simulink model for simulation and to generate C code or stand-alone executable fuzzy inference engines. The editors and viewers of FIS Editor is as shown in Figure 5.3. Description of each editors and viewers are listed in Table 5.1.

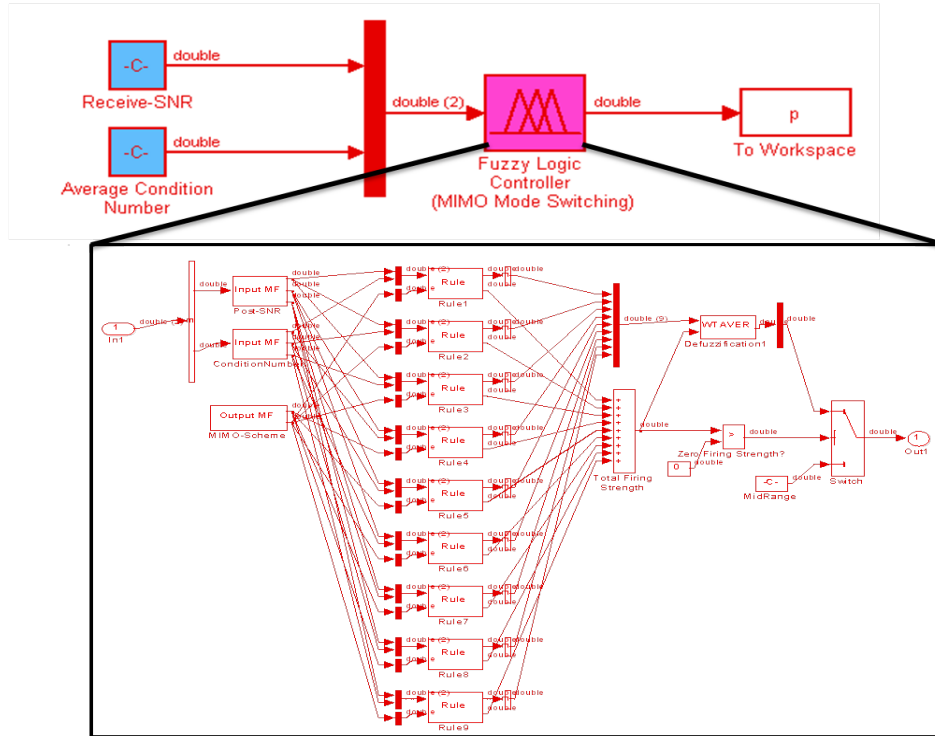


Figure 5.4: FLC in Simulink

MATLAB Function	Description
newfis	Create new Fuzzy Inference System
readfis	Load FIS from File
evalfis	Perform Fuzzy Inference Calculations
addvar	Add variable to FIS
addmf	Add MF's tro FIS
addrule	Add rule to FIS
defuzz	Defuzzify Membershipo Functions

Table 5.2: List of MATLAB Functions for Designing FIS

FIS performance can be evaluated using the Fuzzy Logic Controller (FLC) block in a Simulink model. The Fuzzy Logic Controller block automatically generates a hierarchical block diagram representation for Fuzzy Logic controller designed. This representation uses only built-in Simulink blocks, enabling efficient code generation. The Fuzzy Logic blocks available in Simulink and the detailed representation is as shown in Figure 5.4.

The FIS model can also be designed using the programming functions provided in the Fuzzy Logic Toolbox. Table 5.2 lists few MATLAB Functions to design FIS System.

5.3 Artificial Neural Networks

An Artificial Neural Network (ANN) is an information processing paradigm that is inspired by the biological neural networks, which consists of massively parallel computing systems with large number of simple processors with many interconnections [20]. ANN methodologies consists of basic architecture known as "Neurons". A neuron or nerve cell is a special biological cells that processes information in human brain. Brief description on Biological Neurons and Neural Networks can be found in [21]. ANNs are applied to solve various challenging problems like Classification [22], Clustering, Function Approximation [23–25], Prediction/Forecasting, Medical Imaging Application [27], Optimization and Control related applications [26].

5.3.1 McCulloch and Pitts Model of Neuron

The science of ANN has its first significance appearance during the 1940's, when researchers McCulloch and Pitts [28, 29] tried to emulate the functions of human brain by developing physical model of biological neuron and their interconnections [30]. Their work was focus on a simple neuron, which were considered to be binary with fixed thresholds as shown in Figure 5.5.

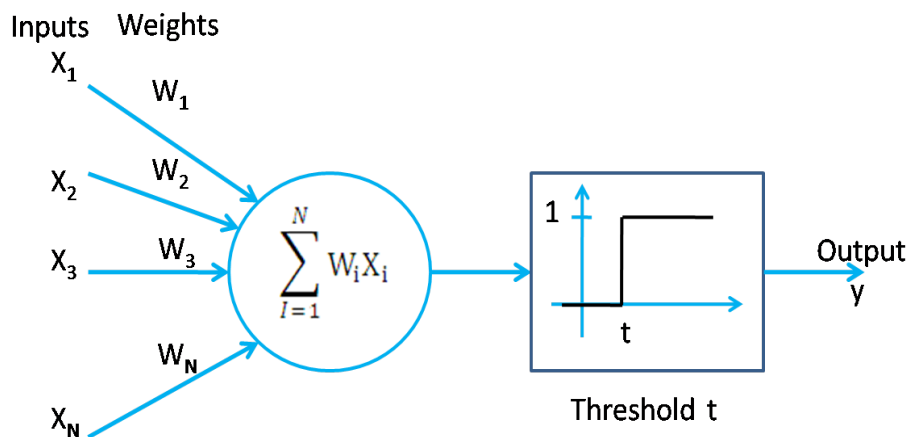


Figure 5.5: McCulloch-Pitts model neuron

The threshold unit receives input from N other units. Input from i^{th} unit is termed as x_i , and the associated weight is w_i . The total input to a unit is the weighted sum over all inputs

$$\sum_{i=1}^N W_i X_i = W_1 X_1 + W_2 X_2 + \dots + W_N X_N \quad (5.1)$$

If this value is below threshold t , the output of the unit is 1 and 0 otherwise. The McCulloch-Pitts model of a neuron is so simple that it only generates a binary output and also the weight and threshold values are fixed. But, it has substantial computing potential. The neural computing algorithm has diverse features for various applications. Thus, we need to obtain the neural model with more flexible computational features. Based on the McCulloch-Pitts model described previously, the general form an artificial neuron can be described in two stages shown in Figure 5.7.

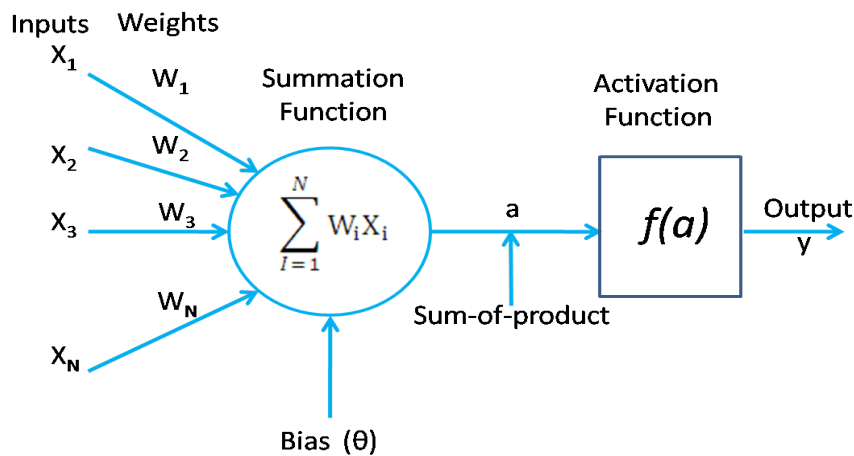


Figure 5.6: Artificial Neuron

In the first stage, the linear combination of inputs is calculated. Each value of input array is associated with its weight value, which is normally between 0 and 1. Also, the summation function often takes an extra input value θ with weight value of 1 to represent threshold or bias of a neuron. The summation function will be then performed as:

$$a = \sum_{i=1}^N W_i X_i + \theta \quad (5.2)$$

The sum-of-product value is then passed into the second stage to perform the activation function which generates the output from the neuron. The activation function “squashes” the amplitude the output in the range of $[0,1]$ or $[-1,1]$ alternately. The behavior of the activation function will describe the characteristics of a neuron model.

5.3.2 ANN Network Architectures

ANNs can be viewed as weighted directed graphs in which artificial neurons are nodes and their weights are connections between neuron outputs and neuron inputs. Based on the connection pattern (architecture), ANNs can be classified into two categories [31, 32]:

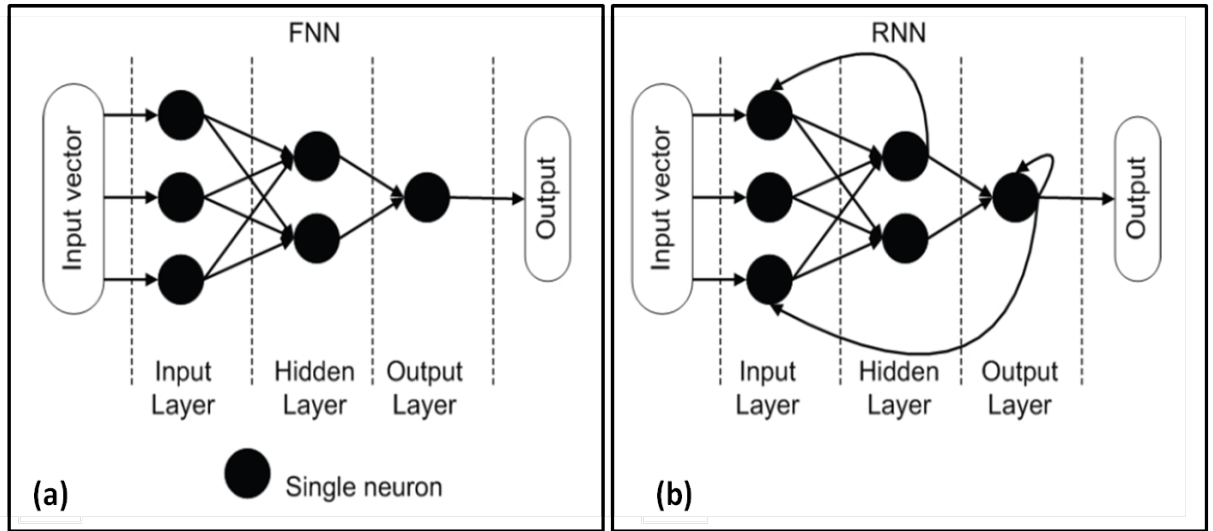


Figure 5.7: (a) Feed-forward (FNN) and (b) Recurrent Neural Network (RNN) Architectures

- Feed-forward Networks:** In this type of network neurons are organized into layers that have unidirectional connection between them. These networks are static in nature as they have no feedback and hence no delays. The output is calculated directly from the input through feedforward connections. They are memory-less networks as their response to an input is independent of the previous network state. Types of Feed-forward networks include: Single-Layer perceptron, Multilayer perceptron and Radial Basis Function networks. Figure 5.7 (a) shows a single layer Feed-forward neural network with n inputs and m outputs.
- Recurrent or Feedback Networks:** These networks are dynamic in nature i.e. the output depends on the current and previous inputs, outputs and states of network. Due to feedback paths, the input to each neuron is modified according to the feedback value and the network enters into a new state. Types of recurrent networks are: Competitive networks, Kohonen's Self-organizing Maps (SOM), Hopfield Network and ART models. Figure 5.7 (b) shows a Recurrent Neural network, which consists of feedback paths from output to input neurons. There can be neurons with self-feedback links.

The ability to learn is a fundamental trait of intelligence of ANN. In learning process, ANN updates network architecture and connection weights from training patterns. ANN's ability to learn from examples makes it attractive for various applications in research field. ANNs learn the underlying rules (like input-output relation) from the given collection of training data. Learning algorithms [33] adjust the weights of ANN using learning rules. Based on learning process there are three types of learning paradigms:

- **Supervised learning:** also known as learning with a “teacher”, means the network is provided with the correct output for every input pattern. Connection weights are then determined so as to allow the network to produce output very close to the correct answers. Examples of supervised learning algorithms are Boltzmann learning algorithm, Learning vector quantization, Back-propagation Adaline algorithm and Perceptron learning Algorithms.
- **Unsupervised Learning:** also known as learning without “teacher”, do not require correct output answers for each input pattern in the training set provided. It explores the network structure in data or correlations between input patterns, and organizes input patterns into categories from these correlations. Unsupervised Learning algorithms include Principal Component Analysis, Associative memory Learning, Kohonen's SOM, Adaptive resonance theory (ART) algorithms.
- **Hybrid learning:** It combines supervised and unsupervised learning i.e. part of the weights are determined through supervised learning and the remaining are obtained through unsupervised learning. Radial Basis Function (RBF) Learning algorithm used for learning in RBF networks using Error-correction and competitive learning rule is an example of Hybrid learning.

5.3.3 Designing Neural Network

The ANN design process follows number of systematic steps [34–36]. It can be design using following steps:

1. **Collection of data:** The data for which the neural network is to be designed, the data for training the networks. It is termed as Inputs and Targets for the Neural networks [data preparation for neural network].
2. **Designing the network:** It includes defining the architecture of Neural Network. it includes defining the number of layers, number of nodes in each layer, defining Transfer functions for each

layer, defining the training algorithm to train the network. Option parts of design includes: Error function for neural network, plotting the data, number of echos.

3. **Training the network:** once the network is designed, it has to be trained to optimize the error function. This process determines the best set of weights and biases for the collected data.
4. **Testing the network:** Finally the designed net is to be tested for accuracy and generalization.

5.3.4 MATLAB Simulation: Neural Network Toolbox

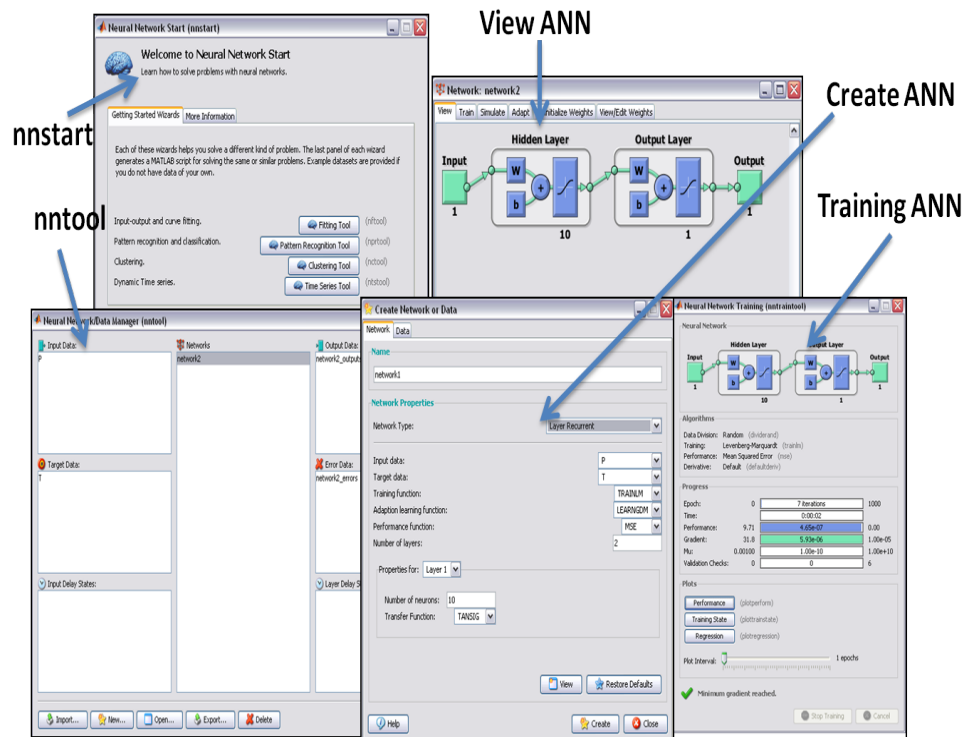


Figure 5.8: Neural Network Toolbox

The MATLAB Neural Network Toolbox [37] provides tools for design, visualization and simulation of ANN. It supports many network paradigms and provides GUI which enables user to design networks. Neural Network Toolbox supports a variety of supervised and unsupervised network architectures. With the toolboxes modular approach to building networks, custom network architectures for specific problem can be developed. The network architecture including all inputs, layers, outputs, and interconnections can be viewed. The features of GUI are as shown in Figure 5.8. The Neural network Start GUI provides examples and data sets for designing neural networks. It consists of Fitting Tool, Pattern recognition Tool, Clustering Tool and Time Series Tool for designing ANN for various Applications.

The toolbox can also be used by basic command-line operations. The command-line operations offer more flexibility than the GUIs, but with some added complexity. Various ANN architectures can be designed using command line functions like *feedforwardnet* for creating a feed-forward neural network. Number of parameters for ANN like number of hidden layer, activation functions, input nodes, training algorithm can be set using numerous MATLAB functions provided in the Toolbox. Example of sample code for designing, viewing, evaluating, training and creating simulink model for Feedforward network with 5 hidden layers is as below:

```
[x,t]=simplefit_dataset; % data set for training ANN
net=feedforwardnet(5) % Creates FNN
net=train(net,x,t); % Training of net
view(net) % View the net designed
y=net(x); % Evaluate net for x input
perf=perform(net,y,t) % Calculate network performance
gensim(net) % Generates simulink model for the net
```

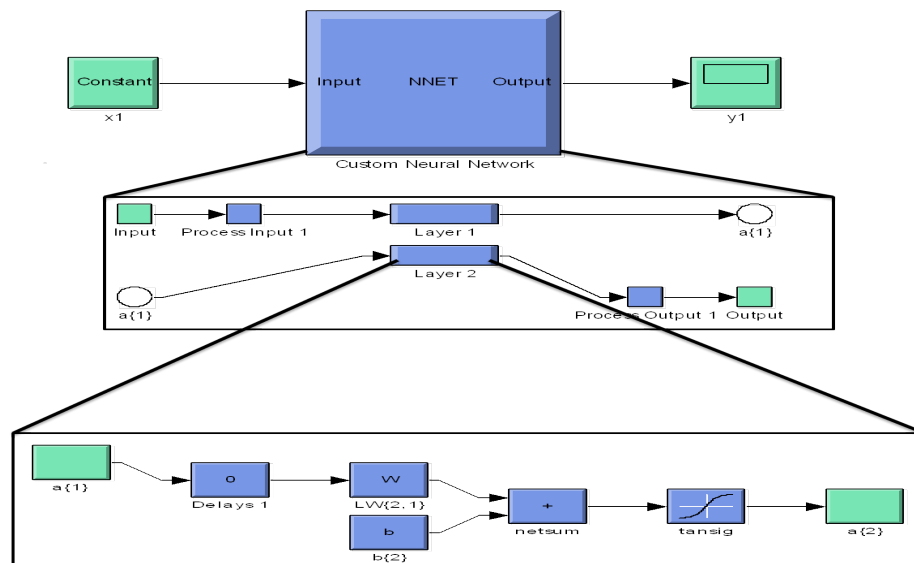


Figure 5.9: Neural Network Simulink model

Alternatively, Networks can be created and trained in the MATLAB environment and automatically generate network simulation blocks for use with Simulink using *gensim* command. This approach also enables users to view networks graphically. Example of Custom neural network created by the *gensim* command for the sample code of feedforward network is as shown in Figure 5.9.

Neural Network Toolbox provides set of blocks for building neural networks in Simulink. These blocks are divided into four libraries:

- Transfer function blocks, which take a net input vector and generate a corresponding output vector
- Net input function blocks, which take any number of weighted input vectors, weight-layer output vectors, and bias vectors, and return a net input vector
- Weight function blocks, which apply a neuron’s weight vector to an input vector (or a layer output vector) to get a weighted input value for a neuron
- Data pre-processing blocks, which map input and output data into the ranges best suited for the neural network to handle directly

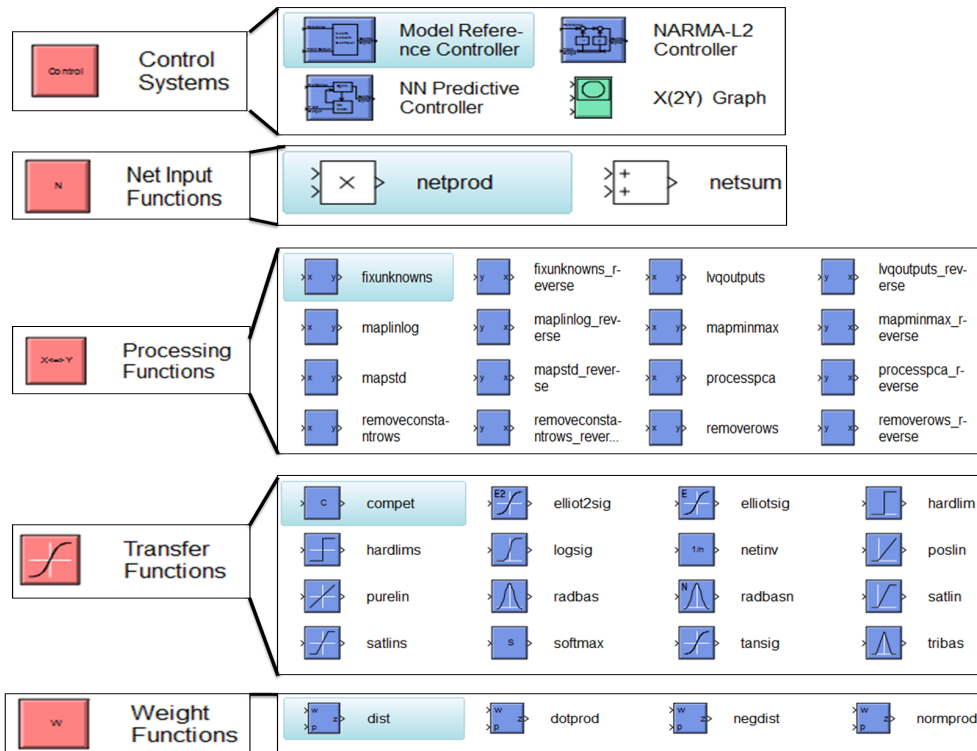


Figure 5.10: Neural Network Toolbox Simulink Blocks

Figure 5.10, shows the set of blocks provides by Neural Network Toolbox for simulating Neural Networks in Simulink. Neural Network Simulink blocks consists of Control Systems, Net Input functions, numerous Pre and Post processing Functions, various Transfer Functions and Weight functions for designing Neural Networks for various applications. Using these blocks ANN Architecture is designed and its performance and analysis is carried out for system analysis.

5.4 Genetic Algorithms

Since 1950s several researchers have studied Evolutionary Systems as an optimization tool for engineering problems. The basic idea in all these systems were to evolve a population of candidate solutions of a given problem, using operators inspired by natural genetic variation and natural selection [39]. In 1970's, the pioneering work of J.H. Holland proved to be significant contribution for various engineering and scientific applications. Holland's book "Adaptation in Natural and Artificial Systems" [40] was instrumental in creating the flourishing field of research in Genetic Algorithms. The well known applications of GA include scheduling, sequencing, reliability design, and image processing [41].

5.4.1 Introduction

Genetic Algorithms are inspired by the mechanism of natural selection, which is a biological process in which stronger individuals are more likely to be winners in a competing environment [42]. GA assumes that the solution of a problem is an individual, which can be represented by a set of parameters. These parameters are known as genes of the chromosomes and can be represented by string of binary values. GAs is a search technique which start with an initial set of random solutions known as population. Each individual in population is called chromosomes, which is a string of binary values. The chromosomes evolve through successive iterations, called generations. During each iteration the chromosome evolve using some measures of fitness. Then the next generation is created, where the new chromosomes called as off-springs, are formed by either merging two chromosomes from current generation using a crossover operator or modifying a chromosome using a mutation operator. New generation is formed by selection, based on the fitness values, some of the parents and off springs are rejected to keep the population size constant. After several iterations the algorithm converges to the best chromosome, which represents the optimum or sup-optimum solution to the problem [43]. Figure 5.11. shows the basic structure of Genetic Algorithms. The Standard genetic Algorithm [42, 44] is given in Algorithm 5.4.1.

Genetic Algorithm tools are available to evaluate the optimization problem. The GA toolkits and libraries available [45, 46] based on C++ programming include GALib, The Genetic Algorithm Utility Library (GAUL), Open Beagle and Java based toolkits include Java Genetic Algorithms Package (JGAP), JAVA API for Genetic Algorithms and JAVA GALib. MATLAB also provides Global Optimization Toolbox for solving Optimization Problems. It consists of Genetic Algorithm Solver as one of the method to solve optimization problems, discussed in following section.

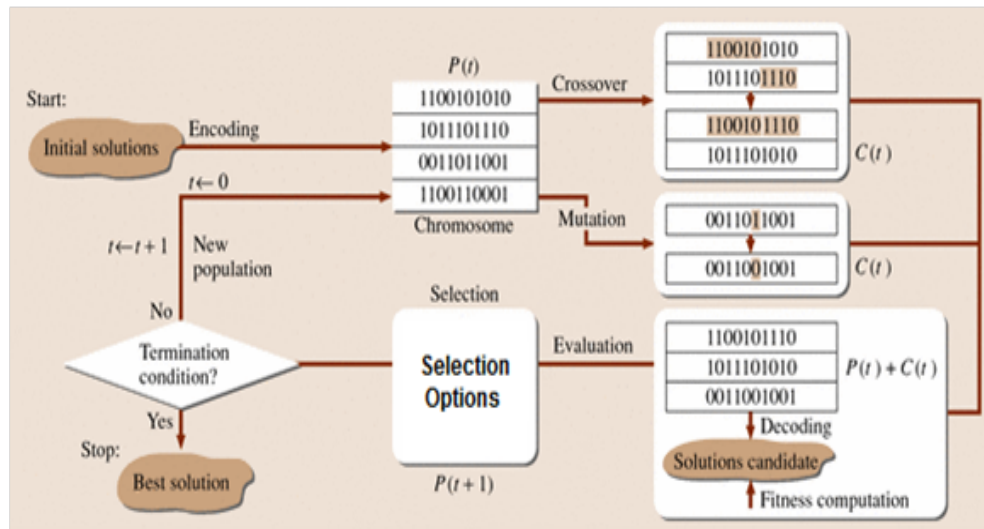


Figure 5.11: Genetic Algorithm Basic Structure

Algorithm 5.2 Standard Genetic Algorithm

- Input Initial Parameters: Fitness Function, Population size, Crossover operator, Mutation operator and stopping criteria.
- Initialize a random population of individuals;
- Evaluate fitness of all initial individual of population;
- while** *stopping criterion not full filled* **do**
 - Select individuals for reproduction;
 - Create offsprings by crossing individuals;
 - Eventually Mutate some individuals;
 - Evaluate its new fitness;
 - Select survivors from actual fitness;
 - Compute New Generation.
- end while**
- Plot SNR v/s Throughput

5.4.2 MATLAB Simulation: Global Optimization Toolbox

MATLAB provides Global Optimization Toolbox which consists of methods that search for global solutions to problems that contain multiple maxima or minima [47]. Methods include global search, multistart, pattern search, genetic algorithm, and simulated annealing solvers. The Genetic Algorithm solves both constrained and unconstrained optimization problems that is based on natural selection, the process that drives biological evolution. The genetic algorithm repeatedly modifies a population of individual using rules modeled on gene combinations in biological reproduction. The steps for the genetic algorithm optimization techniques are as follows:

- 1) Random Initial Population is created using the population options like population size and creation function specified.

2) The algorithm then creates a sequence of new populations. At each iteration, the algorithm uses the individuals in the current generation to create the next population. To create the new population, the algorithm performs the following steps:

- Computing fitness value of each member of the current population.
- Selects members, called *parents*, who contribute their genes to their *children*, based on their fitness.
- Some of the individuals in the current population that have best fitness are chosen as *elite*. These elite individuals are passed to the next population.
- Produces *children* from the parents. Children are produced either by *mutation* or *crossover*.
- Replaces the current population with the children to form the next generation.

3) The algorithm stops when one of the stopping criteria like number of generations, time limit, fitness limit is met.

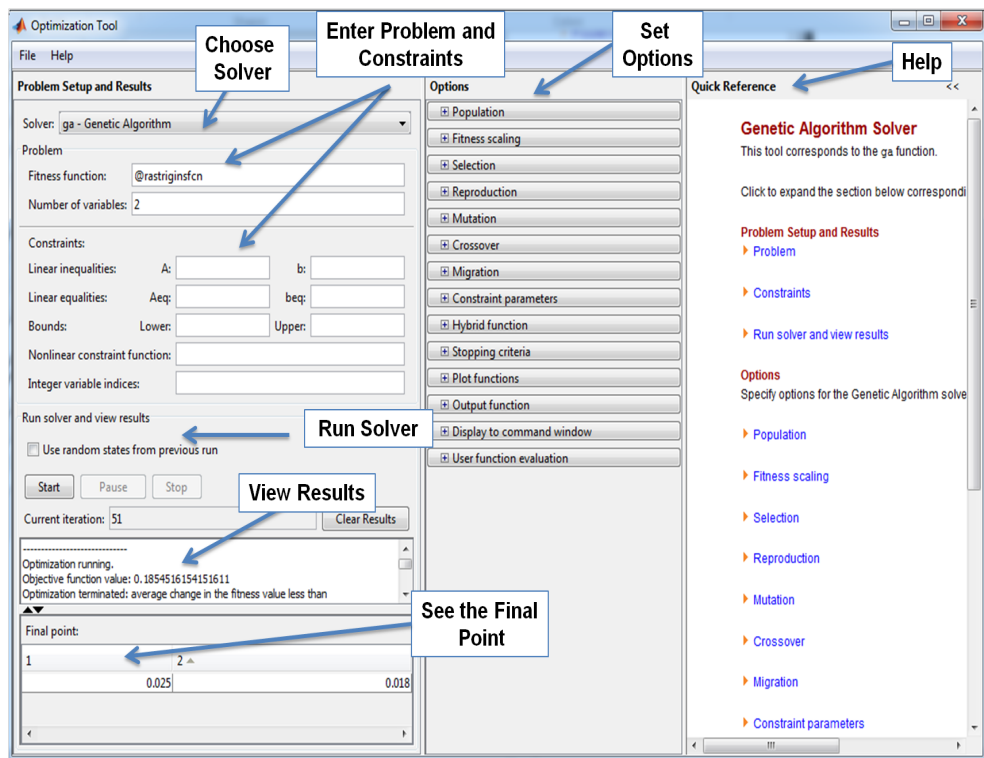


Figure 5.12: Optimization App in Global Optimization Toolbox

The Optimization App provided by the Global Optimization Toolbox is open by using the command: `optimtool` in MATLAB Command Window. This command opens the Optimization App, as shown in Figure 5.12.

Genetic Algorithm Solver options like Population, Fitness Scaling, Mutation options, Crossover options and Stopping criteria is selected based on the optimization function and application. Using Optimization App various plots like best fitness, best individual, Distance, Range and Score Diversity is generated for performance analysis of Genetic Algorithm.

Genetic Algorithm for mixed-integer or continuous-variable optimization, constrained or unconstrained optimization problems can be also solved using MATLAB functions and by specifying algorithm options. Customize Genetic algorithm can be created by modifying the initial population and fitness scaling options or by defining parent selection, crossover and mutation functions. Table 5.3 lists the MATLAB functions for solving problems using Genetic Algorithm.

Functions	Description
ga	Find minimum of function using Genetic Algorithm
gaoptimget	Obtain values of GA options structure
gaoptimset	Create GA options structure

Table 5.3: List of MATLAB Functions for Genetic Algorithm

The genetic algorithm is executed by calling the gaoptimset function and providing with fitness function to optimize and other Genetic Algorithm options.

5.5 Applications of Soft Computing Techniques in Wireless Communication

Wireless communications is rapidly evolving sector with challenges to meet the demands for higher performance and efficiency. Wireless communication systems are associated with much uncertainty and imprecision due to a number of stochastic processes such as time-varying characteristics of the wireless channel caused by the mobility of transmitters, receivers, objects in the environment and mobility of users. This reality has fueled numerous applications of soft computing techniques in mobile and wireless communications [48, 49]. The role of soft computing in the domain of wireless systems can be classified into three broad categories, namely, optimization, prediction and uncertainty management [50]. Evolutionary algorithms are mostly used for optimization. Neural networks and other learning systems are used for different types of prediction tasks. Uncertainties arising due to incomplete modeling and measurements are handled using fuzzy logic, either in stand-alone manner or in conjunction with the optimization and prediction algorithms.

Fuzzy Logic have been applied in numerous areas of Wireless communication such as in channel estimation, channel equalization and decoding [51]. Evolutionary Algorithms (EAs) have been

frequently applied to telecommunication problems in hardware design, network design and data transmission. Genetic Algorithms have been successful in solving various optimization problems in the field of Wireless Communication. Genetic Algorithms has been applied to hardware design applications like antenna design, network routing and assignment [52].It has also been applied to Wireless Sensor Network to optimize system performance [53]. Artificial neural networks have been applied in high-speed communication networks [54], Antenna Design [55]. Literature review of various field areas where soft-computing techniques are applied in Wireless Communication Systems and Wireless Sensor Networks is given in [48,50].

5.6 Concluding Remarks

This chapter discusses various problem solving techniques. The theoretical background for core soft-computing techniques i.e Fuzzy Logic, ANN and Genetic Algorithm is summarized. MATLAB based toolboxes available for designing and testing the performance of application of soft-computing techniques in various areas is discussed in detail. Procedural steps for designing and programming the soft-computing techniques and its usage using SIMULINK is summarized.

Artificial Neural Network Based MIMO Channel Estimation

6.1 Introduction

MIMO Wireless systems have been shown to provide dramatic increase in channel capacity and throughput performance of LTE-A Downlink Physical Layer. MIMO provides promising solutions for the increasing demands for high channel capacity systems. The capacity gain, however, requires perfect knowledge of the instantaneous channel fading at both the transmitter and receiver [1]. The efficiency of channel estimation affects the system performance by introducing a channel estimation error that reduces the channel capacity and by dedication of a fraction of its bandwidth to the transmission of pilots or training symbols [2, 3]. Channel estimation techniques for MIMO Communication systems has been reviewed in [4, 5].

The receiver in MIMO system, requires the knowledge of CSI in order to recover the transmitted signal properly. MIMO channel capacity has been widely investigated under different assumptions on CSI at the receiver or both at the transmitter and receiver [6, 7]. The bounds on Mutual Information with imperfect CSI for time-varying SISO and MIMO channels and their effect on achievable rates is already analyzed in [8–10].

Channel estimation in MIMO systems is an active research area and challenging task. Several channel estimation methods have already been studied by different researchers for MIMO systems. In LTE-A Downlink channel estimation methods, reference symbols are inserted and transmitted over the channel, and are estimated at the receiver [11]. The most efficient training based methods are the Least Squares (LS) method [12], Minimum Mean Square Error (MMSE) method [13, 14] and Adaptive Filtering channel estimation method [15]. Channel estimation by artificial neural network has been deployed in OFDM system, with different neural network architectures [16–20].

ANN based MIMO channel estimation techniques for LTE-A Downlink Physical layer is proposed and discussed in this chapter. The performance analysis of channel estimation techniques in terms of Throughput of Downlink Physical layer is analyzed using LTE-A Link Layer Simulator. The ANN weights are further trained by Genetic Algorithm (GA) to increase the performance of system. Further details of ANN based MIMO Channel estimation design and simulation results are discussed in following sections.

6.2 LTE-A MIMO channel estimation

The distortion imposed by the wireless channel on the transmitted data stream in a MIMO communication system is normally observed in the form of errors at the receiver. The main objectives

of communication system is to minimize the number of these errors and to maximize the throughput of the system. In order to optimize the system performance in response to channel conditions, an estimate of the channel at the receiver is a vital part. A Reference Signal (RS) is a pre-defined signal, pre-known to both transmitter and receiver. RS when transmitted through wireless channel is affected by multipath fading and distortions.

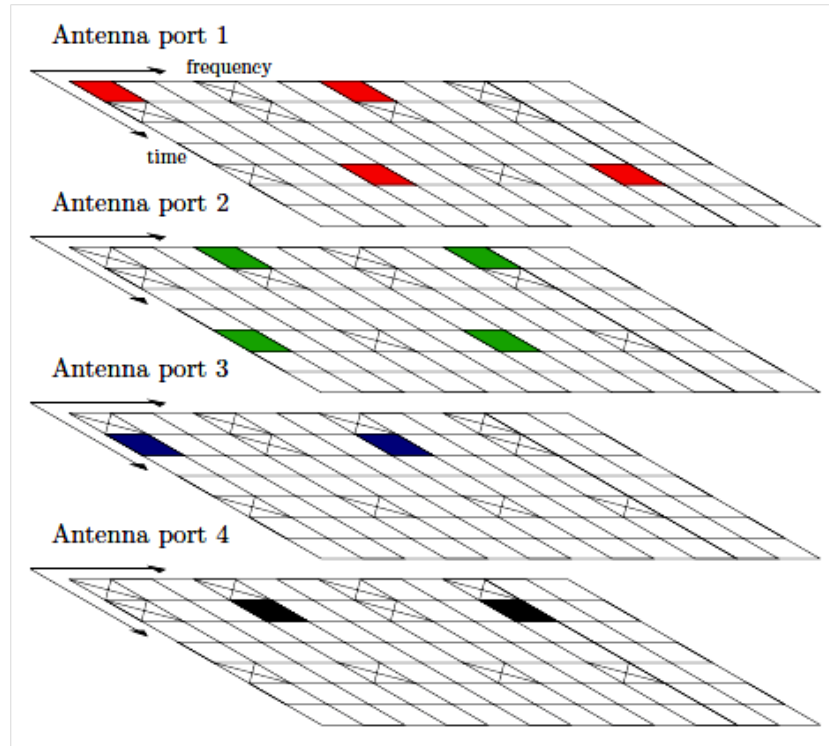


Figure 6.1: Reference Signals for LTE-A antenna ports

In LTE-A, the Downlink transmission uses the OFDMA feature with 15 kHz subcarrier spacing of the resource grid as discussed in Section 4.3. During subcarrier mapping the RS are inserted in both time and frequency directions so that it can be estimated at the receiver [21]. This pilot symbols are used to estimate the channel at given specific locations within a subframe. The RS signals are transmitted with 1,2 or 4 antennas. It is transmitted every first and Fifth OFDM symbol of a slot as shown in Figure 6.1. For the case of two antennas, reference signal is sent on the first OFDM symbol of first antenna and the first OFDM symbol on the second antenna is not used to avoid interference. Using this estimates, the channel across an arbitrary number of subframes can be estimated using interpolation [22]. The pilot symbols in resource grid have unique position which depends on the eNB cell identification number and transmit antenna being used. The pilot symbols are positioned so that they do not interfere with one another and can be effectively used to

estimate the channel gains.

In Release 8, the reference signal is added after precoding i.e Cell-specific Reference Signal (CRS) per antenna. Using the received CRS the UE estimates the wireless radio channel, which is used by the receiver for demodulation of the received signal. In Release 10, the UE-specific reference signal Demodulation Reference Signals (DM-RS) is added to different data streams before precoding. Hence the channel is estimated using DM-RS which provides information about the combined effect of the wireless channel and precoding.

6.3 ANN based MIMO Channel Estimation

ANN are algorithms for optimization and learning based on concepts inspired by research into the nature of the brain [23]. ANN based channel estimation for throughput optimization of LTE-A Downlink Physical Layer is carried out in this work. Different ANN Network Architectures are tested for its effect on channel estimation and hence throughput.

Considering a 2x2 MIMO system, the received symbol y can be written as:

$$y = XH + n \quad (6.1)$$

where H is the channel matrix, n is the AWGN noise at the receiver and X contains the data symbols x_d and pilot symbols x_p . The Least-Squares (LS) channel estimator for subcarriers on which pilot symbols are located, is given by:

$$h_p^{LS} = X_p^H y_p \quad (6.2)$$

where H is for Hermitian matrix. LS channel estimator is obtained by minimizing the square distance between the received reference symbols Y and the transmitted reference symbols X as follows [14, 24]. The channel estimated by the LS channel estimator is used as target for training ANN. The algorithm developed for MIMO Channel estimation in LTE-A Link Level Simulator is given in Algorithm 6.1. As shown in Figure 6.2 X is the transmitted reference symbol through wireless channel and is affected by noise. The received reference symbols is assigned a Y . LS Channel estimator estimates the unknown channel given by H .

The training pairs for ANN is generated using set of reference symbols as input and LS Channel estimate as output pairs. Reference symbols from the training set is presented to the input layer of the network and the error at the output layer is calculated. The error is propagated backwards towards the input layer and the weights are updated. This procedure is repeated for all the training

Algorithm 6.1 ANN based MIMO Channel Estimation Algorithm

- Initialization:

- Assign Received Reference Symbol to variable X
- Assign Reference Symbols to variable Y
- Initialize ANN Simulation Parameters

- Estimate MIMO Channel using Least Square Algorithm and assign to variable $H_{ls_one_channel}$.

- Determine the Real and Imaginary parts of the Estimated channel and Received reference Symbols.

- Design ANN Network Architecture specifying the simulation parameters.

- Generate Training Pairs for ANN by taking Received Reference Symbols as Input and LS Estimated Channel as output ($X, H_{ls_one_channel}$).

- Train the ANN using Training Algorithm Specified.

- Once the ANN is trained, take Received Reference Symbol as input and simulate ANN for Estimated Channel.

signals. At the end of each iteration, test data are presented to ANN and the performance of ANN is evaluated. Further training of ANN is continued till the desired performance is reached. The estimator uses the information provided by received reference symbols of sub channels to estimate the channel.

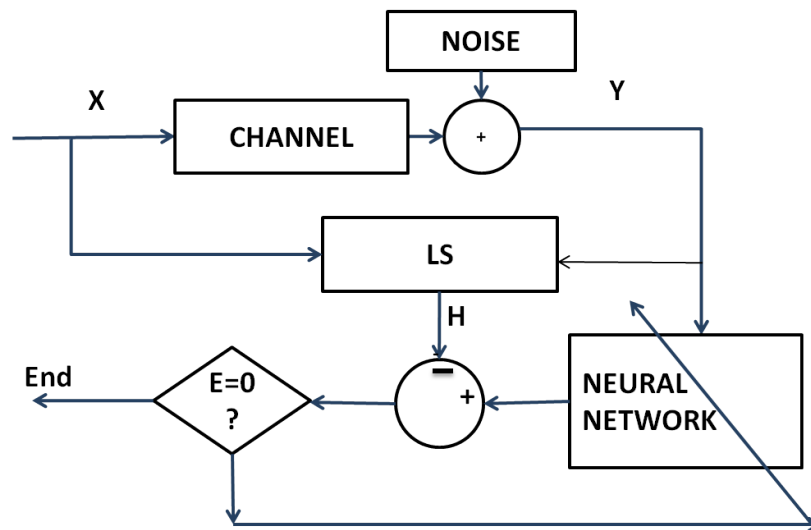


Figure 6.2: ANN based Channel estimation

Four types of ANN Architecture are design for MIMO Channel Estimation for LTE-A Downlink Physical Layer as follows:

- 1). Feedforward Neural Network (FNN): A FNN [25] is one whose topology has no closed

paths. Its input nodes are connected to the output nodes without any feedback paths. The Back-Propagation Algorithm (BPA) uses the steepest-descent method to reach a global minimum. The flowchart of the BPA is given in [26]. FNN consists of one or more hidden layers of sigmoid neurons followed by an output layer of linear neurons as shown in Figure 6.3. This network can be used as a general function approximator. It can approximate any function with a finite number of discontinuities arbitrarily well, given sufficient neurons in the hidden layer.

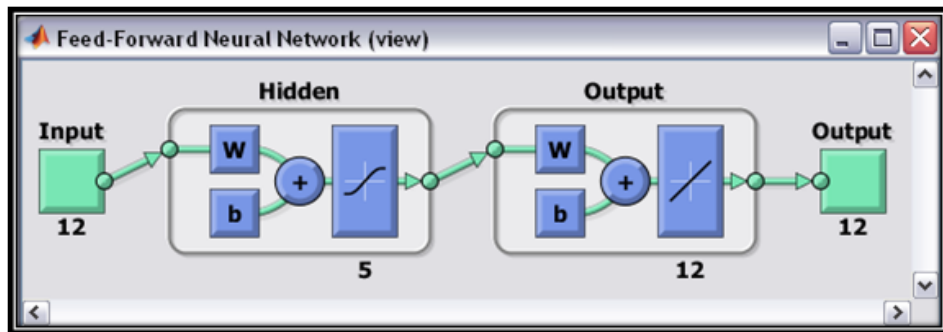


Figure 6.3: Feedforward Neural Network

2). Radial Basis Neural Network (RBNN): It is an alternative to the more widely used Multi-layer network and is less computer time consuming for network training [27, 28]. Radial basis networks consist of two layers: a hidden radial basis layer of radial basis function neurons, and an output layer of linear neurons. as shown in Figure 6.4. The nodes within each layer are fully connected to the previous layer. This network is mainly used for fitting a function application.

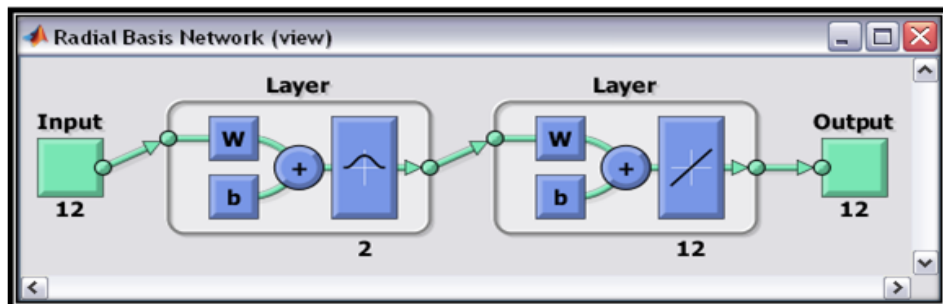


Figure 6.4: Radial Basis Network

3). Layered Recurrent Network (LRN): In the LRN, there is a feedback loop, with a single delay, around each layer of the network except for the last layer. The method of training is similar to that of the FNN. In addition to this, a neuron taking input from the output layer and connected to

the hidden layer as shown in Figure 6.5. The inputs are presented to the input units and the output from the network is calculated. The process is repeated for all the patterns. After finding the system error, the training of the network is based on the steepest gradient method.

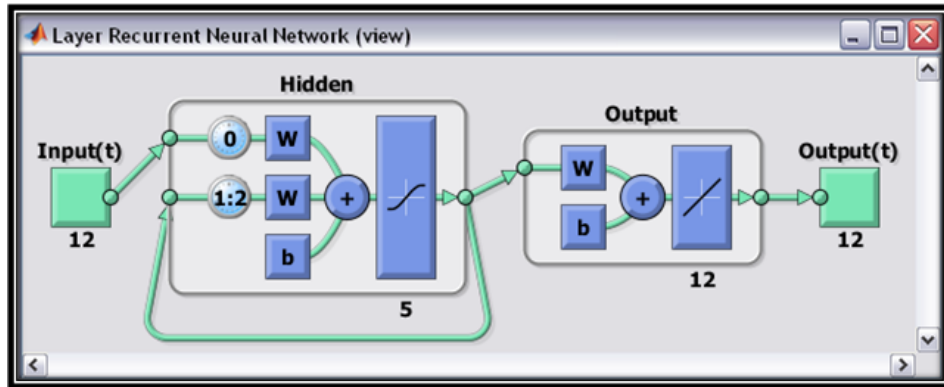


Figure 6.5: Layer Recurrent Neural Network

4) General Regression Neural Network (GRNN): A GRNN [27, 29] is a variation of the radial basis neural networks. A GRNN is often used for function approximation. It has a radial basis layer and a special linear layer. A GRNN does not require an iterative training procedure as back propagation networks. It approximates any arbitrary function between input and output vectors, drawing the function estimate directly from the training data. In addition, it is consistent that as the training set size becomes large, the estimation error approaches zero.

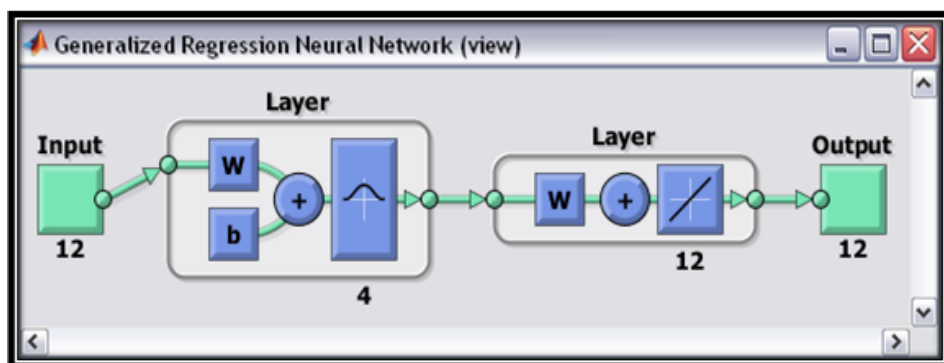


Figure 6.6: Generalized Regression Neural Network

6.3.1 ANN Simulation Parameters and results

ANN based MIMO Channel Estimation methods for LTE-A Downlink Physical Layer are design and simulation is carried out using Neural network Toolbox. The results are validated with

Perfect and LS Channel Estimation methods in LTE-A Link Level Simulator. The functions used for simulation of the ANN Networks are as listed in Table 6.1.

ANN Network	MATLAB Function
Feedforward network	feedforwardnet(hiddenSizes,trainFcn)
Radial Basis Network	newrb(P,T,goal,spread)
General regression Neural network	newgrnn(P,T,spread)
Layered recurrent Neural network	layrecnet(layerDelays,hiddenSizes,trainFcn)

Table 6.1: MATLAB Function to design ANN Networks

The Simulation parameters for the simulation of Channel estimation Techniques for LTE-A Downlink Physical Layer is as given in Table 6.2. GRNN network does not require training using train function, because the *newgrnn* function itself trains the network.

Parameters	FNN	RBNN	GRNN	LRN
Number of Layers	1	1	1	1
Hidden Sizes	5	5	5	5
Training Function	'trainlm'	'trainlm'	-	'trainlm'
Number of Epochs/Iteration	1000	1000	1000	1000
Spread	-	1.0	1.0	-
Goal	-	0.0	0.0	-
layerDelays	-	-	-	1:2

Table 6.2: Simulation parameters for ANN

The simulations are carried out modifying the LTE-A Channel estimator files. The MIMO Channel being complex, the real and imaginary part of the reference symbols and the received reference symbols are generated and two different neural networks are designed to estimate the channel at the receiver. Figure 6.7 shows the throughput analysis for 2x2 MIMO System for Tx-D transmission mode for flat Rayleigh channel. It can be observed that RBFN and GRNN gives better result compared to LS Channel Estimation. FNN and LRN gives worse result when compared to LS Channel Estimation technique. At SNR equal to 20 dB, throughput for perfect channel is 4.8 Mbps and for RBFN and GRNN is approximately same and equal to 4.5 Mbps. LS Channel Estimation gives Throughput of 3.55 Mbps, but FFN and LRN gives approximately same throughput of 2.75 Mbps.

Figure 6.8 shows the throughput analysis for 2x2 MIMO System for CLSM transmission mode for flat rayleigh channel. It can be observed that GRNN gives better result compared to LS Channel Estimation. FNN gives worse result when compared to LS Channel Estimation technique. RBFN

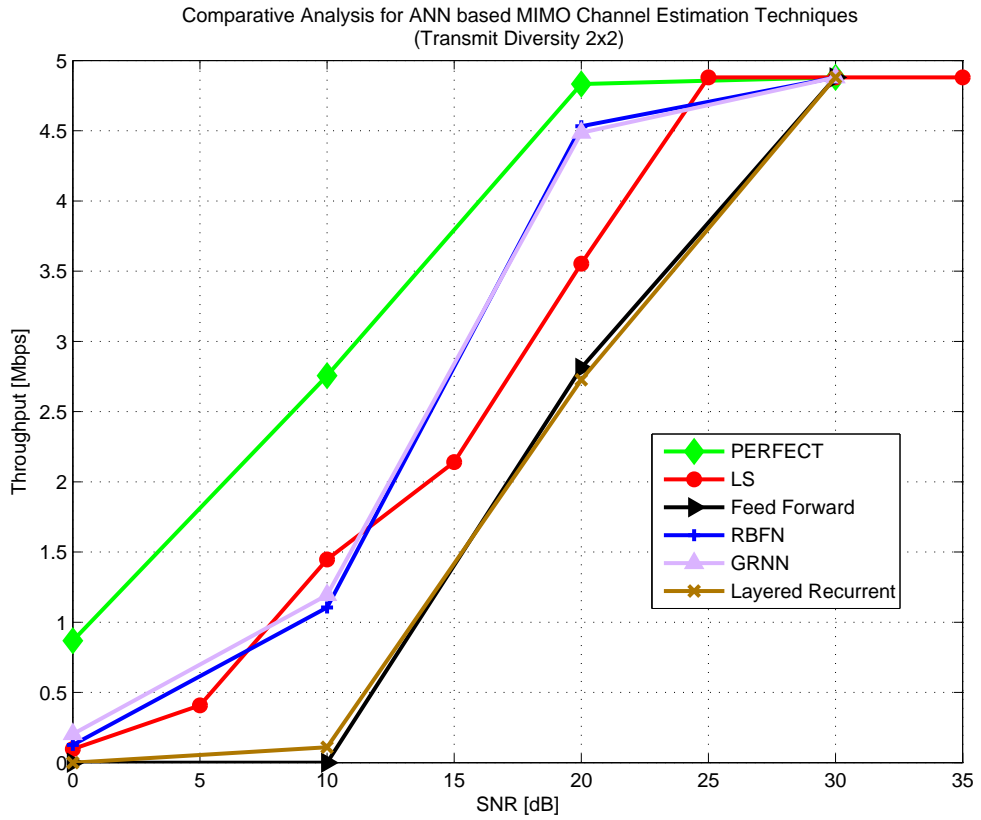


Figure 6.7: Throughput v/s SNR for TxD 2x2 for various ANN Channel estimation

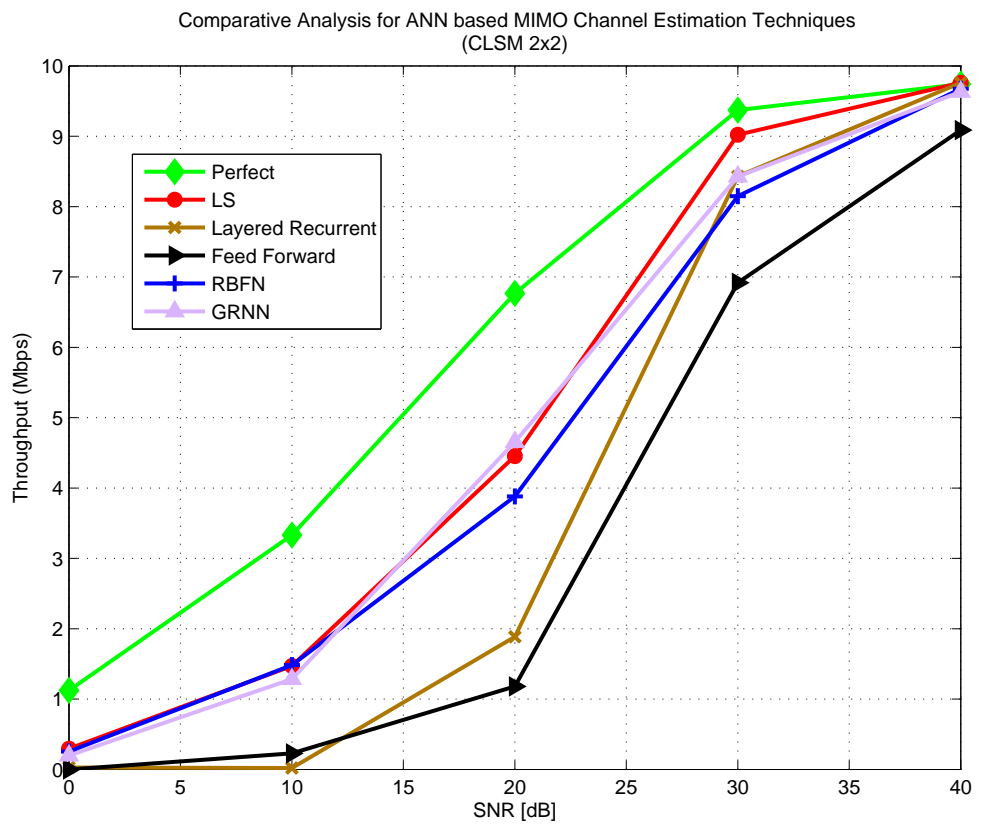


Figure 6.8: Throughput v/s SNR for CLSM 2x2 for various ANN Channel estimation

Network also gives equivalent performance to LS Channel Estimation technique.

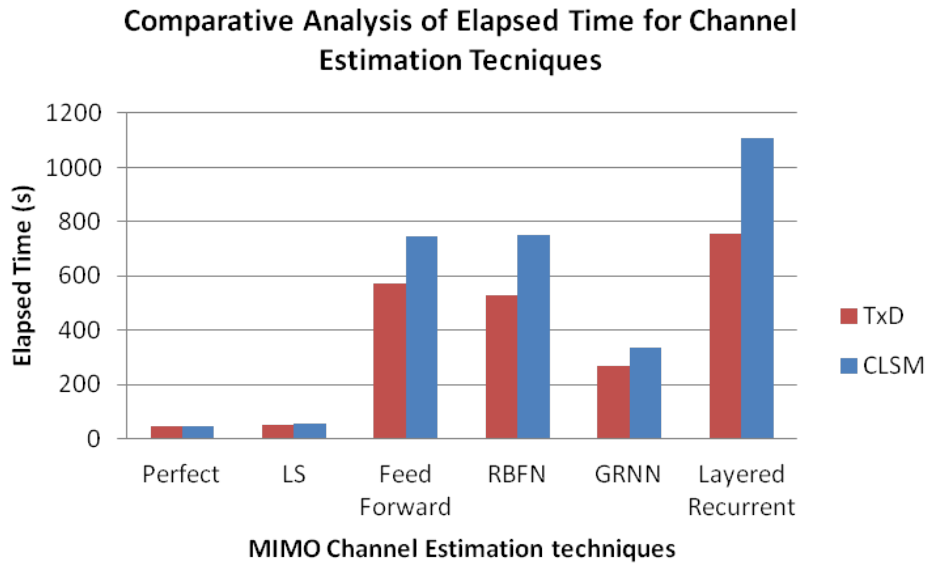


Figure 6.9: Comparison of Elapsed Time for different MIMO Channel Estimation Techniques

Figure 6.9 shows the performance analysis of different ANN based MIMO Channel estimation in terms of Elapsed time for simulation. The results are compared with the perfect channel and LS Channel Estimation Technique. As seen the GRNN Network takes minimum time of all ANN based Channel estimation technique of 266.54s for TxD and for 337.8s CLSM transmission mode. Whereas LRN takes maximum simulation time of for 757.7s TxD and for 1106.77s CLSM mode as it consists of feedback loop and layer delays for simulation.

6.4 ANN trained by Genetic Algorithm for MIMO Channel Estimation

Genetic algorithms are optimization algorithms based on several features of biological evolution. It proceeds in an iterative manner by generating new populations of individuals from the old ones. This algorithm applies stochastic operators such as selection, crossover, and mutation on an initially random population in order to compute a new population [30]. GA are used in conjunction with ANN to set the weights of ANN architectures, to learn ANN topologies and to select training data [31, 32]. GA have been successfully applied to train FNNs using GA for various decision and optimization problems [33–35].

Multi-layer feedforward (MLF) neural networks, trained with a back-propagation (BPA) learning algorithm, are the most popular neural networks. During training, the network topology and/or

the weights and/or the biases and/or the transfer functions are selected based on some training data. In many approaches, the topology and transfer functions are held fixed, and the space of possible networks is spanned by all possible values of the weights and biases [36, 37]. The BPA is a widely used method for FNN learning in many applications [38]. GA is widely used for optimization of parameters of FNN Network like weights and biases, network structures [39, 40]. GAs are found to be superior algorithm for training FNN as compare to BPA [40, 41]. This work has motivated the author to apply the GA for training FNN for MIMO Channel Estimation in LTE-A Downlink Physical Layer.

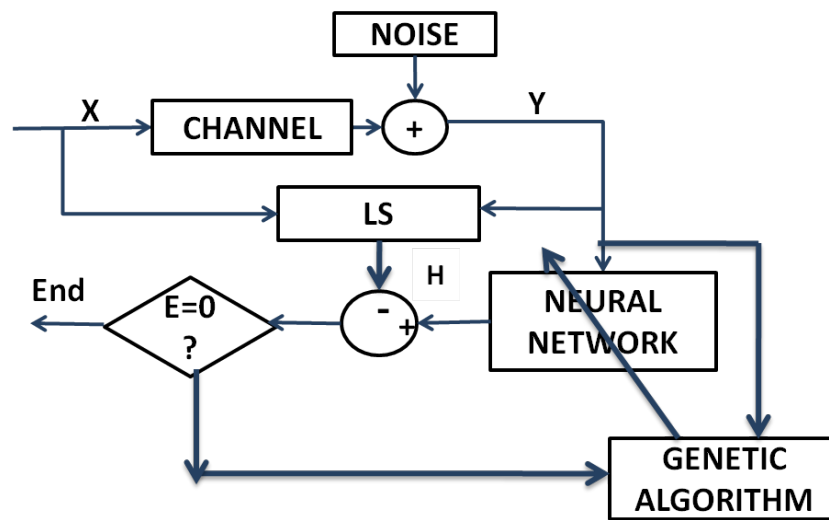


Figure 6.10: ANN-GA based Channel Estimation

BPA [42] is a famous learning algorithms among ANNs. In the learning process, to reduce the inaccuracy of ANNs, BPLAs use the gradient-descent search method to adjust the connection weights. The algorithm for FNN trained by BPA and FNN trained by GA is discussed in detail in [41]. In ANN-BPA, the ANN is trained with transmitted reference symbols. Optimization of the weights is made by backward propagation of the error during training or learning phase. The ANN reads the input and output values in the training data set and changes the value of the weighted links to reduce the difference between the received reference symbol and reference symbol values. The error in prediction is minimized across many training cycles (iteration or epoch) until network reaches specified level of accuracy. A complete round of forwardbackward passes and weight adjustments using all inputoutput pairs in the data set is called an epoch or iteration. The target sample set is presented to the ANN in the form of result or estimated channel obtained by Least Square (LS) complex type matrix. The learning of the ANN is done in the training phase

during which the ANN adjusts its weights according to training algorithm.

Similarly, ANN-GA is designed, the target sample set is presented same as in backpropagation neural network. The training of the ANN is done using GA. In the training phase, the GA adjusts its weights according to the Genetic algorithm applied between the receiver and result of LS estimator. First neural network is initialized with training pair (Inputs and Targets), and then configuration of neural network is done for the data set. A handle to the “MSE _ TEST” function [43] is created, that calculates MSE (mean square error between output and targets of FNN) by changing weights using GA. In GA, lower the error, the higher is the fitness. The weights for which function is to be the lowest will be stored in the neural network and applying Inputs to FFNN, output will give estimated channel output as shown in Figure 6.10.

6.4.1 ANN-GA Simulation Parameters and Result

The ANN-BPA and ANN-GA based MIMO Channel Estimation are simulated in LTE-A Link Level Simulator. Comparative Analysis of these techniques are carried out in terms of throughput v/s SNR for 2x2 CLSM MIMO mode as shown in Figure 6.11. FNN developed for channel estimation, is further optimized in terms of weights and biases of network architecture by GA. MATLAB Toolboxes usage and description for Neural Network and Genetic Algorithm design is discussed in detail Chapter 5. The simulation parameters for MIMO Channel Estimation based on ANN trained by BPA and GA are as in Table 6.3.

Parameters	ANN Trained by BPA	ANN Trained by GA
Number of inputs	1	1
Number of hidden layers	1	1
Number of neurons	5	5
Epoch number / Iteration	1000	100
Training Function / Algorithm	Levenberg- Marquart	Genetic Algorithm
Performance Metric	Mean Square Error	Mean Square Error

Table 6.3: Simulation Parameters for ANN-BPA and ANN-GA for MIMO Channel Estimation

Throughput analysis of proposed methods MIMO Channel estimation techniques are compared with LS channel estimator. It is seen that MIMO Channel estimator based on ANN trained by GA exhibits better performance in terms of throughput and is giving performance similar to Perfect channel from 10 to 15 SNR range. At SNR of 20 dB, ANN-GA has higher throughput of 8.875 Mbps compare to ANN-BPA (8.332 Mbps) and LS (8.673 Mbps) channel estimator.

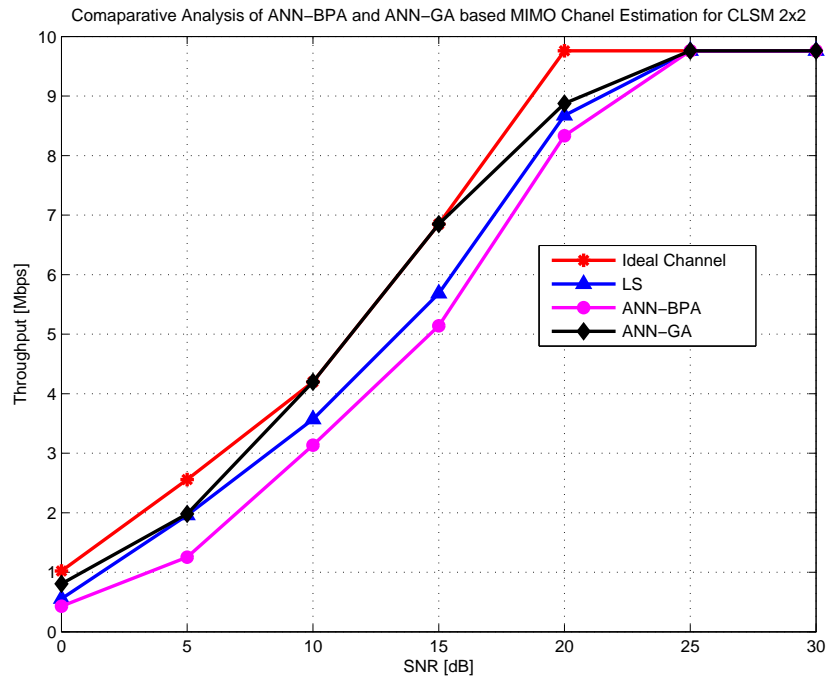


Figure 6.11: Throughput v/s SNR for ANN-BPA and ANN-GA MIMO Channel Estimation

6.5 Concluding Remarks

MIMO Channel Estimation being the vital part for detecting the received data at receiver, is studied in detail in this chapter. The imperfect CSI at receiver affects the Throughput of LTE-A Downlink Physical Layer. Various ANN based MIMO Channel estimation techniques are designed and simulation are carried out in this work. ANN based channel estimation methods developed for channel estimation are based of ANN Architectures: FNN, GRNN, RBFN and LRN. The throughput analysis shows that the proposed techniques gives better performance of the system as compared to traditional LS Channel estimator. The ANN is further trained by GA to optimize the ANN weights to enhance the channel estimation. By using ANN-GA based Channel Estimation technique the throughput can be maximized as compared to traditional LS Channel estimation method.

Fuzzy Logic Decision model for MIMO mode switching

7.1 Introduction

This chapter discusses the FL-Decision model developed for MIMO mode switching to optimize the throughput of LTE-A Downlink Physical Layer. A MIMO system can provide two types of gains: diversity gain and spatial multiplexing gain. Both types of gain can, in fact, be simultaneously achievable in a given channel, but there is a tradeoff between them [1] as discussed in Section 2.4. Most of current research focuses on designing schemes to extract either maximal diversity gain or maximal spatial multiplexing gain [2]. Existing adaptive schemes that switch between spatial multiplexing and diversity are based on various parameters for switching criteria. These parameters include Channel Condition Number [3, 4], Constellation Size [5], Signal-to-Noise Ratio [6, 7], Throughput [8], Probability of MIMO mode [9], and Error Rates [10].

Fuzzy Logic is well suited for nonlinear and complex systems where human knowledge can be utilized. Fuzzy Logic has been successfully applied in various areas of wireless communication systems [11]. This leads to motivation for the switching between MIMO modes using FL Decision model. A similar approach for MIMO Mode and Modulation and Coding Scheme (MCS) selection using Fuzzy Q-Learning was applied for High Speed Packet Access Evolution (HSPA⁺) Systems [12, 13]. This chapter discusses the design of proposed FL Decision model for MIMO mode switching scheme which considers Channel Condition Number and Receive Signal-to-Noise Ratio to decide the appropriate MIMO mode which gives optimal throughput. The FL Decision model designed for MIMO switching considers two MIMO modes: Transmit Diversity and Open Loop Spatial Multiplexing in LTE-A context.

7.2 MIMO Channel Condition Number

The channel condition number is a well known indicator of the spatial selectivity of a MIMO wireless channel [14, 15]. In MIMO context, the condition number indicates the multipath richness of the channel [16]. Many adaptive MIMO systems that have been proposed employ the condition number as a criterion for choosing appropriate MIMO Scheme. The system proposed in [5] chooses either BLAST or STBC based on the instantaneous channel condition number. Extending this scheme, in [4] a “dual-mode” antenna selection scheme is outlined, which uses the condition number to choose between multiplexing and general diversity techniques. Performance of Linear detectors: Zero-Forcing (ZF), Maximum-Likelihood (ML) and Minimum-Mean Square Error (MMSE) has been investigated based on Channel Condition Number. For MIMO Systems,

theoretical investigations and experiments suggest that the performance of linear detectors strongly depends on the channel condition number [17,18]. Channel Condition Number has also been shown to drastically affect the detection and error performance in spatial multiplexing systems [19,20].

Channel Condition Number of MIMO wireless channel measures the independence or correlation between channel paths. Lower the values of channel condition number, low is the correlation between channel paths. Condition number can be used to analyze the causes for throughput issues. The relation between the condition number and its effect on throughput according to industry published approximations is listed in Table 7.1 [21].

Condition Number	Indication
0 dB	Two totally independent channels, ideal condition to achieve maximum throughput
≤ 13 dB	Favorable condition which enables higher throughput as compare to SISO/MISO
13 dB to 19 dB	Medium Correlation which provides marginal throughput improvement
≥ 19 dB	High correlation where MIMO would not be able to increase throughput

Table 7.1: Channel Condition Number and its indications

To obtain high throughput of LTE-A Downlink Physical Layer, the channel condition number should be approximately less than 19 dB. When the channel condition number is high, means the channel paths are highly correlated so the MIMO scheme will not be able to maximize the throughput of the system. Hence the quality of MIMO wireless channel plays a vital role to optimize the throughput of LTE-A Downlink Physical Layer.

7.2.1 Statistics of Demmel Condition Number

MIMO wireless communication system delivers significant capacity gains as compared with conventional SISO system. For a MIMO System with n_T transmit antennas and n_R receive antennas, the performance and capacity of MIMO transmission schemes are dictated by the eigenvalues of instantaneous MIMO channel correlation matrix given by:

$$W = \begin{cases} HH^*, & n_R < n_T \\ H^*H, & n_R \geq n_T \end{cases} \quad (7.1)$$

where H is the channel matrix of MIMO channel gains modeled as Complex Gaussian. MIMO Channel Correlation Matrix W is known to follow a complex Wishart distribution [14]. The Wishart distribution is the multivariate extension of the gamma distribution [22]. The statistical properties

of Wishart matrices have been applied to MIMO applications. The eigenvalue distributions and determinate properties of Wishart matrices have been extensively studied to explore the ergodic capacity of the MIMO channel under different conditions [23, 24]. The eigenvalues of matrix W is denoted by the vector:

$$\lambda \triangleq [\lambda_1, \lambda_2, \dots, \lambda_s], \quad (7.2)$$

with $\lambda_1 \geq \lambda_2 \dots \geq \lambda_s > 0$.

The Condition Number of MIMO Correlation matrix W is defined as:

$$z \triangleq \frac{\lambda_{max}}{\lambda_{min}}, \quad z \geq 1 \quad (7.3)$$

where λ_{max} and λ_{min} are the largest and smallest eigenvalues of W , respectively. Channel Condition Number is a metric which determines the invertibility of a matrix. A condition number close to one indicates a well-conditioned full-rank matrix with equal eigenvalues, whereas a very high condition number implies a near rank-deficient matrix.

The impact of condition number on MIMO channel capacity assuming perfect channel knowledge at the receiver and no knowledge at transmitter for 2x2 system is given by following equation:

$$C = \log_2(\det(I_2 + \frac{\rho}{2}W)) \quad (7.4)$$

$$= \log_2((1 + \frac{\rho}{2}\lambda_{max})(1 + \frac{\rho}{2}\frac{\lambda_{max}}{z})) \quad (7.5)$$

where ρ is SNR and from Equation 7.5 we can say that there is no analytical relation and one-to-one mapping between condition number and MIMO Channel capacity.

The relation between Channel capacity with fixed SNR and varying condition number is shown in Figure 7.1. The effect of channel condition number on channel capacity is shown in Figure 7.2. It is evident that as the channel condition number increases the MIMO channel capacity decreases and vice-versa. We can conclude that channels with low condition number or highly uncorrelated channels yields high MIMO channel capacity.

To get a deeper understanding, the Cumulative Distribution Function (CDF) and Probability Density Function (PDF) of MIMO Channel condition number is studied. For statistical analysis of Channel Condition number the two classes of channels are considered for which, $W \in \mathcal{C}^{s \times s}$ follows

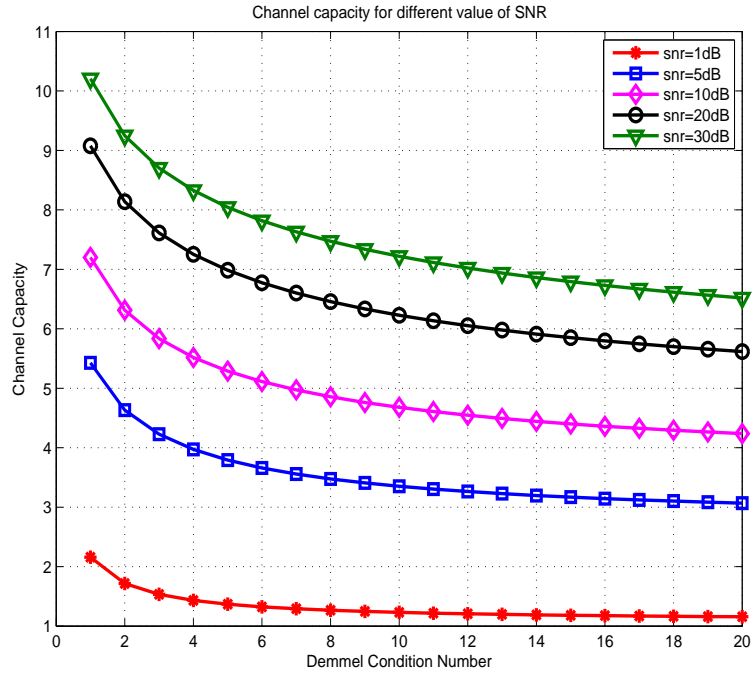


Figure 7.1: Channel capacity with varying SNR

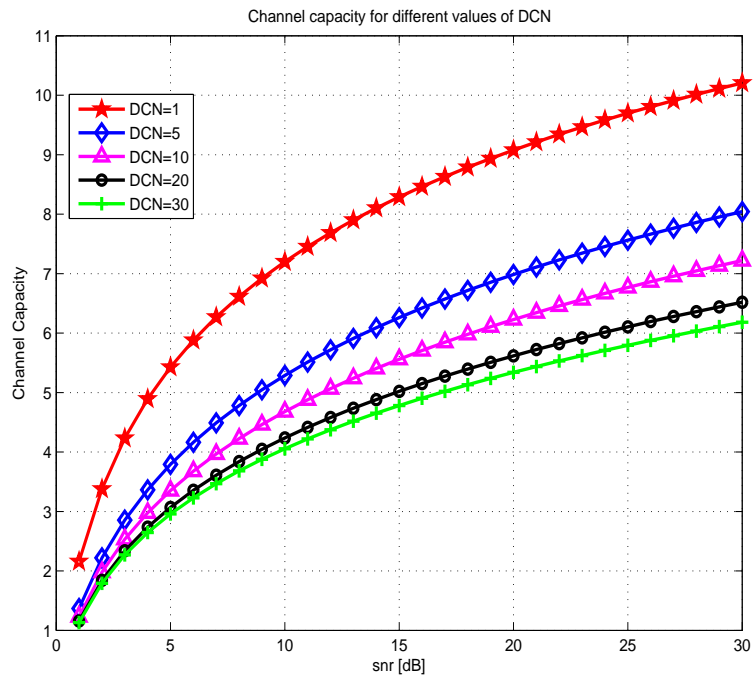


Figure 7.2: Channel capacity with varying Condition Number

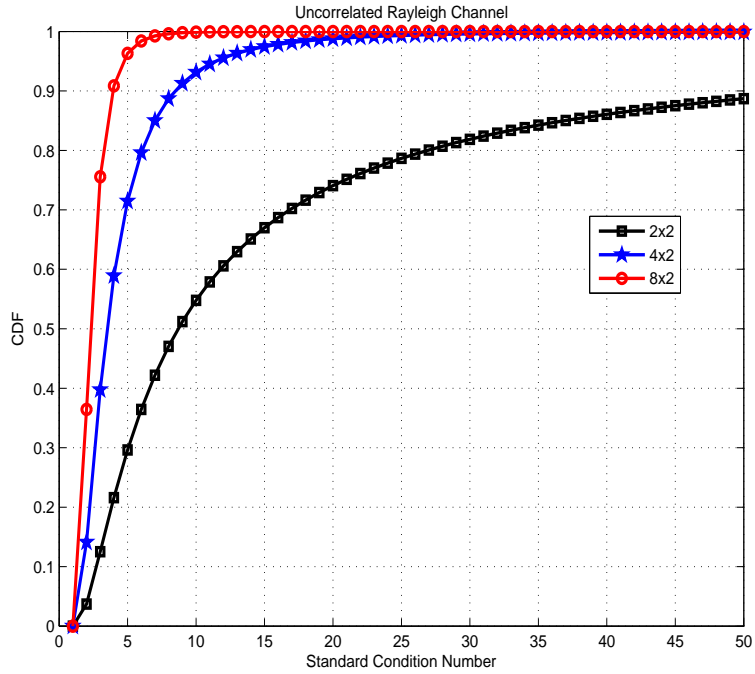


Figure 7.3: CDF of SCN for Uncorrelated Rayleigh Channel

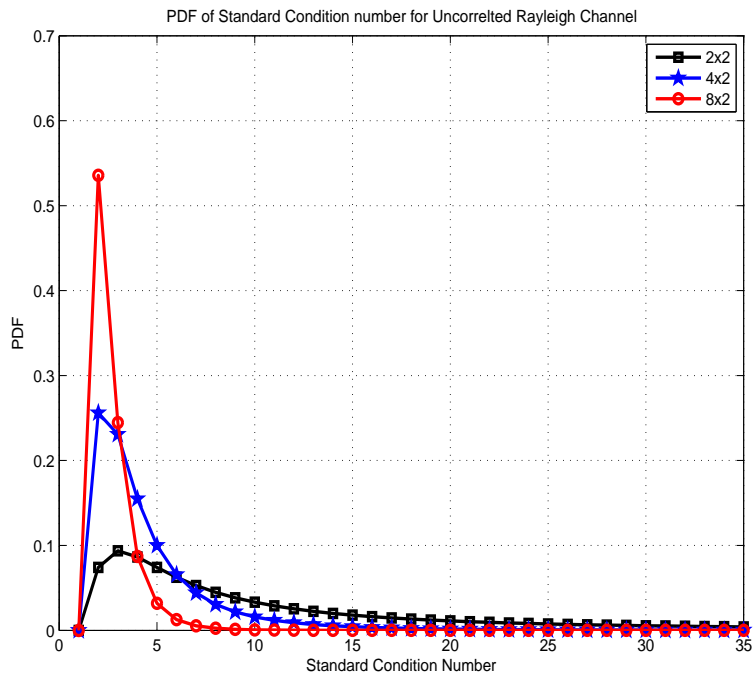


Figure 7.4: PDF of SCN for Uncorrelated Rayleigh Channel

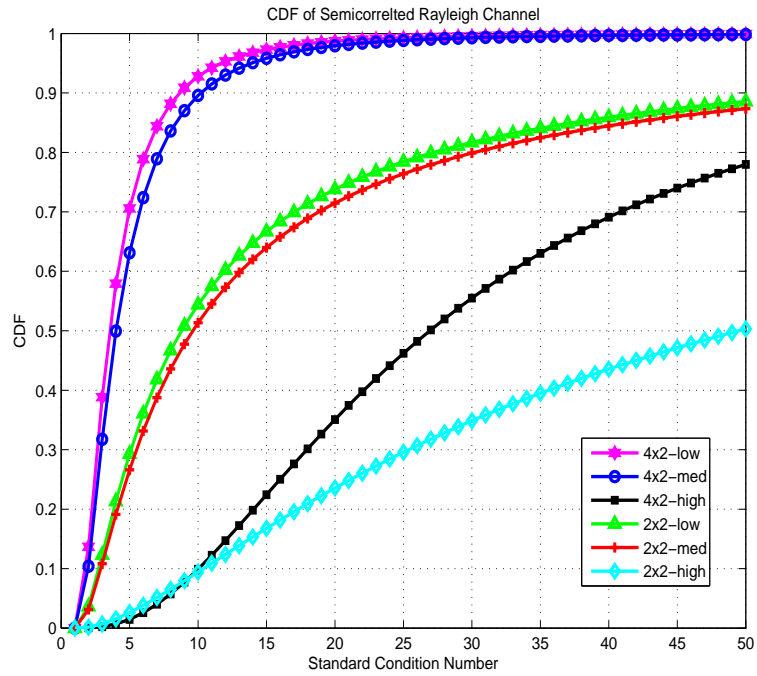


Figure 7.5: CDF of SCN for semicorrelated Rayleigh Channel

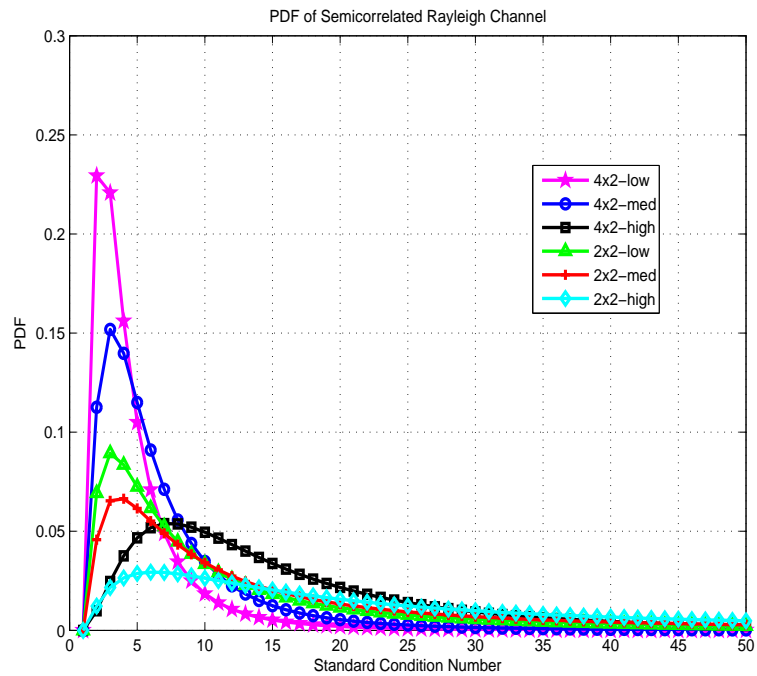


Figure 7.6: PDF of SCN for semicorrelated Rayleigh Channel

Wishart distribution with t degrees of freedom, where $s = \min(n_T, n_R)$ and $t = \max(n_T, n_R)$. Following are the two channel models considered for study:

1). Uncorrelated Rayleigh Fading: The uncorrelated Rayleigh model is valid when the antenna spacing is high enough to induce independent fading, and there is no LoS path between the transmitter and receiver and W is uncorrelated central Wishart matrix.

2). Semi-Correlated Rayleigh Fading: The MIMO spatial subchannels are often correlated due to the limited angular spreads or restrictions on the array sizes. Hence, spatial correlation between is considered for modeling the channel. Here, we have assumed that correlation occurs only at the side with minimum number of antennas, in which case W is semi-correlated central Wishart matrix.

The exact closed form expressions for both the channel cases have been derived in paper [15]. The same equations are used to plot the distributions and densities of Channel Condition Number. As shown in Figure 7.3, CDF of condition number for uncorrelated Rayleigh channel for different antenna configurations. For a system with two receive antenna, as the number of transmit antennas increases, the channel condition significantly improves. The CDF plot for 2x2 system is spread over the entire range [0,1] which indicates the the channel consists of highly correlated paths as compared to 8x2 system. As the number of antenna increases, it leads to improvements of the channel condition number. The PDF of standard condition number is as shown in Figure 7.4. The probability of having low condition number channel is high in 8x2 system when compared to 4x2 and 2x2 system.

The effect of spatial correlation on the channel condition number has been studied by plotting the CDF and PDF for Semi-correlated Rayleigh channel. As shown in Figure 7.5, as the spatial correlation increases the CDF plot spread over the entire region [0,1] and hence the channel becomes ill-conditioned. For low spatial correlation for 2x2 and 4x2 system the channel is well conditioned as compare to medium or high correlation. Hence, correlation in the channel matrix results in ill-conditioned channel and also increases the channel condition number.

Similarly, the PDF plot for different spatial correlation for 2x2 and 4x4 system is as shown in Figure 7.6. The probability of low condition number i.e well conditioned channel is highest in 4x2 system with low spatial correlation as compare to other systems. The probability of ill-conditioned channel is maximum in 2x2 system with high correlation.

7.3 Investigation of Switching Point between TxD and OLSM for 2x2 MIMO

Switching point between various MIMO modes has been investigated in [2, 26]. In context of LTE-A, MIMO schemes Transmit Diversity and Open-Loop Spatial Multiplexing offers trade-off between diversity gain and multiplexing gain. The switching point between both the scheme is studied in conjunction with transmit correlation for consideration of single sided correlation with minimum number of antennas.

Different values of Transmit correlation were considered and its effect on switching point between two schemes are studied. The plots are generated using the Vienna LTE-A Link Level Simulator. As shown in Fig. 7.7, SNR v/s throughput for 2x2 TxD and OLSM the switching point moves towards higher SNR as the transmit correlation increases. Table 7.2 analyses the numerical relation between Transmit Correlation and Switching point between TxD and OLSM.

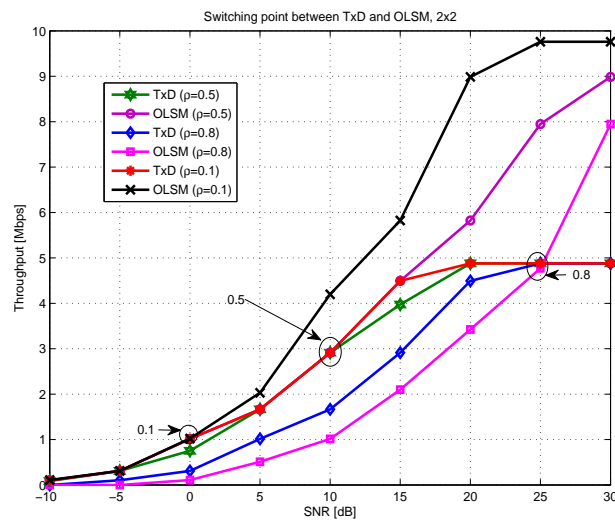


Figure 7.7: Switching point between 2x2 TxD and OLSM for different transmit correlation

Transmit Correlation	Switching Point SNR[dB]
0.1	0
0.5	10
0.8	25

Table 7.2: Switching point between TxD and OLSM for 2x2 MIMO

For transmit correlation of 0.1 the switching point is at 0 dB and for Transmit Correlation of 0.8 the switching point is at 25 dB. As we increase the correlation the switching point moves towards

the higher SNR. The switching point depends on the SNR value and the correlation between MIMO channel paths. Hence the channel condition number which depends on the correlation between channel paths and the Receive SNR can be considered for making decision on switching between TxD and OLSM to maximize throughput. By making decision based on the channel condition and the receive SNR regarding the MIMO mode for transmission can optimize the throughput of LTE-A Downlink Physical Layer.

7.4 FL Decision model for MIMO mode switching

Fuzzy Logic is used for decision making and is capable of dealing with non-linearities and uncertainty in the system. Decision-making in a fuzzy environment is a decision process in which the goals and/or the constraints, are fuzzy in nature. The object of the fuzzy decision methodology is to obtain a decision, optimum in the sense that some set of goals are attained, while observing set of constraints [27].

The MIMO wireless channel is non-linear and continuously time-varying in nature. Hence, the channel condition number and Receive-SNR are fuzzy in nature. The decision regarding switching of MIMO mode is done through the FL Decision model. A heuristic knowledge regarding the Channel Condition Number and Receive-SNR influence the appropriate MIMO mode Switching. This heuristic knowledge can be expressed well in terms of a fuzzy logic using the so-called fuzzy IF-THEN rules. This fact provides the motivation for the design and implementation of FL decision model for MIMO mode switching.

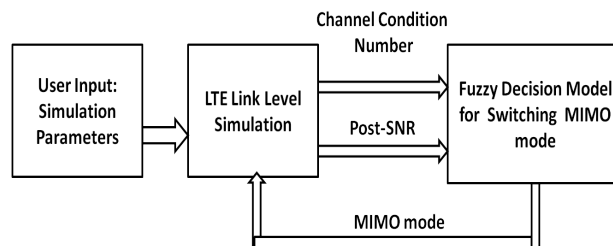


Figure 7.8: Block Diagram for FL Decision based MIMO mode Switching

The FL Decision model is designed using MATLAB based Fuzzy Logic Toolbox [28], which provides a set of GUI editors that builds a Fuzzy Inference System (FIS). As shown in Fig. 7.8, the FL Decision model with two input, one output is designed for MIMO mode switching. Channel condition number and Receive-SNR from receiver are taken as input and MIMO mode output from FL Decision model is feedback to transmitter of LTE-A Link level simulator, which selects the appropriate MIMO mode which maximizes throughput. The characteristics of FL Decision model

Parameters	Characteristic
Type of Fuzzy Inference	Sugeno-Type
Inputs	2
Outputs	1
Antecedent MFs	3 triangular shaped
Consequent MFs	2 singleton type
Aggregation method	MIN
Implication method	MAX
MF overlapping degree	2
Defuzzification method	Weighted average

Table 7.3: Characteristics of FL Decision model

are summarized in Table 7.3. The FL Decision model consists of Fuzzification, Fuzzy Rule Base and Defuzzification block, as described in following sections.

7.4.1 Fuzzification

The crisp inputs to FL Decision model are converted into a set of membership values in the interval $[0, 1]$ in the corresponding fuzzy sets. Three partially overlapping Triangular Membership functions (MFs) are used for input Channel Condition Number and Receive-SNR. Variables for FL Decision model, their membership functions with range are as shown in Table 7.4.

Variables	Channel Condition Number (Input-1)	Receive-SNR (Input-2)	MIMO Mode (Output)
Type of Variable	Fuzzy	Fuzzy	Binary
Type of MF's	Triangular	Triangular	Constant
Range	Low: [0 5.95 12.4] Medium: [11.28 27.91 41.64] High: [40.34 61.49 100]	Low: [-30 -12.4 10.87] Medium: [9.29 14.05 17.5] High: [16.96 53.73 70]	1:OLSM 0:TxD

Table 7.4: Variables for FL Decision model

The linguistic variables used for Channel Condition Number are **Low**, **Medium** and **High**. The range for the Channel Condition Number is decided based on the PDF and CDF of Channel Condition Number as discussed in Section 7.3. Similarly linguistic variable for Receive-SNR are **Low**, **Medium** and **High**. The range for Receive-SNR is decided from the Switching Point be-

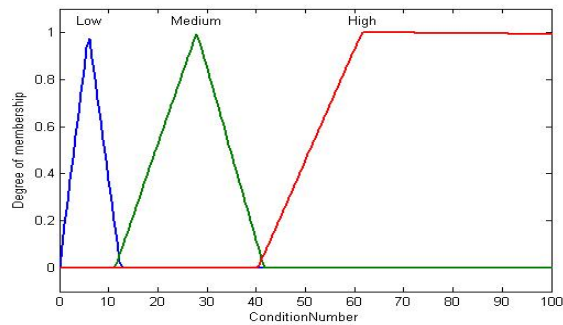


Figure 7.9: Membership function for Channel Condition Number

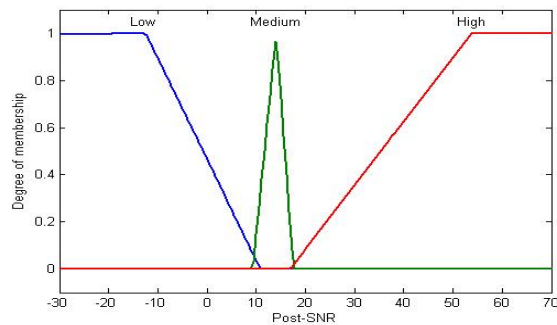


Figure 7.10: Membership function for Receive-SNR

tween MIMO modes (Fig. 7.7). Hence the membership functions of channel condition number and Receive-SNR are designed based on the analysis and simulation results. The Receive-SNR values are designed based on the receive SNR obtained from the simulation results of LTE-A Link Level simulator for various MIMO Schemes, Channel conditions, antenna configurations and Receiver configurations.

The output MF's of the MIMO mode of Sugeno-Type Fuzzy Inference System consists of Singleton MF's. As the switching is to be carried out between two MIMO modes: TxD and OLSM. The output MF's consists of two singleton values, 0 for TxD mode and 1 for OLSM MIMO mode.

7.4.2 Fuzzy Rule Base

The Fuzzy Rule Base is an IF-THEN linguistic rule using the fuzzy input and output sets. This rule base is generated based on an experts heuristic knowledge such as Transmit diversity is preferred if Channel Condition number is high and Receive-SNR is Low. If the Channel condition number is Low it requires high SNR to give better throughput, hence Spatial Multiplexing is preferred. For example, in the case of the rule, “**IF** Channel Condition Number is **High** and Receive-SNR is **High** **THEN** MIMO mode is **TxD**”, an expert thinks that as the Channel condition number

is high, transmit diversity scheme is preferred. In a similar way, the other rules are generated based on human knowledge. According to the fuzzified input value, the fuzzy decision for the MIMO mode is taken based on the Fuzzy Decision Rules. The 9 rules in the form of 3x3 matrix are listed in Table 7.5.

		Receive-SNR		
		Low	Medium	High
Channel Condition Number	Low	TxD	SM	SM
	Medium	TxD	SM	SM
	High	TxD	TxD	TxD

Table 7.5: FL Decision model Rule base

7.4.3 Defuzzification

After the set of Fuzzy rules are applied to the fuzzified input, the output need to be converted to scalar output quantity. The process of converting the fuzzy output is called defuzzification. There are many different mathematical techniques to perform defuzzification. The Weighted-Average method [29] is used to obtain the final output MIMO mode.

7.4.4 FL Decision Algorithm

The FL Decision Algorithm takes the user input as initial parameters for LTE-A Link level simulations. Initial Simulation parameters and selection Choice is as shown in Table 7.6. The basic idea for the FL Decision Algorithm is to use the MIMO mode which maximizes throughput. The decision for appropriate MIMO mode is based on Average Channel Condition Number and Receive-SNR. The pseudo code for FL Decision Algorithm is as shown in Algorithm 7.1.

Algorithm 7.1 FL Decision based MIMO mode Switching Algorithm

- Get User input Simulation Parameters as in Table 7.6.
 - while** *SNRRange* **do**
 - Run LTE sim batch quick test.m
 - Calculate Channel Condition Number and Receive-SNR
 - Fuzzification: Convert crisp input data to fuzzy values using the membership functions
 - Inference: Evaluate the rules in the rule base
 - Output the MIMO mode selected
 - Run LTE sim batch quick test for new MIMO mode
 - end while**
 - Plot SNR v/s Throughput
-

The part of the MATLAB code which performs the fuzzy inference calculation is as given below. The out of the Weighted Average Defuzzification is in the range [0,1]. So the Threshold value of

Parameters	Selection Choice
Antenna Configuration	2x2/4x2
Channel Configuration	Flat Rayleigh/PedA/PedB VehA/VehB
Antenna Correlation	Low/Medium/High
MIMO Mode	Transmit Diversity/ Spatial Multiplexing
Receiver Configuration	Zero-Forcing (ZF)/ Minimum Mean Square Error (MMSE)/ Soft-Sphere Decoder (SSD)
MCS Scheme	1-15

Table 7.6: Initial Selection of Simulation Parameters

0.5 is set to select the MIMO mode. The Channel Condition number and Receive SNR is given as input to fis and the command evalfis performs the fuzzy inference calculation and gives the output, which selects the MIMO mode to be switched based on FL Decision model designed.

```

fis_1=readfis('FIS1.fis'); %read the fis model designed
in=[receive_snr;averageconditionnumber] %create an input vector for fis
out=evalfis(in,fis_1); %evaluate fis for output
if out >= 0.5
    LTE_params.UE_config.mode = 3; %OLSM Config mode is selected
else
    LTE_params.UE_config.mode = 2; %TxD config mode is selected
end

```

7.5 Simulation Parameters and Results

The designed FL Decision model for MIMO mode switching is verified with Vienna LTE-A Link Level Simulator. Graphical User Interface (GUI) is developed in MATLAB, which enables user to select the Initial parameters for Simulation, and observe the switching to the MIMO mode decided by FL Decision model. The GUI also compares the Throughput (Mbps) and Time for processing (sec). Figure. 7.11 shows a snapshot of the GUI for analysis of FL Decision model for

MIMO mode switching.

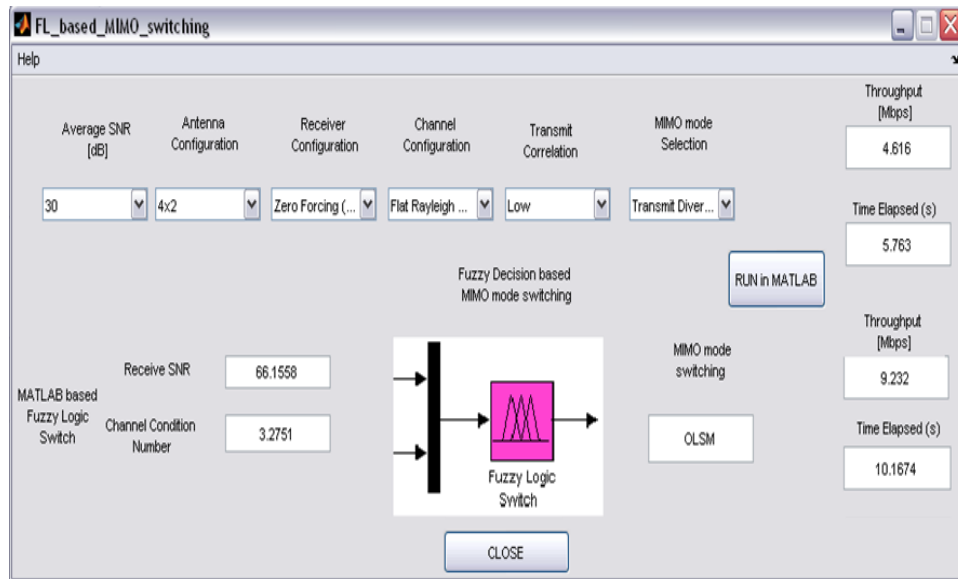


Figure 7.11: User Interface for FL Decision model for MIMO mode switching

The input Channel condition number and the Receive SNR value from the LTE-A receiver are given to the fis model designed for mode switching. By evaluating the fis model developed the MIMO mode output is given to the transmitter for switching the MIMO mode to maximize the throughput. Using the Pop-up menu list the user can select the initial parameters for simulation such as SNR, Antenna configuration, receiver configuration and MIMO mode. After running the simulation using the push button, the results are viewed in display text. For example, for SNR=30dB and MIMO mode selected is Transmit Diversity it gives Throughput of 4.616 Mbps. The obtained average channel condition number for the initial simulation parameter is 3.2751 and the Receive SNR is 66.1558, using this input parameters the MIMO mode selected by FL Decision Model is OLSM and the resultant throughput comes out to be 9.232, which is more as compare to initial MIMO mode Throughput.

Result analysis is carried out for initial mode selection of TxD and OLSM for different antenna configuration for Flat Rayleigh Correlated channel and various transmit correlation as shown in Figure [7.12 - 7.14], respectively.

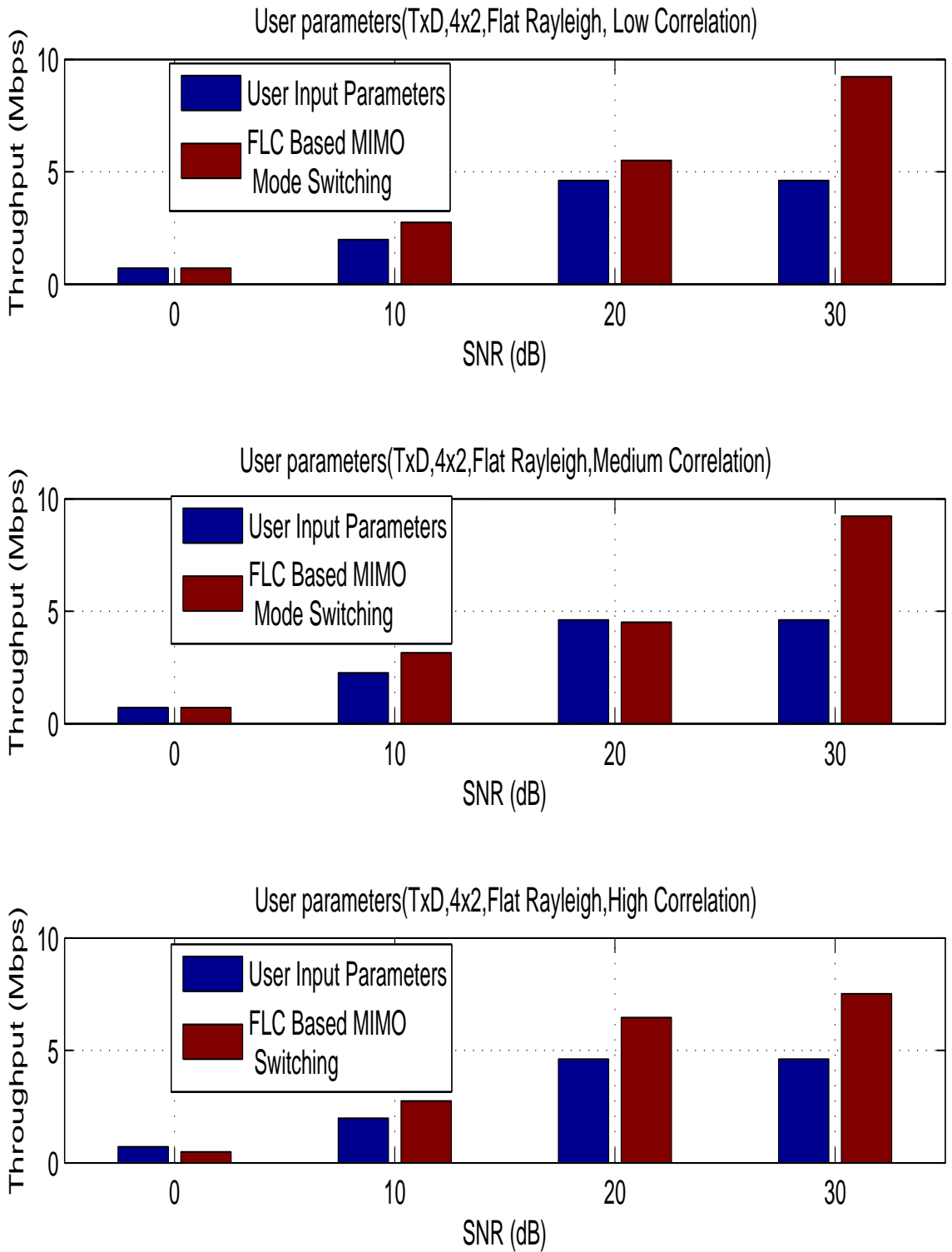


Figure 7.12: Comparative Analysis of FL Decision Model for Initial mode of TxD 4x2

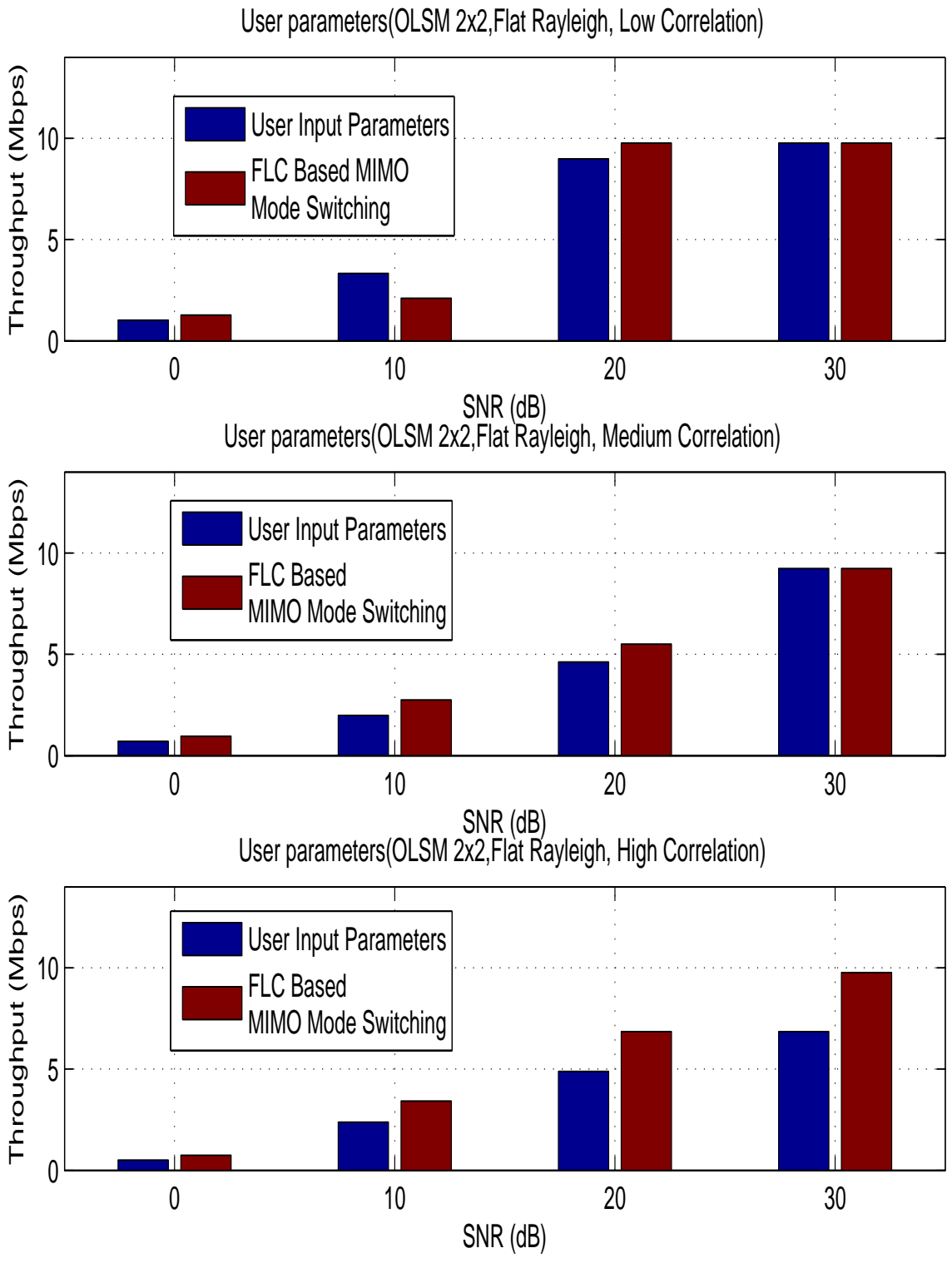


Figure 7.13: Comparative Analysis of FL Decision Model for Initial mode of OLSM 2x2

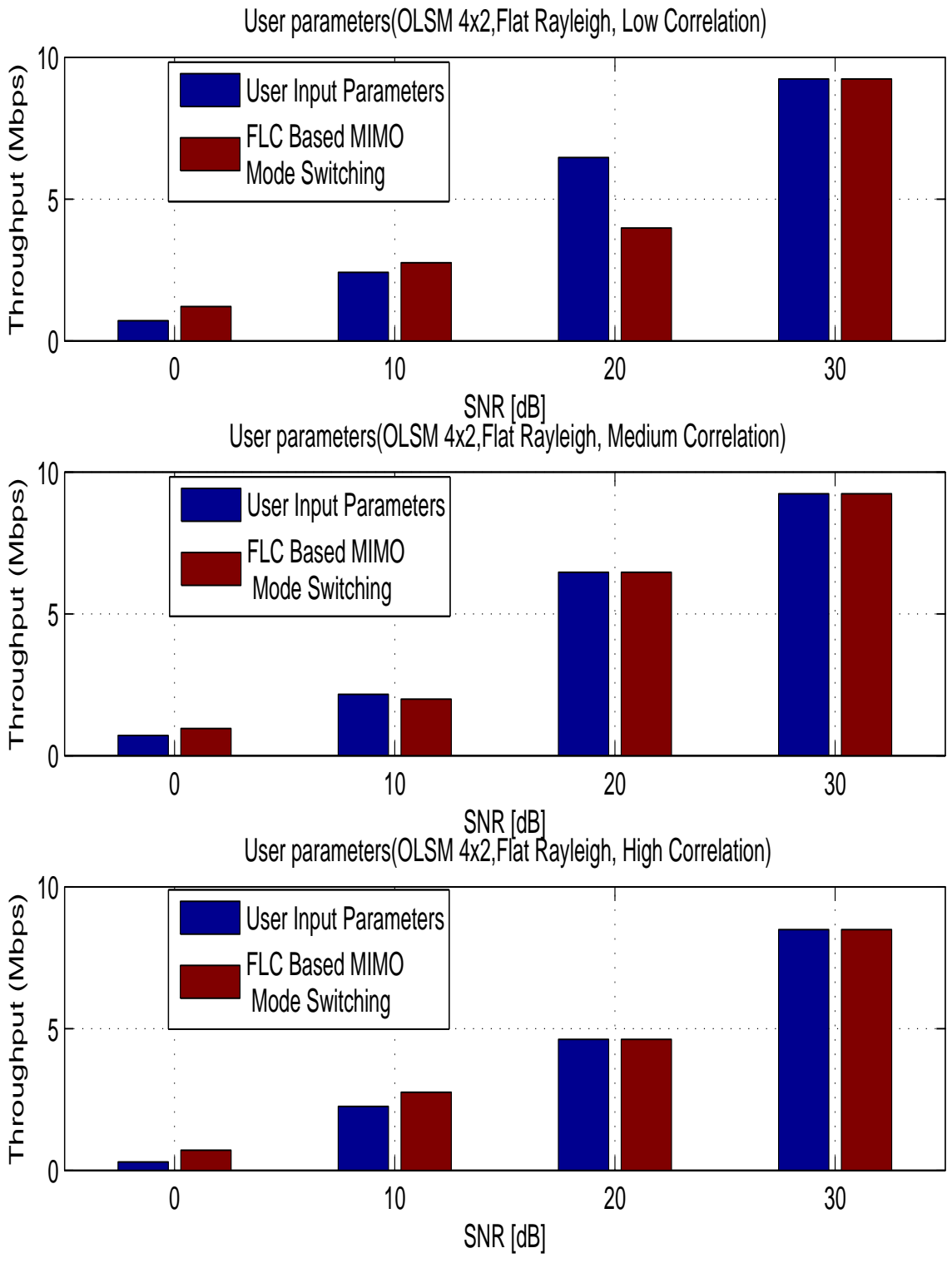


Figure 7.14: Comparative Analysis of FL Decision Model for Initial mode of OLSM 4x2

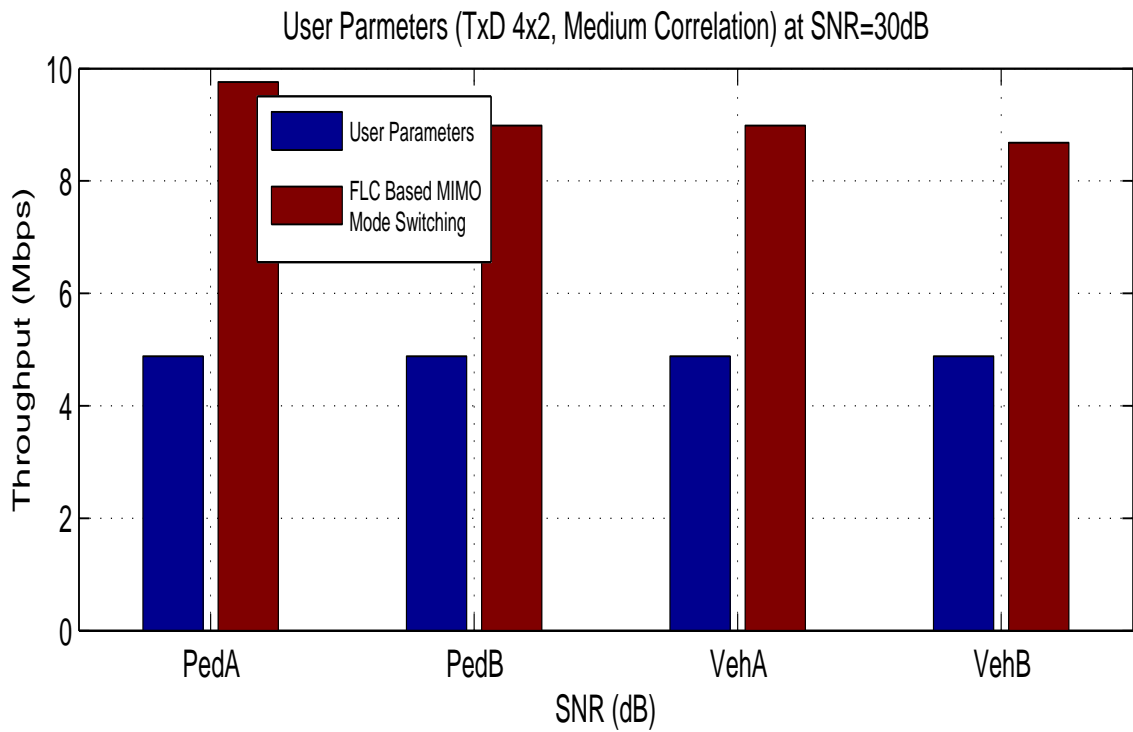
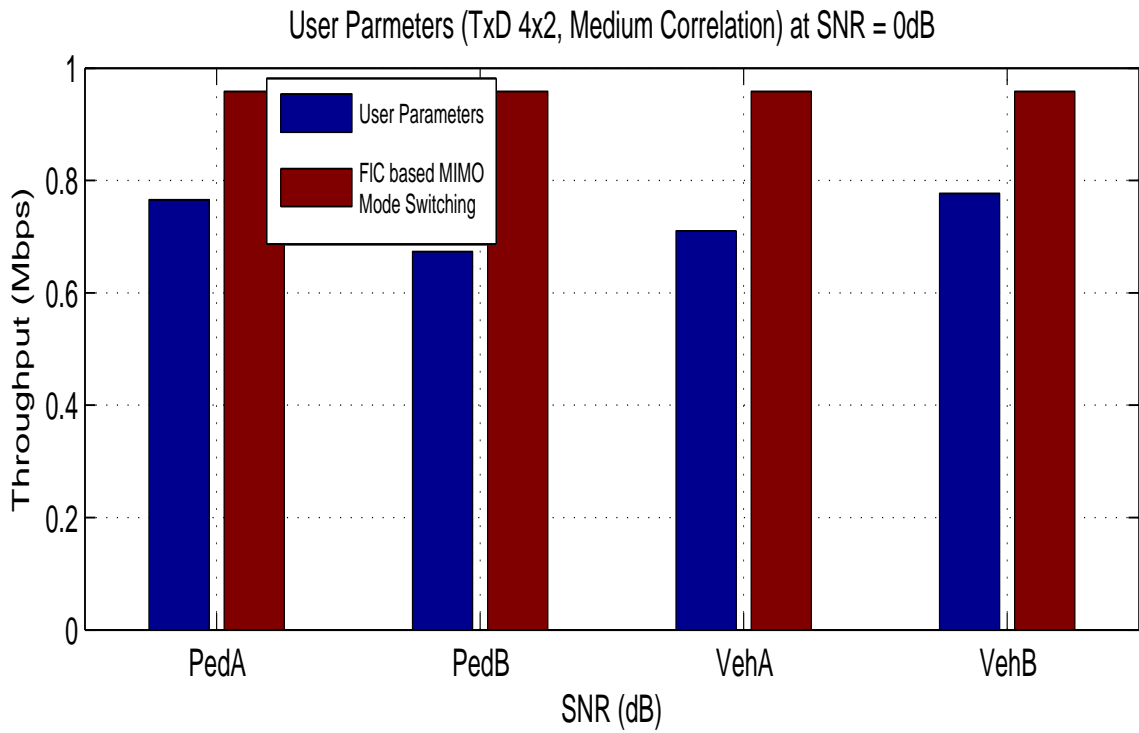


Figure 7.15: Comparative Analysis of FL Decision Model for Initial mode of TxD 4x2.

The FL Decision model developed is also verified for its performance in different channel configuration of PedA, PedB, VehA and VehB channels. The result analysis of Throughput is as shown in Figure 7.15, it can be seen the FL Decision model is able to select the appropriate MIMO mode to maximize the Throughput at Low SNR of 0dB and also at High SNR of 30dB scenario for all channel configurations.

From the comparative analysis we can conclude that for Initial Antenna configuration of 2x2 or 4x2, if initial MIMO mode is TxD or OLSM, the FL Decision model is able to successfully switch to the MIMO mode which gives maximum throughput. The decision made based on the Receive SNR and Channel Condition number is able to optimize the throughput of LTE-A Downlink Physical Layer.

7.6 Conclusion

The chapter discusses the FL-Decision model for MIMO mode switching for Throughput Optimization in LTE Downlink Physical Layer. The model takes into account the channel condition number and the Receive-SNR. The model switches between Transmit Diversity and OLSM Transmission mode of LTE Downlink Physical Layer. Based on the Fuzzy Rule base it takes decision and switches to the appropriate MIMO mode. The rules are designed based on the relation between the Switching point between MIMO modes and Channel Condition Number. The FL Decision Model is able to maximize throughput for LTE Downlink Physical Layer for various Channel Configurations and Antenna Configurations.

Hardware Implementation of Throughput Optimization Algorithms

8.1 Embedded Architecture Implementation

The algorithm developed for Throughput Optimization of LTE-A Downlink Physical Layer are implemented on Spectrum Digital TMS320C6713 DSK and Xilinx Atlys Spartan 6 Development Kit. The embedded architecture implementation of these algorithms are carried out in close-loop testing with MATLAB based LTE-A Link Level Simulator. Figure 8.1 shows the design flow for real-time implementation of proposed algorithms for Throughput Optimization. The Mathworks Model based design FPGA and DSP implementation and verification is discussed in Section 3.3.

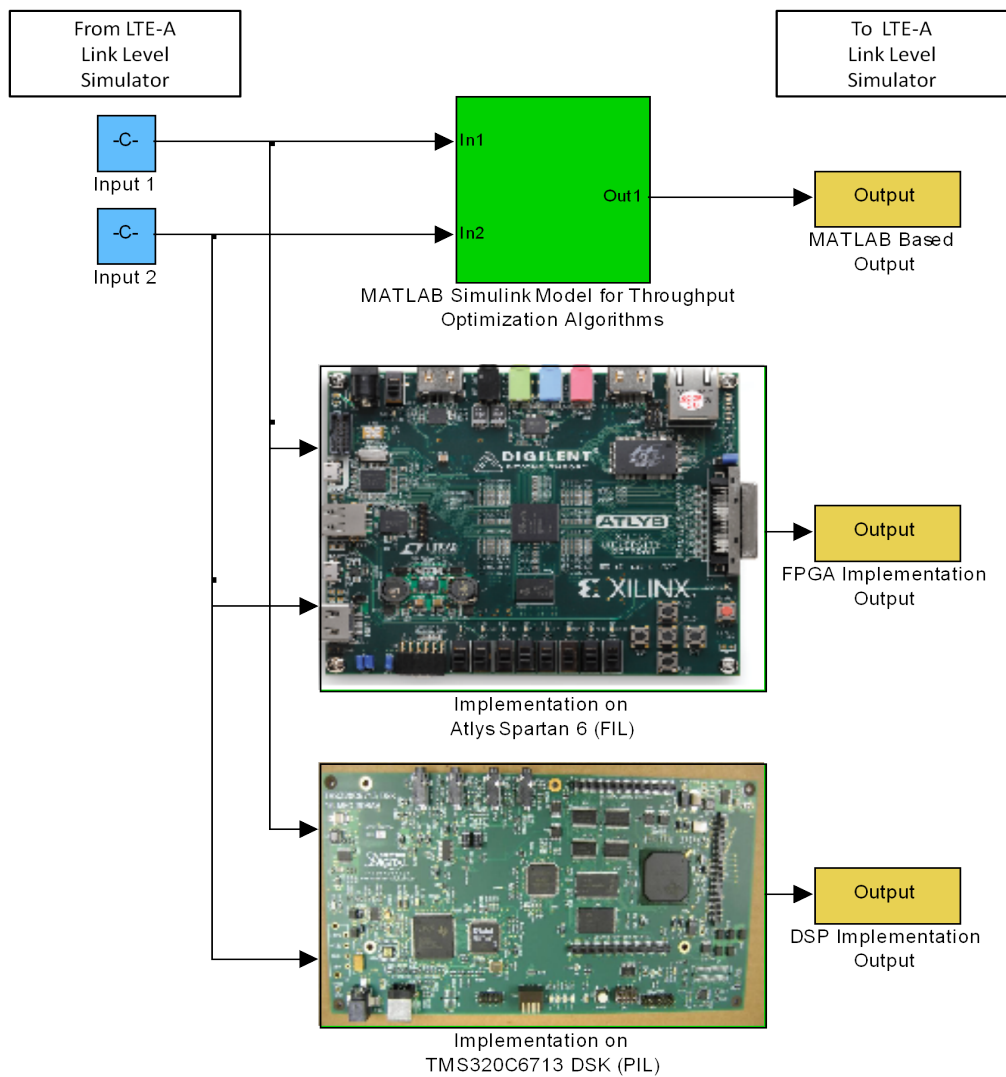


Figure 8.1: Design Flow for Real-time Implementation on Target Hardware

Throughput Optimization of LTE-A Downlink Physical layer is addressed in the research work. Following are the proposed techniques for throughput optimization:

- ANN based MIMO channel estimation techniques are developed which maximizes Throughput of LTE-A Downlink Physical Layer as discussed in Chapter 6.
- Fuzzy Logic Decision model is developed for MIMO mode switching to achieve maximum throughput of LTE-A Downlink Physical Layer discussed in Chapter 7.

8.1.1 XUP Atlys Spartan-6 Development Kit

The Xilinx University Program (XUP) Atlys Development Kit [1, 2] is based on high-capacity Spartan-6 LX45 FPGA [3, 4], and includes the circuits and devices that enable advanced digital system designs. The on-board high-speed DDR2 memory, HDMI ports, Gigabit Ethernet, and advanced clocking and power supply circuits makes the kit an ideal platform for research work as shown in Figure 8.2. The Atlys Functional Block Diagram with all the peripherals and connectivity are shown in Figure 8.3. The Atlys board includes Adept USB2 system, which offers device programming, real time power supply monitoring, automated board tests, virtual I/O, and simplified user data transfer facilities.

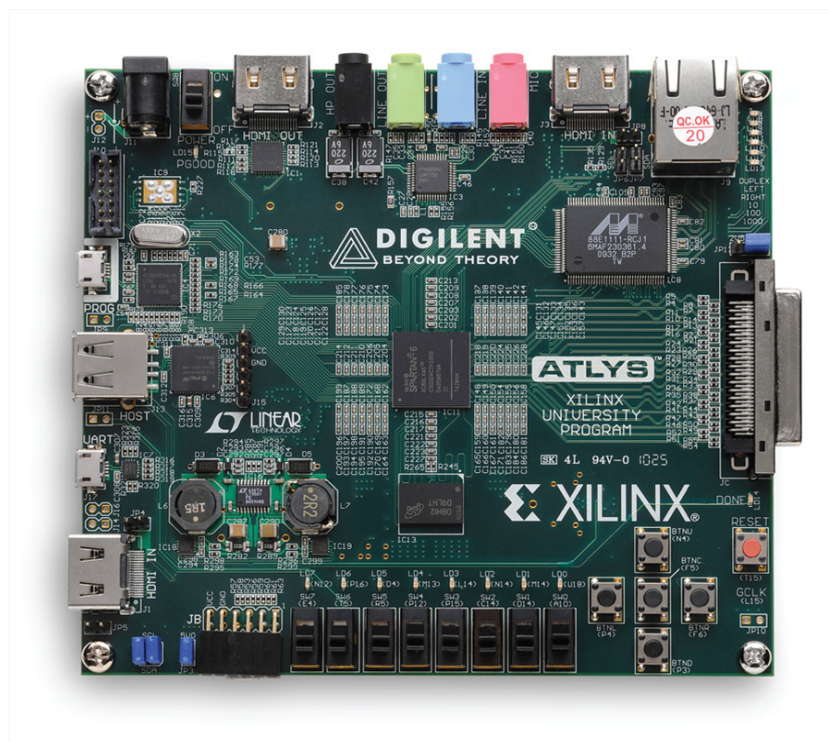


Figure 8.2: XUP Atlys Spartan-6 Development Kit

XUP Atlys Board is one of the supported FPGA devices for FPGA-in-the-loop simulation in MATLAB. FIL Simulation provides the capability to use Simulink models for testing designs in real hardware for any existing HDL code. The FIL process provides synthesis, logical mapping, Place-and-route (PAR), programming file generation and communication channel.

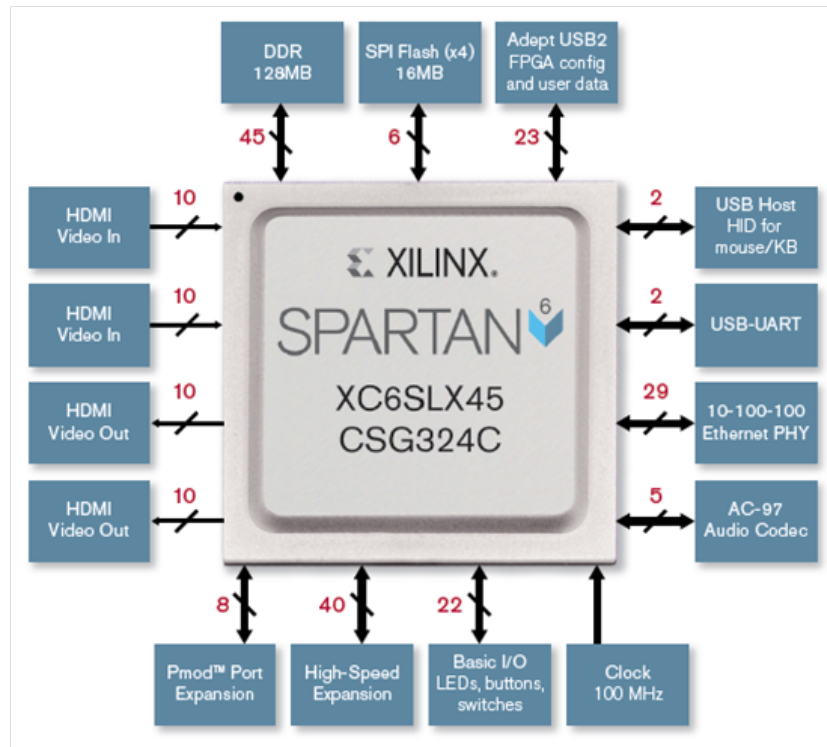


Figure 8.3: Functional Block Diagram of Atlys board

8.1.2 TMS320C6713 DSP Starter Kit

The TMS320C6713 DSP Starter Kit (DSK) [5] is a standalone development platform that enables users to evaluate and develop applications for the TI's TMS320C6713 DSP operating at 225MHz [6] as shown in Figure 8.4. The DSP on the starter kit interfaces to on board peripherals through a 32bit wide External Memory Interface (EMIF) as shown in Figure 8.5. The SDRAM, flash and CPLD are all connected to the bus. EMIF signals are connected to daughter card expansion connectors which are used for third party add in boards. The kit is designed to work with TI's CCS IDE. Code composer communicates with the starter kit through an embedded JTAG emulator with a USB host interface.

MATLAB's Embedded coder toolbox provides Processor-in-the-loop simulation for developed algorithm simulation, testing and validation. DSK C6713 is one of the many Target device which supports PIL Simulation for close loop simulation. The C code generated from the Simulink model

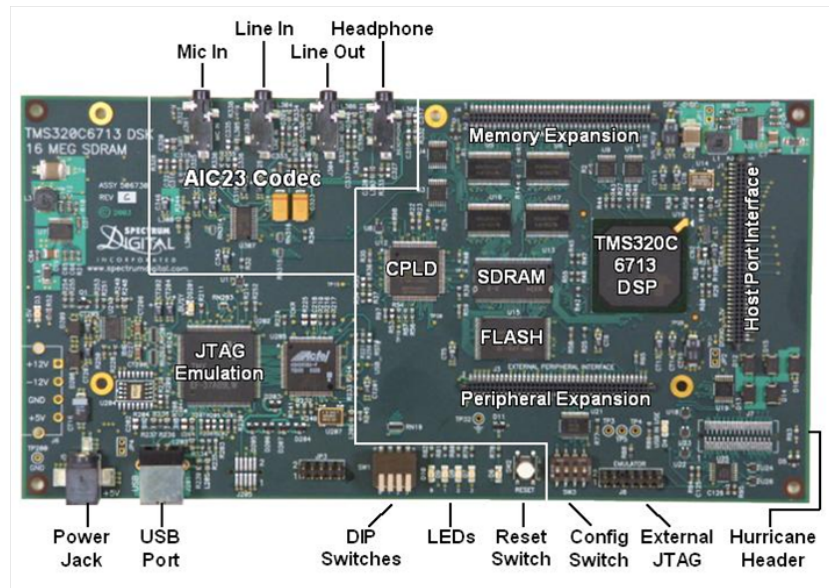


Figure 8.4: TMS320C6713 DSP Starter Kit

runs on actual target and in close loop simulation with MATLAB.

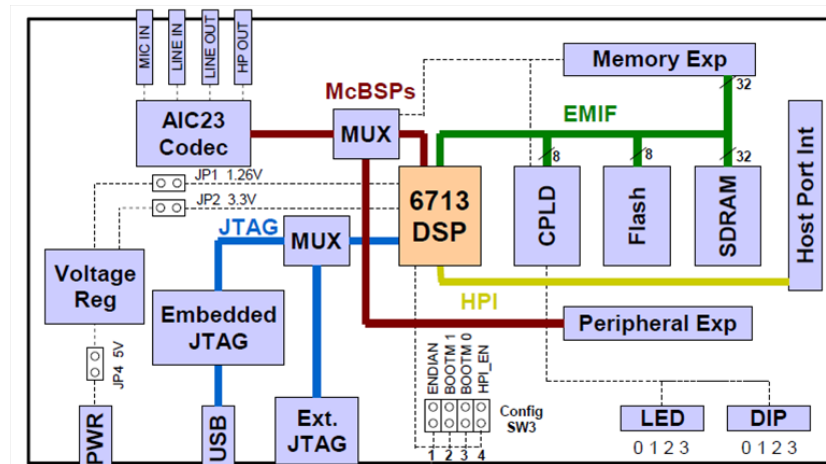


Figure 8.5: Functional Block Diagram of DSK 6713

8.1.3 Implementation of FL Decision model for MIMO mode switching

FL Decision model is designed using Fuzzy Logic Toolbox for MIMO mode switching in LTE-A Downlink Physical Layer. The FL Decision Model consists of two inputs Average Condition Number and Receive SNR and one output is MIMO mode selected. The FL Decision model is converted to Fixed-point model to validate its performance on FPGA and DSP. GUI is designed to ease the throughput analysis of Physical Layer and to perform the real-time implementation on Target Hardware.

8.1.3.1 Implementation on Atlys Spartan 6 Development kit

The FL Decision model is developed for MIMO mode switching to maximize throughput of LTE-A Downlink Physical Layer. The design and simulation results of the Fuzzy Decision model is presented in Chapter 7. The Decision model is verified with the real-time implementation and real-time testing on Atlys Spartan 6 Development kit. Figure 8.6. shows the MATLAB Simulink models for verification on target device.

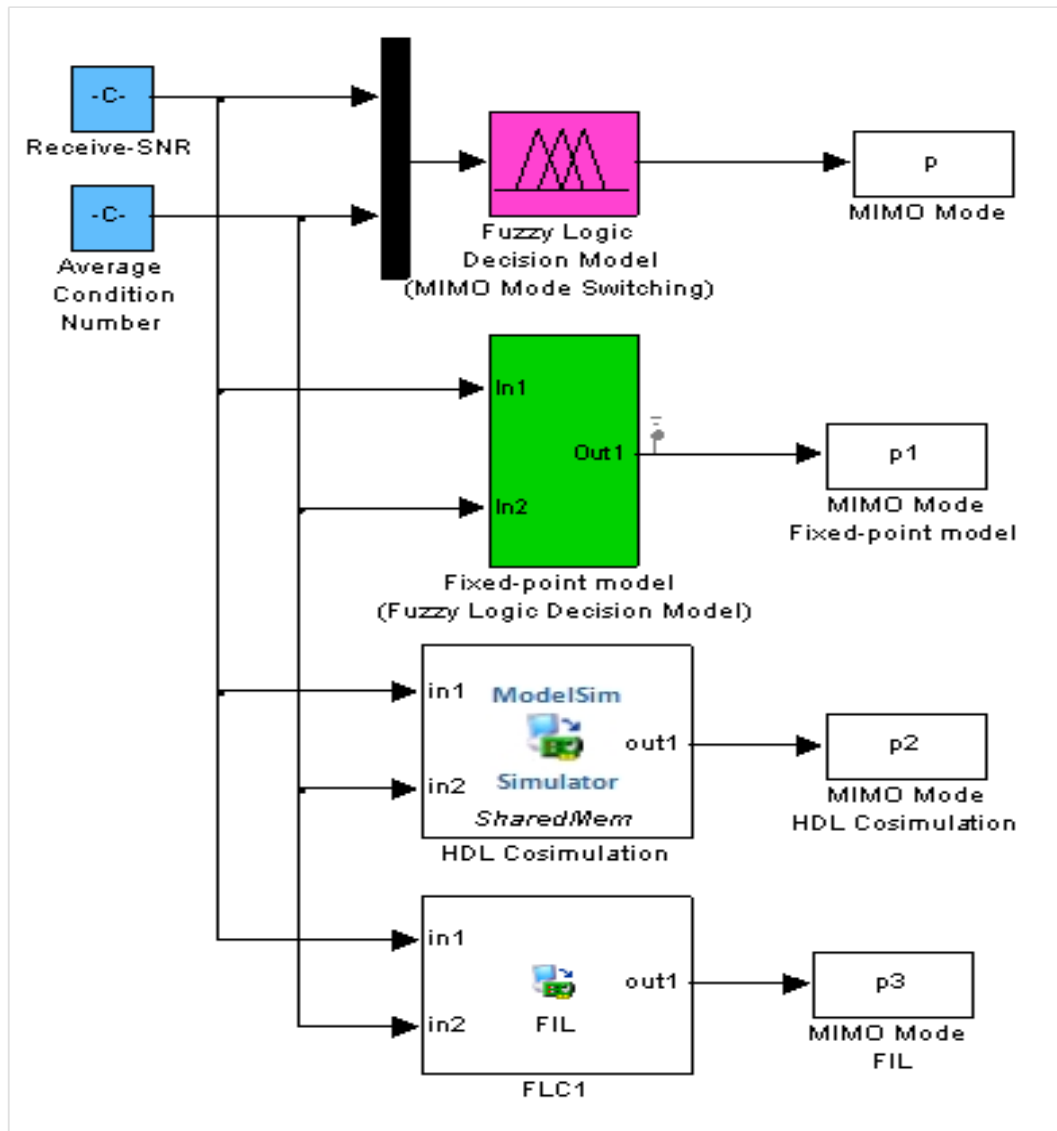


Figure 8.6: Simulink Models for FL Decision model for HDL Co-simulation and FIL Simulation

The steps for Hardware Implementation of Fuzzy Decision model in Atlys Spartan 6 Development kit is as below:

- 1). The simulation model *FLC* is designed using Fuzzy Logic Toolbox and is verified in close-

loop with LTE-A Link Level Simulator. The input membership functions of Channel Condition Number and Receive SNR and Fuzzy Rule base is as given in Section 7.4.

2). The SIMULINK model is converted to Fixed-point model (to implement on FPGA), using Fixed-Point Toolbox.

3). HDL code is developed for the designed Fixed-Point model of Fuzzy Decision model using HDL Workflow Advisor. Using HDL Workflow Advisor we can set the Target Device, prepare the model for HDL Code Generation and HDL code is generated for the Target device specified. FPGA Synthesis and Analysis in Xilinx ISE Design Suite is carried out and the programming file generated is downloaded to the Target.

4). Once the HDL Code is generated, the code is verified with ModelSimXE III 6.2c Simulator using EDA Simulator Link. Figure 8.7 shows the result of ModelSim Simulator, which is same as we got using Fixed-Point model.

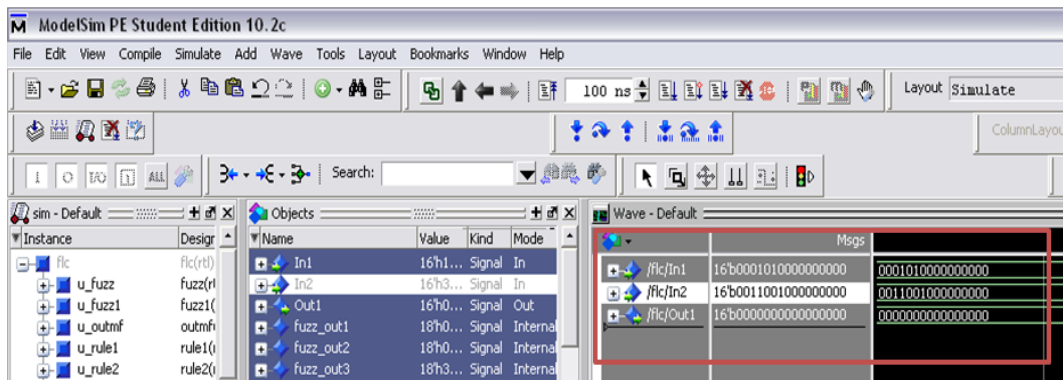


Figure 8.7: ModelSim Simulator Results

5). After verification of the HDL code using ModelSim Simulator, the code is downloaded to the target and the results is verified. FIL simulation mode is used for close-loop simulation with LTE-A Link Level Simulator.

8.1.3.2 Implementation on TMS320C6713 DSP Starter Kit

The MATLAB Simulink Fuzzy Logic Decision model is implemented and real-time testing is done on C6713 DSP Starter kit. The standalone C code of the Simulink model is generated using the Simulink Coder. The generated code for the Target Device C6713 is used for real-time applications, including simulation, rapid prototyping and hardware-in-the-loop testing.

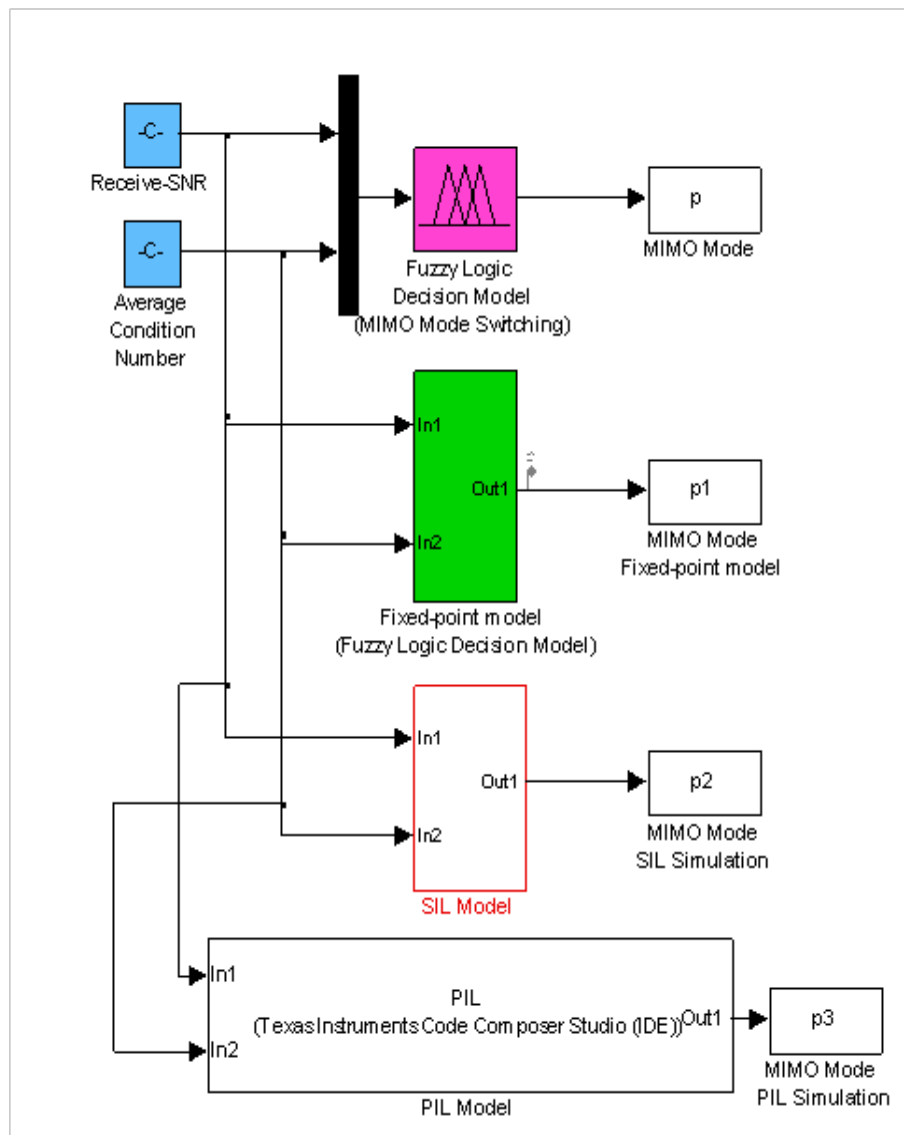


Figure 8.8: Simulink Model for FL Decision model for SIL and PIL Simulation

Using the Simulink Coder the Simulink model is built for C code generation for the Target device specified. Once the code is generated, the SIL simulation is carried out using CCS IDE. The C code is verified with software simulator and then downloaded to the target for in-loop testing. Using PIL Simulation mode, the PIL block is generated and the code is verified with in-loop testing with LTE-A Link Level Simulator. Figure 8.8 shows the MATLAB Simulink blocks for FLC, SIL model and PIL model for Texas Instruments CCS IDE. The snapshot of the CCS IDE is as shown in Figure 8.9.

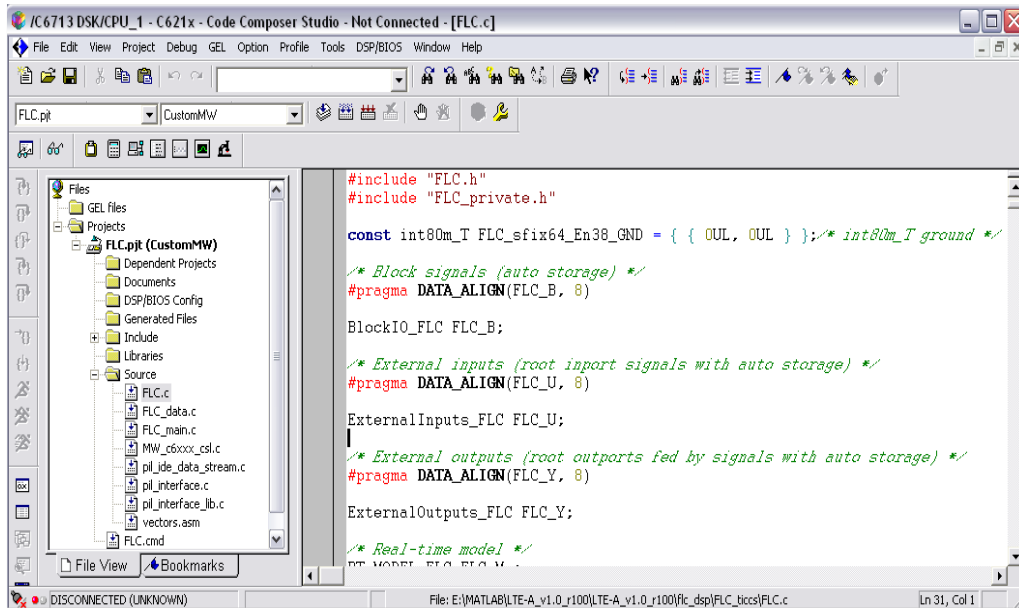


Figure 8.9: Code Composer Studio IDE Window

8.1.3.3 Implementation Results

GUI is developed to ease the Throughput Analysis for FL Decision Model for MIMO mode Switching in LTE-A Downlink Physical Layer. The User Manual and steps for setup for real-time implementation using the GUI is given in Appendix A. The user can select the Initial Simulation parameters using the Pop-up menu editor for Average SNR, Antenna Configuration, Receiver Configuration, Channel Configuration, Transmit Correlation and MIMO mode. The average condition number, Receive SNR and MIMO mode selected using FL Decision model is displayed in GUI.

Simulation results for different Initial Simulation Parameters, with FL Decision Model for MIMO mode switching is implementation on DSP and on FPGA. Figure 8.10-8.15 shows the results of throughput for various six different Case scenarios to test the performance of FL Decision model with different antenna configurations, transmission modes and channel configuration.

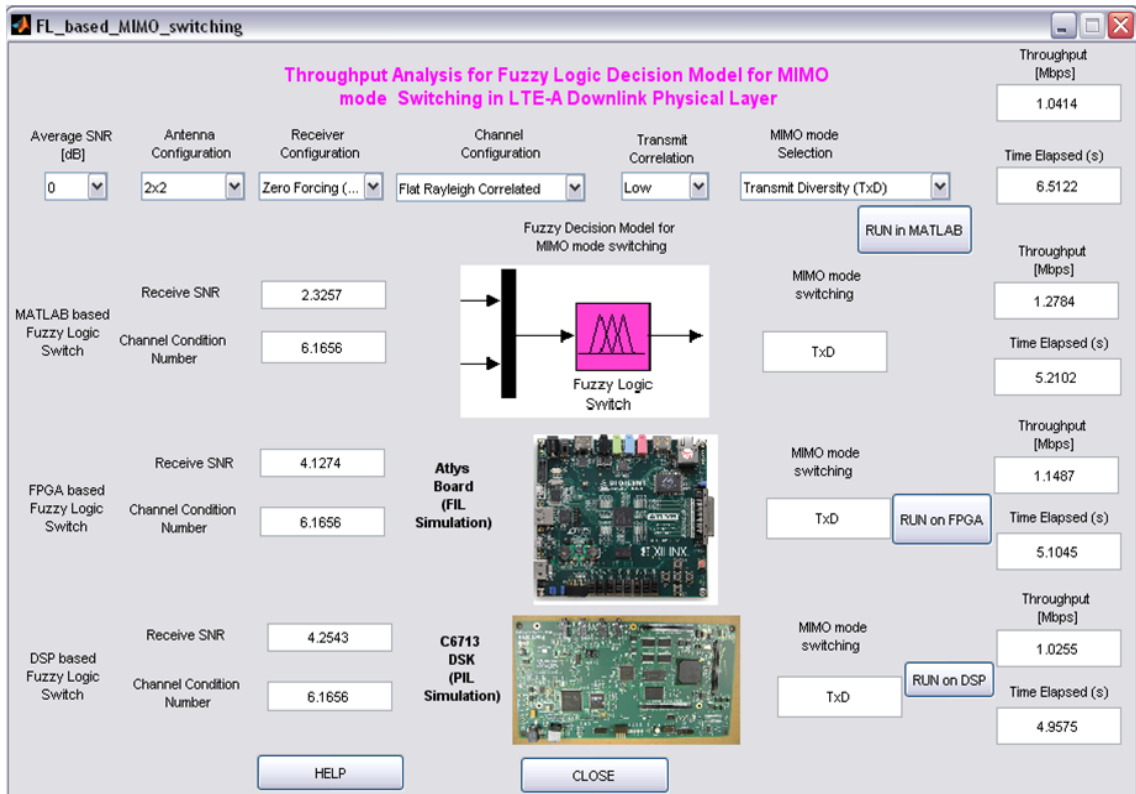


Figure 8.10: Throughput Analysis of Case 1 Scenario

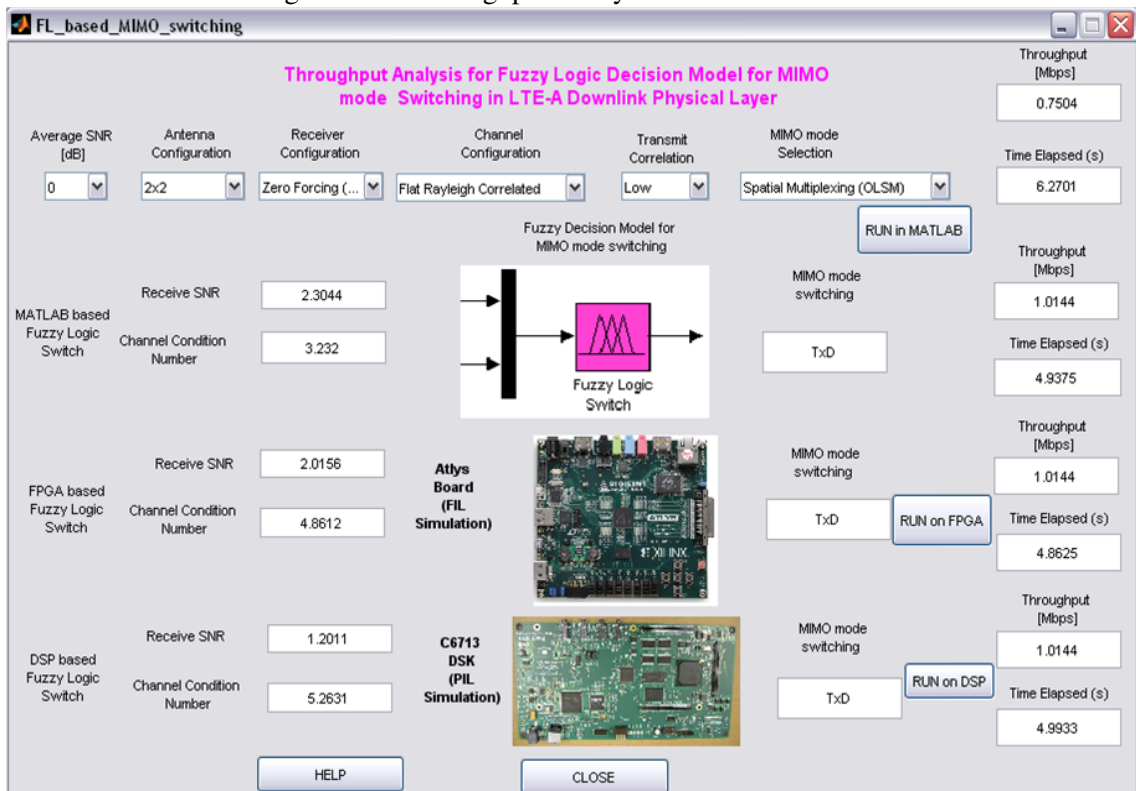


Figure 8.11: Throughput Analysis of Case 2 Scenario

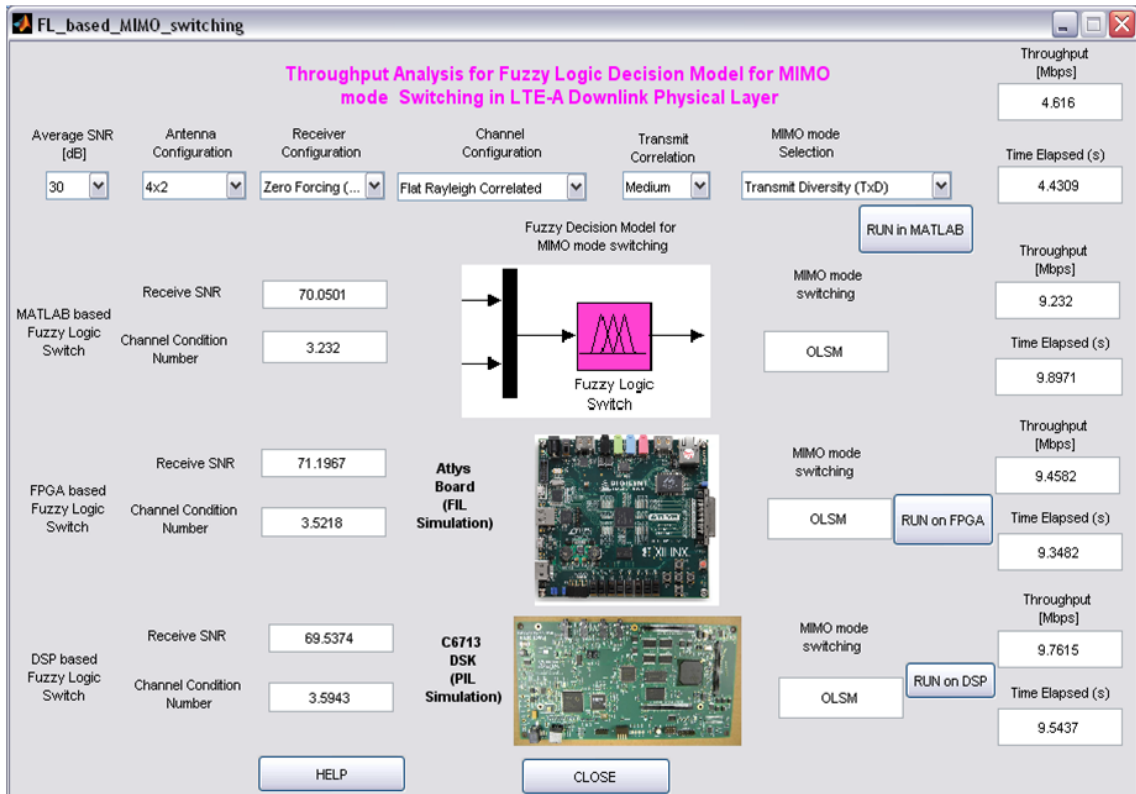


Figure 8.12: Throughput Analysis of Case 3 Scenario

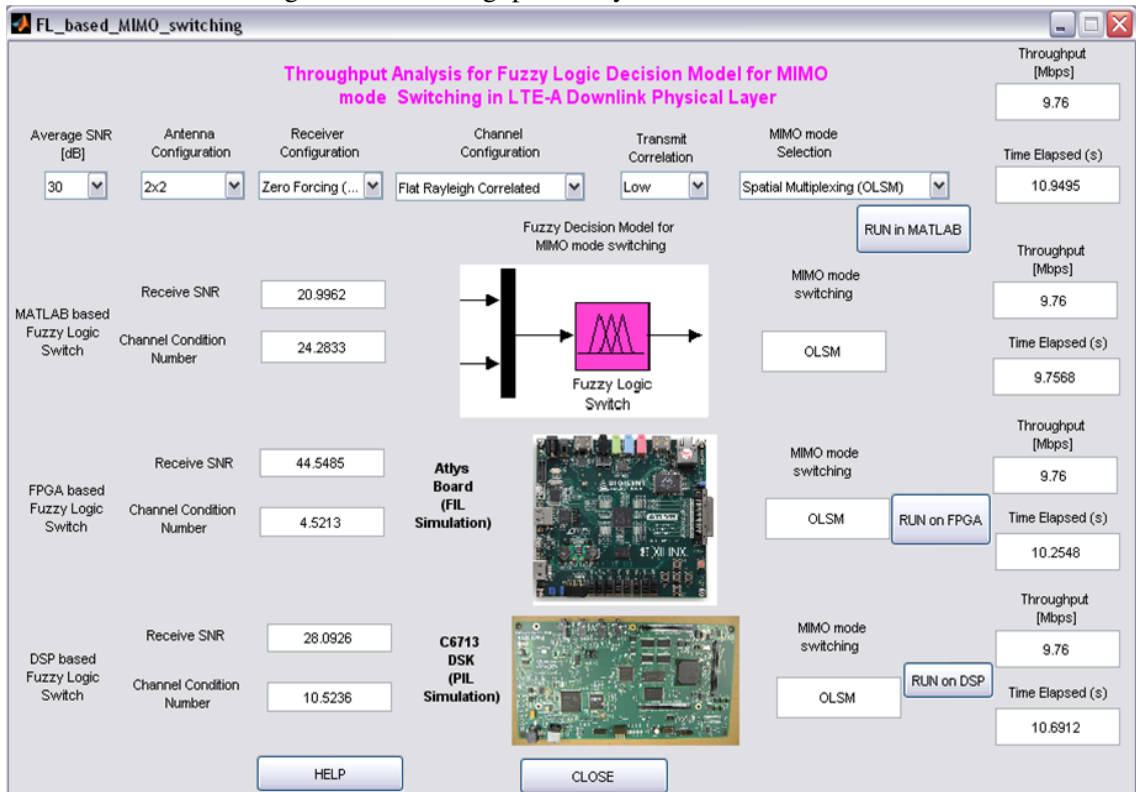


Figure 8.13: Throughput Analysis of Case 4 Scenario

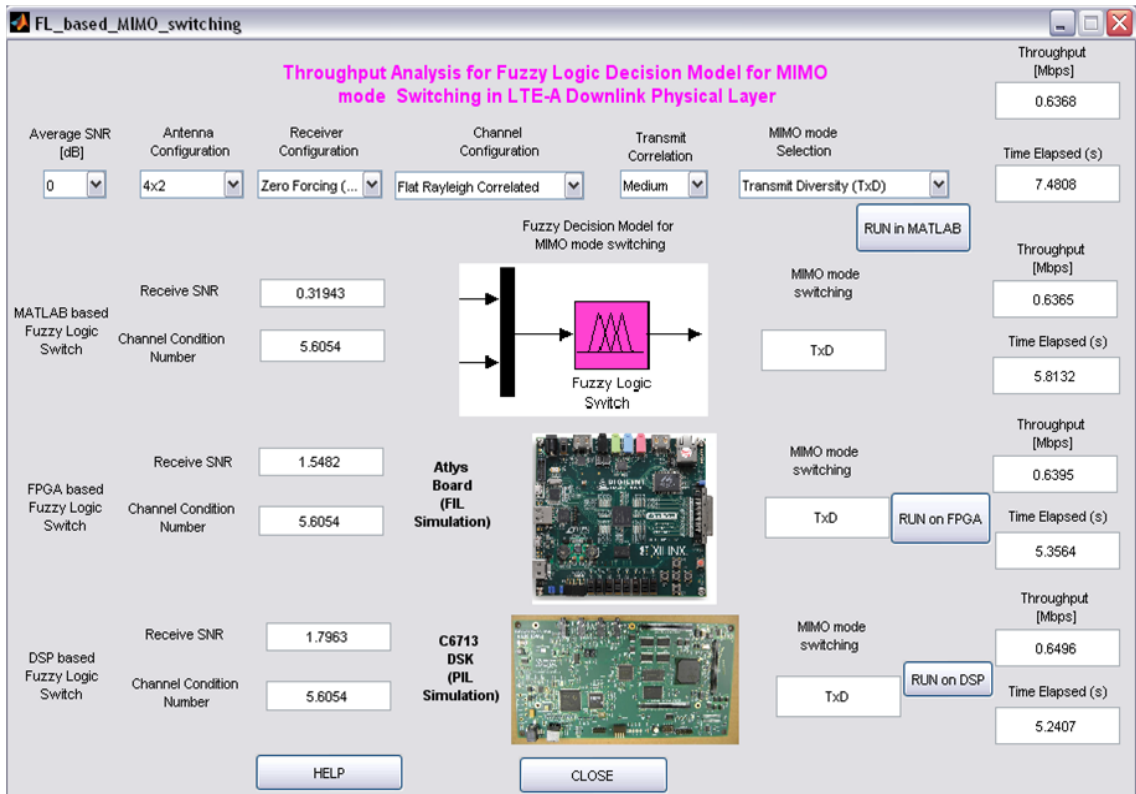


Figure 8.14: Throughput Analysis of Case 5 Scenario

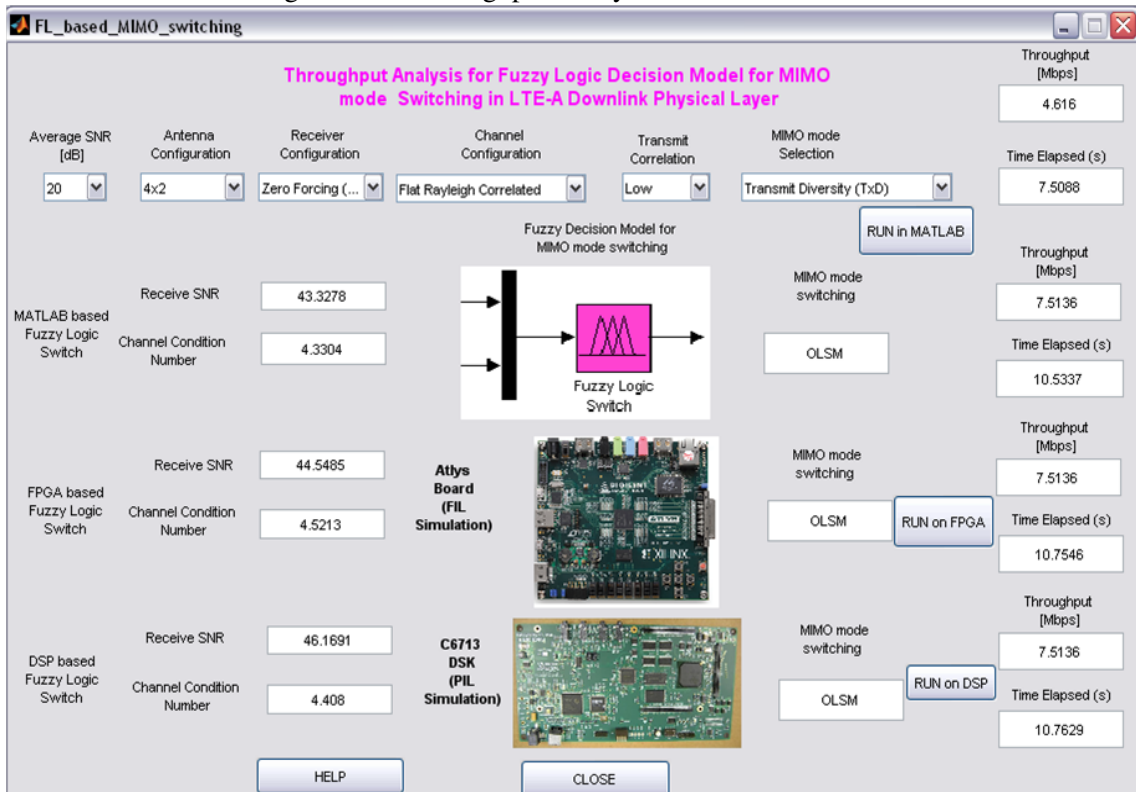


Figure 8.15: Throughput Analysis of Case 6 Scenario

Initial Simulation Parameters Scenarios	Initial Throughput (Mbps)	FL Decision Model Throughput (Mbps)	FPGA Throughput (Mbps)	DSP Throughput (Mbps)
Case 1: 0dB,2x2, Low Correlation, TxD	1.0414	1.2784	1.1487	1.0255
Case 2: 0dB,2x2, Low Correlation, OLSM	0.7504	1.0144	1.0144	1.0144
Case 3: 30dB,4x2, Medium Correlation, TxD	4.616	9.232	9.4582	9.7615
Case 4: 30dB,2x2, Low Correlation, OLSM	9.76	9.76	9.76	9.76
Case 5: 0dB,4x2, Medium Correlation, TxD	0.6368	0.6365	0.6395	0.6496
Case 6: 20dB,2x2, Low Correlation, TxD	4.616	7.5136	7.5136	7.5136

Table 8.1: Summary of throughput results for various case scenarios for FL Decision model

Table 8.1 shows the summary of throughput results for various case scenarios to test the throughput performance of LTE-A Downlink Physical Layer with FL Decision model and its implementation.

8.1.4 Implementation of ANN based MIMO Channel Estimation

The ANN based MIMO Channel Estimation Algorithm developed is discussed in detail in Chapter 6. GRNN based MIMO Channel estimation algorithm is implemented and verified in close-loop with LTE-A Link Level Simulator for Throughput Analysis.

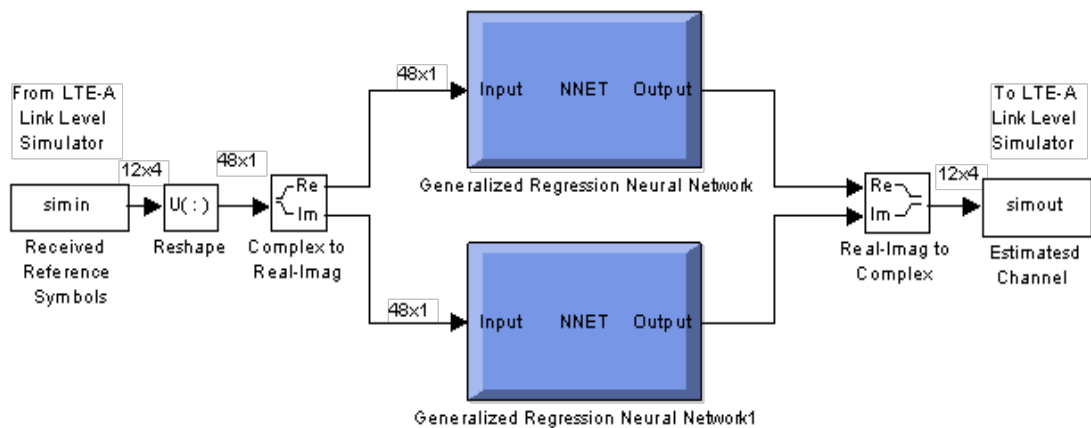


Figure 8.16: ANN based MIMO Channel Estimation Simulink Model

Out of different ANN based MIMO Channel Estimation Techniques, GRNN is implemented as the time taken for the technique is minimum as compared to others and also it gives better per-

formance in terms of throughput as compared to other channel estimation techniques. The input to Neural Network is 12×4 matrix Received reference symbol and output channel estimated is also 12×4 channel matrix. After reshape the input data is 48×1 . The ANN cannot support complex data as input and training data, hence two neural networks are designed one for real part and other for imaginary part. The MATLAB Simulink model for ANN is as shown in Figure 8.16.

If we convert the model to Fixed-point model and consider sfixed data of 16 bits (8 fraction bits), the input should be equal to 48×1 data. So if we assign 16 pins for each data, we need $16 \times 48 = 768$ pins for input and 768 pins for output. Hence, real-time verification of channel estimation algorithm on FPGA is not practically feasible due to limitation of IOB's on Atlys Spartan 6 Development kit.

8.1.4.1 Implementation on TMS320C6713 DSP Starter Kit

The GRNN based MIMO channel estimation technique is implemented on TMS320C6713 DSK. The real-time verification is done with LTE-A Link Level Simulator. MATLAB Simulink model of GRNN based Channel Estimation developed is implemented on C6713 DSK.

Similar procedure as discussed in Section 8.1.3.2 for implementation on TMS320C6713 DSK is followed. Software simulation is verified using Code Composer Studio 3.3 and the code is download to the Target device TMS320C6713 and verified in close loop with LTE-A Link Level Simulator. GUI is developed for Throughput Analysis of ANN Based MIMO Channel Estimation in LTE-A Downlink Physical Layer is developed. Throughput for Perfect, LS, GRNN and DSP based channel estimation can be analyzed in GUI.

8.1.4.2 Implementation Results

GUI is developed for to ease the Throughput Analysis for ANN based MIMO Channel Estimation in LTE-A Downlink Physical Layer. The User Manual and steps for setup for real-time implementation using the GUI is given in Appendix A. The user can select the Initial Simulation parameters using the Pop-up menu editor for Average SNR, Antenna Configuration, Receiver Configuration, Channel Configuration, Channel Estimation Technique and MIMO mode. After running simulation the average condition number, Receive SNR and MIMO mode selected using FL Decision model is displayed in GUI. The comparative analysis for throughput and Elapsed time can be observed. GUI also consists of options for Simulations of GRNN based MIMO channel estimation on TMS320C6713 DSK for throughput analysis.

Simulation results for different Case Scenarios with FL Decision Model for MIMO mode switching implementation on DSP is as shown in Figure 8.17-8.22.

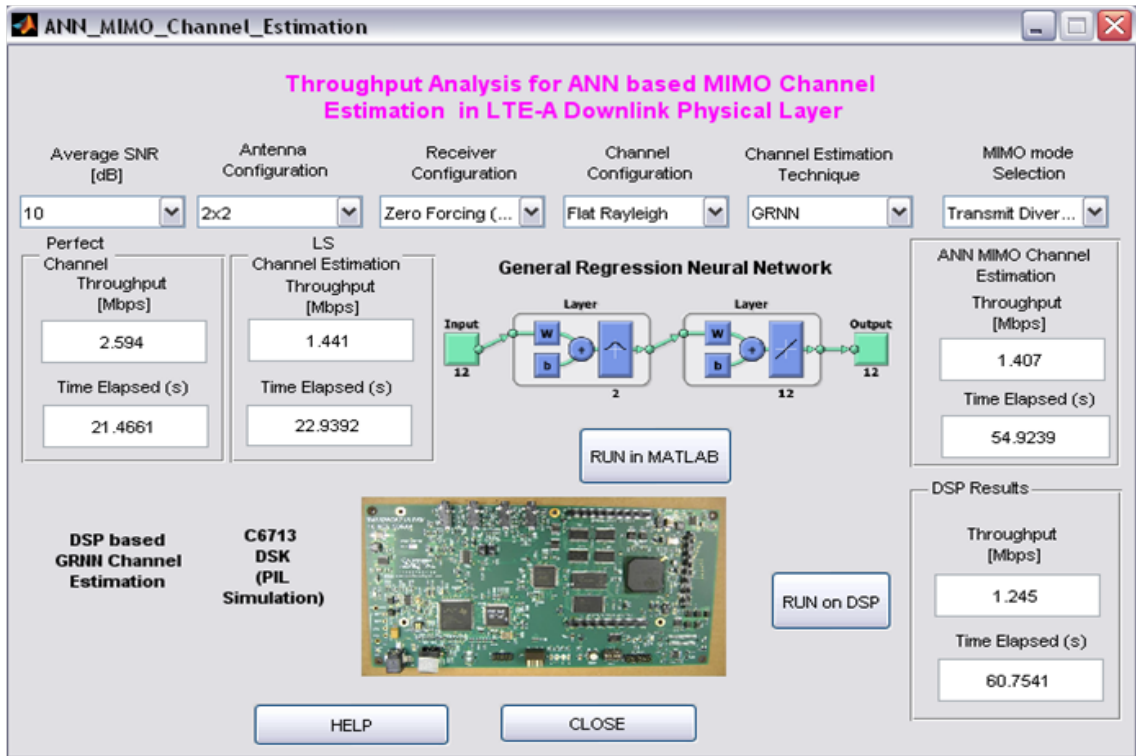


Figure 8.17: Throughput Analysis of GRNN Case 1

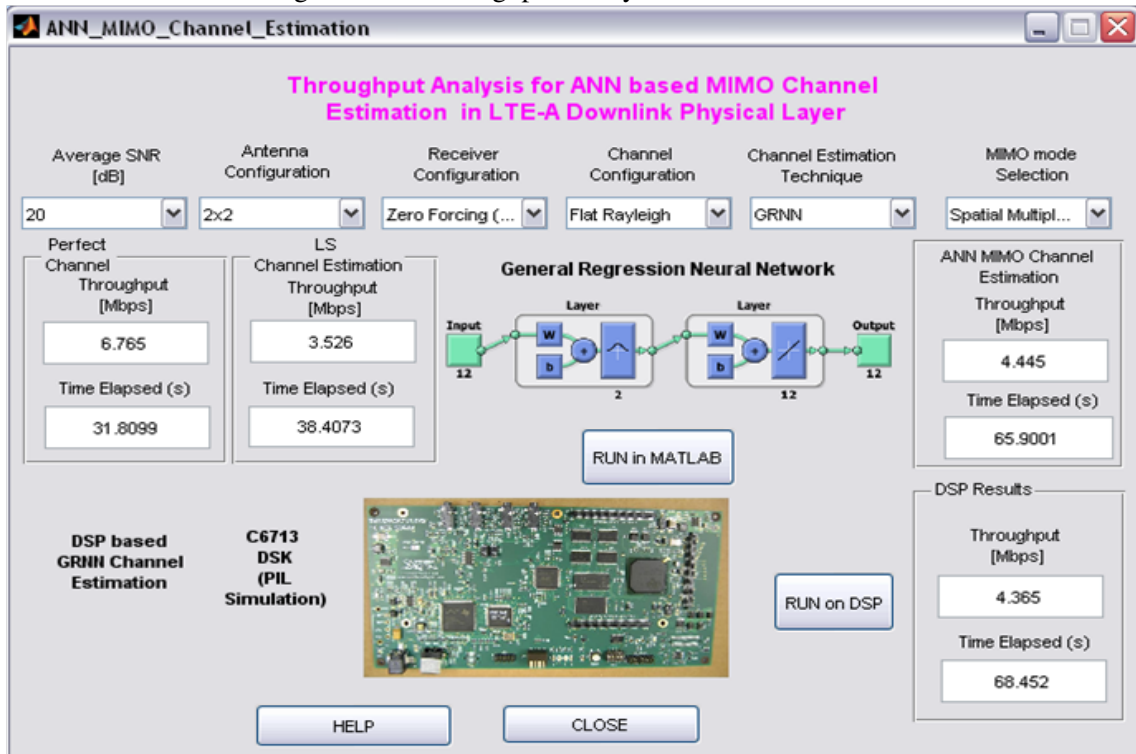


Figure 8.18: Throughput Analysis of GRNN Case 2

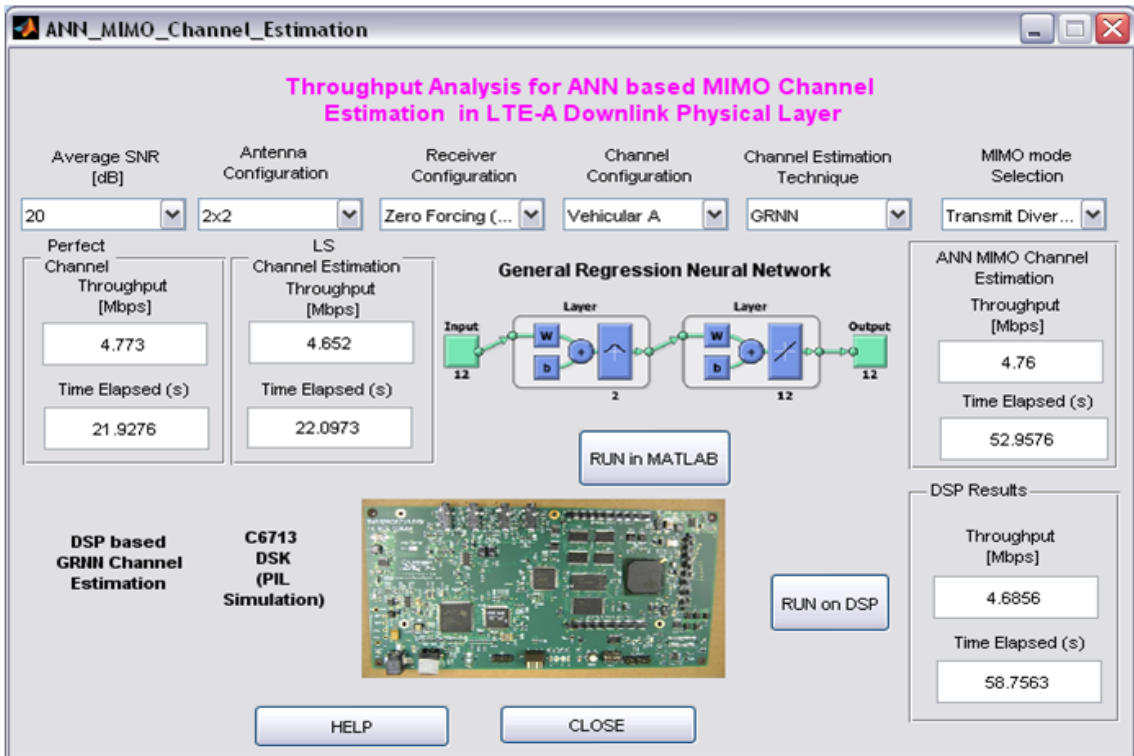


Figure 8.19: Throughput Analysis of GRNN Case 3

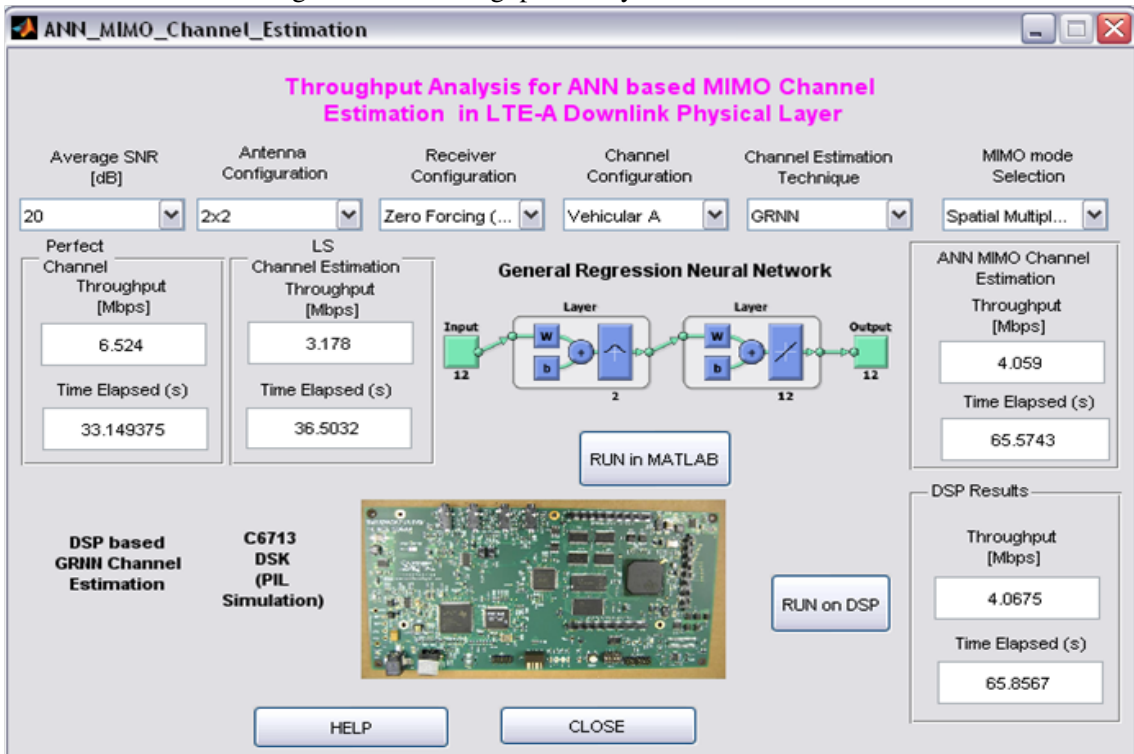


Figure 8.20: Throughput Analysis of GRNN Case 4

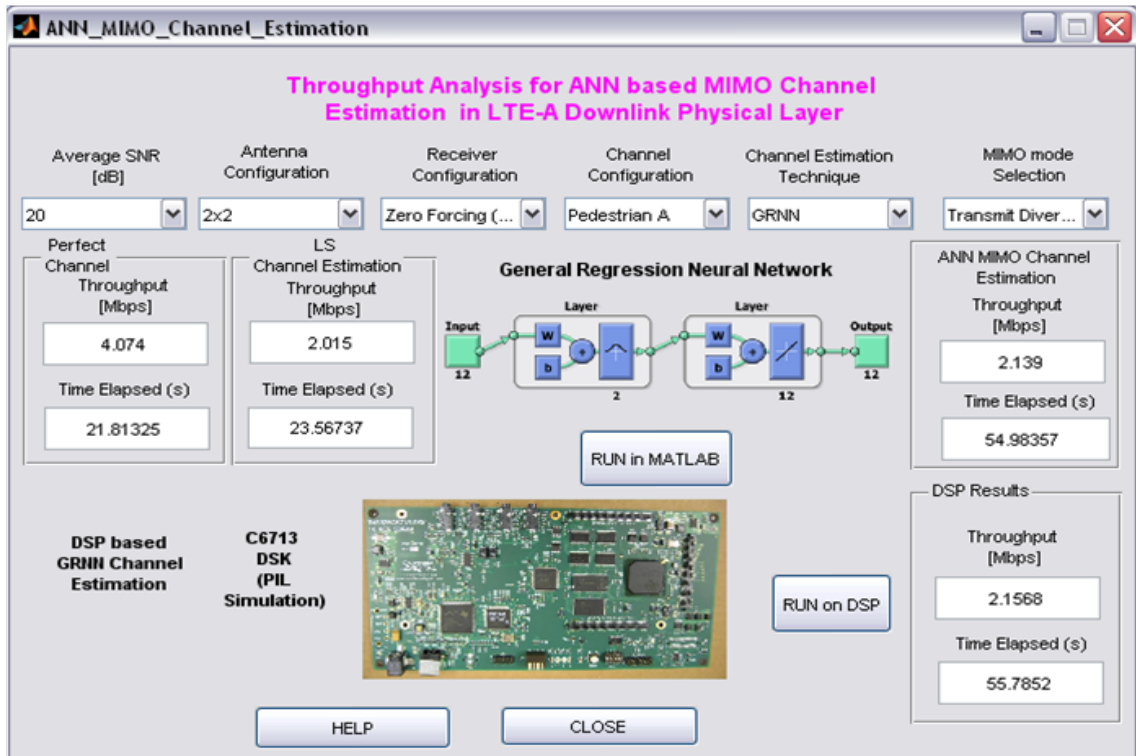


Figure 8.21: Throughput Analysis of GRNN Case 5

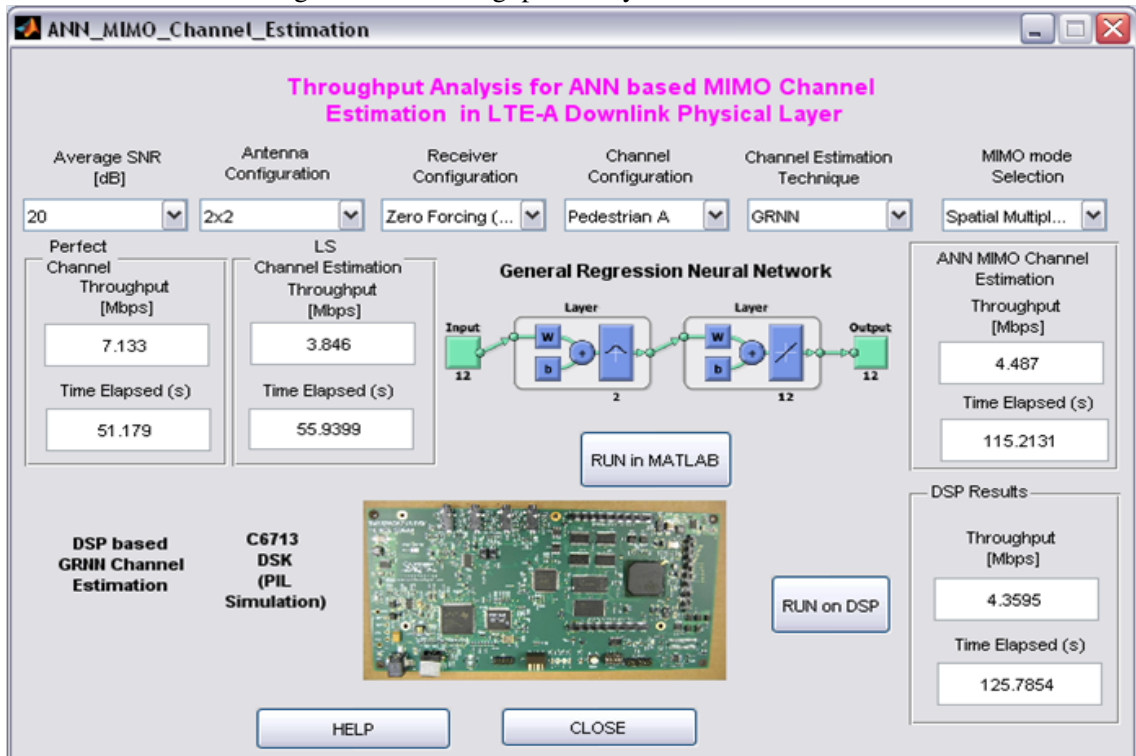


Figure 8.22: Throughput Analysis of GRNN Case 6

Table 8.2 shows the summary of throughput results for different simulation parameters and channel estimation techniques and DSP implementation of GRNN based channel estimation.

Simulation parameters Case Scenarios	Perfect channel (Mbps)	LS (Mbps)	GRNN (Mbps)	DSP (Mbps)
Case 1: 10 dB, 2x2 TxD, Flat Rayleigh	2.594	1.441	1.407	1.245
Case 2: 20 dB, 2x2 CLSM, Flat Rayleigh	6.765	3.526	4.445	4.365
Case 3: 20 dB, 2x2 TxD, Veh A	4.773	4.652	4.76	4.6856
Case 4: 20 dB, 2x2 OLSM, Veh A	6.524	3.178	4.059	4.065
Case 5: 20 dB, 2x2 TxD Ped A	4.074	2.015	2.139	2.1568
Case 6: 20 dB, 2x2 OLSM Ped A	7.133	3.846	4.487	4.3595

Table 8.2: Summary of throughput results for case scenarios for ANN Channel estimation

8.2 Concluding Remarks

This chapter presents the real-time verification of the developed throughput optimization algorithms on Atlys Spartan 6 Development kit and TMS320C6713 DSK. The GRNN based MIMO channel estimation and FL Decision model for MIMO mode switching in LTE-A Downlink Physical layer are implemented on real-time hardware for performance analysis. FL Decision model is implemented on FPGA and DSP and is found to give satisfactory results when compared to MATLAB Simulation result. GRNN MIMO channel estimation is implemented on DSP and gives similar performance to MATLAB Simulation results. Throughput analysis of the algorithms are carried out in close-loop testing with LTE-A Link Level Simulator.

Conclusion and Further developments

9.1 Research Contributions

The contributions of the research work are listed below:

- MIMO Wireless System is the mandatory technology for achieving high channel capacity demands to satisfy the needs of next generation wireless technologies. The theoretical Channel Capacity Analysis for MIMO System is carried out and comparative analysis with SISO, SIMO and MIMO is analyzed. GUI is developed to ease the channel capacity and performance analysis of MIMO Transmission Techniques.
- LTE-A is a pioneer technology to achieve the IMT-Advanced requirements. The MIMO Transmission modes in LTE-A technology are studied in detail. The comparative analysis between Transmit Diversity and Spatial Multiplexing modes is carried out in terms of Throughput and BLER. The Diversity-Multiplexing tradeoff for LTE-A Downlink Physical Layer is analyzed.
- MIMO Channel estimation affects the Throughput of LTE-A Downlink Physical layer. To increase the throughput performance ANN based MIMO Channel estimation techniques are designed and simulations are carried out. The GRNN based MIMO Channel Estimation technique is implemented on TMS320C6713 DSK for throughput analysis.
- Fuzzy Logic Decision model for MIMO mode switching in LTE-A Downlink Physical layer is designed. Throughput can be maximized by selecting the appropriate MIMO mode based on Channel Condition Number and Receive SNR. The FL Decision model developed is implemented on Atlys Spartan-6 Development Kit and TMS320C6713 DSK for throughput analysis.

These contributions are discussed in more detail hereafter.

9.1.1 Channel Capacity Analysis and Conceptual Design of MIMO Wireless System

Theoretical aspects of MIMO Channel capacity is analyzed using MATLAB simulations. The Channel Capacity v/s SNR analysis of i.i.d Rayleigh flat-fading MIMO channel with full CSI at the transmitter and receiver is carried out. From the channel capacity plots we can conclude that, as we increases the number of transmit or receive antennas the channel capacity increases linearly with

minimum number of transmit or receive antennas. For MIMO system Diversity-Multiplexing trade-off is studied. From DMT plots we can conclude that as the diversity gain increases by increasing the number of transmit antennas, the spatial multiplexing gain remains same and vice versa. But both Diversity and Spatial Multiplexing gain cannot not be simultaneously achieved.

The System Design methodology for design and implementation of MIMO Wireless system from initial specifications to wireless platform development is presented in thesis. The Rapid prototyping of MIMO algorithms for real-time testing in conjunction with MATLAB on FPGA and DSP target hardware is carried out. The Mathworks design flow for FPGA and DSP prototyping is described in detail with list of supporting tools available in MATLAB.

9.1.2 Performance Analysis of LTE-A Downlink Physical Layer

The LTE-A Downlink Physical layer is studied in detail. Vienna LTE-A Link Layer Simulator is used for performance analysis of MIMO modes in LTE-A. Throughput and BLER analysis of Transmit Diversity, OLSM and CLSM MIMO modes is carried out. Diversity and Spatial Multiplexing tradeoff is concluded from LTE-A Downlink Physical layer simulations. Spatial multiplexing gives higher throughput as compare to Transmit Diversity Scheme but low BLER. Hence either high throughput can be achieved or low error rates can be obtained. Throughput is analyzed for LTE-A Downlink Physical Layer for different antenna configurations as shown in Figure 9.1. As we increase the number of antennas at transmitter and/or receiver the throughput increases.

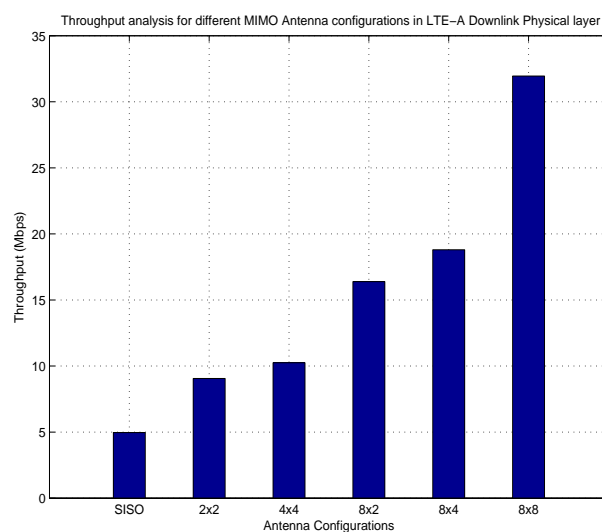


Figure 9.1: Throughput for different antenna configuration in LTE-A Downlink Physical Layer

9.1.3 Throughput Optimization of LTE-A Downlink Physical Layer

9.1.3.1 ANN based Channel Estimation Technique

MIMO Channel Estimation being the vital part for detecting the received data at receiver, is studied in detail. The imperfect CSI at receiver affects the Throughput of LTE-A Downlink Physical Layer. Various ANN based MIMO Channel estimation techniques are designed and simulation are carried out in this work. ANN based channel estimation methods developed for channel estimation are based of ANN Architectures: FNN, GRNN, RBFN and LRN. The throughput analysis shows that the proposed techniques gives better throughput performance of the system as compared to traditional LS Channel estimator. The ANN is further trained by GA to optimize the ANN weights to enhance the throughput of physical layer. By using ANN-GA based Channel Estimation technique the throughput can be maximized as compared to traditional LS Channel estimation method.

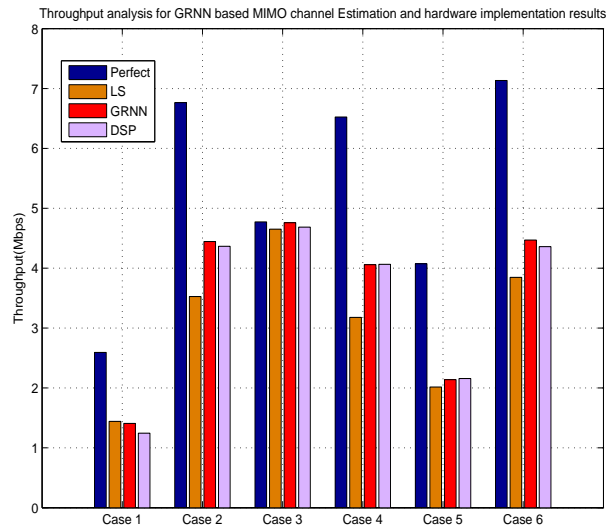


Figure 9.2: Comparison of Throughput for GRNN channel estimation and implementation

The proposed GRNN based MIMO Channel Estimation technique is implemented on TMS320C6713 DSK. Processor-in-loop simulations are carried out for verification of the developed channel estimation technique with LTE-A Link Level Simulator. The hardware implementation of GRNN based channel estimation gives approximately similar results in terms of throughput as of MATLAB Simulations as shown in Figure 9.2 for different Case scenarios.

9.1.3.2 FL Decision model for MIMO mode switching

FL Decision model for MIMO mode switching for Throughput Optimization in LTE-A Downlink Physical Layer is proposed in the research work. The model takes into account the channel condition number and the Receive-SNR and switches between Transmit Diversity or OLSM Trans-

mission mode of LTE-A Downlink Physical Layer. Based on the Fuzzy Rule base it takes decision and switches to the appropriate MIMO mode. The rules are designed based on the relation between the Switching point between MIMO modes and Channel Condition Number. The FL Decision Model is able to maximize throughput for LTE Downlink Physical Layer for various Channel Configurations and Antenna Configurations. Simulation results shows that the FL Decision model is successfully able to select appropriate MIMO mode to maximize throughput of LTE-A Physical Layer.

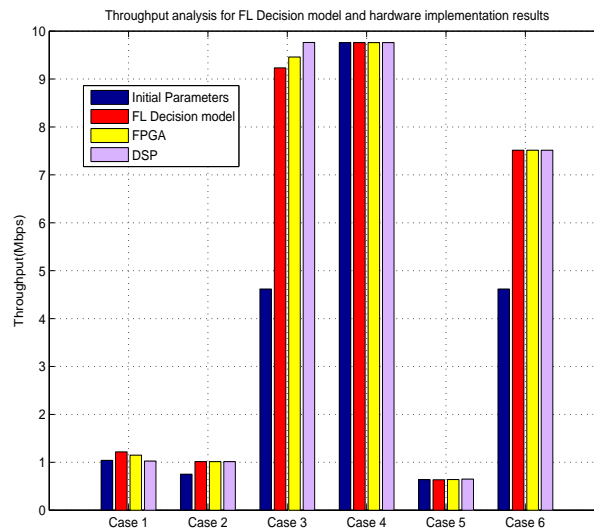


Figure 9.3: Comparison of throughput for FL Decision model and hardware implementation

The proposed FL Decision model is implemented on TMS320C6713 DSK. PIL simulations are carried out for verification of the developed FL based MIMO mode decision model. The proposed FL Decision model is also implemented on Atlys Spartan-6 Development Kit. FIL simulations are carried out for verification of the developed FL based MIMO mode decision model. The hardware implementation of FL Decision model gives approximately similar results in terms of throughput as of MATLAB Simulations as shown in Figure 9.3 for different Case scenarios.

9.1.3.3 GUI developed for performance analysis of MIMO Wireless System

MATLAB based user friendly GUI is developed for “Design and Implementation of Embedded Architecture Using Soft-Computing Techniques for Parametric Optimization of MIMO Wireless System”. Analysis of MIMO Channel Capacity, MIMO Techniques and proposed throughput optimization techniques are simulated and real-time implementation is carried out. The operating procedure of the GUI is described in User Manual in Appendix A. The hardware implementation of the proposed techniques for throughput optimization is verified using PIL and FIL Simulation

through developed GUI as shown in Figure 9.4.

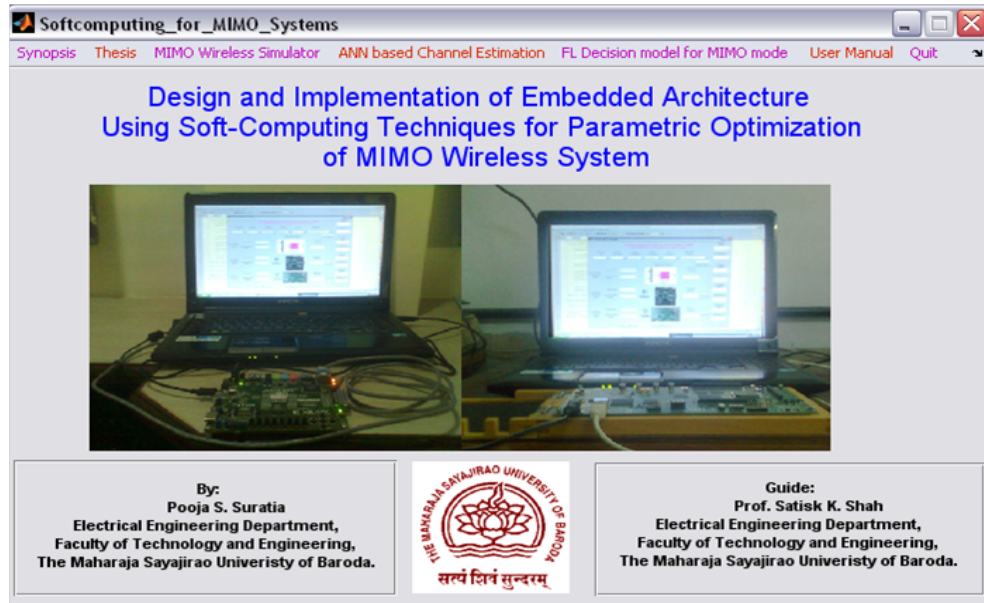


Figure 9.4: GUI for analysis of MIMO Communication System

9.2 Further Developments

Future work will explore some of the research directions as listed below:

- The capacity analysis for Flat Rayleigh fading channel with imperfect CSI at the transmitter and/ receiver can be carried out to gain better insight of the concepts.
- ANN based channel estimation technique developed is for 2x2 MIMO System. The same concept can be further verified with 4x4 or 8x8 MIMO Systems for performance analysis. The DSP and FPGA implementation challenges of the same can be explored.
- Further optimization of the developed ANN architectures for MIMO Channel Estimation can be done. The ANN parameters like connection weights and biases, number of nodes in hidden layer can be further optimized using Optimization algorithms such as GA or Particle Swarm Optimization Algorithm.
- The membership functions and fuzzy rules of the FL decision model can be tuned using Adaptive Neuro-Fuzzy Inference System (ANFIS), which allows FL model to learn the training data.
- The online-training ANFIS model can be implemented on FPGA and DSP for hardware prototyping.

Bibliography

This chapter gives the bibliography which includes the list of references used in each chapter.

Chapter 1

- [1] Rappaport S. et.al. “Wireless Communications: Past Events And a Future Perspective”, IEEE Communication Magazine, pages 148-161, 2002.
- [2] International Telecommunication Union “The world in 2011, ICT facts and figures”. Technical report, International Telecommunication Union, 2011.
- [3] Arogyaswami J Paulraj. et.al. “An Overview of MIMO Communications A Key to Gigabit Wireless”. Proceedings of the IEEE, 92:198-218, 2004.
- [4] Jack H. Winters, Jack Salz, and Richard D. Gitlin “The impact of antenna diversity on the capacity of wireless communication systems”. IEEE Transactions on Communications, 42:1740-1751, 1994.
- [5] R. T. Derryberry et.al. “Transmit diversity in 3G CDMA systems”. IEEE Communication Magazine, 40(4):68-75, April 2002.
- [6] Y. Xiao. “IEEE 802.11n: Enhancements for higher throughput in wireless LANs”. IEEE Wireless Commun., 12(6):82-91, Dec 2005.
- [7] Draft IEEE. “System requirements for IEEE 802.20 mobile broadband wireless access systems”. IEEE 802.20-PD-06 version 14, July 2004.
- [8] H. Ekstroem et.al. “Technical solutions for the 3G Long Term Evolution”. IEEE Wireless Commun., 44(6):38-45, March 2006.
- [9] Jan Mietzner, Robert Schober, Lutz Lampe, Wolfgang H Gerstacker, and Peter A Hoeher “Multiple-Antenna techniques for wireless communications A comprehensive literature survey”. IEEE Communications Surveys and Tutorials, 11(2):87-105, 2009.
- [10] 3GPP TS 36.300. LTE-Advanced (3GPP Release 10) datasheets.
- [11] Jeanette Wannstrom. “LTE-advanced <http://www.3gpp.org/LTE-Advanced/>”. May 2012.

- [12] Juho Lee, Jin-Kyu Han, and Jianzhong Zhang. "MIMO technologies in 3GPP LTE and LTE Advanced". *EURASIP J. Wirel. Commun. Netw.*, pages 1-10, mar 2009.
- [13] C.Mehlfuhrer, M.Wrulich, J.Colom Ikuno, D.Bosanska, and M.Rupp. "Simulating the Long Term Evolution physical layer". In *Proc. 17th European Signal Processing Conference (EUSIPCO 2009)*, pages 1471-1478, Glasgow, Scotland, August 2009.
- [14] C.Mehlfuhrer, J.Colom Ikuno, M.Simko, S.Schwarz, M.Wrulich, and M.Rupp. "The vienna LTE simulators - enabling reproducibility in wireless communications research", *EURASIP Journal on Advances in Signal Processing*, Vol. 2011:1-13, 2011.
- [15] [Online]. Available:<http://www.nt.tuwien.ac.at/ltesimulator/>.
- [16] R. Mysore Rao, W. Zhu, and S. Lang et al. "MultiAntenna testbeds for research and education in wireless communications". *IEEE Communications Magazine*, pages 72-81, Dec 2004.
- [17] T. Kaiser, A. Wilzeck, M. Berentsen, and M. Rupp. "Prototyping for MIMO systems - An overview". *Proc. of the 12th European Signal Processing Conference (EUSIPCO)*, pages
- [18] P. Belanovic et.al. "A consistent design methodology for wireless embedded systems". *EURASIP Journal on Applied Signal Processing*, 16:2598-2612, Oct 2005.
- [19] Mika Vaittinen. "Developing wireless systems with MATLAB and simulink".
- [20] Maria Erman. "Fuzzy Logic Applications in Wireless Communications". IFSA-EUSFLAT
- [21] Amit Kumar, Dr. Yunfei Liu, Dr. Jyotsna Sengupta, and Divya. "Evolution of Mobile Wireless Communication Networks: 1G to 4G". *International Journal of Electronics and Communication Technology*, 1:68-72, 2010.
- [22] Johanna Ketonen. "Equalization and Channel estimation algorithms and implementations for Cellular MIMO-OFDM downlink". University of Oulu Graduate School; Faculty of Technology, Department Of Communications Engineering; Centre For Wireless Communications; Infotech Oulu, Jun 2012.
- [23] D.Han C. Lim. "Robust ls channel estimation with phase rotation for single frequency network in OFDM". *IEEE Transactions on Consumer Electronics*, 52:1173-1178, 2006.

- [24] Kanchan Sharma and Shweta Varshney. "Artificial neural network channel estimation for ofdm system". *International Journal of Electronics and Computer Science Engineering (IJCSE)*, 1(3):1686-1691, 2012.
- [25] J.Sun and Y.Dong-Feng. "Neural network channel estimation based on least mean error algorithm in the ofdm systems". *International Symposium on Neural Networks (ISNN)*, Chengdu, China, 2006.
- [26] Lizhong Zheng and David N. C. Tse. "Diversity and multiplexing: A fundamental tradeoff in multiple antenna channels". *IEEE Trans. Inform. Theory*, 49:1073-1096, 2002.
- [27] R. W. Heath and D. J. Love. "Multimode antenna selection for spatial multiplexing systems with linear receivers". *IEEE Trans. Signal Processing*, 53:3042-3056, 2005.
- [28] Michail Matthaiou, Matthew R. McKay, Peter J. Smith, and Josef A. Nossek. "On the condition number distribution of complex wishart matrices". *IEEE Transactions On Communications*,
- [29] Antonio Forenza, Matthew R. Mckay, Iain B. Collings, and Robert W. Heath. "Switching between OSTBC and spatial multiplexing with linear receivers in spatially correlated MIMO channels". In *Proc., IEEE Veh. Technology Conf*, 2006.

Chapter 2

- [1] European Commission Information Society and Media, "The Networked Future : Mobile and Wireless Communications", European communities, 2006.
- [2] G. J. Foschini and M. J. Gans, "On Limits of Wireless Communications in a Fading Environment when Using Multiple Antennas," *Wireless Personal Communications*, vol. 6, no. 3, pp. 311-335, March 1998.
- [3] E. Telatar, "Capacity of multi-antenna gaussian channels," *Europ. Trans. Telecomm.*, vol. 10, no. 6, pp. 585-595, NovDec. 1999.
- [4] A. J. Paulraj, D. A. Gore, R. U. Nabar, H. Bolcskei, and S. Member, "An Overview of MIMO Communications - A Key to Gigabit Wireless," vol. 92, no. 2, 2004.
- [5] H. Ekstroem, A. Furuskaer, J. Karlsson, M. Meyer, S. Parkvall, J. Torsner, and M. Wahlqvist, "Technical solutions for the 3G longterm evolution," *IEEE Commun. Mag.*, vol. 44, no. 3, pp. 38-45, Mar. 2006.

- [6] B. Sklar, "Rayleigh Fading Channels in Mobile Digital Communication Systems Part I: Characterization," *IEEE Communication Magazine*, pp. 90-100, 1997.
- [7] M. Chiani, M. Z. Win, and A. Zanella, "On the Capacity of Spatially Correlated MIMO Rayleigh-Fading Channels," *IEEE Transactions on Information Theory*, vol. 49, no. 10, pp. 2363-2371, 2003.
- [8] J. H. Winters, "On the capacity of radio communication systems with diversity in Rayleigh fading environment," *IEEE J. Select. Areas Commun.*, vol. JSAC-5, pp. 871-878, June 1987.
- [9] T. L. Marzetta and B. M. Hochwald, "Capacity of a mobile multiple-antenna communication link in Rayleigh flat fading," *IEEE Trans. Inform. Theory*, vol. 45, pp. 139-157, Jan. 1999.
- [10] P. J. Smith and M. Shafi, "On a Gaussian approximation to the capacity of wireless MIMO systems," in *Proc. IEEE Int. Conf. Communications*, vol. 1, New York, NY, May 2002, pp. 406-410.
- [11] C. Shannon, "A mathematical theory of communication," *Bell Syst. Tech. J.*, vol. 27, pp. 379-423 JulyOct. 1948.
- [12] J. G. Proakis, "Digital Communications", New York: McGraw- Hill, 1989.
- [13] D. Gesbert and J. Akhtar, "Breaking the barriers of Shannon's capacity : An overview of MIMO wireless systems," *Telenor's Journal:Teletronikk* pp. 1-9,2002.
- [14] A. J. Paulraj, D. A. Gore, R. U. Nabar, and H. Blcskei, "An Overview of MIMO Communications A Key to Gigabit Wireless," *Proceeding of the IEEE*, vol. 92, no. 2, pp. 198-218, 2004.
- [15] A. Paulraj, R. Nabar, and D. Gore, "Introduction to Space-Time Wireless Communications". Cambridge University Press, 2003.
- [16] D. Seethaler, "Capacity Analysis of MIMO Systems", Thesis, Institute of Telecommunications, Vienna University of Technology, Vienna, Austria, 2006.
- [17] T. Brown, E. Carvalho and P. Kyritsi, "Practical Guide to the MIMO Radio Channel-with MATLAB Examples", John Wiley and Sons Ltd., 2012.
- [18] A. Goldsmith, S. A. Jafar, N. Jindal, and S. Vishwanath, "Capacity Limits of MIMO Channels," *IEEE Journal on Selected Areas in Communications*, vol. 21, no. 5, pp. 684-702, 2003.

- [19] M.T.Ivrlac and J.A. Noseek, "Performance gains of MIMO signal processing" e& i Elektrotechnik und Informationstechnik, Volume 122, Issue 6, pp 210-216, June 2006.
- [20] H. Boelcskei, "Fundamental tradeoffs in MIMO wireless systems," IEEE 6th CAS Symp. on Emerging Technologies: Mobile and Wireless Comm, May 31-Jun, 2004.
- [21] A. Lozano and N. Jindal, "Transmit Diversity vs . Spatial Multiplexing in Modern MIMO Systems," IEEE TRANSACTIONS ON WIRELESS COMMUNICATIONS, vol. 9, no. 1, pp. 186-197, 2010.
- [22] A.Goldsmith, "Wireless Communications", Cambridge University Press, 2005
- [23] A.Goldsmith and P.Varaiya, "Capacity of Fading Channels with Channel Side Information", IEEE Transactions on Information Theory, Vol. 43, no. 6, pp 1986-1992, Nov 1997.
- [24] "BERTool: A Bit Error Rate Analysis GUI- Communications Toolbox", User guide MATLAB.
- [25] J.B.Anderson, "Array Gain and capacity for Known Random Channels with Multiple Element Arrays at Both Ends", IEEE Journal on Selected Areas in Communications, Vol. 18, no. 11, pp 2172-2178, Nov 2000.
- [26] R.S.Blum, "MIMOCapacity with interference", IEEE Journal on Selected Areas in Communications, Vol 21, no. 5, pp 793-801, June 2003.
- [27] T. Tang and R.W. Heath, "Space-time interference cancellation in MIMO-OFDM Systems", IEEE Transactions on Vehicular Technology, Vol. 54, no. 5, pp: 1802-1816, Nov 2005.
- [28] G.J.Foschini, "Layered Space-Time Architecture for Wireless Communication in a Fading Environment When Using Multi-Element Antennas", Bell Labs Technical Journal, Autumn, Lucent Technologies, 1996.
- [29] P.W.Wolniansky, G.J.Foschini, G.D.Golden and R.A. Valenzuela, "V-BLAST: An architecture for Realizing Very High data Rates Over the Rich-scattering Wireless Channel", International Symposium on Signals, Systems and Electronics, pp 295-300, 1998.
- [30] S. M. Alamouti, "A simple transmit diversity technique for wireless communications," IEEE Journal on Selected Areas in Communications, vol. 16, no. 8, pp. 1451-1458, 1998.
- [31] L. Zheng and D. Tse, "Diversity and multiplexing: a fundamental tradeoff in multiple-antenna channels," Information Theory, IEEE Transactions on, vol. 49, no. 5, pp. 1073-1096, 2003.

- [32] L. Ordnez, D. Palomar, and J. Fonollosa, "Fundamental Diversity, Multiplexing, and Array Gain Tradeoff Under different MIMO Channel models," IEEE International Conference on Acoustics, Speech and Signal Processing (ICASSP), 2011, pp. 3252-3255, May 2011.
- [33] K. Azarian and H. El Gamal, "The Throughput-Reliability Tradeoff in Block-Fading MIMO channels," IEEE Transactions on Information Theory, Vol. 53, no. 2, pp. 488-501, Feb. 2007.
- [34] M. A. Hammouda, "The Power-Bandwidth Tradeoff in MIMO Systems," 2012.
- [35] A.M.Tulino, A.Lozano and S. Verdu, "Bandwidth-Power Tradeoff of Multi-antenna Systems in the Low-Power Regime," DIMACS Series in Discrete Mathematics and Theoretical Computer Science, vol. 62, pp. 15-24, American Mathematical Society, 2003.
- [36] F. Heliot, O. Onireti and M.A. Imran, "An accurate Closed-Form Approximation of the Energy Efficiency-Spectral Efficiency Trade-off over the MIMO Rayleigh Fading channel," IEEE International Conference on Communications Workshops (ICC), June 2011.
- [37] J. Mietzner, R. Schober, S. Member, L. Lampe, S. Member, W. H. Gerstacker, P. A. Hoeher, and S. Member, "Multiple-Antenna Techniques for Wireless Communications A Comprehensive Literature Survey," IEEE Communications Surveys and Tutorials, vol. 11, no. 2, pp. 87-105, 2009.
- [38] Nirmalendu Bikas Sinha, R. Bera, M. Mitra, "Capacity And V-Blast Techniques For MIMO Wireless," Journal of Theoretical and Applied Information Technology, 2005.
- [39] Vibhav Kumar Sachan¹, Ankur Gupta, Dr. Avinash Kumar, "Performance analysis of MIMO space diversity technique for wireless communications", 2008 IEEE.
- [40] D. Gesbert, M. Shafi, D. Shiu, P. J. Smith, and A. Naguib, "From theory to practice: An overview of MIMO space-time coded wireless systems," IEEE J. Select. Areas Commun., vol. 21, no. 3, pp. 281-302, Apr. 2003.
- [41] A. Paulraj, R. Narbar, D. Gore, "Introduction to Space-time Wireless communications", Cambridge University Press, 2003.
- [42] V. Tarokh, N. Seshadri, and A. R. Calderbank, "Space-time codes for high data rate wireless communication: performance criterion and code construction," IEEE Transactions on Information Theory, vol. 44, no. 2, pp. 744-765, 1998.

- [43] Min Kim, "Exact BER analysis of OSTBCs in spatially correlated MIMO channels", IEEE Trans. Communication. Vol. 54, no. 8, pp. 1365-1373, 2006.
- [44] Liu Yuyu, Liu Yongzhi, Gao Yanping, "Research and Performance Simulation of OSTBC over Rayleigh Fading Channels," Wireless Communications, Networking and Mobile Computing, 1163-1166, WICOM 2007.

Chapter 3

- [1] A. J. Paulraj, D. A. Gore, R. U. Nabar, and H. Boelcskei, "An overview of MIMO communications - A key to gigabit wireless," Proc. IEEE, vol. 92, no. 2, pp. 198-218, Feb. 2004.
- [2] JA. Garcia-Naya, M. Gonzalez-Lopez and L. Castedo, "An overview of MIMO Testbed technology," Proceedings of the 4th International Symposium on Image/Video Communications over Fixed and Mobile Networks (ISVIC '08), Spain, July 2008.
- [3] T. Kaiser, A. Wilzeck, M. Berentsen, and M. Rupp, "Prototyping for MIMO Systems - An Overview", in Proc. of the 12th European Signal Processing Conference (EUSIPCO), pp. 681-688, Vienna, Austria, Sept. 2004.
- [4] P. Belanovic, B. Knerr, M. Holzer, G. Sauzon, and M. Rupp, "A Consistent Design Methodology for Wireless Embedded Systems", EURASIP Journal on Applied Signal Processing, vol. 16, pp. 2598-2612, Oct 2005.
- [5] J. Terry and J. Heiskala, "OFDM Wireless LANs: A Theoretical and Practical Guide," Sams Publishers, December 2001.
- [6] M. Pelcat, J. Piat, M. Wipliez, S. Aridhi and J. Nezan, "An open framework for Rapid Prototyping of Signal Processing Applications," Design and Architecture for Signal and Image Processing, EURASIP Journal on Embedded Systems, 2009.
- [7] F. Edman, "Digital Hardware Aspects of Multiantenna Algorithms," Thesis, Lund University, 2006.
- [8] P. Murphy, F. Lou, A. Sabharwal, J.P. Frantz, "An FPGA based rapid prototyping platform for MIMO systems", Proc. of Asilomar, vol. 1, pp. 900904, Nov. 2003.
- [9] S. Roy, L. Belanger, "The Design of an FPGA-Based MIMO Transceiver for Wi-Fi", Xilinx DSP Magazine, May 2006.

- [10] P. Greisen, S. Haene and A. Burg, "Simulation and Emulation of MIMO Wireless Baseband Transceivers," *Simulators and Experimental testbeds Design and Development for Wireless networks*, Eurasip Journal on Wireless Communications and Networking, 2010.
- [11] M. Rupp, S. Caban and C. Mehlhruer, "Challenges in Building MIMO Testbeds," *Proceedings 15th European Signal Processing Conference (EUSIPCO)*, Poland, September 2007.
- [12] P. Wolninsky, G. Foschini, G. Golden and R. Venzuela, "V-BLAST: an architecture for realizing very high data rates over the rich scattering wireless channel," *IEEE International Symposium on Signals, Systems and Electronics*, pp. 295-300, Sept. 1998.
- [13] M. Rupp, C. Mehlhruer, S. Caban, R. Langwieser, L. W. Mayer, and L. Scholtz, "Testbeds and rapid prototyping in wireless system design", *EURASIP Newsletter*, vol. 17, no. 3, pp. 3250, Sep. 2006.
- [14] Ettus Research, The USRP product family (2009, <http://www.ettus.com>)
- [15] GNU Radio, The GNU software radio (2009, <http://www.gnuradio.org>)
- [16] Rice University, WARP project: wireless open-access research platform (2009, <http://warp.rice.edu>)
- [17] F. Kaltenberger, R. Gaffar and R. Knopp, "Low-complexity distributed MIMO receiver and its implementation on the OpenAirInterface platform," *Proceedings 20th International Symposium on Personal, Indoor and Mobile Radio Communications*, pp. 2494-2498, Tokyo, Sept. 2009.
- [18] K. Buchenrieder, "Rapid Prototyping of Embedded Hardware/Software Systems," *Design Automation for Embedded Systems*, vol. 5, no. 3-4, pp. 215-221, Kluwer Academic Publishers, 2000.
- [19] E. Dillaber, L. Kendrick, W. Jim and V. Reddy, "Pragmatic Strategies for Adopting Model-Based Design for Embedded Applications", *The Mathworks*, SAE International, 2010.
- [20] S. Note, P. van Lierop, J. van Ginderdeuren, Philips ITCL Belgium, "Rapid Prototyping of DSP systems: requirements and solutions," *Proceedings of Sixth International Workshop on Rapid System Prototyping*, Chapel Hill, NC, pp. 88-96, June 1995.
- [21] C. Madritsch "Rapid Prototyping using Model-Based Design methodology: A Digital Signal Processing lecture case study," *Proceedings of 33rd International Convention on Information*

- and Communication Technology, Electronics and Microelectronics MIPRO, Croatia, pp 849-851, May 2010.
- [22] B.Daya “Rapid Prototyping of Embedded Systems using Field Programmable Gate Arrays,” Summa Cum Laude Thesis, Bachelor of Science in Electrical Engineering, Spring 2009.
- [23] G. Nicolescu and P. Mosterman, “Model-Based Design for Embedded Systems,” CRC Press, Taylor and & Francis Group, 2010.
- [24] S.Ginsburg, ”Model-Based Design for Embedded Systems,” Embedded Computing Conference, ZHAW Winterhur, September 2008.
- [25] R.Cofer and B.Harding, “Rapid System Prototyping with FPGAs Accelerating the Design process,” Embedded technology Series, Newnes, Elsevier Inc. 2006.
- [26] L. Shure, “MATLAB to FPGA using HDL Coder,” MATLAB 2013a. blogs.mathworks.com/loren/2013/04/11/matlab-to-fpga-using-hdl-codertm/
- [27] <http://www.xilinx.com/products/design-tools/ise-design-suite/>
- [28] http://www.mentor.com/company/higher_ed/modelsim-student-edition
- [29] <http://www.synopsys.com/Solutions/EndSolutions/FPGASolution/Pages/default.aspx>
- [30] EDA Simulator Link Getting Started Guide, The Mathworks Inc, 2003-2011.
- [31] B.Rinner, m. Scchmid and R.Weiss,“Rapid prototyping of flexible embedded systems on mult-DSP architectures,” Proceedings Design, Automation and test in Europe Conference and Exhibition, pp. 1530-1591, 2003.
- [32] “Real-Time Workshop For use with Simulink,”User Guide, The Mathworks Inc.
- [33] “Embedded Coder Getting Started Guide,” The Mathworks Inc, 2003-2011.
- [34] Renzo Calcagno et.al ,“Application of Wireless Technologies in Automotive Production Systems”, Comau spa Italy.
- [35] Zhiguo Chen and Wenbo Xu,“Wireless Communication Application in Mobile Robot with Machine Vision” Wireless Communications, Networking and Mobile Computing, WiCom, pp. 24-26 Sept. 2009.

- [36] Datasheet: C8051F340 Full Speed USB Flash MCU Family, Silicon Laboratories.
- [37] The Silicon Laboratories Integrated Development Environment (IDE), <http://www.silabs.com/products/mcu/Pages/SiliconLaboratoriesIDE.aspx>
- [38] Cx51 Compiler, Optimizing C Compiler and Library Reference, for Classic and Extended 8051 Microcontrollers, Users Guide 09.2001, Keil Software.
- [39] Brian W. Kernighan and Dennis M. Ritchie, “The C Programming Language”, Second edition, Prentice Hall Software Series.
- [40] HyperTerminal Private Edition 6.3, by Hilgraeve Inc., Copyright 2001.
- [41] C8051F34X Development Kit Users Guide, Silicon Laboratories.
- [42] Pololu Wixel User’s Guide, 2001-2010 Pololu Corporation <http://www.pololu.com/docs/0J46>
- [43] Datasheet: CC2511, Texas Instruments.
- [44] Eclipse IDE for C/C++ Developers, <http://www.eclipse.org/downloads/packages/eclipse-ide-cc-developers-includes-incubating-components/indigosr2>
- [45] Wireless Serial Application <http://www.pololu.com/docs/0J46/9.b>

Chapter 4

- [1] ITU-R Recommendation M.1457: Detailed specifications of the radio interfaces of International Mobile Telecommunications-2000 (IMT-2000).
- [2] “Guidelines for evaluation of radio interface technologies for IMT-Advanced”, ITU-R Report M.2135.
- [3] Stephen M. Blust, “IMT-Advanced standards for mobile broadband communications,” ITU WRC 2012 Reports www.itu.int/net/newsroom/wrc/2012/features/imt.aspx.
- [4] www.3gpp.org.
- [5] www.3gpp.org/specifications/releases

-
- [6] R1-072444 TSG-RAN WG1-49 R1-072444 “Summary of Downlink Performance Evaluation”, Ericsson, Kobe, Japan, May 7 11, 2007.
- [7] T. Ali-Yahiya, “Understanding LTE and its performance”, Springer New York, 2011.
- [8] 3GPP TS 36.201 V8.3.0 (2009-03), “Evolved Universal Terrestrial Radio Access (E-UTRA); LTE Physical Layer - General Description (Release 8)”
- [9] 3GPP TS 24.301, “Non-Access-Stratum (NAS) protocol for Evolved Packet System (EPS)”
- [10] TS 36.331, “Evolved Universal Terrestrial Radio Access (E-UTRA); Radio Resource Control (RRC); Protocol specification”
- [11] TS 36.323, “Evolved Universal Terrestrial Radio Access (E-UTRA); Packet Data Convergence Protocol (PDCP) specification”
- [12] 3GPP TS 36.322, “Evolved Universal Terrestrial Radio Access (E-UTRA); Radio Link Control (RLC) protocol specification”
- [13] 3GPP TS 36.321: “Evolved Universal Terrestrial Radio Access (E-UTRA); Medium Access Control (MAC) protocol specification”
- [14] 3GPP TS 36.201 V10.0.0 (2010-12), “Evolved Universal Terrestrial Radio Access (E-UTRA); LTE physical layer; General description (Release 10)”
- [15] S. Schwarz, C. Mehlfuhrer, and M. Rupp, “Calculation of the Spatial Preprocessing and Link Adaption Feedback for 3GPP UMTS/LTE,” in Proc. IEEE Wireless Advanced 2010, London, UK, 2010.
- [16] S. Schwarz, M. Wrulich, and M. Rupp, “Mutual Information based Calculation of the Precoding Matrix Indicator for 3GPP UMTS/LTE,” in Proc. IEEE Workshop on Smart Antennas 2010, (Bremen, Germany), February 2010.
- [17] Schwarz, S., Rupp, M., “Throughput maximizing feedback for MIMO OFDM based wireless communication systems”, SPAWC2011.
- [18] 4G Americas, “MIMO Transmission Schemes for LTE and HSPA Networks”, (June 2009).
- [19] 4G Americas, “MIMO and Smart Antennas for 3G and 4G Wireless Systems: Practical Aspects and Deployment Considerations”, (May 2010).

- [20] Lee, J., Han, J. K. and Zhang, J., “MIMO technologies in 3GPP LTE and LTE-Advanced”, EURASIP Journal on Wireless Communications and Networking, 2009, article ID 302092.
- [21] Christopher Cox, “An Introduction to LTE: LTE, LTE-Advanced, SAE and 4G Mobile Communications”, John Wiley and Sons Ltd. 2012.
- [22] “LTE System Multiple Antenna Techniques”, eRAN2.2 (MIMO and Beamforming), HUAWEI TECHNOLOGIES CO., LTD. 2012.
- [23] C. Mehlfrhrer, M. Wrulich, J. C. Ikuno, D. Bosanska and M. Rupp, “Simulating the Long Term Evolution Physical Layer,” in Proc. of the 17th European Signal Processing Conference (EUSIPCO 2009), Aug. 2009, Glasgow, Scotland.
- [24] C. Mehlfrhrer, J. Colom Ikuno, M. Simko, S. Schwarz, M. Wrulich, M. Rupp, “The Vienna LTE Simulators - Enabling Reproducibility in Wireless Communications Research”, EURASIP Journal on Advances in Signal Processing, Vol. 2011, pages 1 - 13, 2011.
- [25] “Vienna LTE Simulators LTE-A Link Level Simulator Documentation”, v1.1 Institute of Telecommunications Vienna University of Technology, Austria.
- [26] <http://www.nt.tuwien.ac.at/research/mobile-communications/lte-a-downlink-link-level-simulator>.
- [27] 3GPP TR 25.943 V10.0.0 (2011-04), “3GPP-Technical Specification Group Radio Access Network;; Deployment Aspects (Release 10)”

Chapter 5

- [1] A. B. Kurhe, S. S. Satonkar, P. B. Khanale, and S. Ashok, "Soft Computing and its Applications," BIOINFO Soft Computing, vol. 1, no. 1, pp. 5-7, 2011.
- [2] K. M. Saridakis and A. J. Dentsoras, "Soft computing in engineering design A review," Advanced Engineering Informatics, vol. 22, pp. 202-221, 2008.
- [3] S.H. Liao, "Expert system methodologies and applications-a decade review from 1995 to 2004," Expert Systems with Applications, Vol. 28, pp.93-103, 2005.
- [4] Y. Dote, S.J. Ovaska, "Industrial applications of soft computing: a review," Proceedings of the IEEE, pp. 1243-1265, 2001, .
- [5] S. Das, A. Kumar, B. Das and A.P.Burnwal, "On Soft Computing Techniques in Various Areas," Computer Science & Information Technology -CSCP, pp. 59-68, 2013.
- [6] Maria Erman. "Fuzzy Logic Applications in Wireless Communications". IFSA- EUSFLAT 2009, pages 763-767, 2009.
- [7] Base Station Placement and Channel Allocation. "Softcomputing in wireless mobile networks". pages 29-34.
- [8] John K.William, Cathy Kessinger, Jennifer Abernethy, Cathy Kessinger and Scott Ellis, " Fuzzy Logic Applications", Artificial Intelligence Methods in the Environmental Sciences, pp 347-377, 2009.
- [9] L.A. Zadeh, "Fuzzy sets," Information Control, Vol. 8, pp. 338-353, 1965.
- [10] Kevin M. Passino and Stephen Yurkovich, "Fuzzy Control", Addison-Wesley.
- [11] Zadeh, L. A. , "Outline of a New Approach to the Analysis of Complex Systems and Decision Processes", IEEE Transactions on System, Man, and Cybernetics, SMC Vol. 3 pp. 28-44, 1973.
- [12] Zadeh, L. A. "The Calculus of Fuzzy Restrictions," Fuzzy Sets and Applications to Cognitive and Decision Making Processes, Eds. Zadeh, L.A. et. al., Academic Press, New York, 1975, 1-39.
- [13] Zadeh, L.A. "The concept of a linguistic variable and its application to approximate reasoning". Information Sciences, Part I: 8, 1975, pp. 199-249; Part II: 8, pp. 301-357; Part III: pp. 43-80.

- [14] Gottwald, S., "Fuzzy Sets and Fuzzy Logic", Vieweg, Wiesbaden, 1993.
- [15] P. Hjek, "Mathematics of fuzzy logic," Kluwer Acad. Publ., Series Trends in Logic, London, 1998.
- [16] G. Chen and T.T. Pham, "Introduction to Fuzzy Sets, Fuzzy Logic, and Fuzzy Control Systems," CRC Press LLC, 2000.
- [17] N.Kataria, "A Comparative Study of the Defuzzification Methods in an Application," The IUP Journal of COmputer Sciences, Vol. IV, No. 4, pp. 48-54, Oct 2010.
- [18] A.J.Rey Amaya, O. Lengerke, C.A.Cosenza, M.S.Dutra and M.J.M.Tavera, "Comparison of Defuzzification Methods: Automatic Control of Temperature and Flow in Heat Exchanger," www.intechopen.com/download/get/type/pdfs/id/8778
- [19] "Fuzzy Logic Toolbox User's Guide," R2011a, The Mathworks, Inc.
- [20] A.K.Jain, J.Mao and K.M.Mohiuddin, "Artificial Neural Networks: A Tutorial," IEEE Computer, Vol. 29, Issue. 3, pp. 31-44, March 1996.
- [21] S.Brunak and B.Lautrup, "Neural Network, Computers with Intuition," World Scientific, Singapore, 1990.
- [22] G.P.Zhang, "Neural Networks for Classification:A Survey," IEEE Transactions on Systems, Man and Cybernetics-Part C:Applications and reviews, Vol. 30, No.4, pp-451-462,Nov. 2000.
- [23] S. Yang, T.O. Ting, K.L. Man and S. Guan "Investigation of Neural Networks for Function Approximation," First International Conference on Information Technology and Quantitative Management, Vol. 17, pp. 586-594,2013.
- [24] H. N. Mhaskar and N. Hahm, "Neural networks for functional approximation and system identification," December, 1995 <http://web.calstatela.edu/faculty/hmhaska/postscript/neursyst.pdf>
- [25] D. Wedge, D. Ingram, D. Mclean, C. Mingham and Z. Bandar, "On global-local artificial neural networks for function approximation ," Neural Networks, IEEE Transactions on, Volume 17, Issue:4, pp. 942 - 952, July 2006 .

- [26] D.H.Kemsley, T.R.Martinez and D.M.Campbell, "A survey on Neural Network Research and Fielded Applications," *International Journal of Neural Networks: Research and Application*, Vol. 2, No. 2/3/4, pp. 123-133, 1992.
- [27] M.Yasmin, M.Sharif and S.Mohsin, "Neural network in Medical Imaging Applications: A Survey," *World Applied Sciences Journal* Vol. 2(1), pp. 85-96, 2013.
- [28] W.W. McCulloch and W. Pitts, "A Logical Calculus of the Ideas Immanent in Nervous Activity," *Bulletin of Mathematical Biophysics*, Vol. 5, pp. 115-133, 1943.
- [29] W. Pitts and W.W. McCulloch, "How We Know Universals," *Bulletin of Mathematical Biophysics*, Vol. 9, pp. 127-147, 1947.
- [30] D. Andina, A. Vega-Corona, J. I. Seijas, J. Torres-Garca, "Neural Networks Historical Review," *Computational Intelligence for Engineering and Manufacturing*, pp 39-65, Springer 2007.
- [31] A Krenker, J. Bester and A.Kos, "Introduction to the Artificial Neural Networks," <http://www.intechopen.com/download/get/type/pdfs/id/14881>
- [32] B.M.Wilamowski, "Neural network architectures and learning algorithms," *Industrial Electronics Magazine, IEEE*, Vol. 3, Issue 4, pp. 56-63, Dec. 2009
- [33] A.Atiya, "Learning Algorithms for neural networks," PhD Thesis, California Institute of technology, 1991.
- [34] D. Kriesel, "A brief introduction to Neural networks," 2005. www.dkriesel.com/_media/science/neuronalenetze-en-zeta2-2col-dkrieselcom.pdf
- [35] E.Inohira and H.Yokoi, "An Optimal Design method for Artificial Neural Networks by using the design of Experiments," *Journal of Advanced Computational Intelligence and Intelligent Informatics*, Vol. 11, No. 6, pp. 2007.
- [36] Anand, "Artificial neural Networks," *Seminar on Computational Intelligence Applications to Renewable Energy*, 2012 www.iitmandi.ac.in/ciare/files/7_Anand_ANN.pdf
- [37] "Neural Network Toolbox User's Guide," R2011a, The Mathworks, Inc.
- [38] P. Robin Jacob, "Design and Implementation of a Fuzzy Inference Engine on an FPGA," MSc. Dissertation Thesis, Department of Electrical Engineering, IIT, Delhi, March 2005.

- [39] Mitchell Melanie, "An Introduction to Genetic Algorithms," A Bradford Book The MIT Press, 1996.
- [40] J.H.Holland, "Adaptation in natural and Artificial Systems: An Introductory Analysis with Applications to Biology, Control and Artificial Intelligence," University of Michigan Press 1975.
- [41] Colin Reeves, "Genetic Algorithms," Handbook of Metaheuristics, International Series in Operations Research & Management Science Volume 57, 2003, pp 55-82.
- [42] K. F. Man, K. S. Tang, and S. Kwong, "Genetic Algorithms: Concepts and Applications," IEEE Transactions on Industrial Electronics, Vol. 43, No. 5, Oct 1996.
- [43] Mitsuo Gen, "Genetic Algorithms and Their Applications," Springer Handbook of Engineering Statistics, , pp 749-773, 2006.
- [44] Ulrich Bodenhofer, "Genetic Algorithms: Theory and Applications," Lecture Notes, Johannes Kepler University, Austria, Austria. Second Edition WS 2001/2002
- [45] Joe Geigel "Genetic Algorithms Tools," www.cs.rit.edu/~jmg/gas/tools.html
- [46] "GA Related Software," www.geneticprogramming.com/ga/GAsoftware.html
- [47] "Global Optimization Toolbox User's Guide," MATLAB, The Mathworks, Inc.
- [48] A. A. Atayero and M. K. Luka, "Applications of Soft Computing in Mobile and Wireless Communications," International Journal of Computer Applications, Volume 45, No.22, pp. 48-54, May 2012.
- [49] L.Wang, "Soft Computing in Communications," Series: Studies in Fuzziness and Soft Computing, Vol. 136, Springer, 2003
- [50] R.K.Ghosh and P.Mitra, "Softcomputing in Wireless Mobile Networks". pp. 29-34, www.iitk.ac.in/directions/feb2006/PRINT~RATAN.pdf.
- [51] Maria Erman, "Fuzzy Logic Applications in Wireless Communications," IFSA- EUSFLAT 2009, pp. 763-767, 2009.
- [52] E.Alba and J.F. Chicano, "Evolutionary Algorithms in Telecommunications," IEEE Mediterranean Electrotechnical Conference, MELECON., pp. 795-798, May 2006.

- [53] J. Fan and D. J. Parish, "Using a Genetic Algorithm to Optimize the Performance of a Wireless Sensor Network," PGNet, vol. ISBN: 1-9025-6016-7, 2007.
- [54] Y.Park and G.Lee, "Applications of neural networks in high-speed communication networks," IEEE Communication Magazine, Vol. n33, Issue. 10, pp. 68-74, Oct 1995.
- [55] C. G. C. and J. C. L. A.Patnaik, D.E. Anagnostou, R.K.Mishra, "Applications of Neural Networks in Wireless Communications," IEEE Antennas and Propagation Magazine, vol. 46, no. 3, pp. 130-137, 2004.

Chapter 6

- [1] T. Yoo and A. Goldsmith, "Capacity of fading MIMO channels with channel estimation error.
- [2] M. Biguesh and A. B. Gershman, "Training-based MIMO channel estimation: A study of estimator tradeoffs and optimal training signals," IEEE Transactions on Signal Processing, vol. 54, no. 3, 884-893, Mar. 2006.
- [3] B. Hassibi and B. M. Hochwald, "How much training is needed in multiple-antenna wireless links?" , Bell Labs Technical Journal, 2000.
- [4] B. Rajan and K. Kumar, "A Survey on Channel Estimation Schemes For MIMO Systems," International Journal of Advanced Research in Electronics and Communication Engineering (IJARECE), Volume 2, Issue 1, January 2013.
- [5] R.S.Ganesh and J.Jaya Kumari, "A Survey on Channel Estimation Techniques in MIMO-OFDM Mobile Communication Systems," International Journal of Scientific & Engineering Research, Volume 4, Issue 5, May-2013.
- [6] E.Telatar, "Capacity of Multi-Antenna Gaussian Channels," European Transaction on Telecommunication (ETT), vol. 10, no. 6, pp. 585596, Nov 1999.
- [7] L. Berriche, K. Abed-Meraim and J. Belfiore, "Investigation of the Channel Estimation Error on MIMO System Performance,"
- [8] M. Medard, "The Effect Upon Channel Capacity in Wireless Communications of Perfect and Imperfect Knowledge of the Channel," IEEE. Transaction on Information Theory, vol. 46, pp. 933-946, May 2000.

- [9] G. Caire and S. Shamai, "On the Capacity of Some Channels with Channel State Information," IEEE. Transaction on Information Theory, vol. 45, pp. 2007-2019, September 1999.
- [10] T. Yoo and A. Goldsmith, "Capacity of Fading MIMO Channels with Channel Estimation Error," in Proc. ICC, Jun 2004, vol. 2, pp. 808-813.
- [11] 3GPP TS 36.211, Evolved Universal Terrestrial Radio Access (EUTRA), Physical Channels and Modulation, (Release 10).
- [12] Johanna Ketonen, "Equalization and Channel estimation algorithms and implementations for Cellular MIMO-OFDM downlink", University of Oulu Graduate School; Faculty of Technology, Department Of Communications Engineering; Centre For Wireless Communications; Infotech Oulu, June 2012.
- [13] C. Lim, D.Han, "Robust LS channel estimation with phase rotation for single frequency network in OFDM", IEEE Transactions on Consumer Electronics, Vol. 52 , pp. 1173-1178, 2006. <http://dx.doi.org/10.1109/TCE.2006.273130>.
- [14] Barnali Dey, Awanish Kumar, Prashant Kumar, Sanjit Lal, Naveen Kumar, Bikash Sharma, "Channel Estimation using LS and MMSE Algorithm", International Symposium on Devices MEMS, Intelligent Systems & Communication (ISDMISC) 2011.
- [15] Saqib Saleem, "Channel Estimation using Adaptive Filtering for LTE-Advanced", International Journal of Computer Science (IJCSI) Issues, Vol. 8, Issue 3, No. 2, May 2011.
- [16] A.Omri, R. Bouallegue, R. Hamila and M. Hasna, "Estimation of highly selective channels for downlink LTE MIMO-OFDM system by a robust neural network", International Journal of Wireless & Mobile Networks (IJWMN), Vol.2, No. 1 (2011), pp. 31-38.
- [17] A. Omri, R. Bouallegue, R. Hamila and M. Hasna, "Channel estimation for LTE uplink system by Perceptron neural network", International Journal of Wireless & Mobile Networks (IJWMN), Vol.2, No. 3, pp. 155-165, August 2010. <http://dx.doi.org/10.5121/ijwmn.2010.2311>.
- [18] Kanchan Sharma, Shweta Varshney, "Artificial Neural Network Channel Estimation for OFDM System", International Journal of Electronics and Computer Science Engineering (IJECS), ISSN 2277-1956/V1N3-1686-1691.

- [19] J.SUN, Y.Dong-Feng, "Neural Network Channel Estimation Based on Least Mean Error Algorithm in the OFDM Systems", International Symposium on Neural Networks (ISNN) 2006, Chengdu, China.
- [20] Sun, J., & Yuan, D. F. (2006). "Neural network channel estimation based on least mean error algorithm in the OFDM systems". Advances in Neural Networks. Berlin: Springer.
- [21] L. Anthony, "Reference Signals and Channel Estimation," Seminar Ausgewhlte Kapitel der Nachrichtentechnik, Nov 2009.
- [22] M. Simko, D. Wu, C.Mehlfuhrer, J. Eilertz and D.Liu, "Implementation Aspects of Channel Estimation for 3GPP LTE Terminals,"
- [23] Dave Anderson and George McNeill, "Artificial Neural Networks Technology, Kaman Sciences Corporation, New York.
- [24] A. Cheema, "Channel Estimation for LTE Downlink," Thesis, Blekinge Institute of Technology, September 2009.
- [25] James A. Freeman, David M. Skapura, "Neural Networks Algorithms, Applications, and Programming Techniques," Loral Space Information Systems and Adjunct Faculty, School of Natural and Applied Sciences University of Houston at Clear Lake, Addison-Wesley Publishing Company.
- [26] Jatinder N.D. Guptaa, Randall S. Sextonb, "Comparing back propagation with a genetic algorithm for neural network training," International Journal of Management Science, pp. 679-684, 1999.
- [27] Shaikh Abdul Hannan, R. R. Manza, R. J. Ramteke, "Generalized Regression Neural Network and Radial Basis Function for Heart Disease Diagnosis," International Journal of Computer Applications (0975 8887) Volume 7, No.13, October 2010.
- [28] [Online].Available: http://home.iitk.ac.in/~mfelixor/Files/Lecture5_RBFN.pdf.
- [29] Donald F. Specht, "A General Regression Neural Network," IEEE Transactions On Neural Networks. Vol. 2. NO. 6. November 1991.

- [30] A. Ghaffari, H. Abdollahi, M.R. Khoshayand, I. Bozchalooi, A. Dadgar and M. Rafiee-Tehrani "Performance comparison of neural network training algorithms in modeling of bimodal drug delivery," *International Journal of Pharmaceutics*, 327, pp. 126138, 2006.
- [31] J.D. Schaffer, D. Whitley and L. Eshelman, "Combination of Genetic Algorithms and Neural Networks: the state of the art," *IEEE Computer Science*, 1992.
- [32] D. Whitley, "Chapter 11: Genetic Algorithms and Neural networks," *Genetic Algorithms in Engineering and Computer Science*, John Wiley and Sons Ltd. 1995.
- [33] D. Whitley and T. Hanson, "Optimizing neural network using faster, more accurate genetic search," J.D. Schaffer (Ed.), *third International Conference on Genetic Algorithms*, CA, pp. 391-396, 1989.
- [34] D. Monatana and L. Davis, "Training Feedforward neural networks using Genetic algorithms," *Proceeding of Eleventh International Joint Conference on Artificial Intelligence*, CA, pp. 762-767, 1989.
- [35] I. Ileana, C. Rotar and A. Incze, "The Optimization of Feed Forward Neural Networks Structure Using Genetic Algorithms," *Proceedings of the International Conference on Theory and Applications of Mathematics and Informatics - ICTAMI*, Greece, pp. 223-234, 2004.
- [36] D. Svozil, V. KvasniEka and J. Pospichal, "Introduction to multi-layer feed-forward neural networks," *Chemometrics and Intelligent Laboratory Systems*, No. 39, pp. 43-62, 1997.
- [37] G. Bebis and M. Georgiopoulos, "Feed-forward neural Networks: Why Network size is so important," *IEEE*, pp. 27-31, 1994.
- [38] B. Choi, J. H. Lee and D. H. Kim, "Solving local minima problem with large number of hidden nodes on two-layered feed-forward artificial neural networks," *Neurocomputing*, vol.71, no.16-18, pp.3640- 3643, 2008.
- [39] M. L. Huang and Y. H. Hung, "Combining radial basis function neural network and genetic algorithm to improve HDD driver IC chip scale package assembly yield," *Expert Systems with Applications*, vol.34, no.1, pp.588-595, 2008.
- [40] R. S. Sexton and J. N. D. Gupta, "Comparative evaluation of genetic algorithm and backpropagation for training neural networks," *Information Sciences*, vol.129, no.1-4, pp.45-59, 2000.

- [41] Z. Che, T. Chiang and Z. Che, "Feed-forward neural networks training: a Comparison between genetic algorithm and Back-propagation learning algorithm," *International Journal of Innovative Computing, Information and Control* Volume 7, Number 10, October 2011.
- [42] D. E. Rumelhart, G. E. Hinton and R. J. Williams, "Learning representations by back-propagating errors," *Nature*, vol.323, no.6088, pp.533-536, 1986.
- [43] [Online].Available: <http://www.mathworks.in/support/solutions/en/data/1-EFLUUB/index.html?product=NN&solution=1-EFLUUB>

Chapter 7

- [1] L. Zheng and D. N. C. Tse, "Diversity and multiplexing: A fundamental tradeoff in multiple antenna channels," *IEEE Trans. Inform. Theory*, vol. 49, pp. 1073-1096, 2002.
- [2] A. Forenza, M. R. McKay, I. B. Collings, and R. W. Heath, "Switching between OSTBC and spatial multiplexing with linear receivers in spatially correlated mimo channels," in *Proc., IEEE Veh. Technology Conf*, 2006.
- [3] T. H. Chan and M. Hamdi, "A link adaptation algorithm in MIMO-based WIMAX systems," *Journal Of Communications*, vol. 2, pp. 1624, 2007.
- [4] R. Heath, Jr. and D. Love, "Multimode antenna selection for spatial multiplexing systems with linear receivers," *IEEE Transactions on Signal Processing*, vol. 53, no. 8, pp. 3042-3056, Aug 2005.
- [5] R. W. Heath and A. J. Paulraj, "Switching between multiplexing and diversity based on constellation distance," in *Proc. Allerton Conf. Commu., Contr., and Comput.*, Monticello, IL, USA, Oct 2000.
- [6] M. U. Sheikh, R. Jagusz, and J. Lempiinen, "Performance evaluation of adaptive MIMO switching in long term evolution," in *IWCMC. IEEE*, 2011, pp. 866-870.
- [7] M.S. Kim and Y.-H. Lee, "Effective SNR based MIMO switching in mobile wimax systems," in *Proc. Wireless Broadband World Forum (WBWF)*, Oct 2007.
- [8] Z. Zhang and L. Qiu, "Throughput-based mode switching for MIMO ARQ systems in presence of transmit correlation," *Journal of Systems Engineering and Electronics*, vol. 24, no. 1, pp. 1-10, Feb 2013.

- [9] D. W. Dongdong Li and M. Al-Shalash, "Probability based MIMO mode selection and switching system and method for wireless systems," U.S. Patent US20 100 290 553 A1, Nov 18, 2010.
- [10] W. L. et.al, "Investigation of adaptive multi-antenna switching strategy in TD-LTE systems," in Progress In Electromagnetics Research Symposium Proceedings, Moscow, Russia, August 2012, pp. 19-23.
- [11] A. M. Maria Erman and E. Rakus-Andersson, "Fuzzy logic applications in wireless communications," in IFSA/EUSFLAT Conf., 2009, pp. 763- 767.
- [12] W.-C. Chung, C.-J. Chang, K.-T. Feng, and Y.-Y. Chen, "An mimo configuration mode and mcs level selection scheme by fuzzy Q-learning for HSPA+ systems," IEEE Transactions on Mobile Computing, vol. 11, no. 7, pp. 1151-1162, 2012.
- [13] Y.-Y. C. Wen-Ching Chung and C.-J. Chang, "HARQ control scheme by Fuzzy Q-learning for HSPA+," in VTC Spring. IEEE, 2011, pp. 1-5.
- [14] D. I. L. Michail Matthaiou and C.-X.Wang, "On analytical derivations of the condition number distributions of dual non-central wishart matrices," IEEE Transactions On Wireless Communications, vol. 8, pp. 1212-1217, 2009.
- [15] M. Matthaiou, M. R. McKay, P. J. Smith and J. A. Nossek, "On the condition number distribution of complex wishart matrices," IEEE Transactions On Communications, vol. 58, pp. 1705-1717, 2010.
- [16] D. S. B. Erceg, P. Soma and A. J. Paulraj, "Capacity obtained from multiple-input multiple-output channel measurements in fixed wireless environments at 2.5 GHz," in Proc. International Conf. Commun. (ICC), New York, USA, May 2002, pp. 396-400.
- [17] L. Zhou and M. Shimizu, "A novel condition number-based antenna shuffling scheme for D-STTD OFDM system," in Vehicular Technology Conference. IEEE, 2009, pp. 1-5.
- [18] G. M. Johannes Maurer and D. Seethaler, "Low-complexity and fulldiversity MIMO detection based on condition number thresholding," in IEEE International Conference on Acoustics, Speech, and Signal Processing (ICASSP), Honolulu, Hawaii, USA, April 2007, pp. III-61- III-64.

- [19] V. K. D. Wubben, R. Bohnke and K. D. Kammeyer, "MMSE-based lattice-reduction for near-ml detection of mimo systems," in Proc. ITG Workshop Smart Antennas, Munich, Germany, Mar 2004, pp. 106-113.
- [20] D. S. H. Artes and F. Hlawatsch, "Efficient detection algorithms for MIMO channels: a geometrical approach to approximate ml detection," IEEE Trans. Signal Processing, vol. 51, pp. 2808-2820, 2003.
- [21] J.Zik and B.Hoeffler, "Maximizing LTE MIMO Throughput using Drive Test Measurements," PCTEL RF Solutions. www.rfsolutions.pctel.com/artifacts/MIMOThroughputDriveTestWebinar.pdf
- [22] S. W. Nydick, "The Wishart and Inverse Wishart Distributions," pp. 119, 2012.
- [23] M. Kang and M.-S. Alouini, "Largest eigenvalue of complex Wishart matrices and performance analysis of MIMO MRC systems," IEEE J. Sel. Areas Commun., vol. 21, no. 3, pp. 418-426, Apr. 2003.
- [24] S. Jin, M. R. McKay, X. Gao, and I. B. Collings, "MIMO multichannel beamforming: SER and outage using new eigenvalue distribution of complex noncentral Wishart matrices," IEEE Trans. Commun., vol. 56, no. 3, pp. 424-434, Mar. 2008.
- [25] J. W. Demmel, "The probability that a numerical analysis problem is difficult," Math. Comput., vol. 50, pp. 449-480, 1988.
- [26] A. Forenza, M. R. McKay, A. Pandharipande, R. W. Heath, and I. B. Collings, "Adaptive MIMO transmission for exploiting the capacity of spatially correlated channels," Vehicular Technology, IEEE Transactions on, vol. 56, no. 2, pp. 619-630, 2007.
- [27] M. OHagan. "A fuzzy decision maker". [Online]. Available: <http://www.csee.wvu.edu/classes/cpe521/old/Reading%20Assignment%204%20-%20Hagan%20-%20Fuzzy%20decision%20making.pdf>
- [28] "Fuzzy Logic Toolbox," User's Guide, R2011a Mathworks.
- [29] J. J. Saade and H. B. Diab, "Defuzzification techniques for fuzzy controllers," Trans. Sys. Man Cyber. Part B, vol. 30, no. 1, pp. 223-229, Feb 2000.

Chapter 8

- [1] “Versatile FPGA Platform for University Classroom and research Environments- Atlys Spartan-6 Development Kit,” Xilinx, Inc. 2010.
- [2] “Atlys Board Reference Manual,” Doc: 502-178, Digilent, Inc. 2013.
- [3] “The Low-Cost Programmable Silicon Foundation for targeted Design Platform Spartan-6 FPGAs,” Xilinx, Inc. 2010.
- [4] “Spartan-6 Family Overview,” DS 160(v2.0) Xilinx, Inc. 2011.
- [5] “TMS320C6713 DSK Technical Reference,” Spectrum Digital, Inc. 2003.
- [6] “TMS320C6713 Floating-Point Digital Signal Processor,” SPRS186L, Texas Instruments, Inc. 2005.

Appendix A: User manual for GUI of Embedded Architecture Using Soft-Computing Techniques for Parametric Optimization of MIMO Wireless System

GUI is developed for “Design and Implementation of Embedded Architecture Using Soft-Computing Techniques for Parametric Optimization of MIMO Wireless System”. GUI is user friendly environment using which the MIMO Capacity analysis and throughput analysis of proposed algorithms in the research work is carried out. Also, the real-time implementation on Atlys Spartan 6 Development kit and TMS320C6713 DSK is carried out. Following is the operating procedure for GUI with description.

Operating Procedure of GUI

1) Open the GUI by writing “Softcomputing_ for_ MIMO_ Systems” in MATLAB Command window. Figure A. 1 shows the GUI for “Design and Implementation of Embedded Architecture Using Soft-Computing Techniques for Parametric Optimization of MIMO Wireless System”.

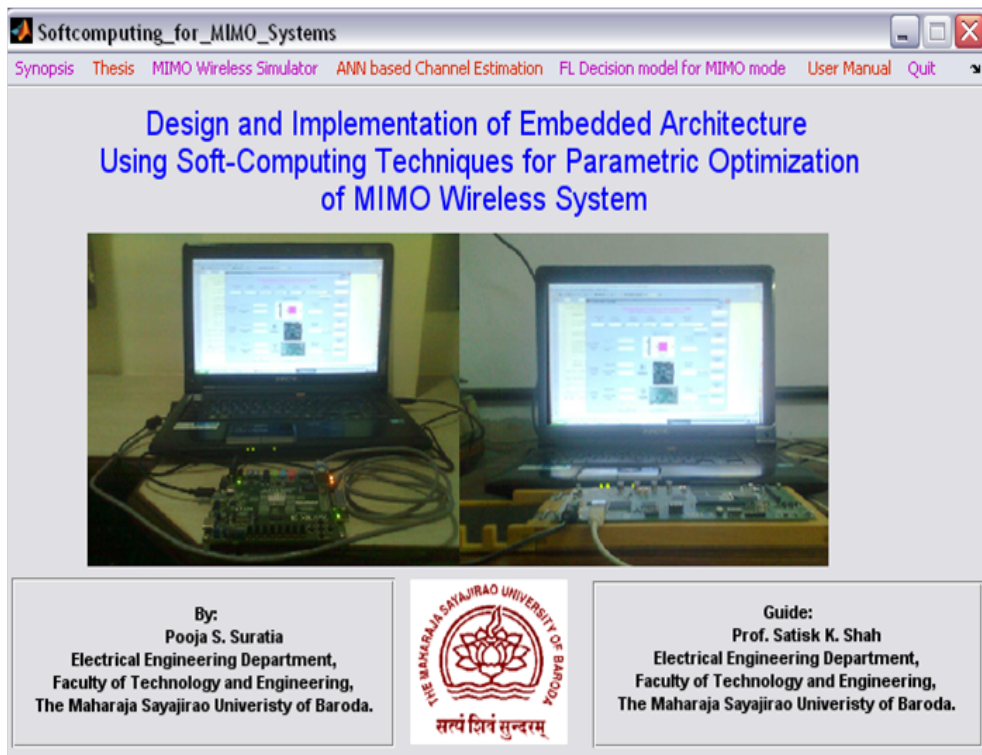


Figure A. 1: GUI for Design and Implementation of Embedded Architecture Using Soft-Computing Techniques for Parametric Optimization of MIMO Wireless System

The menu bar gives the options to view documents (synopsis, thesis and user manual) and to open other GUI for performance analysis of MIMO Wireless Simulator, ANN based Channel Estimation and FL Decision model for MIMO mode switching.

2) MIMO Wireless Simulator is a user friendly GUI based simulator for Capacity and performance analysis of MIMO Wireless System as shown in Figure A. 2. Two MIMO transmission techniques: Spatial Multiplexing and Diversity Techniques can be analyzed using the simulator.

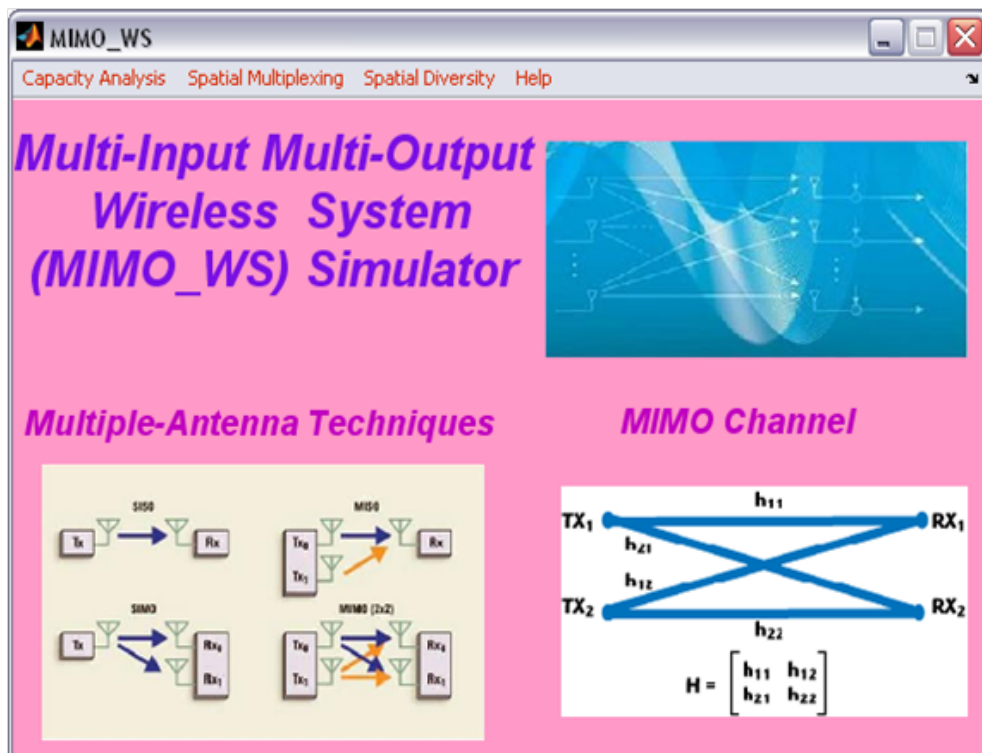


Figure A. 2: GUI for MIMO Wireless Simulator

As shown in Figure A. 3 MIMO-WS is able to carry out the Capacity Analysis for various antenna configurations, performance analysis for Spatial Multiplexing- V-BLAST technique for different receivers. It can also do the analysis of various spatial diversity techniques like MRC, Alamouti, OSTBC and STTC. From the selection of techniques from menu editor, another GUI window pop ups, and the user can vary parameters like Antenna Configuration (2X2, 4X4 or 8X8) and Type of Modulation (BPSK, QPSK, 8-PSK, 16-PSK) as shown in Figure A. 4. When the user pushes the push button labeled with “PLOT”, the BER v/S SNR plot is displayed. For comparative analysis the user can “HOLD FIGURE” and select other configurations and can “PLOT” the graph for further analysis. The “CLEAR FIGURE” push button will clear the axes for other plots.



Figure A. 3: Features of MIMO Wireless Simulator

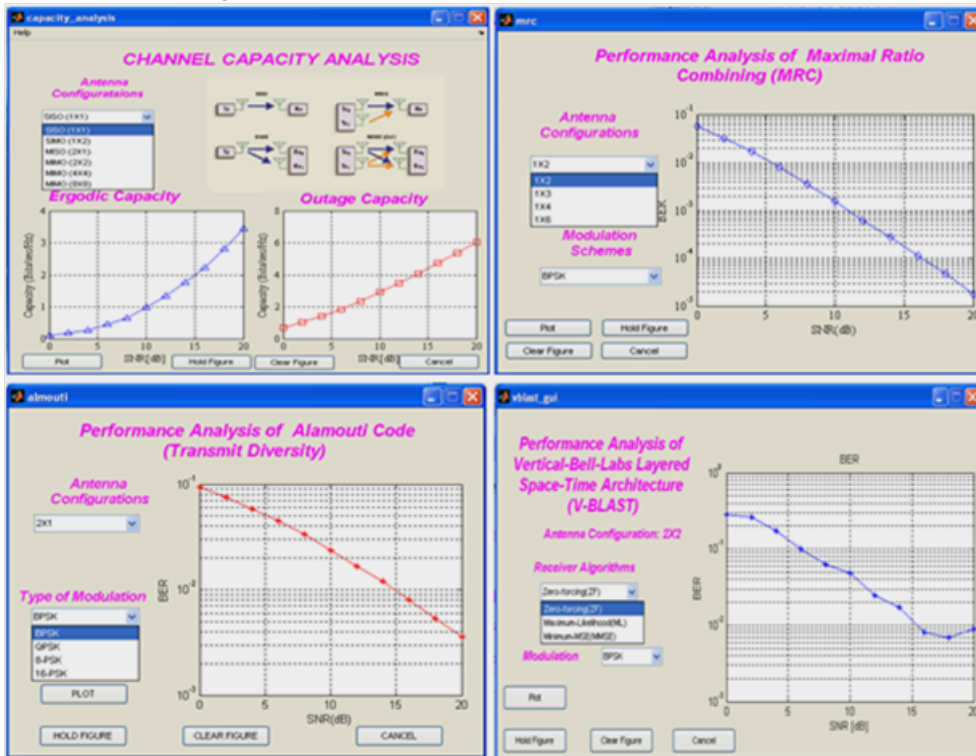


Figure A. 4: MIMO WS GUIs for performance analysis

The GUI for STTC Code Design and performance analysis is as shown in Figure A. 5. The STTC GUI gives option to select the Code design or performance analysis through radio buttons.

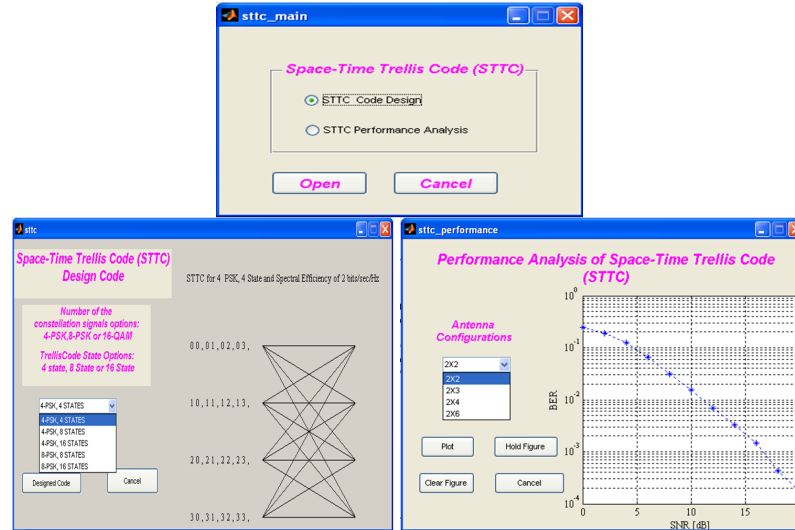


Figure A. 5: STTC performance analysis GUI

3) From the menu bar FL Decision model for MIMO mode, it opens the GUI for “Throughput Analysis for Fuzzy Logic Decision model for MIMO mode switching in LTE-A Downlink Physical Layer” as shown in Figure A. 6. The GUI allows user to set initial simulation parameters using the pop-up menus. “RUN in MATLAB” push buttons starts the simulation and displays the throughput and elapsed time for User parameters.

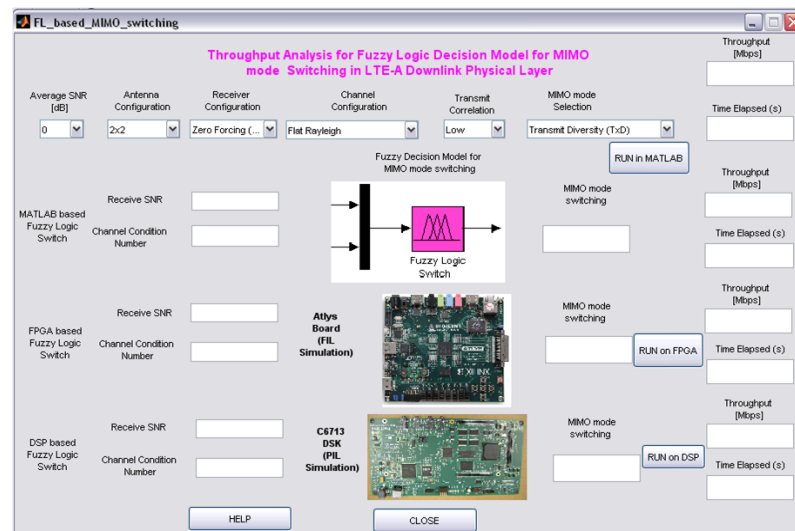


Figure A. 6: GUI for FL decision model for MIMO mode switching

For real-time implementation on Atlys board, connect the USB cable, power supply and Gigabit

Ethernet cable to the kit. Then open the Simulink model “fuzzy_ switching_ modified_ fixedpoint_ new”. Then double click the FIL model, from the Function Block parameters, Load the program to the XUP Atlys board as shown in Figure A. 7. The implementation is done using the push button “RUN on FPGA”.

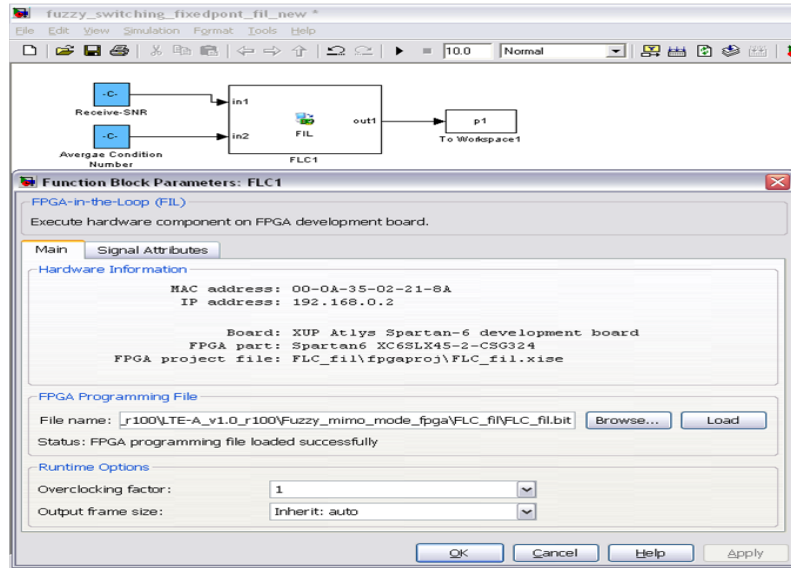


Figure A. 7: Programming XUP Atlys board through MATLAB FIL model

For real-time implementation on TMS320C6713 DSK, connect the USB cable and power supply to the kit. Then open the Simulink model “fuzzy_ switching_ fixedpoint_ pil”. Set the Configuration parameters as shown in Figure A. 8.

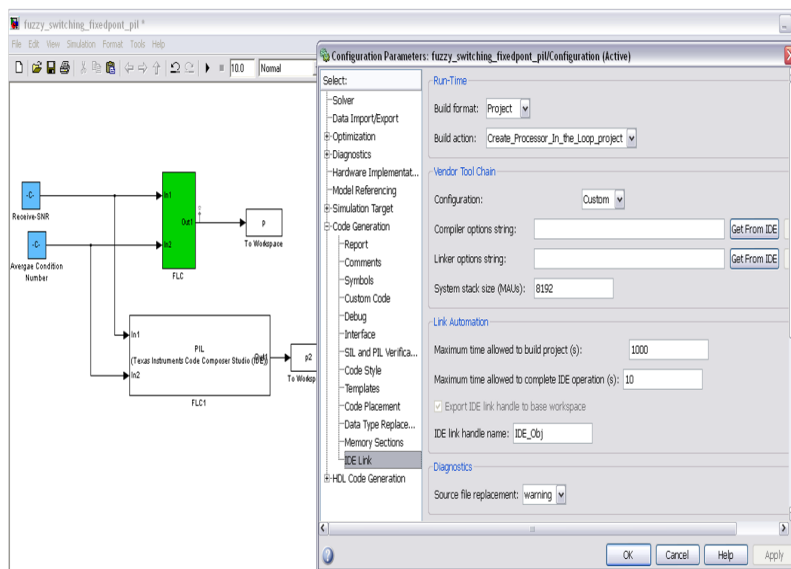


Figure A. 8: Programming C6713DSP through MATLAB PIL model

Then right click the FLC model, and Build Subsystem. The Connectivity Configuration to CCS is generated and is automatically connected to CCS and the PIL block is created. Connect the PIL model in the Simulink file and the output To Workspace. The implementation is done using the push button “RUN on DSP”. The results are viewed in GUI.

4) From the menu bar ANN based Channel Estimations, it opens the GUI for “Throughput Analysis for ANN based MIMO channel estimation in LTE-A Downlink Physical Layer” as shown in Figure A. 9.

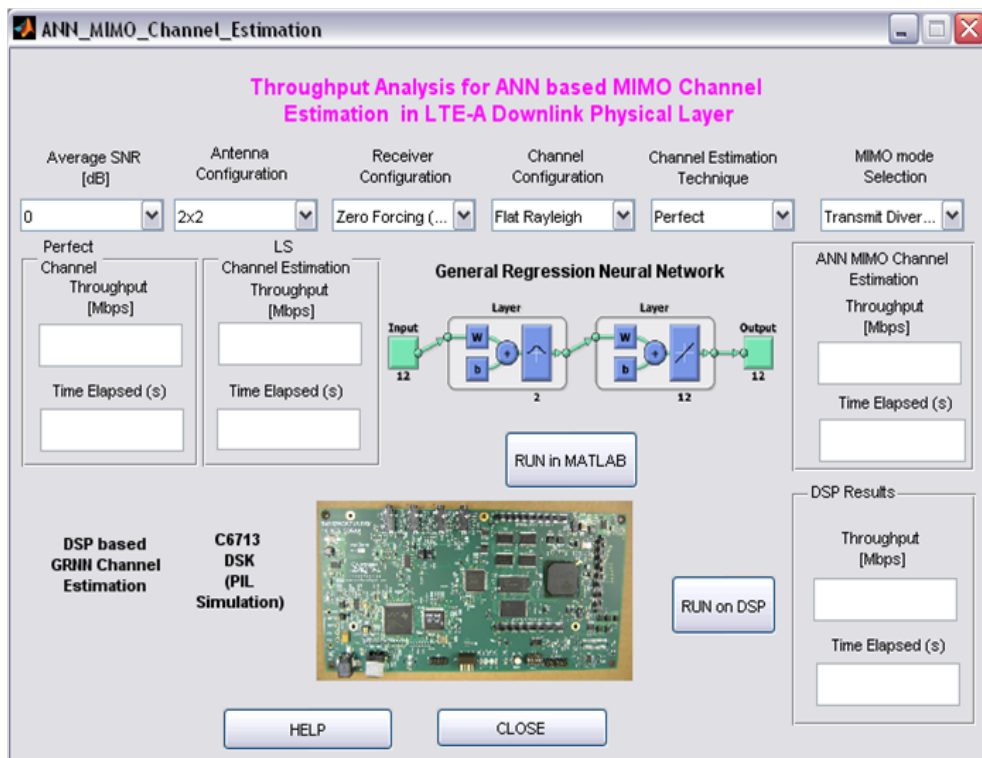


Figure A. 9: GUI for Throughput Analysis for ANN based MIMO channel estimation

For real-time implementation on TMS320C6713 DSK, connect the USB cable and power supply to the kit. Then open the Simulink model “grnn_channelest_pil”. Follow the similar procedure as in Step 3 for implementation on DSP. The implementation is done using the push button “RUN on DSP”. The results are viewed in GUI.

Appendix B: Development Tools and Software programs

This appendix gives list of Software development tools and Hardware development tools used for implementation of proposed techniques on FPGA and DSP.

Software Development Tools	Description
MATLAB 7.12.0.635 (R2011a)	It is an interactive environment for algorithm development, data visualization, data analysis, and rapid prototyping.
LTE-A Link Level Simulator LTE-A_ v1.0_ r100	It simulates test scenarios for analysis of LTE-A Downlink Physical Layer
Xilinx ISE Design Suite 14.6	It is a tool for HDL code design, synthesis and analysis for FPGA Development.
ModelSim PE Student Edition 10.2c	It is HDL Simulator to simulate, verify and debug the HDL Code developed
CCStudio v3.3 6713 DSK CCStudio	It comprises of compilers for TI TMS320C6713 and tools for development and debugging
SiLabs IDE v4.2	It consists of Keil C compiler to develop C code for Wireless Control of FTE Robot .
Eclipse IDE Release 3.7.0	It is used to develop C code for Wireless module.
Pololu Wixel Configuration Utility	To program Wireless module with Wireless Serial Application.

Table B. 1: Software Development Tools with Description

Hardware tools	Description
XUP Atlys Spartan-6 Development Kit	For real-time implementation of throughput optimization techniques on Spartan-6 FPGA.
Spectrum Digital TMS320C6713 DSK	For real-time implementation of throughput optimization techniques on TMS320C6713 DSP.
SiLabs Microcontroller Development kit	It is used to develop and debug the C . code developed for FTE Robot
FTE Robot	Mobile Robot with various features
Pololu Wireless Wixel Modules	To implement Wireless Control of FTE Robot.

Table B. 2: Hardware Development Tools with Description

Table B.3 gives the Fuzzy Inference files developed for FL Decision model for MIMO mode switching in LTE-A Downlink Physical Layer.

FIS Files	Description
FIS_decision.fis	FL Decision model for MIMO mode Switching

Table B. 3: FIS Files

Table B.4 lists the MATLAB files developed for simulation of the proposed techniques.

MATLAB Files	Description
Softcomputing_for_MIMO_Systems	To open the main GUI for developed Soft-Computing Techniques
MIMO_WS	To open GUI MIMO Wireless Simulator and simulation of performance analysis
LTE_sim_test_allmodes	To compare throughput of MIMO configuration in LTE-A Downlink Physical layer
LTE_sim_test_ann_simulink	To simulate and test the performance of ANN based MIMO channel Estimation techniques developed .
LTE_sim_test_fmodel	To simulate and test the performance of FL Decision model for MIMO mode switching
LTE_channel_estimator_ann	To simulate and test the performance of MIMO Channel estimation based on ANN architectures
ANN_MIMO_Channel_Estimation	Simulation and Implementation FL Decision model for MIMO mode switching
FL_based_MIMO_switching	Simulation and Implementation of GRNN based MIMO Channel Estimation Technique

Table B. 4: MATLAB files with Description

Table B.5 lists the Simulink models developed for ANN based MIMO channel estimation and FL Decision model for MIMO mode switching.

Simulink Model Files	Description
fuzzy_switching_fixedpont_fil_new.mdl	For FIL simulation of FL Decision model
fuzzy_switching_fixedpont_pil.mdl	For PIL Simulation on DSP of FL Decision model
grnn_channelest_pil	PIL Simulation on DSP of GRNN based MIMO Channel estimation

Table B. 5: MATLAB Simulink model files

Figure B.6 lists the user friendly GUI developed for performance analysis of MIMO Wireless Systems.

GUI Files	GUI Description
Softcomputing_for_MIMO_Systems.fig	Design and Implementation of Embedded Architecture Using Soft-Computing Techniques for Parametric Optimization of MIMO Wireless System
MIMO_WS.fig	MIMO Wireless Simulator
Capacity_analysis.fig	Capacity Analysis of MIMO Wireless Systems
sttc_performance.fig	Performance analysis of STTC code design and BER
vblast_receiver_compare.fig	Performance analysis of VBLAST Receiver techniques
diversity_compare_figure.fig	Performance analysis of Diversity Techniques for MIMO Wireless
ANN_MIMO_Channel_Estimation.fig	Throughput Analysis for ANN based MIMO Channel Estimation
FL_based_MIMO_switching.fig	Throughput Analysis for FL based MIMO mode switching

Table B. 6: GUI Figure files

Appendix C: Photo Gallery

The FTE Robot with wireless module is shown in Figure B. 1. The setup for Wireless Control of FTE Robot through remote computer is shown in Figure B. 2.

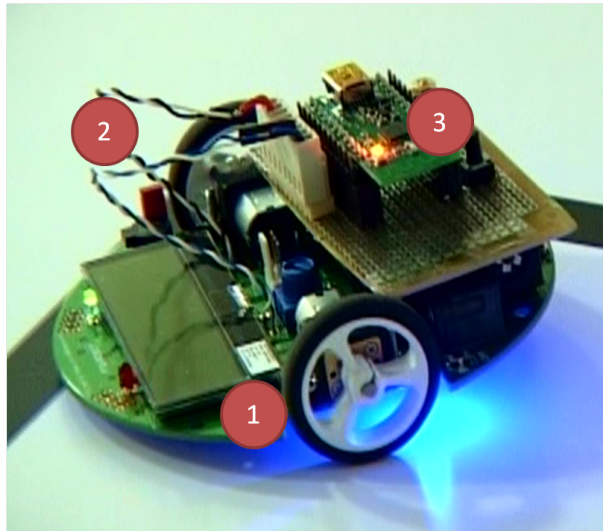


Figure B. 1: FTE Robot with Wireless module: 1)FTE Robot, 2)Connecting wires between Robot and Wireless Module and 3)Wireless Module.

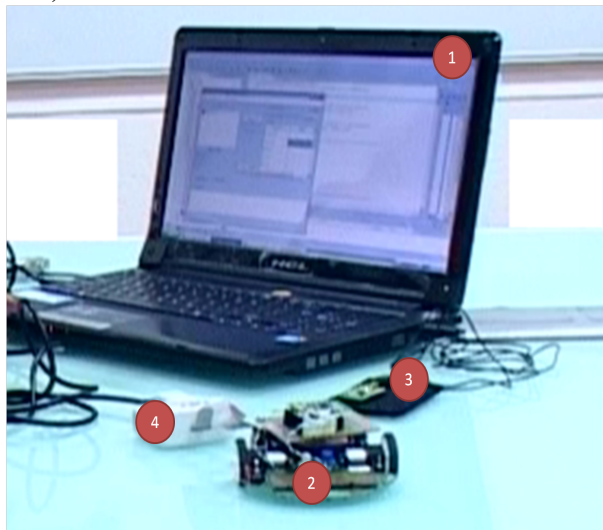


Figure B. 2: Wireless Control of FTE Robot setup: 1)Remote Computer, 2) FTE Robot with wireless module, 3) Transmitter Wireless Module, 4) JTAG Adapter Connector

The real-time implementation and testing of proposed algorithm for throughput optimization of LTE-A Downlink Physical Layer are done on TMS320C6713 DSK. The DSK is shown in Figure B. 3. Figure B. 4 shows the setup for real-time testing of algorithms in close-loop with MATLAB based LTE-A Link Level Simulator. Intel Core2Duo CPU 2.20GHz, 2.96 GB of RAM has installed MATLAB based LTE-A Link Level Simulator, CCS IDE and related toolbox useful for verification of algorithms.

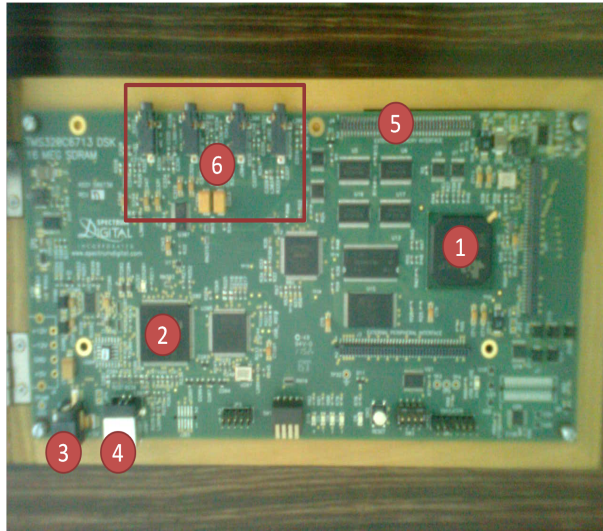


Figure B. 3: DSP Starter Kit: 1)TMS320C6713 DSP, 2)JTAG Emulation, 3)Power Jack, 4)USB Port, 5)Memory Expansion and 6)AIC23 Codec with peripherals



Figure B. 4: DSP Setup: 1)CPU Core2Duo with Software tools installed, 2)TMS320C6713 DSK, 3)Power Cable and 4)USB Cable

The real-time implementation and testing of proposed algorithm for throughput optimization of LTE-A Downlink Physical Layer are done on XUP Atlys Spartan-6 Development kit. The Atlys board is shown in Figure B. 5. Figure B. 6 shows the setup for real-time testing of algorithms in close-loop with MATLAB based LTE-A Link Level Simulator. Intel Core2Duo CPU 2.20GHz, 2.96 GB of RAM has installed MATLAB based LTE-A Link Level Simulator, Xilinx ISE Design Suite and related toolbox useful for verification of algorithms.

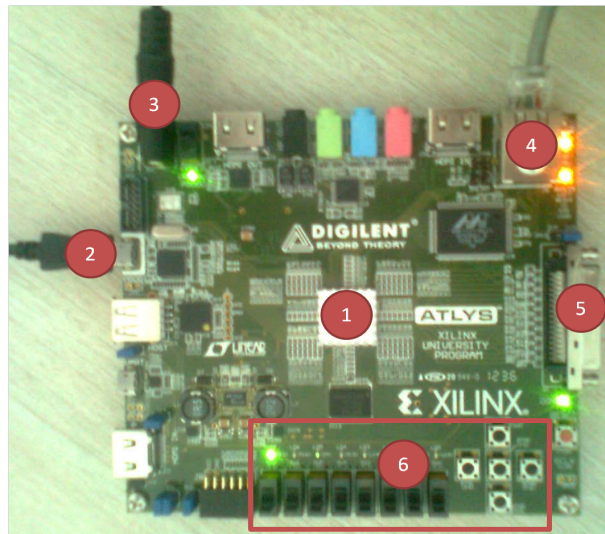


Figure B. 5: XUP Atlys Board: 1)Spartan-6 LX 45, 2)Adept USB Port, 3)Power Jack, 4)Ethernet connector, 5)VHDC connector and 6)LEDs, Slide Switches and Push buttons



Figure B. 6: FPGA Setup: 1)CPU Core2Duo with Software tools installed, 2)USB cable, 3)Power cable, 4)Atlys board, 5)Gigabit Ethernet crossover cable

Appendix D: Research Publications

• *Journal Publications*

- Pooja S. Suratia and Satish K. Shah, “Conceptual Design of MIMO Wireless Communication System” , International Journal of Advanced Research in Computer and Communication Engineering [IJARCCE], Vol. 1, Issue 5, July 2012, ISSN : 2278 1021.
- Pooja S. Suratia and Satish K. Shah, “Performance Analysis of Open and Closed Loop Spatial Multiplexing in LTE Downlink Physical Layer”, Proceedings of IEEE International Conference on Communications, Network and Satellite (ComNetSat), Indonesia, pp. 60-63, July 2012. DOI: 10.1109/ComNetSat.2012.6380777
- Satish K. Shah, Pooja S. Suratia and Nirmalkumar S. Reshamwala, “Comparative Performance Analysis of ANN Based MIMO Channel Estimation for downlink LTE-Advance System employing Genetic Algorithm”, The International Journal of Soft Computing and Software Engineering [JSCSE], Vol. 3, No. 3, Special Issue: The Proceeding of International Conference on Soft Computing and Software Engineering 2013 [SCSE13], San Francisco, CA, U.S.A., March 1-2, 2013. DOI: 10.7321/jscse.v3.n3.111
- Nirmalkumar S. Reshamwala, Pooja S. Suratia, Satish K. Shah, “Study of ANN Configuration on Performance of Smart MIMO Channel Estimation for Downlink LTE-Advanced System”, International Journal of Computer Network and Information Security [IJCNIS], Vol. 5, No. 11, September 2013. DOI: 10.5815/ijcnis.2013.11.04

• *International Conferences*

- Pooja S. Suratia and Satish K. Shah, “Performance Analysis of Open and Closed Loop Spatial Multiplexing in LTE Downlink Physical Layer”, IEEE International Conference on Communications, Network and Satellite (ComNetSat), Indonesia, pp. 60-63, July 2012. DOI: 10.1109/ComNetSat.2012.6380777
- Satish K. Shah, Pooja S. Suratia and Nirmalkumar S. Reshamwala, “Comparative Performance Analysis of ANN Based MIMO Channel Estimation for downlink LTE-Advance System employing Genetic Algorithm”, International Conference on Soft Computing and Software Engineering 2013 [SCSE13], San Francisco, CA, U.S.A., March 1-2, 2013. DOI: 10.7321/jscse.v3.n3.111

- ***National Presentations and Technical Awards***

- Pooja Suratia, “GUI Based MIMO-WS (Multi-Input Multi-Output Wireless Simulator) for Capacity and Performance Analysis”, State Level Paper Contest- Control, Microcomputer, Electronics and Communication (CMEC), organized jointly by IETE and Electrical Engineering Department, Faculty of Technology and Engineering, The Maharaja Sayajirao University of Baroda, February 2011. The paper received **Second Prize**.
- Pooja Suratia, “Design and Implementation of Wireless Control of FTE Embedded Robot”, State Level Paper Contest- IT Security with 4G communication (ITS4GC), organized jointly by IETE-Vadodara and The Institution of Engineers IE(I)-Vadodara, April 2012. The paper received **First Prize**.
- Pooja Suratia, “Performance Analysis of ANN Based MIMO Channel Estimation for downlink LTE-Advanced System”, National Level Paper Contest- Soft Computing for Processing, Security Networking and Communication (SCPSNC), organized jointly by IETE and Electrical Engineering Department, Faculty of Technology and Engineering, The Maharaja Sayajirao University of Baroda, January 2013. The paper received **First Prize**.
- Pooja Suratia, “Throughput Optimization of LTE Downlink Physical Layer employing Fuzzy-Decision model for MIMO mode switching”, National level Paper Contest- Target Technologies in Computing, Automation and Communication (TTAC), organized jointly by IETE-Vadodara and The Institution of Engineers IE(I)-Vadodara, March 2014. The paper received **First Prize**.

- ***Sponsored Grant***

The project is approved by Department of Science and Technology under Women Scientist Scheme (WOS-A) for three years and has received total amount of Rupees 19,95,000/- for the implementation of the project at Electrical Engineering Department, Faculty of Technology and Engineering, The Maharaja Sayajirao University of Baroda, Vadodara.

Appendix E: Training Programs attended based on Research Work

- ISTE approved Short Term Training Programme on “MIMO Wireless Communication Systems”, 26th to 31st December 2011 conducted by Department of Electronics and Communication Engineering, Institute of Technology, Nirma University, Ahmedabad.
- Workshop on “Power Line Communication and IT Enabled Energy Metering”, 15th to 19th May 2012, organized by Electrical Engineering Department, The Maharaja Sayajirao University of Baroda in Technical Association with IETE-Vadodara Center.
- Workshop on “Spoken Tutorial for Latex and Scilab” on 25th and 26th June 2012 at ITM Universe, Vadodara in association with Spoken Tutorial Project, IIT Bombay.
- Workshop on “ASIC and FPGA Design”, 1st September 2012, conducted by Electronics and Communication Department, IETE Chapter, SVIT-Vasad and CorEL Technologies, Bangalore.
- Short Course on “MIMO/OFDM Based Advanced 4G Cellular Networks”, 11th to 13th January 2013, organised by Department of Electrical Engineering IIT Kanpur and BSNL-IITK Telecom Center of Excellence.
- Workshop on “Simulation of Wireless Communication Systems”, 24th and 25th August 2013 conducted by Department of Electronics and Communication Engineering, Institute of Technology and organized by Centre for Continuing Education (CCE), Nirma University, Ahmedabad.
- Five days program on “Performance Analysis of MIMO Wireless Communication Systems” 5th to 9th March 2014 conducted by Department of Electronics and Communication Engineering, Institute of Technology and organised by Centre for Continuing Education (CCE), Nirma University, Ahmedabad.